MOLECULAR AND BIOCHEMICAL PHARMACOLOGY OF MITOCHONDRIAL ENZYMES IN THE MALARIA PARASITE *PLASMODIUM FALCIPARUM*

Thesis is submitted in accordance with the requirements of the University of Liverpool for the degree of Doctor of Philosophy

By

ROSLAINI ABD MAJID

B.Sc. BioMedical (Hons) (Nott. Trent, UK)

M.Sc Medical Parasitology (Malaysia)

October 2011

Declaration

This thesis is the result of my own work. The material contained in the thesis has not been presented , nor is currently being presented, either wholly or as a part, for any other degree or other qualification.

The research work was carried out in the Liverpool School of Tropical Medicine, University of Liverpool, United Kingdom.

ROSLAINI ABD MAJID (2011)

Dedications

First and foremost, I would like to dedicate this work to my loving memory of my late mother Hajjah Neh Isahak who passed away in August 2009. Since you left, my life is never the same again. I will always miss you and love you. You are always in my heart, my thoughts and prayers. May your soul rest in peace. Al-fatihah.

Abstract

The mitochondria of malaria have big potential to be explored as a drug targeting site. This is due to the differences in the composition of the *Plasmodium* respiratory complex compared with the human host. The *Plasmodium* respiratory chain consists of 2 unique dehydrogenases PfNDH2 and MQO which are only encoded in prokaryotic cells. Apart from these two, the *Plasmodium* bc_1 complex has low amino acid similarity when compared to the bc_1 complex of other eukaryotes. Currently the only approved antimalarial drug targeting *Plasmodium* mitochondria is atovaquone. This drug is used in combination with proguanil (Malarone™) and is widely used for the curative and prophylactic treatment of malaria. Atovaquone, a 2-hydroxynaphthoquinone, is a competitive inhibitor of the quinol oxidation (Q_o) site of themitochondrial cytochrome bc_1 complex. Inhibition of this enzyme results in the collapse of the mitochondrial membrane potential and subsequent parasite death. However, atovaquone resistance developed very soon after its implementation as malaria chemotherapy. Previous studies have established that the resistance of the parasite is the result of mutations in the bc_1 Q_o. To date we are the first group to elucidate the genotype and biochemical characterisation of the atovaquone resistant *P. falciparum* TM90C2B. The GeXP multiplex quantitative PCR (qPCR) revealed that a number of genes encoding energy metabolism proteins and genes associated with redox control are upregulated in the resistant parasite compared to the atovaquone sensitive strain 3D7. This has been supported by automated sequencing results which indicate the presence of a single point mutation in the DNA sequence of TM90C2B cytochrome *b* which resulted in the substitution of tyrosine by serine at position 268. The drug sensitivity assays and kinetic studies were conducted in order to understand the phenotypic consequences of this mutation. As expected, TM90C2B strain was resistant to almost all electron transport chain inhibitors. The enzymological characterisation of TM90-C2B bc_1 complex (steady-state decylubiquinol:cytochrome oxidoreductase assay) showed that enzyme turnover was approximately 50% of the atovaquone-sensitive strain with a threefold increase in K_m for decylubiquinol (3D7 : V_{max} = 97.4 ± 5.1 nmol cyt *c* reduced/min/mg protein, K_m = 5.5± 1.1 mM dQH_2, IC_{50} 6 nM, K_i = 0.6 nM; TM90C2B : V_{max} = 60.2 ± 3.2 nmol cyt *c* reduced/min/mg protein, K_m = 18.5± 2.6 mM dQH_2, IC_{50} 600 nM, K_i = 162 nM). The other mitochondrial respiratory complexes' specific activities were also measured using samples prepared from Percol® fractionation. Apart from Complex II, we also managed to demonstrate the specific activities of the other complexes'. The PfNDH2 and bc_1 complex proteins of TM90C2B strain had 50% less activity than the 3D7 strain.This was supported by data from western blot analysis showing a decrease in PfNDH2 and ISP proteins content of the TM90C2B compared to the 3D7 strain. In addition to this study, we also characterised the *Plasmodium falciparum* mitochondrial malate quinone oxidoreductase (MQO). MQO is involved in the electron transport chain, oxidising malate to oxaloacetate in the oxidative arm of *Plasmodium* tricarboxylic acid cycle (TCA cycle). This enzyme contains a flavin cofactor which donates electrons to cytochrome bc_1 complexvia reduction ofubiquinone to ubiquinol. The bioinformatic analysis data indicates that PfMQO is a

membrane-bound mitochondrial protein with only one transmembrane domain. The *PfMQO* gene was successfully amplified from genomic DNA of 3D7 *P. falciparum* and cloned into 2 expression vectors pET-15b and pUC19. The presence and orientation of the gene in the respective vector were confirmed by restriction enzyme analysis and automated sequencing. The putative *PfMQO* gene (1566 bp) was successfully amplified and predicted to produce an approximately 60-kDa protein. Only when the *PfMQO* gene was cloned into pET15b was overexpression of the recombinant protein achieved. The recombinant PfMQO was purifiable under denaturing conditions due to its insolubility and formation of inclusion bodies. This protein is inactive and appears to be improperly folded thus producing the inconsistent results of the kinetic analyses. In conclusion, our study provides new insights into the understanding of the molecular and biochemical regulation of atovaquone resistant parasites through a mutation in the bc_1 complex. The partial characterisation of PfMQO is a starting point for the development of a new drug target in *Plasmodium* mitochondria by taking into account the uniqueness of this enzyme which is not found in the human host.

Contents

List of Figures

List of Tables:

List of Appendices

Acknowledgements

Special thanks to The Malaysian Government and Universiti Putra Malaysia for providing a scholarship to enable me pursue PhD study at Liverpool School of Tropical Medicine.

I would like to acknowledge my supervisors Dr Giancarlo Biagini and Prof Steve Ward for their supervision, continued support and encouragement throughout this PhD.

I express my sincere gratitude to Dr Ashley Warman for establishing my practical aspects in molecular biology, Dr Nick Fisher for managing to teach me the kinetic studies and Dr Muhammed Al-Hilal for his dedicated work and introduce to me the basic technique in malaria parasite culture and IC_{50} techniques.

To Katerine, Alice and Alison thank you very much for help proof reading my thesis draft. I am very grateful to Ashley for his commitments, corrections and suggestions. Your comments were extremely valuable and help so much on my writing skills.

Big thanks to Miss Alison Mbeakini "aiyai aiyai" for inspirational argument every morning before I started my culture work. Thanks also to my French tag team Mr Thomas Antionne, for continuous support when fighting with Alison and also for exchanging scientific knowledge's. I must also thank to other staff members of MBP group; Jill, Taj, Enrique and David.

My heartiest thanks to my PhD friends, Susan, Archana, Upali, Kwanan "Kung", Susana, Dr Tiago, Teresa and Khairul many thanks for all of you. We have been together for four years and we are really enjoyed the moments in the culture suite while taking care of our precious malaria parasites. Although malaria causes many deaths, but in our studies we felt very disappointed if it is not growing well. To new generation of PhD friends, Murad, Taghrid, Aiman and Muhammaed, wish you are best of luck.

For new friends in PhD room, Dr Alex, Dr Ruksana, Dr John, and Dr Pamela nice to know all of you even in a short time. Their commitments in study always give me inspirational to write my thesis. And last and not least to Mr Dariel thanks for sharing ideas about Mayan theory of 2012, I really hope it is not going to be happen. I feel very grateful having such good memories and friends throughout of my study in LSTM (2007-2011).

My acknowledgements would not be complete without profound recognition of my examiners; Dr. Mark J.I. Paine and Professor Angus Bell, for their building comments on my Thesis. I truly appreciate.

As for my past head of Departments Assoc. Prof. Dr. Malina Osman and the current Dr. Rukman , Terima kasih. I am very grateful.

Lastly but not the least, Jane Banda, let it be penned down that words can not express how grateful I am for the tireless support and proof-reading my write-up.

Publications and Presentations

Work in this thesis has been presented for publication, or is in preparation for publication, and has been presented at meetings in the following forms:

Publication:

Nicholas Fisher*, Roslaini Abd Majid*, Mohammed Al-Hilal, Thomas Antoine, Ashley Warman, David J Johnson, Hilary Ranson, Paul M O'Oneill, Stephen A Ward# and Giancarlo A Biagini# (2012). Molecular and Biochemical Characterisation of the Atovaquone Resistant Phenotype in the Malaria Parasite *Plasmodium* falciparum. *The Journal of Biological Chemistry*, 287:13,9371-9741.

Publication in Preparation:

Electron Competion and membrane potential generation in *Plasmodium falciparum*

Nichlos Fisher*, Thomas Antoine*, Roslaini Abd Majid, Mohammed Al-Helal, Ashley Warman, Paul M O'Neill, Stephen A Ward# and Giancarlo A Biagini#

*Join first authors

#Join corresponding authors

Presentations:

Molecular & Biochemical Characterisation of Atovaquone Resistance in the Malaria Parasite *Plasmodium falciparum* (TM90-C2B)

Has been presented at the following meetings:

1. 16th European Bioenergetics Conference - Warsaw, 17-22 July 2010 (Poster)
2. BSP Spring, Trypanososomiasis/Leishmaniasis & Malaria Meetings 2010, Cardiff University (Poster)

Abbreviations

ADP	Adenosine diphosphate
APS	Ammonium persulfate
ATP	Adenosine triphosphate
ATV	Atovaquone
bp	Base pairs
BSA	Bovine serum albumin
cDNA	Complementary DNA
CQ	Chloroquine
CoQ	coenzyme ubiquinone
CSP	circumsporozoite protein
DCPIP	2,6-dichlorophenolindophenol
DEPC	Diethyl pyrocarbonate
DHODH	Dihydroorotate dehydrogenase
DHFR	Dihydrofolate reductase
DHPS	Dihydropteroate synthase
DMSO	Dimethyl sulphoxide
DNA	Deoxyribonucleic Acid
DV	Digestive vacuole
EDTA	Ethylenediamine-tetraacetic acid
EPR	Electron paramagnetic resonance
ETC	Electron transport chain
EtOH	Ethanol
FAD	Flavin Adenine Dinucleotide
FMN	Flavin mononucleotide
FPPIX	Ferripritoporphyrin
Gu-HCl	Guanidine hydrochloride
HEPES	(4-(2-hydroxyethyl)-1-piperazineethanesulfonic acid

IC_{50}	50% inhibitory concentration
IPTG	Isopropyl-β-D-thiogalactopyranoside
ISP	Rieske Iron protein
kbp	Kilobase pairs
kDa	Kilodaltons
MDH	Malate dehydrogenase
MQO	Malate quinone oxidoreductase
MtDNA	mitochondrial DNA
mtETC	mitochondrial electron transport chain
NADH	β-Nicotinamide-Adenine-Dinucleotide (reduced form)
NADPH	β-Nicotinamide-Adenine-Dinucleotide – Phosphate (reduced form)
Ni-NTA	nickel-nitrilotriacetic acid
O.D	Optical density
OAA	Oxaloacetate
PBS	Phosphate Buffer Saline
PCR	Polymerase chain reaction
PfCRT	*P. falciparum* chloroquine resistance transporter
PfMDR	*P. falciparum* multidrug resistance 1 gene
Pgh1	P-glycoprotein homolog 1
ROS	Reactive oxygen species
QN	Quinine
QH_2	Ubiquinol
Q_i	Ubiquinone reduction site
Q_o	Ubiquinol oxidation site
qPCR	Quantitative Polymerase chain reaction
RBCs	Red blood cells
RNA	Ribonucleic acid
SD	Standard deviation
SDS	Sodium Dodecyl Sulfate
SE	Standard error

SERCA	Sarco/endoplasmic reticulum Ca2+-ATPase
SP	Sulfadoxine-pyrimethamine
X-Gal	5-Bromo-4-chloro-3-indoyl-beta-D-galactopyranoside
TAE	Tris/Acetate/EDTA
TBE	Tris/Borate/EDTA
TBS-T	Tris buffered saline and Tween-20
TCA	Tricarboxcylic acid cycle
UV	ultra violet
WHO	World Health Organisation

Chapter 1.0: Introduction

1.1 History of Malaria: Key Discoveries

The word malaria comes from the latin word '*mal aria*', which means 'bad air'. This is due to the close relationship between the disease and the swamp area (261). Malaria parasites were for the first time ever reported in 1880 by a French physician and military surgeon Charles Alphonse Laveran (1845-1922) in the Roman Campagna. He found the cresent-shaped bodies in the blood of patients who had become infected under the light microscope. He gave the name of the organism as *Oscillaria malariae*. He also described swamps and low humid plains were the most favourable environments for malaria. However, swamp itself is not a main cause of the disease. In 1886, Camillo Golgi (1843-1926) discovered the parasite produced asexually by multiple fission and the symptoms of the fever were due to the release of the parasite from infected RBC.

Diagnosis of malaria began with the invention of methylene blue and eosin stain by Dimitri Romanowsky. He demonstrated the nucleus and the cytoplasm of the organism are differently stained. However, the result was not reproducible after being repeated by other investigators. The problem was resolved with the invention of a similar stain by Gustav Giemsa (1867-1948). This Giemsa stain, is still the gold standard stain for diagnosis of human malaria parasites.

The sexual stages of the parasite were revealed by two medical students from Johns Hopkins University of Baltimore, Maryland USA in 1897. They demonstrated the sexual

stages of the parasite are formed from two sex cells, micro and macrogametocytes. The concept of exflagellation was firstly described in the formation of male gametocyte from microgamete.

The mode of transmission of malaria parasites was first discovered by Sir Ronald Ross. Sir Ronald Ross, a British physician in the Indian Medical Service, demonstrated the presence of the parasite in dissected mosquitoes, which were fed with infected blood from the malaria patient. His work was published in British Medical Journal in December 1897. In the subsequent year, he proved that female mosquitoes are the vector in malaria transmission. This study was continued by Professor Giovanni Batistta Grassi who successfully demonstrated that only the *Anopheleine* genus can act as the vector for malaria transmission. Historical accounts of malaria are described by Irwin B. Sherman entitled "A Brief History of Malaria and Discovery of the Parasite's Life Cycle" (238).

1.2 Malaria Epidemiology

In the year 2010, the World Health Organisation (WHO) World Malaria Report estimated 240 million cases and about 781,000 deaths globally in 2009 (278). 40% of the World's population are at risk of contracting malaria mainly in tropical and subtropical countries (Figure 1.1); mainly in Sub-Saharan Africa, South East Asia, China, Central and South America. The climatic conditions in these areas provided the favourable environments to support the Anopheline mosquito breeding sites. Malaria has caused a negative impact on the economic status of these countries. In Africa only, it is estimated to cost $12 billion US per annum in lost productivity and 25% of all deaths recorded in children under the age of

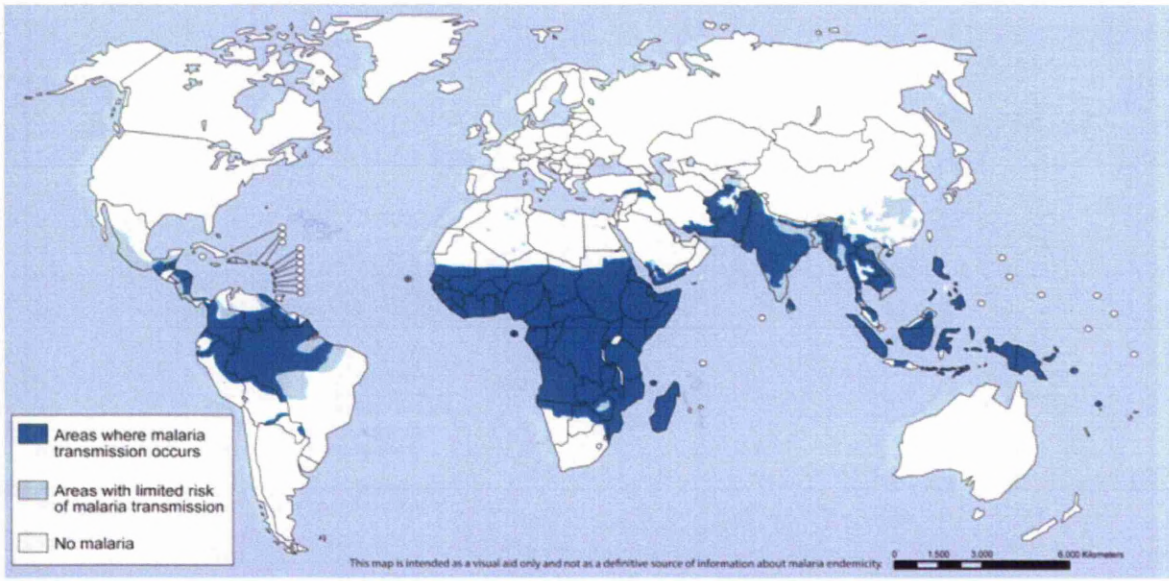

Figure 1.1: Geographical Distribution of Malaria

World map showing malaria endemic countries areas at risk of transmission in 2008. Dark blue colour indicates areas where high transmission occurs mainly in tropical areas of Asia, the Americas and Sub-Saharan Africa. Light blue indicates areas with limited risk and white areas representing malaria free countries (279).

five (244).

Human malaria is caused by one or a combination of four species of *Plasmodium* parasites namely *P. falciparum*, *P. vivax*, *P. ovale* and *P. malariae*. Recently, *P. knowlesi* the primate malaria has also been reported to be responsible for human malaria cases in South East Asia (39). These species can be distinguished via morphological structure, clinicopathology and their geographical distribution (although *P. knowlesi* and *P. malariae* can only be distinguished using molecular-based methods). *P. falciparum*, pre-dominantly found in sub-Saharan Africa causes 90% of fatality mainly in young children. *P. vivax* is the second most widespread species but rarely causes fatality. *P. ovale* is restricted to West Africa regions, while *P. malariae* is found worldwide with low frequency (278).

Malaria is transmitted through biting of female *Anopheles* mosquitoes. 400 species of *Anopheles* mosquitoes have been recorded worldwide. 60 species are served as malaria vectors and 30 species are the major species for malaria transmission (261).

1.3 Malaria Life Cycle

The malaria parasite has a complex and multistage life cycle. All malaria parasites undergo almost similar life cycles (5). Figure 1.2 describes the life cycle of malarial parasites. It begins with injection of sporozoites by an infective female *Anopheles* mosquito during a blood meal. The sporozoites then travel actively through the bloodstream to the liver and invade the hepatocytes. The sporozoites invade the Kupffer cells within which they are enclosed in a parasitophorous vacuole then invade the hepatocytes. As the sporozoites enter

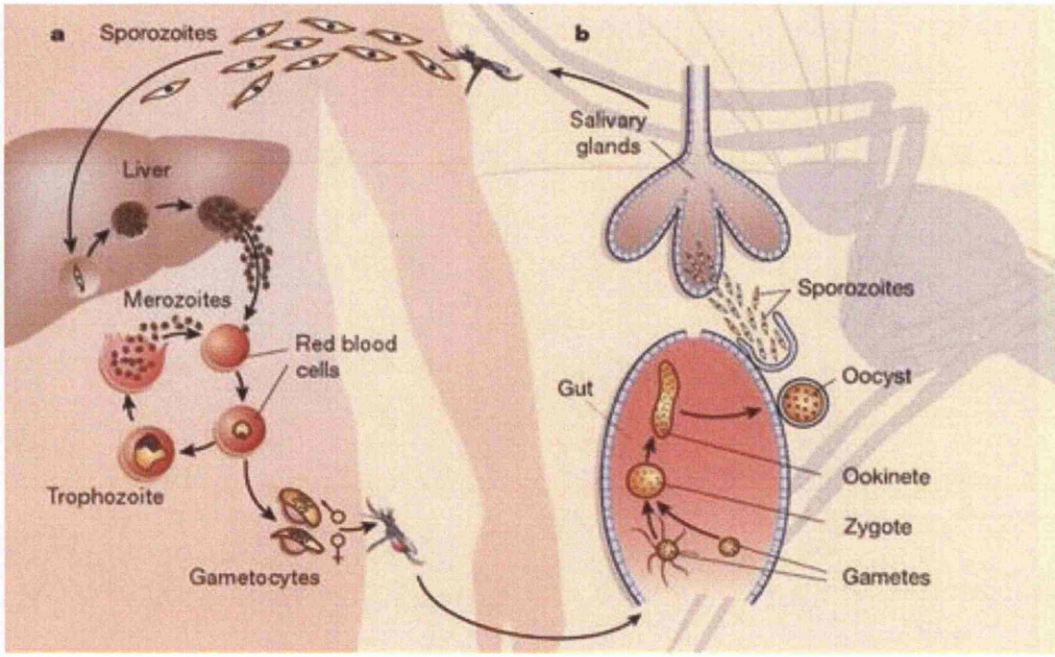

Figure 1. 2: The Life Cycle of Malarial Parasites

(A) *Plasmodium* life cycle in the human host (asexual stage), showing the inoculation of sporozoites into the circulation thus end up in the liver cells. In the liver cells, the sporozoites develop into merozoites which are released from the hepatocytes into blood circulation and eventually infect the red blood cells. A merozoite then develops into a trophozoite, multiply into a schizont and finally new merozoites are released when RBC ruptures. A fraction of the merozoites develop into gametocytes.

(B) The life cycle of malaria parasites in the mosquito host (sexual stage). The sexual reproduction starts when the female *Anopheles* mosquito takes a blood meal from an infected person. In the process it ingests male and female gametocytes. The gametocytes develop into male and female gametes which fertilise within the mosquito midgut to form a zygote which develops into a motile ookinete. The ookinete penetrates the mosquito midgut and forms the oocyst on the outer surface of the epithelium. The matured oocyst filled with sporozoites eventually burst to release sporozoites which travel to the mosquito salivary glands. Adapted from Wirth (2002).

the hepatocytes, they undergo morphological changes leading to the formation of mononucleated forms. The nucleus start to divide and the cytoplasm grows substantially to form schizonts. After completion of the nucleus division, the cytoplasm segments and individual merozoites are formed. The mature schizonts can produce up to thousands of merozoites per hepatocyte occupying the entire cytoplasm. This phase is known as the exoerythrocytic cycle (119). The number of merozoites produced at this cycle varies between species. Approximately, 2000 merozoites produced for *P. malariae,* 10,000 for *P. ovale* and *P. vivax*, and up to 30,000 merozoites for *P. falciparum* (83). Some species, including *P. vivax* and *P. ovale* undergo dormant periods in the liver in the form of hypnozoites in the liver in the form of hypnozoites. Instead of immediate asexual proliferation, the hypnozoites will only be reactive from several weeks to several years after the primary infection. This dormant period is responsible for the relapse of the disease (138).

Upon the rupture of mature schizonts, the merozoites are released into the sinusoids of the liver and invade RBCs. The invasion of RBCs by merozoite is coordinated by the apical organelles and result in the invagination of the RBCs plasma membrane to form parasitophorous vacuole (PV), which surrounds the parasite and separates it from the RBC cytosol (38, 85). The pathological manifestation is started during the intraerythrocytic stage. Within the PV, the parasite matures through serial developmental stages. In those particular cells, the parasites undergo a tropic period and develop into ring forms (young trophozoites). The parasites mature into trophozoite stages about 18-28 hours after RBC invasion. Within the digestive vauole (DV) in the RBCs, the trophozoites obtain nutrients from digested haemoglobin. The degraded haemoglobin is used as an amino acid source for the parasite and the remaining haem is converted into hemozoin , also known as malaria pigment (12). At this stage, the parasite RNA and protein synthesis occur at the highest level and DNA synthesis is

initiated (8). The parasite nucleus continuously multiplies to produce two or more nuclei and subsequently matures into schizonts. Finally, the schizont undergoes cytokinesis and abundant merozoites are released from ruptured schizonts, which infect the other RBCs and iniate another intraerythrocytic developmental stage.

Apart from the asexual multiplication, some merozoites differentiate into female and male gametocytes. During a blood meal from an infected person, the female *Anopheles* mosquito ingests the gametocytes. In the mosquito gut, the gametocytes shed the erythrocyte membrane and transform into female and male gametes (macro and microgametes). The macrogamete does not undergo much morphological changes where as the nucleus of the microgamete actively divides forming a thread-like microgamete which tears free from the original structure. This process is referred to as exflagellation. The female and male gametes then fuse to form a zygote which undergoes elongation and in about 18 hours forms the motile ookinates, which later penetrates the gut wall of the mosquito, establishes itself beneath the basal lamina and form oocysts. The oocysts eventually undergo multiple rounds of asexual replication to form sporozoites. The numbers of sporozoites produced vary between species; for example, 4,000 to 10,000 for *P. falciparum*. Duration of sporogony also varies between species for instance; 10 to 12 days for *P. falciparum*, 5 days for *P. vivax* and *P. ovale* and 5 to 23 days for *P. malariae*. the These sporozoites are released and travel to the salivary gland of the mosquito which finally invaded the mosquito salivary gland cells (166). This mosquito is highly infective and will injected the sporozoites into the human body allowing the cycle of infection to be continue between human and mosquito hosts.

1.4 Malaria Pathogenesis

P. falciparum causes the most severe form of malaria infection. The clinical manifestations of malarial symptoms are associated with the rupture of infected RBCs during the blood stage of the parasites's life cycle. The common complications related to malaria infection include fever, metabolic acidosis, hypoglycaemia, respiratory distress and severe anaemia, cerebral malaria and in pregnant women can cause abortions, still births which may result in hospitalisation and death (275).

In severe malaria, tissue hypoxia largely contributes to organ failure. The mechanis of hypoxia due to malaria was proposed by sequestration of parasitized RBCs which involve cytoadherence, rosette formation and deformation of the RBCs. Miller et al. (2002) described sequestration and rossetting as two factors which attribute to complicated disease outcomes. Within the infected RBCs, the *Plasmodium* parasites adjust the erythrocyte surface causing the infected RBCs to adhere to the vascular endothelium (143). Cytoadherence is mediated by the antigenically variant *P. falciparum* erythrocyte membrane protein 1 (PfEMP-1) on the surface of the infected RBCs (143). Kyes et al. (2001) postulated that PfEMP1 is anchored on the surface of parasitized RBCs in electron dense knobs through interactions with RBC cytoskeleton proteins and parasite encoded proteins, including knob-associated histidine rich protein (KAHRP) (132). The roles of other surface antigens (RIFIN and STEVOR) in the pathogenesis of malaria are still not well ellucidated. However, based on the size, structure and expression patterns between RIFIN and STEVOR, these proteins are speculated to be involved in antigenic variation (148, 149).

PfEMP-1 acts together with CD36, intracellular adhesion molecule 1 (ICAM-1) and chondroitin sulphate A (CSA) to promote infected RBCs adherence to the endothelial cells. Previous studies show that the PfEMP-1 mediated adhesion to ICAM-1 plays an important role in the pathogenesis of cerebral malaria (273). Meanwhile, the adhesion of PfEMP-1 to CSA contributes to pregnancy-related malaria (104). Sequestration to the endothelium is also detected in other organs including the heart, liver and kidneys resulting in the blockage of microvascular blood flow in the affected organs (175). The sequestration of the parasites to the deep microvascular tissues thus prevents the infected RBCs to be cleared by the spleen and helps the parasite to evade the host immune system (175). Rosetting is the second phenomenon of *P. falciparum* infected RBCs that spontaneously bind to uninfected RBCs. Rosetting enhances microvascular obstruction in the targeted organs which exacerbates the pathophysiology of severe malaria. These processes are mediated by the interaction between PfEMP-1 adhesion molecule, CR1 and other several receptors that are expressed on the surface of infected RBCs (224).

1.4.1 Anaemia

Anaemia remains the most common and serious complication associated with malaria infection. Severe anaemia occurs when the concentration of haemoglobin is less than 5 g/dL (60). Excessive burden of the plasmodial parasite leads to the invasion and rupture of the infected RBCs, resulting in severe haemolytic anaemia in the infected hosts (231). There are a few mechanisms attributable to the destruction and production of the RBCs including lysis of the infected and uninfected RBCs (214), splenic sequestration of RBCs (214, 216), dyserythropoiesis and bone marrow suppression (1) and also co-infections with bacteria (15).

Due to the invasion of plasmodial parasites, infected RBCs undergo several changes on their surface thereby reducing their membrane deformability, leading to rapid sequestration in the spleen (95). Apart from that, the uninfected RBCs are also destroyed via phagocytosis and cleared by the reticuloendhothelial system (RES) (144). The high level of *P. falciparum* erythrocyte-membrane proteins (PfEMP-1) in the plasma during the infection may adhere to the uninfected RBCs and remove them from the circulation via initiation of the antibody response or complement cascade (95). In humans, severe anaemia is caused by the high ratio of uninfected to infected RBC clearance in the ratio 12 to 1 (174). The anaemia may resolve with antimalarial therapy and blood transfusion (60, 249).

Dyserythropoiesis occurs when the bone marrow is unable to function accordingly due to immune response triggered by the host, resulting in low levels of reticulocytes, as seen during *P. falciparum* infection (211). The T_h1 cytokines such as IL-6, IFN-γ and TNF-α, other inflammatory mediators and parasite-derived hemozoin potentially suppress haematopoiesis, a biological process of producing the RBCs in the bone marrow. This exacerbates anaemia in the infected hosts (95). Recent findings show that IL-4, a T_h2 cytokine may also be responsible for the dyserythropoiesis (95). Co-infections with helminth or bacteria may extend the severity of malarial anaemia as well due to their activation of the immune system (98, 173).

1.4.2 Cerebral malaria (CM)

The cytoadhering mechanical blockage caused by the infected RBCs through sequestration in microvessels is reported to be involved in the pathogenesis of CM .The obstruction pertubs blood flow, causing hypoxia of the neurons and glial cells as well as haemorrhages. The accumulation of infected RBCs in the brain is shown to promote

chemotactic, inflammatory and toxic mediators that can further accelerate the microvascular obstruction through positive-feedback mechanism (113).

Monocytes potentially secrete coagulation factors that may contribute towards brain sequestration in CM patients (92), whereas neutrophils are found to trigger the release of pro-inflammatory cytokines such as TNF-α, IL-12, IL-18 and IFN-γ that are implicated in CM. As the neuthrophils deplete, downregulation of T_h1 cytokines is accompanied by reduction of the monocytes sequestration and microhaemorrhages in the brain, thus limiting the damage caused by CM as demonstrated in *in vivo* studies in mice infected with *P. berghei* (183) Excessive production of inflammatory cytokines aggravate the inflammation process giving rise to coma and seizures in CM (161). $CD8^+$T cells are involved as well by increasing the permeability of the blood-brain barrier through perforin-dependent mechanisms (212).

The malaria parasites also release soluble malarial toxin known as glycosylphosphatidylinositol (GPI) that triggers the production of TNF-α and IL-1 cytokines by macrophages (232). GPI alone or in combination with IFN-γ is capable of generating the inducible form of nitric oxide synthase (iNOS) and amplify the production of nitric oxide (NO) in the host tissues which is usually in low levels (190). Up-regulation of intracellular adhesion molecule-1 (ICAM-1) and vascular cell adhesion molecule-1 (VCAM-1) in the host cells is also implied the pathogenesis of CM (116).

1.4.3 Fever

Fever is the most common symptom observed during malaria infection. It is associated with vomiting, malaise, joint pain and to some extent convulsions which is common among children (198). The innate immune response has been recognised as the host's first-line of

defence against the parasite during the early stage of infection by inducing inflammation and fever (233). RBC rupture activates the macrophage system through antibody-dependant and independent phagocytosis (161). Upon invasion by the parasites, the infected host immune system recognises the parasitic deoxyribonucleic acid (DNA) via Toll-like receptor-9 (TLR-9) and subsequently induces fever. Engagement of TLRs is more likely to trigger the transcription of nuclear factor kappa-light-chain enhancer of activated B cells (NF-κB) in the nucleus to produce pro-inflammatory cytokines (205). The activation of inducible cyclooxygenase-2 (COX-2) may also increase the synthesis of prostaglandin, changing the set point of the host thermaregulatory centre and ultimately leading to fever (125).

Furthermore, the pathogenesis of malarial fever has been thought to arise from various pro-inflammatory cytokines released by parasite-induced host immune cells (207). As mentioned earlier, the release of GPI upon the rupture of RBCs is capable of inducing the production of TNF-α and IL-1 by the macrophages. The release of IL-1, a pyrexia-related cytokine may cause paroxysmal fever and chills (207). Several groups of researchers have acknowledged the importance of TNF-α in the pathogenesis of fever in malaria as they found a positive correlation between serum concentration of TNF-α and the degree of pyrexia during malaria (123). Apart from that, IFN-γ also possesses a pyrogenic property that mediates through the induction of IL-1 and TNF-α during the clinical paroxysms (7).

1.5 Malaria Chemotherapy and Drug Resistance

At present there is no effective malaria vaccine, and therefore chemotherapy remains the mainstay of malaria control by clearing the parasites from the infected host. To date

antimalarial drugs can be classified according to their chemical structures or biological activities i.e targeting specific stages in the life cycle or interruption of the specific cellular metabolic pathways in the malaria parasite. Summaries of the classification of the antimalarial drugs are shown in Table 1.1 and Table 1.2. The action of antimalarial drugs targeted on the specific subcellular organelles are illustrated in Figure 1.3.

The emergence of antimalarial drug resistance is arises from a combination of several factors such as host population, overuse of drugs for prophylaxis and incomplete therapeutic treatments of infected patients. This is might due to related to lack of the compliance of the drugs or usage of counterfeit drugs which are defective their stated doses. Resistance is also being associated with genetic alteration in the parasites therefore affected the drugs metabolic pathways in the parasite (187). The summary of the molecular basis of drug resistance in human malaria parasite *P. falciparum* is illustrated in appendix 1.

1.5.1 Quinine and its Derivatives

Quinine is the oldest antimalarial drug, used by the native population of Peru for centuries to treat fevers and chills. In 1944 the active alkaloid compound of quinine was successfully isolated from pulverised bark of the cinchona tree (115). The structure of the quinoline ring system is used to synthesise other quinoline derivatives such as 4-aminoquinolines as the example of chloroquine, the most used antimalarial in malaria endemic areas. Other drugs in this category include amodiaquine, primaquine, piperaquine and mefloquine. Halofantrine and lumefantrine (benflumetol) are two drugs which were chemically synthesised by manipulation of the quinoline portion of the 4-quinoline methanols and replacement with a different aromatic ring system to form ary amino alcohols (Figure 1.4) (187).

The mechanism of action of these antimalarial drugs is through the inhibition of the formation of crystallised hemozoin (malaria pigment) in the parasite digestive vacuole (DV). The development of malaria parasites in infected erythrocytes depends on the degradation of haemoglobin of the host cells as a source of nutrients. The degradation of haemoglobinproduced a large amount of free haem or ferriprotoporphyrin IX (FPPIX) in the parasite DV which is toxic to the parasites (76). In malaria parasites the FPPIX is oxidised and dimerised to beta hematin followed by crystalisation into hemozoin which is non-toxic to the parasite and accumulates in the DV (202). 4-Aminoquinolines and their derivatives bind to FPPIX in DV thus interfering with the detoxification of FPPIX (an eythrocytic haemoglobin by-product into hemozoin (59, 71). The toxic form of haem monomer is believed to generate oxidative radicals that in turn permeabilise the parasite membrane, ultimately leading to parasite killing (295).

Chloroquine was introduced as an antimalarial drug in 1943 and has been the main-stay for falciparum malaria treatment for many years before resistance being reported (6). Resistance emerged approximately 10 years after its introduction, along the Thai-Cambodian border in 1957, at the Colombia-Venezuela border in the 1959 and all sub-Saharan Africa 1980s (177). From genetic epidemiology the resistance to chloroquine spread from Southeast Asia to Africa in the late 1970s (177). The chloroquine resistance is associated with mutations in the transporter proteins which are located on the DV or the plasma membrane of the parasite (187). The major transporter proteins in the malaria parasite are PfCRT, PfMDR1 (PfPGH1), PfNHE1 and PfMRP1. The underlying mechanism(s) underpinning chloroquine resistance are not completely understood and several hypotheses have been presented. One hypothesis that has received support is the "Charge drug leak" model. This model states that

Table 1.1: Classification of the Major Antimalarial Drugs According to their Chemical structures

Drugs compound	Drugs
4-aminoquinolines	amodiaquine, naphthoquine, , piperaquine, chloroquine, Tert-butyl isoquine, hydroxchloroquine
8-aminoquinolines	primaquine, diethylprimaquine, bulaquine, tafenoquine
sulfonamides	sulfadoxine, sulfadiazine, sulfamethoxazole
Amino alcohols	lumefantrine, halofantrine, mefloquine,quinine
Antifolates	pyrimethamine, proguanil, dapsone, cycloguanil, chlorproguanil
Hydroxynapthaquinones	atovaquone
Antibiotics	trimethoprim, azithromycin, tetracycline, fosmidomycin, mirincamycin, doxycyclin, thiostrepton
Endeperoxide	artemisinin, artemether, artesunate, artemisone, dihdroartemisinin
others	riboflavin, pentamidine, cycloheximide, N-acetyl-D-penicillamine, deferoxamine, pyroaridine

Table 1.2: Classification of the Antimalarial Drugs According to the Different Stages in the Life Cycle of the Parasite

Developmental Stages	Drugs
Intraerythrocytic schizontocidal drugs	quinine, chloroquine, amodiaquine, mefloquine, halofantrine, pyronaridine, atovaquone, pyrimethamine, sulphadoxine, artimisinins, tetracycline, clindamycin tafenoquine, amodiaquine
Tissue schizontocidal drugs	primaquine, tafenoquine, proguanil, tetracycline, pyrimethamine
Gametocytocidal drugs	primaquine, tafenoquine, proguanil, tyetracycline, pyrimethamine.
Hypnozoitocidal drugs	primaquine
Sporonticidal drugs	proguanil, chloroguanidine, pyrimethamine, atovaquone

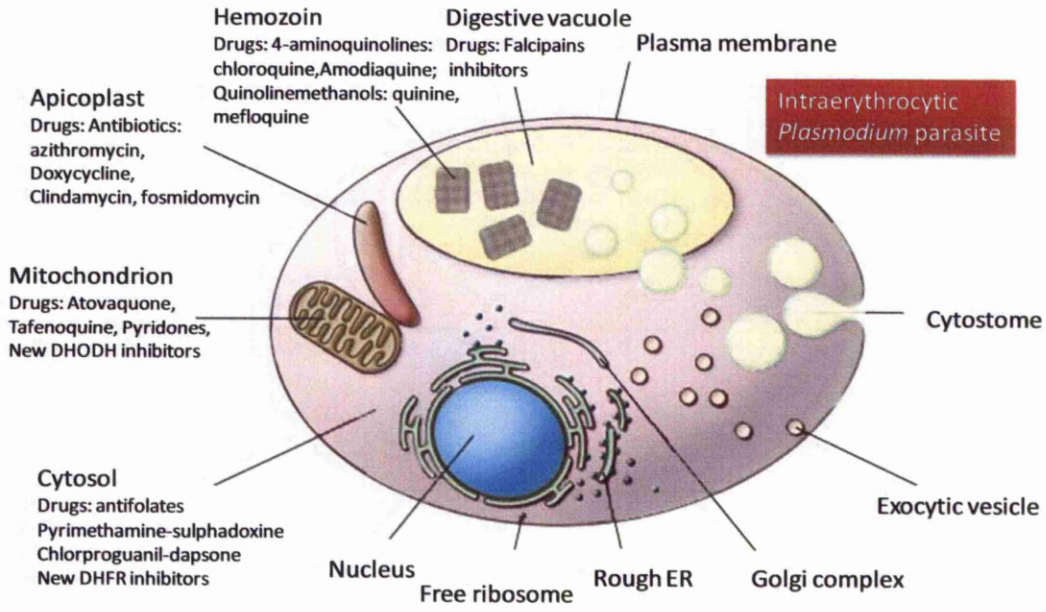

Figure 1.3: Illustrated Picture of Antimalarial Drugs Targeted at the Specific Subcellular Organelles

The 4-aminoquinolines (e.g chloroquine and amodiaquine), and the quinolinemethanols (e.g quinine and mefloquine) act inside the DV of the parasite. The falcipain inhibitors targeted to the cycteine proteases. Antibiotics e.g azithromycin, doxycycline and clindamycin act inside the apicoplast (plastid like organell) by inhibit protein translation. Atovaquone and selected compounds inhibit electron transport in *Plasmodium* mitochondrion. The antifolate drugs act by disrupting *de novo* biosynthesis of folate in cytosol. The action of artemisinin and its derivatives is still actively investigated. Adapted from Greenwood et al. (2008).

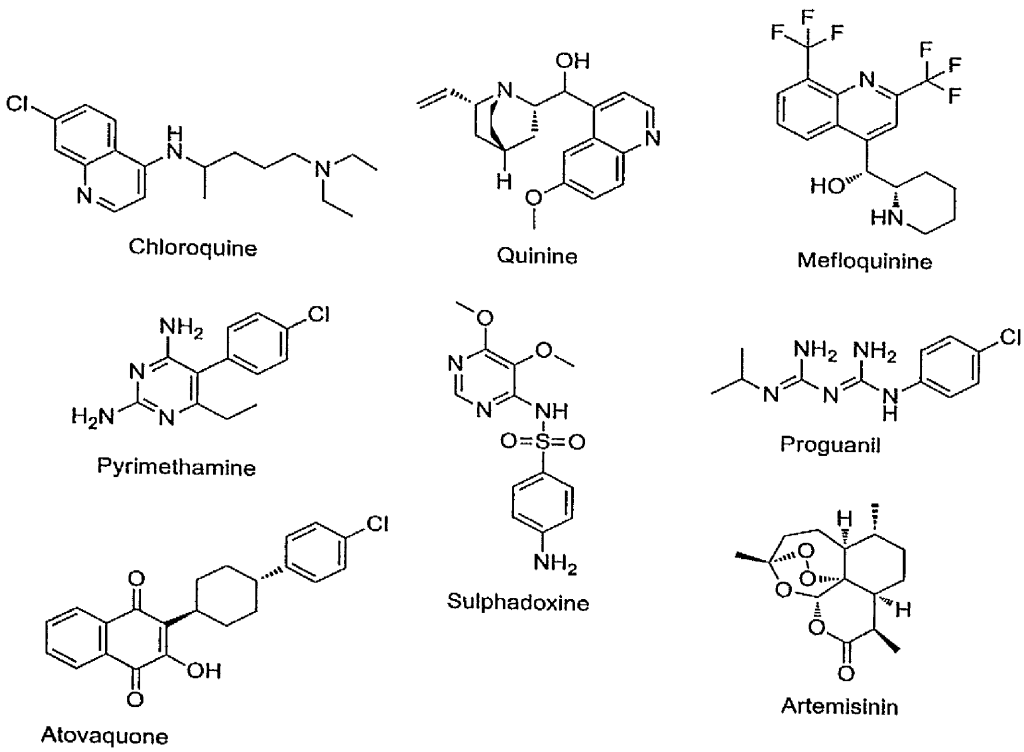

Figure 1.4: The Chemical Structures of Some Antimalarial Drugs

Chloroquine, quinine, and mefloquine are 4-substituted quinolines that interfere with haeme polymerization; sulfadoxine, pyrimethamine, and cycloguanil are substrate analogs that interfere with folate metabolism. In humans, proguanil is converted by CYP2C19 and CYP3A4 to form cycloguanil. Atovaquone acts through destabilisation of the malaria parasite cytochrome bc_1 complex, thus causing proton leakage at to occur at this site. Artemisinin is newer antimalarial with a novel molecular structure. Several mechanisms have been proposed e.g the activation of endoperoxides which bind to Fe^{2+} (haem) therefore generating oxygen radicals and inhibiting the sarco/endoplasmic reticulum Ca $^{2+}$-ATPase (SERCA).

mutations in PfCRT (principally the K76T) enables protonated chloroquine (CQ^{++}) to tranverse the DV membrane thereby reducing the DV chloroquine concentration (17, 187).

Mutations in *pfmdr1* are commonly associated with those in *pfcrt*. However the pattern of the mutation of *pfmdr1* is different based on geographical locality, for example South American mutant strains have mutations in amino acids S1034C, N1042D and D1246Y while the Southeast Asia and Africa counterpart is often associated with N86Y amino acid. (209). The relationship between *pfmdr* and *pfcrt* is not well understood, but is it hypothesised that *pfmdr* mutations are responsible for increasing chloroquine resistance (in K76T *pfcrt* parasites) to levels which result in clinical failure. This hypothesis is supported by evidence that shows that although the K76T *pfcrt* mutation is found in all chloroquine clinical failures, this mutation alone is not predictive of clinical failure.

1.5.2 Antifolate Drugs

Antifolate drugs can be classified into 2 groups: Class 1 and Class II. The Class I or sulfa group consists of sulfadoxine and dapsone. Sulfa drugs inhibit the dihydropteroate synthase enzyme (PfDHPS) activity of the bifunctional hydroxymethylpterin pyrophosphokinase (HPPK)-DHPS protein. DHPS is responsible for the *de novo* synthesis of folate coenzymes (187). Class II antifolate drugs are pyrimethamine and proguanil. Class II antifolate inhibit the dihydrofolate reductase (PfDHFR) activity of the bifunctional DHFR/thymidylate synthase enzyme (187). DHFR present in both parasite and human host is an essential enzyme for synthesis of the reduced form of folate (tetrahydrofolate). Tetrahydrofolate is involved in several metabolic pathways including one carbon transfer reactions and synthesis of DNA. Sulfadoxine-pyrimethamine (SDX-PYR) (SP;Fansidar^{TM}) was introduced as a combination therapy in 1970s to overcome the CQ resistance problem in

Africa (115). Antifolate combination therapy is currently used as intermittent preventive malaria treatment in pregnant women and infants in malaria endemic areas. SP is used as the drug of choice whenever the ACT (artemisinin combination therapy) supply is not available or in the poor countries where the cost of ACT is prohibitively expensive (181).

The rapid emergence of antifolate resistance is due to point mutations in both targeted enzymes (PfDHPS and PfDHFR). Partial pyrimethamine resistance is identified due to a point mutation at codon 108 of *pfdhfr* gene that changes serine to asparagines (101). The severity of the resistance is increased with further mutation at codons 51 (asparagines to isoleucine, N51I) and/or 59 (cysteine to arginine, C59R) (164). Another mutation at codon 161 (isoleucine to leucine, I164L) was detected among isolates from South America and Asian countries that cause triple mutation of the *pfdhfr* gene. Five mutations of the *pfdhps* gene at codons 436 (serine to alanine/phenylalanine, S436A/F; alanine to glycine, A437G; lysine to glutamic acid, K540E; alanine to glycine, A581G; alanine to serine or threonine, A613S/T) were identified to be associated with sulphadoxine drug resistance (259). Mutation at the 437 codon of *pfdhps* gene has been identified as a causative factor in the emergence of mutation at codons 581 and 613 for the SP resistance in *P. falciparum* isolated from patients in the African continent. Mutations at these codons are widely spread in South America and South East Asia, and are associated with high-level SP resistance (168). Another factor that contributes to the SP treatment failure is associated with *pfdhps* double mutant (A437G/K540E) and the *pfdhfr* triple mutant (S108N/N51I/C59R) from the pfdhfr/pfdhps quintuple mutant haplotype (141).

1.5.3 Artemisinins

Artemisinin (Qinghaosu; active compound) is an extract from the *Artemisia annua* (Chinese wormwood) and has been used as a herbal remedies for many centuries for many illnesses including malaria in China (277). The first clinical trial of artemisinin was conducted in China in 1975 and subsequently it was introduced as an antimalarial drug in 1979. This drug has low toxicity and high efficacy against all types of human malaria parasites including those resistant to conventional antimalarial treatment (154).

The chemical structure of the active qinhaosu is ilustartes in Figure 1.3. The artemisinin has a unique trioxane structure ($C_{15}H_{22}O_5$) with an endoperoxide bridge (C-O-O-C), lacking the nitrogen containing ring system which is found in most antimalarial drugs (172). However the setback of this compound is low solubility (57) as well as elimination half-life its short 0.5-1.4 h (22).

To improve the solubility of artemisinin, semi-synthetic artemisinin derivatives have been developed. These include: artemether, artesunate, dihydroartemisinin (DHA), artenimol, artemotil. These artemisinin derivaties are used widely and given in combination therapy (ACT) with other antimalarial drugs (17). Currently ACT is used mainly in the treatment of uncomplicated malaria (193). The combinations of artemisinin derivatives which are currently used as ACT include: artemether-lumefantrine (Coartem®) (most commonly applied worldwide), artesunate-sulfadoxine-pyrimethamine, dihydroartemisinin-piperaquine and artesunate-pyronaridine (278).

The mechanism of action of artemisinin and artemisinin derivatives is not fully elucidated and still debatable (65). It has been hypothesised that artemisinin activity is due to cleavage of the endoperoxide bridge and haem-iron degradation leading to a formation of reactive carbon radicals that alkylate essential biomolecules in the food vacuole of the parasite (209). The detail of the biochemical reaction of artemisinin was described by O'Neill et al., (2010). They concluded that the interaction of the drug is not only on heme degradation but also with free intracellular reduced iron species. This interaction thus activates the artemisin activitity to bind to macromolecules throughout the whole parasite(195). At the cellular level artemisinin was reported to interact with phospholipids and to cause oxidative membrane damage (99, 187).

Eckstein-Ludwig et al. (2003) reported that artemisinin inhibits PfATP6 (sarco/endoplasmic reticulum calcium-dependent ATPase SERCA). The inhibition of PfATP6 is said to lead to the disruption of Ca^{2+} homeostasis in the parasite. This has been supported by *in vitro* study in *X. laevis* oocytes that showed the activity of PfATP6 is inhibited by ART but is not affected by other antimalarial drugs (58). The exact location of PfATP6 is still not fully elucidated, however recent study showed the effect of artemisisnin is through the disruption of DV and not on the endoplasmic reticulum. Based on this finding they speculate that PfATP6 is located in the DV of the parasite (45).

Artemisinin resistance has not been documented until 2010 on the Thai-Cambodian border (52). However the direct evidence of the resistant mechanisms were not well understood. Results from the sequencing data did not show any correlation between artemisinin resistance and *pfcrt*, *pfmdr1* or *pfatp6* genes. Further studies have to be carried out to determine the genetic and biochemical bases of the artemisinin resistance mechanisms.

Nevertheless the worrying signs are that ACT clinical failures are on the increase in South East Asia.

1.5.4 Hydroxynaphthoquinones (Atovaquone) and the *P. falciparum* bc_1 Complex

Hydroxynaphthoquinone compounds have been identified to act as competitive inhibitors of ubiquinone (CoQ) since then 1940s. However, these compounds showed poor bioavailability, lack of metabolic stability and high plasma protein binding (14). Exploration of this class of compound was carried out by Wellcome Laboratories UK in the 1980's. The study conducted by Fry and Pudney developed a hydroxynaphthoquinoe recognised as (2-[*trans*-4-(4'-chlorophenyl)cyclohexyl]-3-hydroxy-1,4-napthoquinone), known commonly as atovaquone, which targets the mitochondrial cytochrome bc_1 complex in *Plasmodium* parasites (79).

To minimise atovaquone resistance/clinical failure, this drug is given in combination with proguanil (antifolate drug). An *in vitro* study showed proguanil as having a synergistic effect when given with atovaquone (130). Combination of atovaquone-proguanil was introduced in Europe in the mid 1990s and in 2000 it was recognised as antimalarial drug by the U.S Food and Drug Administration (FDA). The combination atovaquone-proguanil when given in a fixed dose tablet drug combination (Malarone®) produced a 97% curative rate compare to 67% when atovaquone was given as monotherapy (158). However, due to the high cost of production this drug is used mainly as chemoprophylaxis for travellers visiting malaria endemic areas (130).

Atovaquone is a lipophilic hydroxynaphthoquinoe and can be regarded as a structural analogue to coenzyme ubiquinone (CoQ). Atovaquone has been used in the treatment of infections by apicomplexan parasites *Plasmodium spp.*, *Toxoplasma gondii, Thieleria spp.* and *Babesia spp.* (246). It is suitable for the treatment of multidrug resistant parasites (245, 264). However when used as a monotherapy it has been shown to give rise to an unacceptable high recrudescence rate of ~30% (157).

1.5.4.1 Mechanism of Action

Studies on atovaquone have shown that this compound binds to cytochrome *b* in the bc_1 complex of the inner mitochondrial membrane of the malaria parasite. The cytochrome bc_1 complex (also known as Complex III) is responsible for the electron transfer from ubiquinol to cytochrome *c*. The electron transport is linked to the translocation of protons across the inner mitochondrial membrane, resulting in the generation of a membrane potential, a key feature of an active mitochondrion (14).

Atovaquone acts by selectively inhibiting the mitochondrial electron transport in parasite mitochondria without affecting human mitochondrial functions. Atovaquone binds to the quinol oxidation site of cytochrome *b* known as the Q_o, at a site, close to the conserved PEWY region, which itself is located close to the iron-sulphur binding region of the hinge protein. Binding at this site inhibits catalytic turnover of the enzyme, resulting in the depolarisation of the mitochondria and a loss of mitochondrial function, which includes disruption of pyrimidine biosynthesis, specifically by the loss of activity of dihydroorate dehydrogenase (DHODH) (130, 203, 208).

Various studies have been conducted to determine the molecular mechanism of atovaquone on the cytochrome bc_1 complex. The most extensive studies have been carried out using the yeast model *Saccharomyces cerevisiae* (reviewed in (14, 130). Studies using Electron Paramagnetic Resonance (EPR) spectroscopy show that yeast cytochrome bc_1 complex demonstrate the formation of a hydrogen bond between the hydroxyl group on napthoquinone ring of atovaquone and His181 of the mobile Rieske iron sulphur protein located proximal to cytochrome *b* (14, 130). The hydroxyl group of the hydroxydioxobenzothiazole is ionised when the inhibitor is bound to the Q_o site. The second hydrogen bond is formed at the carbonyl group at the position 4 on the quinone ring via a water molecule with Glu-272 of cyt *b* to stabilise the structure. As a result of these interactions, atovaquone binding to the Rieske protein near cytochrome *b* has the effect of lowering the midpoint potential of the Rieske protein cluster (130). The molecular model of atovaquone interaction with *S. cerevisae* bc_1 complex is illustrated in Figure 1.5.

As described earlier, atovaquone is given in combination with proguanil, an antifolate, to curb the rapid acquisition of resistance to atovaquone. Proguanil inhibits dihydrofolate reductase (DHFR) via its metabolite cycloguanil. However the combination of cycloguanilwith atovaquone fails to produce a synergistic effect (203). It is suggested that proguanil acts by inhibiting the mitochondrial phosphate transporter and thereby synergises with the inhibitory activity of atovaquone (Painter et al., 2007). However there is no data at present to support this hypothesis and it should be added that no *in vivo* synergy between proguanil and atovaquone has been reported and this may therefore be a red herring as in most people proguanil is rapidly metabolised to cycloguanil.

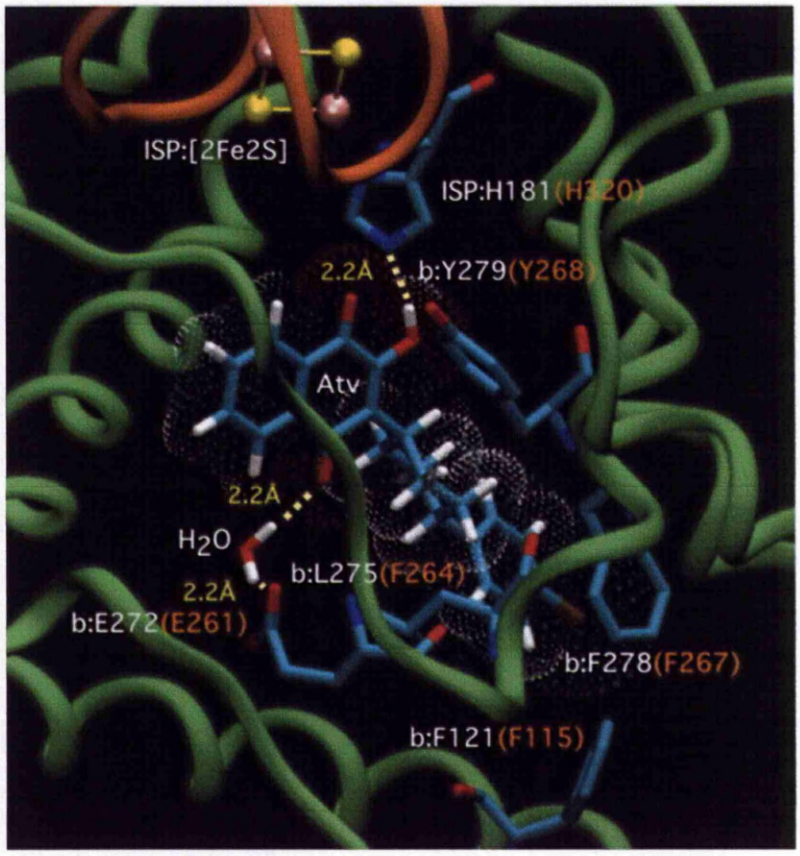

Figure 1.5: Diagram of the Interactions of Atovaquone with the Yeast bc_1 Q_o Site

Molecular model of atovaquone (Atv) docked into the Q_o site of yeast cytochrome bc1 complex (3CX5.PDB), showing hydrogen bonding to Rieske protein residue His181 and cytochrome b residue Glu272 (via bridging water molecule). Yeast residues are labelled in white, with the corresponding *P. falciparum* residues labelled in orange. The cytochrome b polypeptide backbone is represented in green, with the Rieske protein backbone in brown. The [2Fe2S] cluster of the Rieske protein is represented in CPK form (sulphur: yellow, iron: pink). Hydrogen bonds are indicated by yellow dotted lines. A 1.4 Å-radius CPK dotted surface has been added around the docked atovaquone molecule to aid visual clarity. The side chain of H181 is shown in the imidazolate conformation, although it has not been established which group contributes the hydrogen atom in the putative hydrogen bond between this residue and the (ionisable) naphthoquinone hydroxyl of atovaquone. Adapted from Fisher et al. (2012).

1.5.4.2 Atovaquone Resistance Mechanisms in *Plasmodium falciparum*

As mentioned, atovaquone is extremely potent against *P. falciprarum* malaria, however when use as a monotherapy it causes an unacceptable level of drug failure due to parasite resistance (14, 35, 130). The sequencing data obtain from resistant parasites shows the presence of point mutations spanning the codons 271-284 at the site of ubiquinol oxidation site (Q_o) of the bc_1 complegene (235). This region consists of 13 amino acids within the e-f helix to transmembrane helix F1 of the cytochrome *b* which contains a universal PEWY sequence (245). The most common mutation is detected at amino acid position 268 where tyrosine is replaced with serine (Y268S). The Y268 amino acid is highly conserved across the apicomplexa phylum (14). Polymorphisms also detected at the 268 codon are Y268N or Y268C, however both mutations are rarely reported (3).

In the malaria parasite, cytochrome *b* is encoded by the mitochondrial DNA (mtDNA) (3, 84). The polymorphism of the gene encoded by mtDNA is reported in mammals to exhibit 10 x higher mutation rate than nuclear DNA (3, 36). The mechanisms of the polymorphisms might due to due to spontaneous base substitution or insertions which accumulated the time and also due to the multi-copy nature of the mitochondrial cytochrome *b* gene (62). Cytochrome *b* is highly exposed to ROS which are produced in Complex III mitochondria and also possibly due to poor proof reading by the mitochondrial DNA polymerase (186, 217). Study in malaria parasites showed a rapid mutation rate (10^5) of *Pfcytb* (84), but the recent study showed the rate was lowered by 100-1000 times (3, 135).

1.5.4.3 Mechanisms of Atovaquone Binding in the Yeast Model

The *S. cerevisae* yeast model has been used to elucidate the resistance mechanisms in *P. falciparum* bc_1 complex. *S. cerevisae* is easily grown and the crystal structure of the bc_1 complex is available thus facilitating the study of *P. falciparum* mutations (68, 114). Mutations in yeast bc_1 complex can be directly introduced through transformation therefore the expressed mutated protein can be purified and crystallised to get the structure of the protein.

The mutation of Y268S in *P. falciarum* was introduced into yeast bc_1 genome resulted a mutation at amino acid residues Y279S of *S. cerevisae*. This mutation of Y279S is also located in e-f helix component of the Q_o site (269-295) which consists of PEWY (68, 130). The atovaquone inhibition study was conducted and showed that the mutation is responsible for alteration of atovaquone binding to bc_1 complex of mutated yeast (68, 130). The IC_{50} value of the mutated yeast was 4000 nM compared to the sensitive strain. The study on the steady state turnover of the bc_1 complex showed the mutant yeast has a slower rate (decreased 30%) compared to the wild type strain (14, 68, 130).

1.6 Vaccines for Malaria

For a long time development of malaria vaccines has been dependent on the study of parasite surface antigens and on the discovery of potential target antigens recognised by the sera of immune adults. The target of malaria vaccines generally followed three strategies of immunisation, namely pre-erythrocytic liver stage, the blood stage or the sexual stage (transmission-blocking vaccines). Pre-erythrocytic stage vaccine consists of antigens or antigen subunits produced on the surface of sporozoites and/or the stage of the parasite. This

vaccine targets the *Plasmodium* sporozoite thus preventing invasion of the host hepatocytes and finally eliminates the parasites from the infected individuals. The blood stage or asexual vaccine is targets the merozoite preventing their invasion of RBCs and eventually prevent the clinical manifestations of malaria infections. Transmission blocking vaccines are specifically designed to break transmission target molecules that are unique to gametocytes or to subsequent mosquito stages(257).

1.6.1 Pre-erythrocytic Vaccines

The circumsporozoite protein (CSP) contains a central repeat region containing 37 repeats of the amino acids sequence asparagines-alanine-asparagine-proline (NANP) and flanked on each side by non-repetitive regions containing T cell epitopes. The central repeat region is encoded by the immunodominant surface antigen on the sporozoite of the human malaria parasite *P. falciparum* (46, 257). It has been demonstrated that the antibody response in malaria infected humans is elicited against the central region of CSP. The mechanism of action of the CSP antibody against this region is by sloughing off the protein coat, therefore blocking the invasion into the hepatocytes (10). Several clinical trials have been conducted using either a synthetic peptide or a recombinant protein containing multiple copies of *P. falciparum* CSP B-cell epitopes. Results from these trials showed that the vaccines only conferred partial immunity, with low antibody titres against sporozoites in the vaccinated groups (10). At the later stage, more advanced adjuvants and carrier protein systems are introduced and incorporated into the vaccine formulation. Use of the adjuvant system improves the immunogenicity of CSP based vaccine. With the advent of molecular biology technique, the recombinant CSP based vaccine was created and recognised as RTS,S vaccine. RTS,S vaccine is a recombinant protein composed of amino acids 207 to 395 of the central repeat region (R) and T cell epitopes (T) of *P. falciparum* CSP fused with a 226-amino acid

polypeptide chain of the hepatitis B surface antigen (S) as a carrier matrix (225). The recombinant constructs then was co-expressed in *S. cerevisiae* (S) which assembles it into antigenic particles. The RTS,S vaccine formulation consists of the liposomal based Adjuvant System AS01 or AS02 which contains the immunostimulants monophosphoryl lipid A and QS21 (saponin derivative extracted from the bark of the *Quillaja saponica* tree). Subsequently, the efficacy of RTS/S recombinant vaccine had shown progressive improvements resulting in improved efficacy in vaccinated and challenge groups (26, 91). To date, in November 2011, London-based GlaxoSmithKline (GSK) released the recent clinical data from phase 3 clinical trials of RTS,S (Mosquirix) vaccine. The clinical Phase 3 results showed that RTS,S caused 54% reduction in clinical malaria cases and 47% reduction in severe malaria (4). The Phase 3 clinical study showed that the RTS,S vaccine is highly safe with tolerability profiles. The protective immunity conferred by RTS,S vaccine lasts up to 4 years and interestingly no evidence of a post-immunisation "rebound" has been detected among the vaccinated group (257).

1.6.2 Blood Stage Vaccines (Asexual Erythrocytic Stage)

The asexual erythrocytic stage of the malaria parasite's life cycle begins with the release of merozoites from infected hepatocytes. This is followed by rapid invasion of RBCs and further intraerythrocytic development stages leading to the rupture of merozoites from the parasitized RBCs. The released merozoites then re-infect new RBCs or differentiate into the sexual stages of the parasite. Clinical outcomes caused by *Plasmodium* occur mainly during the erythrocytic stage of the parasite's life cycle. Most erythrocytic stage vaccine candidates are developed based on antigens that coat the surface of the invasive parasites. The immune

response generated against the erythrocytic stages is primarily antibody mediated with the added support of $CD4^+$ T-cell activity and cytokine production (86).

The first merozoite surface protein rigourously studied is PfMSP1. This antigen is believed as the best candidate of many proteins expressed on the merozoite surface and being targeted for vaccine development. The vaccine formulation is similar to the RTS,S vaccine using the hepatitis B surface antigen as a carrier matrix. Several clinical trials were done to evaluate the efficacy of the vaccine in immunised people in the malaria endemic areas. Results from the clinical trial data show that MSP1 vaccine enables to produce antibodies in adult exposed to *P. falciparum* but it had no protective efficacy against clinical malaria in children (197). The drawback of the MSP1 antigen is the extensive genetic diversity that may contribute to the lack of efficacy of the vaccine (257).

The apical membrane antigen 1 (AMA-1) is another candidate for the development of erythrocytic stage vaccine. The AMA-1 resides in the apical complex of the merozoite (210) and plays a vital role in the success of RBC invasion by merozoites (178). The AMA-1 antigens are among the most higly conserved proteins in apicomplexan groups (21). The AMA-1 has 62 polymorpic amino acids, representing more than 15% of the amino acid sites and distributed over three domains of AMA-1 protein (253). The greatest polymorphism is detected in domain I amino acids cluster that plays a vital role in RBC invasion.and is located near to a hydrophobic pocket of the AMA-1 protein (9). An *in vitro* study showed that antibodies against AMA-1 antigen are naturally acquired and confer protection of RBCs from the invasion by merozoites (106). Two AMA-1 based vaccines are already at the stage of efficacy trials in humans. The first one is the bivalent AMA-1 recombinant vaccine that is based on 3D7 and FVO *P. falciparum* strains. This vaccine was expressed in *Pichia pastoris*

and adjuvanated with aluminium hydroxide developed by the Malaria Vaccine Development Branch of the National Institute for Allergy and Infectious Disease of the U.S National Institute of Health. A phase II clinical trial of this vaccine was carried out in adults and children in Mali although the results were unsatisfactory (226). The second one is a monovalent AMA-1 formulated vaccine using RTS,S adjuvant systems (AS01 and ASO2). This vaccine showed highly immunogenic responses when tested in a similar population (256). However, higher degrees of polymorphism in coding regions were observed (253) therefore may limits its success as a vaccine candidate.

The PfEMP1 is another candidate for erythrocyte stage vaccines. PfEMP1 is encoded by the *var* multigene family (243) and transported to the surface of infected RBC. An *in vivo* study using severe model of malaria showed that the PfEMP1 recombinant vaccine constructed in Semliki forest virus (SFV) prevents the sequestration of *Plasmodium* parasite infected RBCs in mouse (33). Another study in *E.coli* host system using PfEMP1 variant (ITvar9/R29var1) also produced antibodies against the recombinant antigen of PfEMP1(87). Even though this vaccine had shown promising results, the designing of this vaccine is not straight forward due to a large genetic variation of the *var* gene. Designing vaccine using PfEMP1 conserved epitopes that are highly immunogenic is perhaps a better approach to address this problem.

One of the latest development in malaria erythrocyte vaccine is published by a group of scientists from Oxford's Jenner Institute, UK and the Kenyan Medical Research Institute using the *P. falciparum* reticulocyte binding protein homologue 5 (PfRH5). PfRH5 is expressed as a 63 kDa protein and localised at the apical end of the merozoite. The PfRH family consisting of six genes (*PfRH1*, *PfRH2a*, *PfRH2b*, *PfRH3*, *PfRH4* and *PfRH5*) play an

important role in ligand-receptor interaction (55) except *PfRH3* (255). Doughlas et al. (2011) are using the full-lenght of *P. falciparum PfRH5* gene and cloned into replication–deficient adenovirus human serotype 5 (AdHU5) which is one of the most promising result in malaria vaccine develpoment. The vaccination trial was carried out in animal models and showed that the PfRH5 was able to induce IgG antibodies, which are recognised by native malaria parasites. The enzyme-linked immunosorbent assay (ELISA) also demonstrated that the recombinant PfRH5 vaccine produced a high level of antibody titres (10, 000 units/ml serum). The authors also indicate that the anti-PfRH5 IgG antibodies were more effective than antibodies produced by PfAMA1 and PfMSP1 antigens when tested against *P. falciparum* 3D7 parasites (53).

1.6.3 Transmission-Blocking (TB) Vaccines

TBV are designed to induce an immune response in the human host that are capable of blocking the parasite's growth in the mosquito host. This is a novel and promising approach in malaria vaccine development for avoiding selection pressure within the host that favours "vaccine resistant" parasite (51). Pfs25 and Pvs25 are two leading TB vaccine candidates. Both proteins are expressed on the surface of ookinetes in the mosquito stages of *P. falciparum* and *P. vivax* respectively. Data from animal studies showed that both antigens are able to induce strong transmission blocking activity (179). However, an early clinical trial showed that the anti-Pfs25 antibodies were detected but had marginal activity in blocking the transmission (124). Meanwhile, other human trials using recombinant Pvs25 were able to inhibit parasite development in mosquitoes but the levels of protection were too low for an effective vaccine (162).

1.6.4 Multi-stage, Multi Antigens Vaccines

Malaria parasites have a complex life cycle and bigger genome size than bacteria or viruses. Ideally, a multiantigenic approach is the best approach to stimulate immune responses thus conferring protection from malaria. The NYVAC-Pf7 and SPf66 are the two *Plasmodium* vaccine candidates in the development of multi-stage vaccine for malaria.

The NYVAC-Pf7 vaccine is a genetically engineered, multistage, multiantigenic and highly attenuated vaccinia virus consisting of seven *P. falciparum* genes (43). Clinical phase I and II trials showed that the NYVAC-Pf7 was safe and well tolerated in all vaccinated volunteers; however, the immune responses observed were variable.

The SPf66 vaccine was the first multiangtigen vaccine to undergo extensive field studies. This vaccine comprises a synthetic "hybrid construct" containing amino acid sequences of MSP1 antigen linked by the central repeat of the pre-erythrocytic antigen (206). The results from various clinical trials conducted in Asia and Africa showed that the vaccine did not produce significant protective efficacy (254). Attempts to develop DNA based vaccine (142) and recombinant vaccinia viruses (196) were also unsuccessful.

1.6.5 Attenuated Whole-Organism Vaccines

A purified, radiation-attenuated, metabolically active and non-replicating sporozoite vaccine (PfSPZ) was manufactured from aseptically raised mosquitoes (108). This vaccine conferred 90% protective efficacy when delivered by bites of at least 1,000 irradiated mosquitoes. Nevertheless, this vaccine did not have significant protective efficacy when administered by intradermal or subcutaneous routes (61). A study in monkeys showed that the

vaccine produced highly protective efficacy when administered intravenously (61). To date, the attenuated whole parasite vaccines have received significant attention by a number of research groups around the globe due to the promising vaccination results shown in monkeys (167). On the other hand, development of attenuated whole organism vaccines is hampered by inadequate quantities of sterile, metabolically active and non-replicating sporozoites that are safe, well tolerated and immunogenic in human. The next obstacle is the method of delivery as the size of the PFZ measures 0.5-1.0 μm x 7-10 μm, in order to confer more than 85% protection.

1.7 The Apicoplast of Malaria Parasite

The apicoplast is a plastid-related organelle that present in almost all parasites of the apicomplexan group i.e *Plasmodium*, *Toxoplasma*, *Crytosporidium*, *Eimireia*, *Babesia* and *Thileria* spps. This is a single non-photosynthetic plastid eukaryotic cell that was acquired by the secondary endosymbiosis of plastid containing red alga (170). Therefore, this organelle is surrounded by three or four membranes. Except for Cryptosporidium which loses the apicoplast over time, this plastid organelle is maintained in the rest of the apicomplexan parasites although it is no longer involved in photosynthesis (111, 192). During the intraeythrocytic stages, the apicoplast closely resembles the *Plasmodium* mitochondrion (248, 269). Like the *Plasmodium* mitochondrion, the apicoplast is structurally elongated and branches out during schizogony. This has been supported by the electron micrographs that revealed a 'spherical body' of apicoplast closely associated with the single mitochondrion of *Plasmodium* parasites (192). At the later stage of schizogony, the branched apicoplast continuously divides, so that each newly formed merozoite carries a new apicoplast in their cytoplasm (268).

The *P. falciparum* apicoplast posseses a circular ~35-kb genome, high number of A+T content and completely lacks any genes related to photosynthesis. As a result of the establishment of the endosymbiont, majority of the apicoplast genes are transferred into the parasite nucleus (165). Therefore, majority of the genes are encoded by nuclear genes and only less than 50 proteins are encoded by the apicoplast genome both of which produce gene products targeted into the organelles (169). The *P. falciparum* genome revealed approximately 10% of the nucleus encoded proteins likely to be targeted to the apicoplast (82). Data from pharmacological and genetic studies in *Toxoplasma* and *Plasmodium* have consistently demonstrated that the apicoplast is essential for parasite growth (191).

Studies by (Ralph et al., 2004, Seeber and Soldadi-Favre, 2010) showed that the apicoplast is involved in the biosynthetic pathways for fatty acids, isoprenoids, iron sulphur cluster assembly and segment of the haem pathways. In the photosynthetic algae these metabolites are generated by chloroplast through the photosynthesis pathway. Since the photosynthesis is abandoned in apicomplexans group, the energy for metabolites generation is carried out in the parasite cytoplasm (155, 236). Several studies have shown that several antibiotics can inhibit the apicoplast DNA replication, transcription and translation therefore leading to death of the parasites (44, 90). Some antibiotics namely ciprofloxacin, rifampicin and thiostrepton can cause an immediate effect whereas tetracycline and clindamycin result in the delayed death of the parasites (44, 90). To date, some of these antibiotics are currently used in combination therapies for malaria.

The biosynthetic pathways for fatty acids and isoprenoid precursors appears to be the only *de novo* synthesis machine for malaria parasites and differs from the other mammalian cells (82, 251). Like in bacteria and plants, fatty acid biosynthesis in *Plasmodium* parasites is

via type II fatty acid synthesis (FAS II) pathway, which consists of single enzymes acting in concert to catalyse the condensation, dehydration and reduction reactions (219).

Type I fatty acid biosynthesis pathway in eukaryotic cells consists of fatty acid synthase which contains all enzymatic reactions sites important for fatty acid synthesis. However, not all apicomplexan parasites have retained the type II FAS synthesis pathway. For example in *Crytosporidium* spp.the fatty acid synthesis is performed via type I FAS pathway. Meanwhile in the apicomplexan parasites *T. gondii* and *Eimeria tenella* have both types (FAS I and II) of fatty acid synthesis pathways (271, 296).

In FAS II pathway, acetyl-CoA is required in the first step of the pathway, and is provided by the pyruvate dehydrogenase complex (PDH) within the apicoplast (75, 171). Acetyl-CoA is carboxylated by acetyl-CoA carboxylase to form manoyl-CoA which is the committing step in the fatty acid biosynthesis. In malaria parasite, type II fatty acid synthesis is only essential for malaria parasite at late liver cell development. An i*n vitro* study showed that the *Plasmodium* FAS was inhibited by antimicrobial drugs thiolactomycin and triclosan. Thiolactomycin is an inhibitor of the condensing enzymes FaB (β-ketoacyl-ACP synthase I), FabF (β-ketoacyl-ACP synthase II) and FabH (β-ketoacyl-ACP synthase III) (274) and triclosan acts on FabI (enoyl-ACP reductase) activity in FAS II pathway (251). Triclosan also produced positive results in parasitic clearance of mice infected with the rodent malaria parasites *P. berghei* (251).

Another important biosynthetic pathway in apicoplast of the *Plasmodium* parasites is the non-mevalonate dependent isoprenoid biosynthesis. Isoprenoids is derived from a simple

five-carbon precursor isopentenyl pyrophosphate (IPP) and its isomeric form dimethylallyl pyrophosphate (DMAPP). The IPP is synthesised in 2 different pathways: i. using intermediate mevalonate e.g in animals and fungi, ii. 1-deoxy-D-xylulose-5-phosphate (DOXP) pathway e.g in apicomplexan parasites, bacteria and plants. *In vitro* and *in vivo* studies showed that the antibiotic fosmidomycin inhibits the DOXP reductoisomerase thus killing the parasites (189, 281).

The *Plasmodium* apicoplast is also involved in haem synthesis. Haem is an essential prosthetic group of cytochromes and is involved in oxygen and electron transport in the *Plasmodium* mitochondria. *Plasmodium* parasites generate haem through DOXP pathway and also from digested haemoglobin of host cells (250). Haem synthesis in *Plasmodium* parasites involves a number of enzymatic reactions which take place in different cellular compartments i.e in the apicoplast, mitochondrion and possibly the cytosol (219). The first step in the reaction is the synthesis of δ-aminolevulinate from glycine and succinyl-CoA. This process is catalysed by δ-aminolevulinate synthase which is located in the mitochondrion (228, 270). The subsequent reactions are carried out by enzymes located in the apicoplast (228, 269). This haem synthesis is completed using three enzymes namely HemF (coproporphyrinogen oxidase), HemG (protoporhyrinogen oxidase) and HemH (ferrochelatase). The HemH contains N-terminal targeting peptides thus suggesting these enzymes are located in the *Plasmodium* mitochondria (219). On the contrary, HemG does not possess an obvious N-terminal targeting peptide, suggesting that this protein is located in the *Plasmodium* cytosol. However, the prediction of *Plasmodium* HemF location is difficult because it contains several introns at the N-terminus (219).

1.8 Mitochondria: Background

In eukaryotic organisms mitochondria are involved in cellular respiration via 5 major complexes namely Complex I, Complex II, Complex III, Complex IV and Complex V (Figure 1.6) embedded in the inner mitochondrial membrane which lead the generation of ATP as an energy source (54, 221). This bioenergetic process starts after glucose is broken down through the glycolytic pathway in the cytosol. The breakdown of glucose produces pyruvate which is the end product of the glycolysis. Glucose is then converted into acetyl CoA by decarboxylation and enters the TCA cycle in the mitochondrial matrix producing CO_2 as a bi-product as well as many intermediates required for amino acid and fatty acid biosynthesis. During the TCA cycle, electrons are released from NADH or $FADH_2$ to ubiquinone to supply the mitochondrial respiratory chain. The movement of electrons in the respiratory chain thus initiates the membrane electrochemical gradient where protons are translocated in and out from the mitochondrial matrix and finally ATP is generated via ATP hydrolysis by plasma membrane ATPase (Complex V).

1.8.1 The Mitochondrial Genome

The linerised form of the 6-kb malaria parasite mitochondrial DNA (mtDNA) is the smallest genome among the eukaryotic cells. The parasite mtDNA contains 30-100 copies of the genome which encode only three subunits belonging to the mitochondrial electron transport chain (mtETC): subunits 1 and III of cytochrome c oxidase (cox I and cox IV of Complex IV), a cytochrome b subunit of ubiquinol-cytochrome c reductase (Complex III) and fragmented ribosomal RNA genes (62, 139, 263).

MtDNA is T-rich and highly conserved among apicomplexan phylogeny (63, 121). The transcription of the mtDNA is highly active during the late trophozoite and early schizont compare to the ring stage (139). To date, there is not so much information related to the mtDNA during gametogenesis and in the life cycle of the parasites in the mosquito host.

1.8.2 Malaria Parasite Bioenergertics: Glycolysis, the TCA cycle and Mitochondrial Electron Transport

1.8.2.1 Glycolysis

Blood-stage malaria parasites rely mainly on glycolysis for energy generation. Glucose from the plasma enters into the *Plasmodium* cytoplasm and is subsequently degraded to lactate via the anaerobic Embden-Meyerhoff-Parnas (EMP) pathway. Studies by Roth Jr et al. (1988) showed that infected RBC use 100 fold more glucose (mainly during trophozoite and schizont stages) than non-infected erythrocytes. Glucose is used in *Plasmodium* metabolic pathways for nucleic acid biosynthesis, amino acid biosynthesis the TCA cycle and lipid biogenesis. 60-70% of the glucose consumed by *P. falciparum* is incompletely oxidised to lactic acid and only a small amount of glucose is oxidised to form CO_2 and ATP (199). A number of studies have shown that the twelve glycolytic enzymes in *Plasmodium* are highly conserved and tightly co-regulated throughout the intraerythrocytic life cycle (25, 82). The glycolytic pathway in *Plasmodium* is illustrated in Figure 1.7. Plasma glucose is arried into the parasite by the hexose transporter located on the surface of infected RBC. The level of hexokinase expression is reported higher during active infection (133, 240) therefore also increases substrate entry into the parasite penthose phosphate pathway.

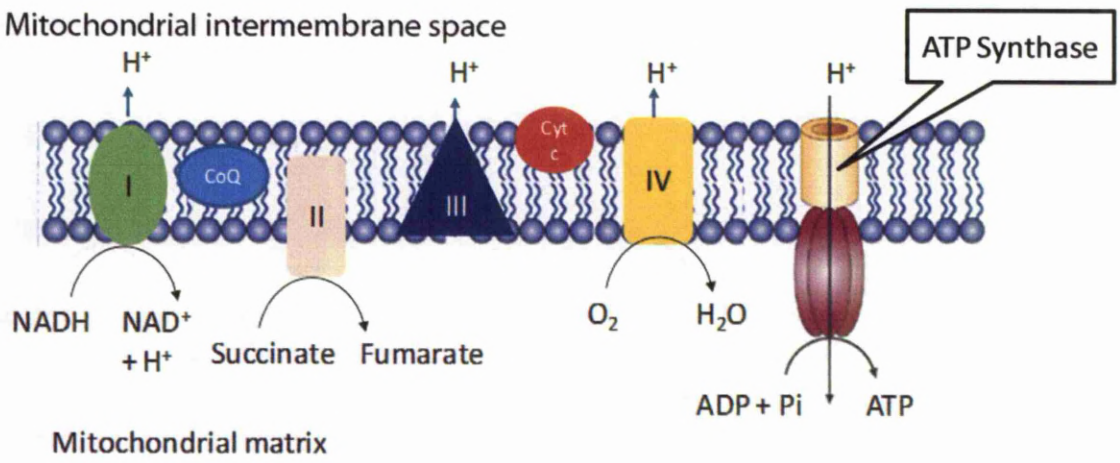

Figure 1.6: The Mammalian Mitochondrial Respiratory Complex

The respiratory complex of the mammalian mitochondrial dehydrogenases consists of Complex I (NADH dehydrogenase), Complex II (succinate dehydrogenase), Complex III (bc_1 complex) Complex IV (cytochrome oxidase) and Complex V (ATPase). The ubiquinone and cytochrome c are 2 mobile electron carriers in the inner mitochondrial membrane. The electrons pass via complex I and II and are accepted by ubiquinone resulting in the generation of ubiquinol. Ubiquinol is net oxidised by the bc_1 complex (III) which in turn reduces cytochrome *c*. Finally cytochrome *c* is oxidised by O_2, the terminal electron acceptor. Electron flow through these complexes is coupled with translocation of protons from the matrix into the intermembrane space thereby generating an electrochemical gradient which in turn is used to generate ATP via complex V (ATP synthase).

Glucose-6-phosphate isomerase (GPI) catalyses the conversion of glucose-6-phosphate to fructose-6-phosphate. Phosphofructokinase (PFK) catalyses the formation fructose-1,6-bisphosphate from fructose-6-phosphate. Fructose-1,6-biphosphate is cleaved to form two different triose phosphates glyceraldehyde-3-phosphate (G-3-P) and dihydroxyacetone phosphate (DHAP) using the aldolase enzyme. Only glyceraldehyde-3-phosphate is oxidised to form 1,3-bisphosphoglycerate (1,3-DPG) by glyceraldehyde-3-phosphate dehydrogenase (GAPDH). DHAP is converted to form G-3-P using triose phosphate isomerase (TPI) thus re-entering the glycolytic pathway.

The following steps in the glycolytic pathway are recognised as a source of ATP production in malaria parasite. These enzymes' subunits are described in the *Plasmodium* genome database (82). The phosphoryl group of 1,3-DPG is phosphorylated to form 3-phosphoglycerate (3-P-glycerate) by phosphoglycerate kinase (PGK) and 2 molecules of ATP are generated at this stage. 3-P-glycerate is converted to 2-phosphoglycerate (2-P-glycerate) by phosphoglycerate mutase. This is followed by the conversion of 3-P-glycerate to phosphoenolpyruvate (PEP) catalysed by enolase enzyme. Eventually, PEP transfers its phosphoryl group to ADP thus generating 2 molecule of ATP. This reaction is catalysed by pyruvate kinase (PK).

In eukaryotic cells pyruvate is oxidised by mitochondrial pyruvate dehydrogenase (PDH). PDH has been recognised as an essential enzyme responsible for connecting the glycolytic pathway and TCA cycle and catalyses the conversion of pyruvate to acetyl-CoA in the mitochondrial matrix. However in malaria parasites the PDH enzyme is not expressed as

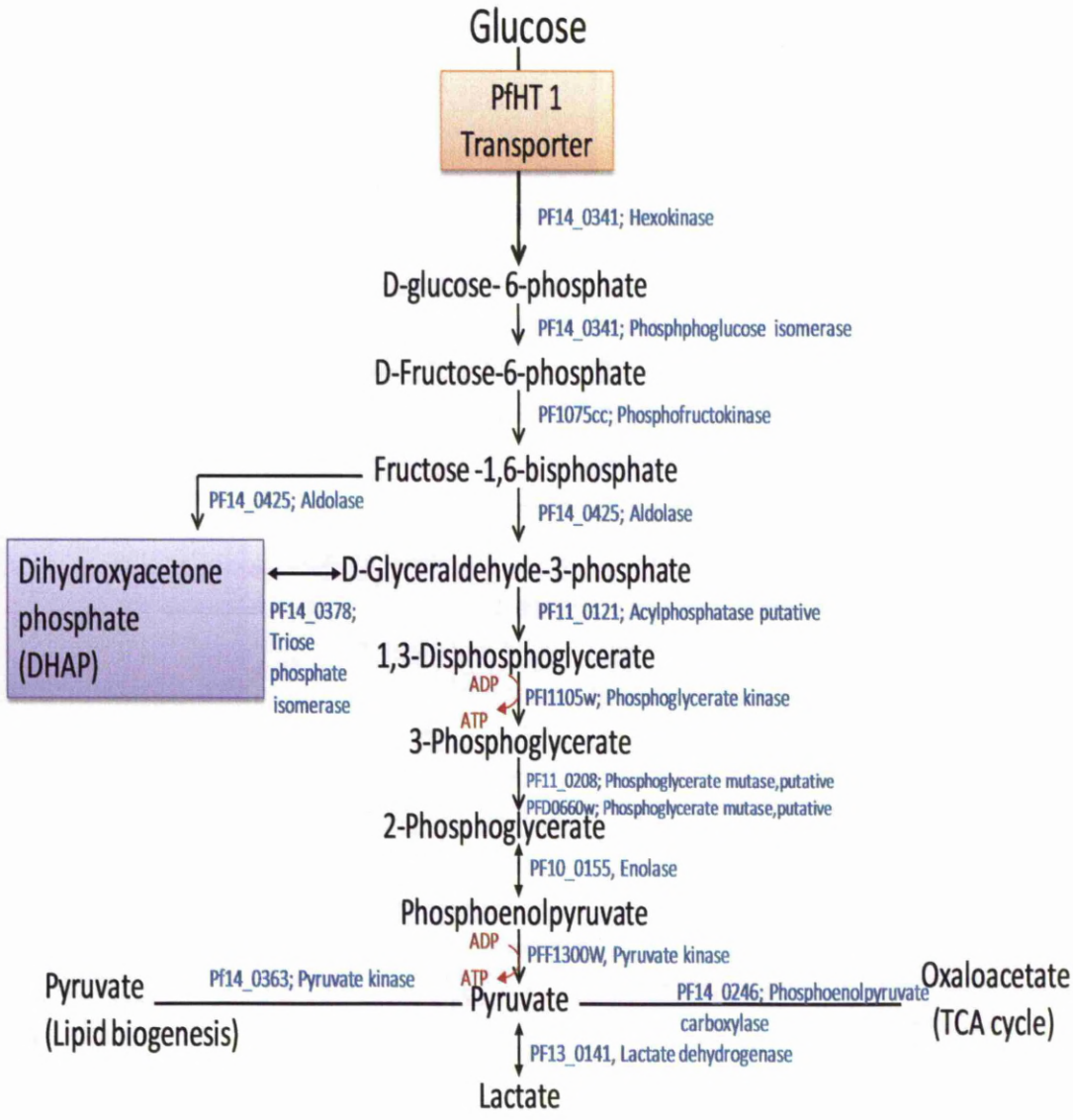

Figure 1.7: Malaria Parasite Glycolytic Metabolite Pathway

The component enzymes of the glycolysis pathways are encoded in the *Plasmodium* genome. Glucose from host plasma protein is transported into the parasite via the hexose transporter which located on the surface of infected RBC. Glucose was degraded by *Plasmodium* glycolytic enzymes thus producing lactate as an end product. The *Plasmodium* glycolytic pathway produces 2 molecules ATP as a carbon source for their cellular activities. The oxidation of phophoenolpyruvate (PEP) produces 2 molecules of pyruvate for the production of lactate (fermentation) and for lipid biogenesis in the apicoplast. Oxidation of pyruvate also produced OAA to enter the *Plasmodium* TCA cycle. Adapted from Daily et al. (2007).

originally predicted by Sherman (1998). Instead, Foth et al. (2005) demonstrated that the PDH enzyme complex is detected in the parasite apicoplast and used for generation of acetyl-CoA for lipid biogenesis. The formation of large quantities of lactic acid by the parasite would have implications for cytosolic pH. To mitigate this, the parasite removes lactic acid via a monocarboxylate transporter on the parasite surface membrane (40).

In most eukaryotic cells despite using glycolytic pathways, glucose can be generated via gluconeogenesis, the reverse mechanism of glucose synthesis from pyruvate. However, in the *P. falciparum* this mechanism is not available due to the unavailability of fructose bisphosphatase an enzyme which is essential for gluconeogenesis. This has been proved by the unavailability of this gene in the *Plasmodium* genome(82) On the other hand the parasite genome encodes phosphoenolpyruvate carboxykinase (PEPCK; PF13_0234) which is an important enzyme for gluconeogenesis which converts oxaloacetate (OAA) and ATP back to phosphoenolpyruvate (PEP) and CO_2. However, a study by Olszewski et al (2010) failed to detect the present of PEPCK activity *in vitro*. However, a study by Hayward (2000) demonstrated the upregulation of this enzyme during the sexual life cycle in mosquito host. PEP is then converted into pyruvate by pyruvate kinase. The *P. falciparum* genome has 2 genes encoded for pyruvate kinase (PF10_0363 and PFF1300w). Pyruvate kinase is already characterised and demonstrated to be involved in lipid biosynthesis in the apicoplast of the parasite whereas the activity of PFF1300w is still not understood (160).

The parasite genome also encodes phosphoenolpyruvate carboxylase (PEPC; PF14_0246) which is an essential enzyme in plant photosynthesis (82). The PEPC enzyme was successfully been purified from *P. berghei* (199). In *P. falciparum*, PEPC is demonstrated involved in the process of reconversion of PEP from OAA. Later, with the

presence of inorganic phosphate (P_i), NADH efficiently reduces OAA to malate by cytoplasmic malate dehydrogenase (MDH) (102).

The OAA generated by PEPC is also converted to aspartate by aspartate transaminase (PFB0200c) when the cellular aspartate level is low. Bulusu *et al.* (2011) demonstrated the role of aspartate in the *Plasmodium* asexual life cycle. Aspartate is used for protein, purine and pyrimidine biosynthesis. However this phenomenon does not exist in *in vitro* culture since aspartate is supplied in the growth medium. Instead of converting into aspartate, OAA is reduced to malate by cytoplasmic MDH (199). This is supported by their previous study on radiolabbeled glucose showing the active involvement of PEPC catalysing the conversion of OAA to malate (200).

1.8.2.2. The Malaria Parasite TCA Cycle

The *P. falciparum* genome encodes all the necessary enzymes for TCA cycle (82). These enzymes are actively synthesised during the asexual blood life stages (25).

The first step in the *Plasmodium* TCA cycle is the production of citrate by citrate synthase using OAA and acetyl-CoA as substrates. *Plasmodium* has a citrate synthase homologue (PF10_0218) which has an N-terminal presequence to transport this protein into the *Plasmodium* mitochondrion (257). However in a recent study by Olszewski et al. (2010) demonstrated that the entry point for the TCA cycle in the malaria parasite is α-ketoglutarate (2-oxoglutarate) instead of citrate. From their study it was demonstrated that the TCA cycle in the malaria parasite is branched and not cyclic as in the canonical TCA cycle present in most higher eukaryotic cells (Figure 1.8). The two brances of the *Plasmodium* TCA architecture

are: the oxidative branch (following the canonical TCA cycle) and the reductive branch which is run in the reverse of the standard direction. However, only the reductive branch is responsible for the *Plasmodium* TCA cycle (200).

Two amino acids glutamine and glutamate have been identified as the major carbon sources which feed the cycle. The degradation of host haemoglobin produces glutamine and glutamine is then is converted to glutamate by *Plasmodium* glutamate synthase (PF14_0334) and finally converted to 2-oxoglutarate by glutamate dehydrogenase (GDH). The *P. falciparum* genome encodes 3 different genes for GDH: an NADP-dependent enzyme (PF14_0286), cytosolic NADP-GDH (PF14_0164) and fungal type NAD-dependent GDH (PF08_0132). An NADP -dependent enzyme is hypothesise targeted to the apicoplast which supply NADPH for biosynthetic reactions within the *Plasmodium* apicoplast (199).

The cytosolic NADP-GDH enzyme is speculated to be involved in redox homeostasis producing cytosolic 2-oxoglutarate (223). The cytoplasmic 2-oxoglutarate enters the mitochondrion through the malate:oxoglutarate antiporter (200) and eventually provides a carbon source to the TCA cycle.

1.8.2.2.1 The Reducing Branch of the Plasmodium TCA Cycle

The reducing arm of the *Plasmodium* TCA cycle is started by the reduction of 2-oxoglutarate to isocitrate by isocitrate dehydrogenase enzyme 2 (IDH2). In higher eukaryotic cells the isocitrate dehydrogenase (IDH) enzyme is available in 3 isoforms: mitochondrial NADP-dependent (IDH1), mitochondrial NAD-dependent (IDH2) and cytosolic NAD-dependent (IDH3).

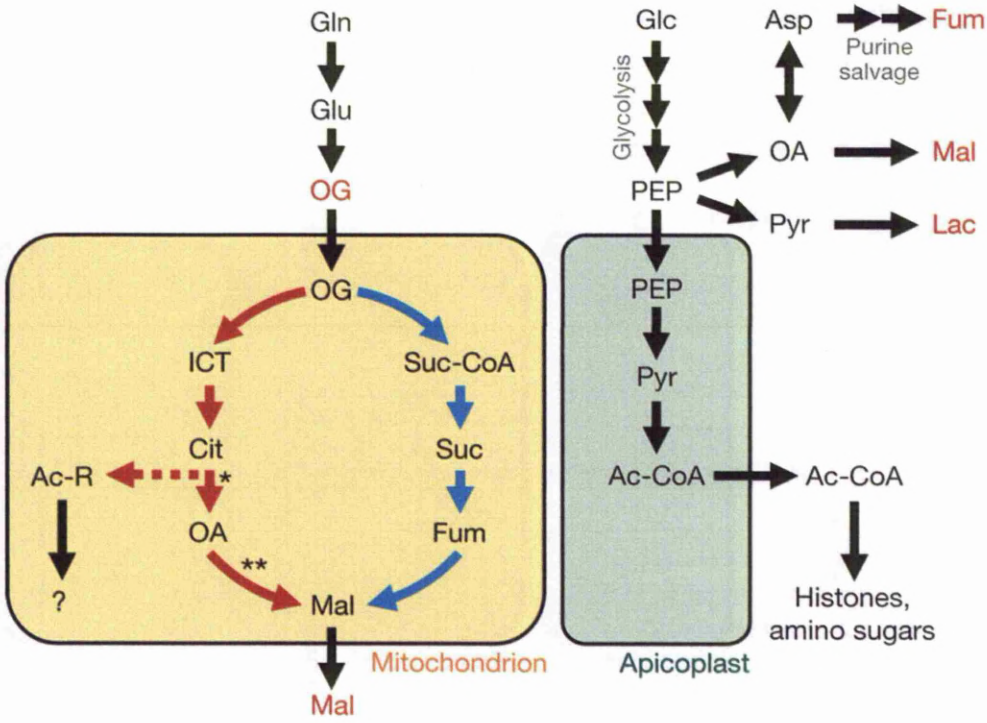

Figure 1.8: The Branched Tricarboxylic Acid Cycle in *P. falciparum*

The TCA cycle in *Plasmodium* mitochondria is structurally divided into reductive and oxidative pathways. Red arrows present the reductive pathway and blue arrows depict the oxidative pathway. Only reductive pathway is responsible for the *Plasmodium* TCA cycle. The reduction of citrate to OAA produced acetyl CoA, but the cellular function and the catalytic enzyme in this process are still unclear. The apicoplast acetyl-CoA is responsible for lipid biogenesis. Glutamate and glutamine are 2 amino acids that feed the cycle which converted to alpha ketoglutarate /2-oxoglutarate and enter the *Plasmodium* mitochondrial matrix. Asterisk (*) indicates the specific enzyme responsible for the citrate cleavage step but its location are unclear. Double asterisk (**) represents enzymes malate quinone oxidoreductase (MQO) or malate dehydrogenase (MDH) catalysing the conversion of OAA to malate. Abbreviations: Gln, glutamine; Glu, glutamate; OG, 2-oxoglutarate; ICT, isocitrate; Cit, citrate; Ac-R, acetate/acetyl-CoA; Ac-CoA, acetyl-CoA; OA, Oxaloacetate; Mal, malate; Suc, succinyl; Suc-CoA, succinyl-CoA; Fum, fumarate; Glc, glucose; Asp, aspartate; PEP, phosphoenolpyruvate; Pyr, pyruvate; Lac, lactate. Both oxidative and reductive branches of the *Plasmodium* TCA cycle produced malate which is transported out from *Plasmodium* mitochondria. Adapted from Olszewski et al. (2010).

. In the oxidative mode, isocitrate is oxidised to 2-oxoglutarate using IDH3 producing O_2 and reducing NAD^+ and $NADP^+$. However in *P. falciparum* the mitochondrial genome encodes only mitochondrial $NADP^+$ dependent isocitrate dehydrogenase IDH2 (PF13_0242) (288) which uses $NADP^+$ as a cofactor. The parasite's mitochondrial NADP(H) specific glutamate dehydrogenase (PF14_0164) and glutamate oxidation provide the cofactor for the *P. falciparum* IDH2. Therefore, due to the absence of the IDH3, it is suggested that the *P. falciparum* TCA cycle uses the branched architecture (200).

The PfIDH2 amino acid sequence has been identified, containing a mitochondrial presequence signal (leader sequence) and shown to be highly upregulated during oxidative stress (288). As mentioned earlier this enzyme uses oxidative $NADP^+$ instead of NAD^+ as a cofactor. The *Plasmodium* mitochondria require NADPH for anti-oxidant protection from ROS which are highly synthesised in the mitochondria (186, 288).

The next step in the reductive TCA branch is the isomeration of isocitrate to citrate catalysed by mitochondrial aconitase (PF13_0229). Aconitase is a reversible enzyme which can oxidised citrate to isocitrate or vice versa.

The *Plasmodium* genome encodes two citrate synthase homologues (PF10_0218) and PFF0455w (25, 82) occupied with an N-terminal presequence signal to transport this protein into the *Plasmodium* mitochondrial matrix (258). From metabolomic data, citrate is shown to be cleaved (deacetylation) into OAA followed by the reduction of OAA to malate (200). The reduction of citrate is catalysed by reversible citrate synthase enzyme. This is different from the canonical TCA cycle where the action of citrate synthase is irreversible. However a study

in fatty acid oxidation shows that citrate synthase can be reversed to catalyse the reduction of citrate to OAA (105). The reduction of OAA to malate generates acetyl-CoA which is transported from mitochondria into the cytoplasm and thereafter transported into the parasite nucleus to produce nucleic acids (DNA and RNA). The OAA is reduced to malate in the final step of the *Plasmodium* TCA cycle. The reduction of OAA to malate is catalysed by mitochondrial malate enzyme (either MDH or MQO) (200).

1.8.2.2.2 The Role of the Oxidative Branch of *Plasmodium* TCA Cycle

Due to the TCA cycle in *Plasmodium* being performed only by the reductive arm, the role of the oxidative arm of *Plasmodium* TCA has drawn new interest in the metabolic study of the *P. falciparum*. As mentioned earlier the *Plasmodium* genome encodes all the enzymes which are involved in the canonical TCA cycle (25, 82)

The oxidative arm is started by the conversion of 2-oxoglutarate to succinyl-CoA by alpha ketoglutarate dehydrogenase complex (PF08_0045). Succinyl CoA has been identified as a precursor enzyme for the cellular *de novo* haem biosynthesis pathway in *Plasmodium falciparum* (265, 269). According to the normal canonical TCA cycle, succinyl Co-A is converted to succinate by succinyl-CoA synthase (PF11_0097) and GTP is generated. The *Plasmodium* genome indicates the presence of alpha and beta subunits of succinyl-CoA synthase (PF11_0097 and PF14_0295) (82, 269).

Succinate then is oxidised to fumarate by succinate dehydrogenase which is the Complex II of the *Plasmodium* electron transport system. Oxidation of succinate supplies electrons to the mitochondrial respiratory chain via the reduction of FAD to $FADH_2$.

A study on the fate of fumarate in the oxidative branch was carried out by Bulusu *et al,* (2011). From the NMR study of the free parasite preparation, fumarate is incorporated into nucleic acids and proteins by biosynthesis (aspartate, alanine and glutamate). They reported that cytosolic *Plasmodium* fumarate is formed via the purine salvage pathway in the parasite cytoplasm. The *Plasmodium* fumarate pool in the parasite cytoplasm is transported into the mitochondria via the malate oxoglutarate transporter. The presence of this transporter in the *Plasmodium* genome was demonstrated using real time PCR (RT-PCR) analysis (Bulusu et al., 2011).

The role of fumarate in pyrimidine biosynthesis was demonstrated by Painter et al. (2007) using transgenic parasites bearing the *S. cerevisae DHODH* (*SCDHODH*) gene. Unlike *PfDHODH*, the *ScDHODH* gene product is localised in the cytoplasm and uses fumarate as electron acceptor which is produced from the purine salvage pathway in *Plasmodium* (27, 203).

Fumarate is then converted into aspartate and malate by the reversible fumarate hydratase (PFI1340w). The oxidation of fumarate to malate is catalysed by the fumarate hydratase Type 1. Pf fumarate hydratase/fumarase is unique and different from Type II fumarate hydratase which is found in yeast or mammalian cells. Pf fumarate hydratase has a resemblance to bacterial fumarate hydratase (73, 287). From the Kyoto Encylopedia of Genes

and Genomes (KEGG) database it is demonstrated that fumarate can be converted into three amino acids, glutamate, aspartate and alanine (27, 122). Glutamate is also derived from the degradation of host haemoglobin thus used as a precursor to initiate the TCA cycle in the *Plasmodium* parasite. Aspartate provides the carbon skeleton for the backbone of the pyrimidine ring in *de novo* pyrimidine synthesis in *P. falciparum*. In the parasite mitochondria fumarate is converted to malate by fumarate hydratase. Malate is then oxidised into OAA which is catalysed by the MQO enzyme. Bulusu et al., (2011) demonstrated that the oxidation of malate is mainly carried out by malate quinone oxidoreductase (MQO; PFF0815w) which is one of dehydrogenase enzymes in the*Plasmodium* electron transport system.

1.8.2.3 The Role of Malate in *P. falciparum* Metabolic Pathways

Malate is an essential substrate involved in central carbon metabolism of eukarytotic and prokaryotic cells. In the TCA cycle of the eukaryotic cells, malate is oxidised into OAA by mitochondrial malate dehydrogenase (MDH). Oxidation of malate to OAA thus reduces NAD^+ to NADH therefore supplying the electrons tothe electron transport chain and finally ATP is generated.

Figure 1.9 depicts the malate aspartate shuttle in eukaryotic cells. This process is started when the OAA is converted into malate by cytosolic MDH thus re-oxidising the NADH (from glycolytic pathway) to NAD^+. The malate passes the mitochondrial inner membrane via the malate–α-ketoglutarate transporter. Within the mitochondria, malate is oxidised to OAA by mitochondrial MDH and NAD^+ is converted into NADH which passes electrons to the mitochondrial respiratory chain. The transamination of OAA to aspartate is

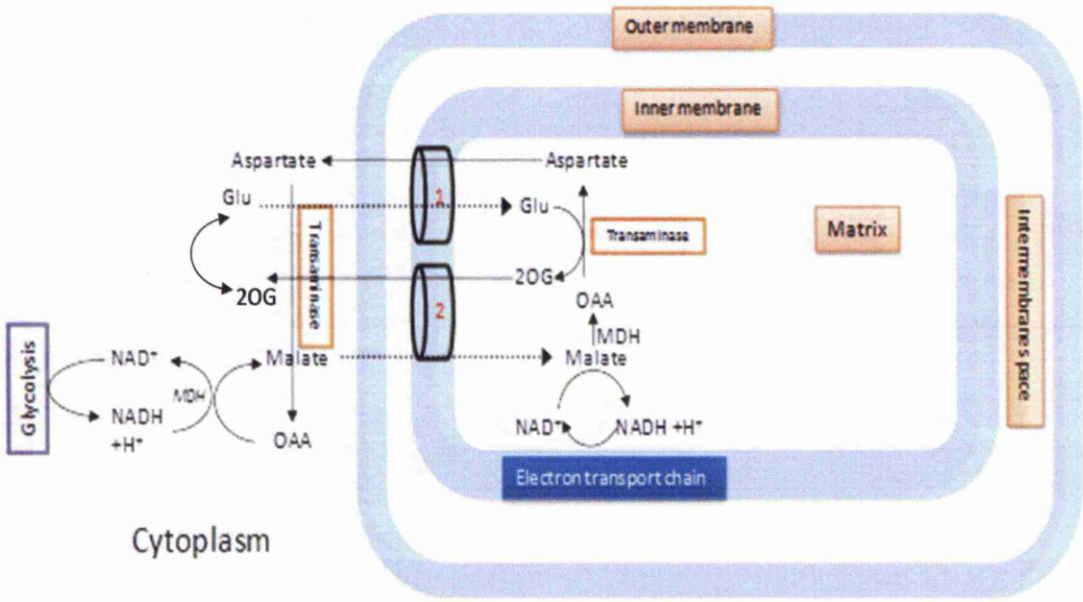

Figure 1.9: The Malate Aspartate Shuttle of Mammalian Cells

(1) Glutamate aspartate transporter and (2) malate-α-ketoglutarate transporter. Cytosolic NADH from the glycolytic pathway provides equivalents to OAA. OAA is reduced to malate by cytosolic malate dehydrogenase. Malate is transported into the mitochondrial matrix via the malate-α-ketoglutarate transporter. Within the matrix, malate is oxidised into OAA by mitochondrial MDH and passes 2 reducing equivalents to NAD^+. OAA is transaminated to aspartate by aspartate aminotransferase and transported back into the cytosol via the glutamate-aspartate transporter. Aspartate is re-transaminated back to OAA to complete the cycle. During the transamination process, glutamate is converted into 2-oxaloacetate/alpha-ketoglutarate (in the mitochondrial matrix) and cytoplasmic 2-oxaloacetate re-converted to glutamate using the same enzyme, aspartate aminotranferase. Abbreviations: Glu, glutamate; 2OG, 2-oxaloacetate; OAA, oxaloacetate; MDH, malate dehydrogenase.

catalysed by the aspartate aminotransferase enzyme. During the transamination of OAA to aspatate, glutamate is converted to α-ketoglutarate by glutamate dehydrogenase. α-ketoglutarate is then transported out from mitochondrial matrix via the malate–α-ketoglutarate transporter and aspartate is passed out via the glutamate aspartate transporter. The cytosolic OAA is then regenerated back through the transamination of aspartate by aspartateaminotransferase and α-ketoglutarate is re-converted to glutamate by reversible glutamate dehydrogenase in the intermembrane space (cytoplasm) (159).

Meanwhile the metabolic fate of malate in the *Plasmodium* mitochondria is slightly different from other eukaryotic cells. As mentioned in **section 1.8.2.2** the metabolomic study conducted by Olszewski et al. (2010) showed that malate is produced as an end product in both oxidative and reducing branches of the *Plasmodium* TCA cycle. The excreted mitochondrial malate in the cytoplasm was demonstrated by the presence of radiolabelled malate, citrate and 2-oxoglutarate in the culture medium. They have proposed that the conversion of malate to OAA is catalysed by PfMDH and malate quinone oxidoreductase (PfMQO). However a recent study by Bulusu et al. (2011) shows that the oxidation of malate to OAA is mainly performed by MQO. The oxidised OAA is transported out from matrix mitochondria via the malate-oxoglutarate transporter. The oxidation of malate to OAA thus feeds electrons directly to the *Plasmodium* respiratory chain. Figure 1.10 shows the diagrammatic presentation of malate in the *Plasmodium* metabolic pathways.

The oxidation of fumarate to malate is catalysed by the fumarate hydratase in the parasite mitochondria. Malate is then transported out from the mitochondrial matrix via the malate-alpha-ketoglutarate transporter. This transporter is encoded in the *Plasmodium* genome (PF 08_0031) and its expression validated by RT-PCR (27). However this

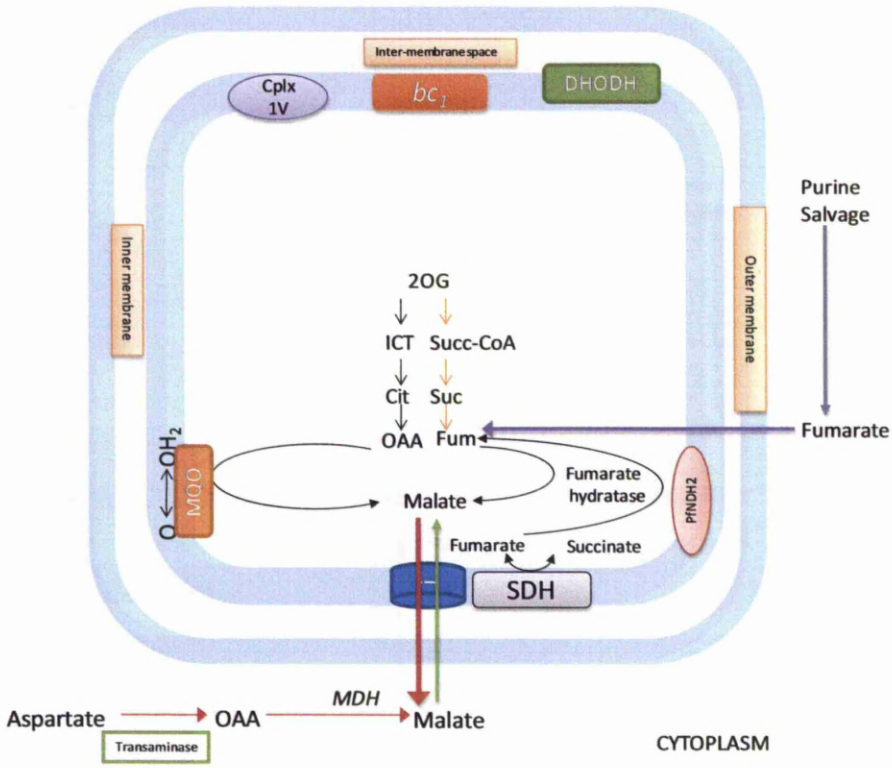

Figure 1.10: The Malate Aspartate Shuttle in the *Plasmodium* Parasite

Malate has been recognised as the end product from both oxidative and reducing branches of the *Plasmodium* TCA cycle. Malate can also be synthesised through fumarate oxidation using fumarate hydratase (fumarase) within the *Plasmodium* mitochondrial matrix. The OAA in the reductive branch is converted to malate by mitochondrial MQO enzyme. Malate than is transported out from the mitochondrial matrix via the malate-oxoglutarate tranporter. Abbreviations: 2OG, 2-oxoglutarate; ICT, isocitrate; Cit, citrate; OAA, oxaloacetate; Fum, fumarate; Succ, succinate; Succ-CoA, Succinyl-CoA; MDH, malate dehydrogenase; MQO, malate quinone oxidoreductase; QH_2, ubiquinone; Q, ubiquinol; DHODH, dihydroorotate dehydrogenase, bc_1, cytochrome bc_1 complex; PfNDH2, *P. falciparum* type II NADH:ubiquinone oxidoreductase, Cplx IV, Complex IV.

mechanism is not yet fully elucidated. In normal physiological condition only a small amount of OAA is transported out from mitochondria via malate-alpha-ketoglutarate transporter. The mitochondrial OAA is normally transported out via a glutamate-aspartate shuttle which is not encoded in the *Plasmodium* genome (269).Olszewski and Llinas (2011) speculated that OAA could directly transport out from mitochondria without being transaminated to aspartate in the mitochondrial matrix. However transamination of the cytoplasmic OAA can be performed in the cytoplasm where OAA is converted to aspartate by the aspartate aminotransferase (PfAAT). PfAAT is encoded in the *Plasmodium* genome (PFIT_PFB0200c) and confocal microscope study depicts PfAAT in the *Plasmodium* cytoplasm and not in the mitochondria (27). The cytoplasmic aspartate is then integrated into *Plasmodium* purine salvage pathways and also into the synthesis of proteins and *de novo* pyrimidine biosynthesis.

At the same time the cytoplasmic OAA is converted to malate by cytosolic MDH, oxidising NADH to NAD^+. Like in other eukaryotic cells malate is transported back to the mitochondria via a malate-oxoglutarate shuttle, and NAD^+ is converted to NADH to supply electrons to the mitochondrial respiratory system in the parasite.

1.8.2.3 The Malaria Parasite Electron Transport Chain

Plasmodium mitochondrial electron transport (mtETC) consist of 5 dehydrogenase enzymes namely NADH type 2 dehydrogenase (rotenone-insensitive complex 1), succinate dehydrogenase (complex II), ubiquinone-cytochrome c oxidoreductase, malate-quinone oxidoreductase (MQO), dihydroorotate dehydrogenase (DHODH) and glycerol-3-phosphate dehydrogenase (Figure 1.11). These dehydrogenase enzymes require their respective substrates to operate which are, NADH, succinate, malate, DHO and glycerol-3-phosphate.

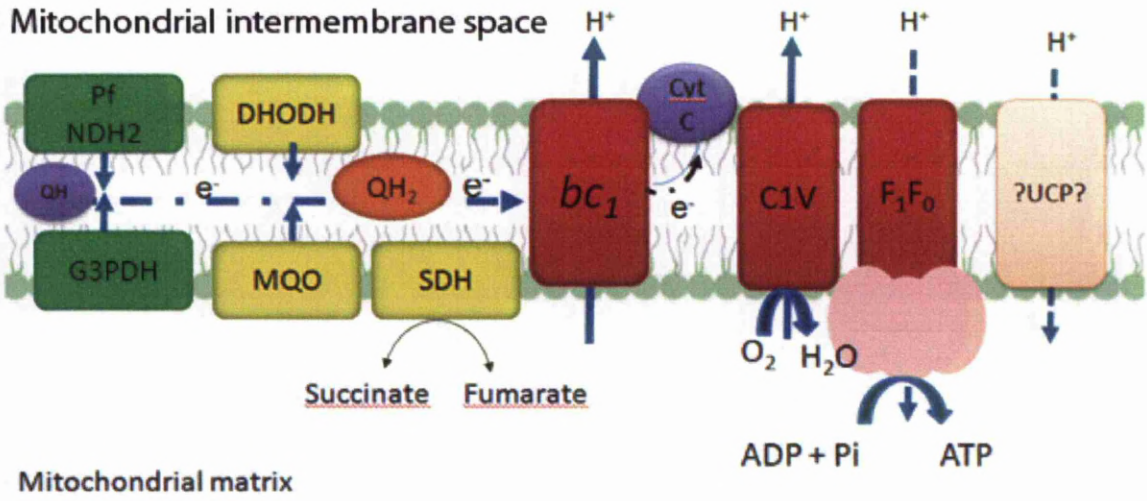

Figure 1.11: Schematic Drawing of the Organisation of the Mitochondrial Respiratory Complexes of *P. falciparum*

The chain consists of PfNDH-type II NADH: quinone oxidoreductase, DHODH (dihydroorotate dehydrogenase), G3PDH (glycerol-3-phosphate dehydrogenase), MQO (malate quinone oxidoreductase), SDH (succinate dehydrogenase), bc_1 (cytochrome bc_1 complex), Cyt c (cytochrome c), CIV (cytochrome oxidase), F_1F_0ATPase (Complex V) and UCP (putative uncoupling protein). Electrons are generated by mitochondrial dehydrogenases and passed to ubiquinone (QH). Re-oxidation of QH2 releases 2 H^+ to mitochondrial intermembrane space and passes electrons to bc_1 complex. The electrons are continuously passed to cytochrome c. Finally, the cytochrome c uses the electrons and H^+ to reduce O_2 to H_2O. The *Plasmodium* genome lacks F_0 the subunit (subunits a and b) which is essential for ATP generation. Fisher et al.(2007) described the presence of a proton leak via the *Plasmodium* F_1F_0 respiratory chain to enable the maintenance of high transmembrane proton potential (ψ_m). Another theory of re-entrance of protons into the mitochondrial matrix is through uncoupling protein (UCP). Adapted from Fisher, et al. (2009).

These dehydrogenase are involved in reduced ubiquinol and then reoxidised its to ubiquinone by the bc_1 (Complex III). This redox reactions is proceeded with a reduction of ubiquinone cytochrome c. Finally, the reduced form of cytochrome c is oxidised by a cytochrome c oxidase (Complex IV) and molecular oxygen to yield water. A membrane potential is generated although this is not then used to generate ATP via Complex V. Probably, a small amount of ATP is generated in order to complete the proton circuit (66)

1.8.2.3.1 PfNDH2 (Alternative NADH dehydrogenase) (PF10735c)

Complex I, rotenone-sensitive NADH dehydrogenase, is an enzyme which oxidise NADH (generated in the TCA cycle) and finally feeds electrons into the respiratory chain of the mitochondrion. Oxidation of NADH is coupled to the reduction of ubiquinone and this process is coupled with proton translocation across the inner membrane, generating a trans-membrane potential. The *Plasmodium* genome lacks a canonical Complex I and instead contains an alternative (rotenone insensitive) type II NADH:ubiquinone oxidoreductase (PfNDH2) (66, 82). PfNDH2 has a single subunit and has homologs in plants, bacteria and yeast but not in animals (139, 219, 269). Structurally PfNDH2 is a membrane bound protein located on the membrane external side of the inner mitochondrial membrane facing the cytosol (19, 262).

PfNDH2 has a FAD prosthetic group in comparison to typical NADH dehydrogenase which have flavin mononucleotide (FMN) and multiple FeS centres. PfNDH2 does not couple a redox reaction to proton pumping. Fisher et al. (2007) demonstrated that PfNDH2 is a major contributor of electrons to the *Plasmodium* respiratory chain (e.g. 50% of total flux is derived from PfNDH2 compared to only 1% by DHODH).

1.8.2.3.2 DHODH (Dihydroorotate dehydrogenase) (PFF0160c)

DHODH is a flavoenzyme located in the inner membrane of *Plasmodium* mitochondrion (140) and is a key enzyme in the biosynthetic pathway for the synthesis of pyrimidines. It also serves to regenerate ubiquinone in the *Plasmodium* respiratory chain.

There are two types of DHODH, known as DHODH type 1 and DHODH type II. Type II DHODH is an integral membrane protein, localised in the inner mitochondrial membrane with the active site facing the intermembrane space. It is found in most eukaryotic cells and also in some of Gram positive bacteria and *S. cerevisae* (49, 203). Unlike type II DHODH, type I DHODH is located in the cytosol and uses fumarate or NAD^+ or $NADP^+$ as an electron acceptor to re-oxidise the flavin (FMN) prosthetic group. A study in *S. cerevisae* showed that the oxidation of DHODH to oorate is responsible for the reduction of fumarate to succinate in the TCA cycle (294).

The synthesis of pyrimidine in *Plasmodium* species are unusual compared to the other eukaryotic organisms. In *Plasmodium*, *de novo* pathway is the only pathway supplies pyrimidines for cell growth using a the dihydroorotate enzyme (151, 203). Unlike eukaryotic cells, *Plasmodium* cannot scavenge pyrimidines and is totally depended on the *de novo* pyrimidine synthesis for generation of *Plasmodium* DNA and RNA, glycoproteins and phospholipids. Dihydroorotate interacts with DHODH which is located facing the intermembrane space. Dihydroorotate is oxidised to generate orotate which is transferred out from the *Plasmodium* mitochondrion to the cytosol. The activity of DHODH has been shown to be maximal at the trophozoite and schizont stages of *Plasmodium* asexual development (140).

1.8.2.3.3 Succinate-ubiquinone Oxidoreductase (Succinate dehydrogenase; Complex II)

Mammalian mitochondrial Complex II consists of four subunits (Sdh1, Sdh2, Sdh3 and Sdh4). Sdh3 and Sdh4 are two hydrophobic anchor b-type cytochromes bound to a soluble heterodimer of Sdh1 and Sdh2. Electrons are transferred from Sdh1 to a ubiquinone binding pocket within Sdh2 and subsequently transferred to Sdh3 and Sdh4 in the inner mitochondrial membrane (109, 290). Succinate dehydrogenase is the only enzyme in the mitochondria which is involved in electron transfer in the respiratory chain and also oxidises succinate to fumarate in the TCA cycle in the mitochondrial matrix.

Two subunits of the Complex II have been identified in the *Plasmodium* genome. These are Fp,Sdh1 (flavoprotein; PF10_0334) and IP,SdhB (an iron-sulphur protein; PF0630w). Both are hydrophilic subunits bound to the matrix side of the inner mitochondrial membrane (31, 82). The existence of Sdh 3 and Sdh 4 is as yet unconfirmed.

In a bioinformatic study, Mogi and Kita (2009) reported the putative identification of the two 'missing' subunits using similarity searches. At this stage however, these data are not confirmed and other candidates have been put forward by other laboratories (Biagini, personal communication).

1.8.2.3.4 Glycerol-3-phosphate Dehydrogenase

P. falciparum has NAD^+ linked (PFL0780w) and FAD linked (PFC0275w) glycerol-3-phosphate dehydrogenases (G-3-PDH) (269). G-3-PDH is a part of the glycerol shuttle which provides an alternative way for transferring electrons to the mitochondrial ubiquinone. The

cytosolic NAD+ linked glycerol-3-phosphate dehydrogenase catalyses the reduction of dihydroxyacetone phosphate (DHAP) to glycerol-3 phosphate with concurrent oxidation of cytosolic NADH.

The glycerol-3-phosphate then is transported to the mitochondrial intermembrane space and re-oxidised back to dihydroxyacetone phosphate using mitochondrial glycerol-3-phosphate dehydrogenase. The oxidation of glycerol-3-phosphate thus generates electrons which pass via the FAD cofactor to ubiquinone.

1.8.2.3.5 Malate Quinone Oxidoreductase (MQO; PFF0815w)

MQO is a lipid-dependent, peripheral membrane-bound flavoprotein which catalyses the oxidation of malate to oxaloacetate. This enzyme is a membrane associated protein containing a FAD prosthetic group (185). From biochemical studies MQOs can be divided into two major families which are MQO 1 and MQO 2. The actinobacterial MQO including *Mycobacterium smegmatis* and *Corynebacterium glutamicum* belong to one major bacterial MQO family (MQO1), while most ε-proteobacterial *Escherichia coli*, *Helicobacter pylori*, *Campylobacter jejuni*, and apicomplexan (*P. falciparum*, *Toxoplasma gondii*, *Babesia bovis*) ones are members of the second group of MQO (MQO2) (182).

1.8.2.3.6 Complex III (Cytochrome bc_1 or ubiquinol-cytochrome c oxidoreductase)

Cytochrome bc_1 or ubiquinol-cytochrome c oxidoreductase is an essential enzyme of the cellular respiration in many eukaryotic cells including metazoa, fungi and protozoan parasites. Cytochrome bc_1 is located in the inner mitochondrial membrane of eukaryotic cells.

The functional complex is 480 kDa consisting of two monomeric units of 10 to 11 polypeptides. The catalytic core of the cytochrome bc_1 consists of cytochrome *b* (CYTb), cytochrome c1 (PF14_0597) and the Rieske iron-sulphur protein (ISP) (PF14_0373) which are encoded by mtDNA whilst the other subunits are encoded by nuclear DNA.

Cytochrome bc_1 catalyses the electron transfer from ubiquinol to cytochrome *c*, coupled with the vectorial translocation of protons, thus generates a transmembrane electrochemical gradient (proton motive force) used for ATP production by F_0F_1-ATP synthase (Complex V). The catalytic mechanism of the bc_1 complex is known as the Q cycle which was first postulated by Mitchell in 1975 (68, 130).

1.8.2.3.6.1 The Q cycle

The crystal structure of the cytochrome bc_1 shows the presence of presence of redox prosthetic groups which are cytochrome c1 and iron sulphur (ISP). This group consists of two membrane domains associated with large hydrophilic regions. While the cytochrome b is containing predominantly hydrophobic protein with 8 transmembrane helices connected with 2 heme b (heme b_H and heme b_l) and 2 quinol binding sites. The Q_l site is the core of the cytochrome b and is topographically proximal to the matrix side in the inner mitochondrial membrane. Q_0 is located at the interface of cytochrome b and the Rieske protein proximal to outer surface of inner mitochondrial membrane (68, 130).

The mitochondrial Q cycle is illustrated in Figure 1.12. The mitochondrial redox system can be divided into two phases. The first phase starts by the diffusion of ubiquinol

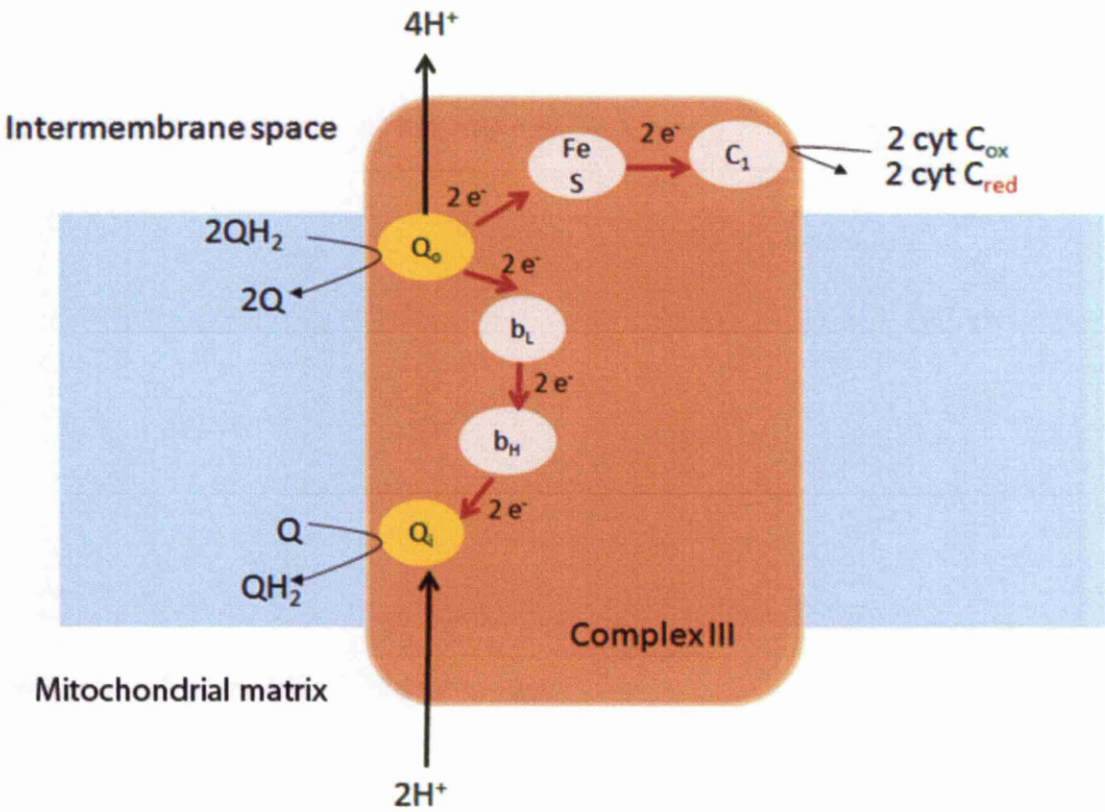

Figure 1.12: The Schematic Drawing to Illustrate the Q cycle in the Mitochondrial *bc1* complex

The *bc1* Q cycle starts when ubiquinol (QH_2) binds to the Q_o (quinol oxidation site) within the complex. The first electron is transferred to the Rieske protein (Fe-S) which is then transferred to cytochrome *c*. QH is then in a semiquinone anionic state, $CoQ^{\cdot-}$. The second electron is transferred to the heme b1 site and converts $CoQH^{\cdot}$ to CoQ. CoQ diffuses out from the Qo site to the mitochondrial intermembrane space. An electron from b_I is transferred to b_H and thus passes the electron to Q_i (quinone reduction site) thus generating stable $CoQH^{\cdot-}$. The second phase of Q cycle is similar to the first phase, in which 2 protons are translocated out into intermembrane space. 2 H^+ from the mitochondrial matrix oxidise CoQ.- to form ubiquinol which later diffuse from the Q_i binding site.

(QH_2) generated from the mitochondrial dehydrogenase enzymes. Ubiquinol binds to Q_o site and is oxidised thus releasing 2 protons and 2 electrons. The 2 protons are released into the intermembrane space. Deprotonated ubiquionol in the form of a semiquinone anionic state (CoQ.-) transfers 1 electron through the iron–sulphur cluster of the Riske protein and cytochrome c_1 and finally transfers the electron to cytochrome c to supply electrons to feed the mitochondrial electron transport chain. The second electron is transferred to the heme b_l which oxidises the semi-quinone to ubiquinone (CoQH.- to CoQ). The electron at heme b_l is transferred to the heme b_H and is finally transferred to the quionone reduction site (Q_i) thus generating a stable CoQ.- radical firmly bound to Q_i binding site.

The second phase of the Q cycle is similar to the first half. The second molecule of ubiquinol (QH_2) binds to the Q_o site and oxidised to CoQH.- at the Qi binding site. This process releases another 2 protons into the intermembrane space. The second electron is transferred to heme b_l and transferred to the heme b_H site. This electron is then transferred to CoQ.- which is firmly bound to Q_i site. 2 protons from the mitochondrial matrix oxidise CoQ.- to form ubiquinol which later diffuse from the Q_i binding site to form part of the ubiquionol pool.

In summary, during the mitochondrial Q cycle 2 molecules of ubiquinol are oxidised to quinone at Q_o site and 1 molecule of quinone is reduced at Q_i site. 4 protons are translocated out to the intermembrane space (2 protons per 1 quinol oxidation). During this cycle electrons are translocated from ubiquinol to feed the mitochondrial respiratory chain and to regenerate ubiquiol to supply the ubiquinol pool in inner mitochondrial membrane.

1.8.2.3.4 Complex IV (cytochrome c oxidase)

Mitochondrial complex IV is a terminal oxidation step in the mitochondrial respiratory chain. Complex IV is a heme-copper oxygen reductase which is involved in complete reduction of dioxygen to water therefore promotes the translocation of protons across the mitochondrial inner membrane and finally generates membrane potential across the mitochondrial membrane.

Plasmodium cytochrome c oxidase consists of 3 catalytic subunits; CoxI, CoxII and CoxIII. The subunits Cox1 and CoxIII of the *Plasmodium* Complex IV are encoded by mtDNA, whilst the subunit Cox II is encoded by nuclear DNA (269).

The *Plasmodium* Complex IV belongs to the haem copper oxidase superfamily which is involved in the respiratory chain by accepting the electrons from cytochrome *c*. Electron pass to the Cu_A followed by transfer to the CU_B copper within the CoxII subunit (64, 269). Protons are translocated across the inner mitochondrial membrane thus contributing to the membrane potential ($\Delta\psi$) and membrane electrochemical gradient. *Plasmodium* CoxII consists two nuclear encoded subunits known as CoxIIa (PF14_0288) and CoxIIb (PF13_0327) (80). The role of CoxIII is not well understood and it is believed to be involved in proton translocation across the inner mitochondrial membrane (110).

Studies conducted by Krungkrai (1993), Srivastava, Rottenberg et al. (1997) Uyemura et al. (2000), Uyemura et al. (2004) show that the activity of *Plasmodium* Complex IV can be inhibited by potassium cyanide.

1.8.2.3.5 F_1F_0-ATP synthase (Complex V)

Complex V in eukaryotic cells is responsible for completing the process of oxidative phosphorylation. ATP is generated through serial steps in the inner mitochondrial membrane; mtETC, oxidative phosphorylation and the electrochemical gradient across the mitochondrial membrane and finally the generation of ATP from ADP and inorganic phosphate (Pi).

Complex V contains F_1 and F_0 subunits. The F_1 sector of the complex V is a detachable structure and consists of 3 α subunits, 3 β subunits, γ, δ, Ɛ and oligomycin sensitivity conferring protein (OSCP) subunits. The F_0 subcomplex is integral membrane protein, acting as a proton channel and consisting of 3 subunits a, b and ~ 12 copies of c.

ATP is synthesised from energy derived from vectorial proton translocation from the mitochondrial matrix through the F_0 a to the c subunits. Rotational movement in the c subunit is linked to a central stalk of the F_1 portion and ATP is generated at the active site of the beta subunits.

The *P. falciparum* genome contains all of the ATP synthase subunits with the exception of F_0 *a* and *b* subunits, which have yet to be identified (82, 265, 269). Subunit *a* has been identified as an essential part for the generation of ATP from F_1F_0-ATP complex. The absence of a and b subunits is also reported in other *Plasmodium* species (e.g *P. yoelii*) (30, 266). Due to the absent of the complete set of F_0F_1 ATP complex, many researchers have hypothesised that the *Plasmodium* parasite does not rely on oxidative phosphorylation for ATP generation; however the "missing" subunits are not conserved at the primary sequence

level in any species, and therefore given that still ~40% of the genome is not annotated, their absence should not necessarily be concluded to mean that the complex is not functional.

1.8.2.3.6 Uncoupling Proteins (UCPs)

In eukaryotic cells energy conservation/transduction is performed by using the proton gradient to drive ATP synthesis and/or transport. As described a number of complexes can pump protons in order to generate a proton gradient, however in order to complete the circuit, enzymes/transporters are also required to allow protons back in to the mitochondrial matrix, i.e. the leak. In addition to Complex V, a number of proteins have been shown in eukaryotic cells to be able to perform this role: these proteins are known as uncoupling proteins (UCPs).

Evidence for the presence of UCPs in *Plasmodium* was presented by Uyemura et al., (2004). The western blot analysis result showed that the UCPs in *P. berghei* using antibodies raised against plant uncoupling mitochondrial protein (PUMP). There have however not been any further studies to support/contradict this work and the presence and role of UCPs in *Plasmodium* remain at present undefined.

1.9 *Plasmodium* Mitochondria as A Drug Target

As described, the mitochondria of *Plasmodium* contain a number of typical components, which are not found in higher eukarytotic mitochondria, such as the PfNDH2 and MQO dehydrogenases. The absence of these dehydrogenases in the human host has led some researchers to propose that these enzymes may be good drug targets for the development of new antimalarials. This work necessitates however the generation of

functional enzyme either purified or from enriched heterologous expression systems in order to perform high-throughput screens or *in silico* rational-drug design. In the case of PfNDH2, recombinant enzyme has been reported (70) and a drug discovery project is currently in progress. In the case for MQO however, no recombinant protein is as yet available, and this knowledge gap is addressed in Chapter 5 of this thesis, where attempts to generate recombinant MQO are described.

The DHODH of *Plasmodium* has also been validated as a drug target and a number of studies have been performed to generate novel inhibitors (23, 37, 239). These studies rely on exploiting small differences in the active site of *Plasmodium* and human DHODH and currently these projects have advanced to the late pre-clinical phase (see Medicines for Malaria Venture portfolio, www.mmv.org).

As described earlier, the parasite bc_1 is a *bona fide* drug target with atovaquone (constituent of Malarone^{TM}) a registered antimalarial drug. Due to the expense of atovaquone and the presence of resistant mutants strains, researchers are attempting to develop alternative compounds; these include (i) pyridones, analogues of clopidol (289, 291), (ii) acridines and acridinediones (18) and (iii) quinolones (284).

For the development of these bc_1 inhibitors, it would be of benefit to have further information regarding the mechanism of atovaquone resistance in the parasite bc_1, as any information is based on that derived from model organisms (e.g. yeast). This knowledge gap is addressed in the first two results chapters of this thesis (Chapter 3 and 4) which describe the molecular and biochemical characterisation of an atovaquone resistant isolate (TM902CB).

1.10 Objectives

The general objective of the thesis was to take a multidisciplinary approach to study key bioenergetics enzymes of the malaria parasite mitochondria. Atovaquone sensitive and resistant parasites have been compared at the level of gene expression and at the biochemical level with the aim to uncover the complex mechanisms underpinning atovaquone resistance, both at the enzyme level and at the pathway/cellular level. In addition a major objective of this study was to isolate and purify the putative malate quinone oxidoreductase (MQO) of *P. Falciparum* 3D7 with the view to validating this enzyme as a potential drug target. Specifically the objectives of this thesis were;

1. To perform a comprehensive gene expression study detailing the expression profile of energy metabolism genes in atovaquone sensitive and resistant parasites.
2. To perform a detailed biochemical analysis of the parasite bc_1 and related respiratory enzymes from atovaquone sensitive and resistant parasites and to relate these data to observe expression data obtained in the Chapter 3.
3. To clone, express and purify *P. falciparum* 3D7 parasite putative MQO in order biochemically to characterise this enzyme and potentially to generate small molecule inhibitors.

Chapter 2: General Materials and Methods

2.1 *In vitro* Cultivation of the Blood Stage Malaria Parasite

Continuous *in vitro* cultivation of malaria parasites was maintained under appropriate conditions according to the method described by Trager and Jensen (1976). All the procedures were carried out under sterile conditions in a NUAIRE BioHazard Class II laminar flow cabinet. Using sterile equipment, blood stage parasites were grown in complete culture medium RPMI 1640 (Sigma Aldrich, UK) with added of 10% human O positive type serum which was compatible with the type of erythrocytes used, 25 mM HEPES, and 0.02 mg/ml gentamicin in 75-cm^2 tissue culture flasks (Nunc^{TM}). The O positive serum used was continuously supplied by Royal Liverpool Hospital, UK.

2.2 Preparation of Uninfected Erythrocytes

Group O positive human blood was obtained from the regional Blood Transfusion Centre, Liverpool UK. The blood was screened for antibodies to pathogens such as Hepatitis virus (HBV) and human immunodeficiency virus (HIV). The RBCs were centrifuged at 3,000 rpm for 5 minutes at room temperature. The serum and buffy coat were discarded and the RBCs were then resuspended in 30-40 ml RPMI 1640 medium with added of 25 mM HEPES and 0.02 mg/ml gentamicin (Sigma Aldrich, UK). The suspension was centrifuged at 3,000 rpm for 5 minutes at room temperature. This step was repeated three times and the washed RBCs were kept at 4 °C and used within one week. After one week the remaining blood was disposed of following standard tissue and blood disposal procedure.

2.3 Preparation of HEPES

One molar HEPES (N-[2-hydroxyethyl] piperazine-N'-[2-ethanesulfonic acid] stock solution (Sigma Aldrich, UK) was used to regulate the pH shift in culture media. The solution was prepared in distilled water and the pH was adjusted to 7.4 using 5 M NaOH. The maintenance of pH is critical to the *in vitro* growth: the HEPES buffer is used to maintain physiological pH despite the acidity problems that resulting from the large amount of lactic acid produced by the malaria parasite. The solution was filtered, sterilised and stored at 4 °C.

2.4 Maintenance of Parasite Growth

The parasite growth was monitored daily by Giemsa-stained thin smears and observed under a light microscope (100 x magnification). For this, one drop of the RBCs (~ 60 μl) were aseptically taken from the culture flask and transferred onto a glass microscope slide. The monolayer thin blood smear was prepared, fixed in absolute methanol for 10 seconds and subsequently stained in 10% Giemsa (BDH Chemical, UK) for 10 minutes. The percentage of parasitemia was counted in 500 cells (infected and non infected RBCs). The optimum level of the infected RBCs in a 75-cm^2 culture flask should be in the range of 5-6%. After determination of parasitaemia, the parasite culture was centrifuged at 2,000 rpm for 5 minutes at room temperature. The supernatant was discarded and the parasitised RBC pellet resuspended in complete RPMI 1640 culture medium and flushed with a gas mixture. The parasite culture haematocrit was usually maintained at 2%.

2.5 Gas Phase

The parasites were gassed to reproduce the conditions usually encountered within human hosts. The composition of the gas during the gas phase is critical to the development

of the parasite. The most favourable atmosphere was provided according to the protocol described by Scheibel et al. (1979), but using the following gas composition: 3% CO_2, 4% O_2 and 93% N_2 (BOC, Guilford, UK) (230). This gas mixture was passed through a sterile pipette into the parasite culture for 30-60 seconds. For the drug sensitivity assay, malaria parasites were grown in 96 well plates and incubated in a humidified gas tight chamber. The chamber was gassed for approximately 3 minutes, followed by 48 hour incubation at 37 °C.

2.6 Cryopreservation of Parasites

For cryopreservation, ring stage parasites at 6% parasitemia were stored in liquid nitrogen. Parasite cultures were centrifuged at 2,000 rpm for 5 minutes at room temperature, supernatant discarded and the pellet resuspended in an equal volume of filtered sterile cryopreservation solution consisting of 0.95% (w/v) NaCl (Sigma Aldrich, UK), 4.2% D-sorbitol (Sigma Aldrich, UK) and 2% (v/v) glycerol (Sigma Aldrich, UK). The mixture was transferred into cryotubes and stored in a liquid nitrogen tank.

2.7 Retrieval of Cryopreserved Parasites

Parasite retrieval involved removing the cryotube from the liquid nitrogen tank and thawing either at room temperature or in a water bath at 37 °C. The culture was transferred into a 15-ml tube and centrifuged at 2,000 rpm for 5 minutes at room temperature. The supernatant was discarded and equal volume of thawing solution (3.5% NaCl) was added to the pellet. This resuspension was centrifuged at 2,000 rpm for 5 minutes. Again, the supernatant was removed, 10 ml of complete RPMI 1640 culture medium added and a repeat centrifugation done at 2,000 rpm for 5 minutes. Following the centrifugation, the supernatant was discarded and the parasite pellet resuspended in 15 ml RPMI complete culture media. The

parasite mixture was then transferred into a 25-cm^2 culture flask, the parasite culture gassed and incubated at 37 °C then closely monitored.

2.8 Synchronisation of Parasite Culture

A continuous parasite culture usually exhibits a mixture of parasites in different stages of their life cycle. Asynchronous cultures were therefore synchronised before use in drug sensitivity assays or when isolating DNA and RNA materials from the parasites. The synchronisation process was achivied by 5% w/v of D-sorbitol treatment (Lambros and Vanderberg 1979). The synchronisation of parasite culture was induced by a selective destruction of the trophozoite and schizont stages of the parasite. The effect of sorbitol on the parasite membrane cell is still not clear (146). For this procedure, the parasite culture was centrifuged at 2,000 rpm for 5 minutes at room temperature and the supernatant discarded. Approximately 1 ml of the parasite pellet was resuspended in 5 ml of 5% of D-sorbitol and incubated at room temperature with intermittent shaking. This was followed by centrifugation at 2,000 rpm for 5 minutes and the pellet was resuspended in 5 ml RPMI complete media. The mixture was centrifuged as above, the supernatant discarded and 35 ml of RPMI medium added to the parasitised RBC pellet then transferred into a 72-cm^2 culture flask. The gassing phase was applied as described above and the flask incubated at 37 °C.

2.9 Preparation of Free Parasites from Erytrocytes

Prior to western blot and kinetic studies, the malaria parasites were extracted from the erythrocytes. The synchronised culture (~10% trophoziotes) was centrifuged at 2,000 rpm for 5 minutes and the supernatant discarded. The pellet was saponised using PBS and 20 mM

glucose, using a final saponin concentration of 0.15%. The mixture was gently shaken for 30 seconds then centrifuged at 2,500 g for 5 minutes at 4 °C. The supernatant was carefully discarded and the pellet resuspended in cold (filtered) sterile intracellular buffer (110 mM KCl, 30 mM NaCl, 2 mM $MgCl_2$, 20 mM glucose and 5 mM HEPES) pH 7.4 followed by centrifugation at 3,000 g for 5 minutes at 4 °C . This step was repeated 3 times and finally the parasite pellet was resuspended in 1.0 ml intracellular buffer. This wet preparation was then used to check the viability of free parasites under a light microscope. The pellets were kept at -80 °C for future use.

2.10 Glycerol Bacterial Stock

E. coli glycerol stock was prepared using 50% (v/v) sterile glycerol stock and 500 µl of bacterial suspension in Luria Bertani broth (LB) consisting of tryptone, yeast extract and NaCl (Sigma Aldrich, UK) with appropriate antibiotics. The bacterial suspension was kept at -80 °C for future use.

2.11 Agarose gel electrophoresis

Agarose gels were used to separate the DNA fragments in the PCR products or from the restriction enzyme digestions. In this study 12.5% agarose gels were prepared (Sigma Aldrich, UK) in 1 x Tris.acetate.EDTA (TAE) consisting 40 mM Tris, 20 mM acetic acid, 1 mM EDTA pH 8.0 (Sigma Aldrich, UK). The mixture was heated for 2 minutes in a microwave oven and cooled at room temperature before adding 0.5 µg/ml of ethidium bromide (Sigma Aldrich, UK). The gel solution was poured into a gel cast on flat surface to avoid bubbles. DNA samples and 6 x loading dye (Invitrogen, UK) were mixed in 1.5 ml tube and followed by quick centrifugation. The DNA samples were loaded and electrophorosed for

30- 40 minutes at a constant current of 90 volts. Once completed, the gel was visualised by UV illuminator (SYNGENE BIOIMAGING, UK) and analysed using Genetools analysis software (Syngene Synoptics Ltd. Cambridge, UK). The DNA fragments were compared with DNA Molecular Weight marker (Invitrogen, UK).

2.12 Determination of Protein Concentration

The Bradford assay (Bradford, 1976) was carried out to determine the protein concentration used for SDS gel electrophoresis and to quantify the specific enzyme activity from free parasite preparations. The reaction was set up using the Bio-Rad Reagent (Bio-Rad, UK) and diluted with distilled water in a 1:4 ratio. A standard curve was generated using bovine serum albumin (Sigma Aldrich, UK) at concentrations ranging from 0.2-0.9 mg/ml. The protein samples were prepared in a serial dilution ranging from 1 in 2.5 to 1 in 35. In this assay, 2 µl of unknown protein concentration was used. For accuracy 3 replicates were performed. The automated dispenser, Varioskan (Varioskan™, Thermal Corporation),was used to resuspend 200 µl Bradford Reagent into a 96 well plate. The plate was incubated for 5 minutes at room temperature. Finally, the protein concentration was analysed using Skant® Software (Varioscan™ , Thermo Corporation) with the absorbency was set at 595 nm.

2.13 SDS Gel Electrophoresis

SDS gel electrophoresis is a technique used to separate protein samples according to their molecular weight. In order to get good separation of protein samples, the right percentage must be selected. The percentage of resolving gels used included 12.5%, 10% or 7.5%. The monomer solution of resolving gel consisted of Acrylamide/bis-acrylamide

solution, (30%/0.8% w/v) (Bio-RAD, UK) distilled H_2O, 1.5 M Tris-HCl (pH 8.8) (Sigma Aldrich, UK), 10% (w/v) SDS (Sigma Aldrich, UK), 20% ammonium persulphate (APS) (Sigma Aldrich, UK) and 10 µl N,N,N\N'-tetramethylethylenediamine (TEMED) (Fluka, UK) per 10 ml gel mix. The monomer solution was mixed gently and poured into glass plates assembled by instructions from the Mini-Protean III Electrophoresis Manual (Bio-RAD UK). The gel was overlaid with water-saturated n-butanol to ensure an even surface and reducing conditions for polymerisation. After the gel had polymerised, the butanol was removed by capillary action using a paper towel. The stacking gel, a 4% monomer solution, was prepared with the following: 0.6-ml 30% (w/v) arylamide/bis (Bio-Rad, UK), 3.05 ml H_2O, 1.25-ml 0.5 M Tris-HCl (pH 6.8), 50-µl 10% (w/v) SDS, 25-µl APS and 5-µl TEMED. This mixture was poured over the resolving gel with the comb fitted and allowed to polymerise for 30 minutes at room temperature.

2.14 Sample Preparation for SDS-PAGE

The different protein sample concentrations were determined using Bradford assays as described in section **2.12**. For each sample, 20 to 50 µg of the protein sample was mixed with an equal volume of 2 x sample loading buffer (50 mM Tris-HCl, pH 6.8, 2% SDS, 10% (v/v) glycerol, 1% (v/v) β-Mercaptoethanol, 12.5 mM EDTA, 0.02 % (w/v) bromophenol Blue). Prior to gel loading, the samples were boiled for 5 minutes at 90 °C. The proteins were separated on SDS-PAGE using 1 X SDS- running buffer (0.196 M glycine, 48 mM Tris-base, 0.04% (w/v) SDS, pH 8.3) at a constant current of 60 milliamps for 60 minutes. For immunoblotting, protein samples were run on duplicate gels; one gel for immunoblotting and the other for stained with Expedion instant blue (a Comassie Blue based staining solution) (Expedion, UK). Staining was carried out for 30 minutes with slow agitation, followed by destaining in distilled water. The prestained, broad range protein marker Spectra^{TM} Multicolor

Broad Range Protein Ladder (Fermentas, UK) was then used to estimate the resulting protein band sizes.

2.15 Silver Staining

The eletrophorosed SDS gel used for silver staining was washed using distilled water for 30 minutes. The gel was then incubated in 0.03% (w/v) sodium hydrosulphite for 2 minutes and again washed in distilled water. This was then incubated in 0.1% (w/v) silver nitrate solution (0.2 g $AgNO_3$, 200 ml H_2O, 0.02% formaldehyde) for 40 minutes before finally washing with distilled water. The reaction was stopped using silver stopping solution (5% (v/v) acetic acid) for 2 hours at room temperature.

2.16 Western Blot Analysis

For immunoblotting, the SDS gel was not stained but equilibrated in Towbin's transfer buffer (20 mM Tris-HCl, pH 8.3, 150 mM glycine, 20% (v/v) methanol) for 15 minutes at 4 °C. A sheet of nitrocellulose membrane and six sheets of 3-mm Whatman filter paper were cut to the size of the gel and soaked in transfer buffer for 5 minutes at 4 °C. The separated proteins were then transferred from the gel to the membrane using a Mini Trans-Blot® Electrophoretic Transfer Cell (Bio-Rad, UK) for 1 hour at 250 milliamps.

After the transfer, the membrane was immersed in blocking buffer consisting of 3% skim milk in TBS-T (137 mM NaCl, 20 mM Tris, 0.1% Tween-20) at 4 °C overnight, then incubated with primary polyclonal antibody in blocking buffer supplemented with 3% (v/v) skimmed milk at room temperature for 2 hours. The blot was washed 3 times (10 minutes per

wash) in 1 x TBS-T. The membrane was incubated for 1 hour in horseraddish peroxidase conjugated secondary antibody at a dilution of 1:10,000 in blocking buffer and slowly agitated at room temperature. Following incubation, the membrane was washed 3 times (10 minutes per wash) with 1 x TBS-T buffer. After washing, the membrane was incubationed with 1:4 ratio of developing solutions A:B (Amersham General Health, UK) for 5 minutes. The membrane was then placed in a cassette and exposed to Kodax BioMax MR Film (Kodax, UK). The intensity of the signal was adjusted depending on the time of exposure, in this case between 5 and 60 minutes.

Chapter 3: The Expression Profiles of Selected Metabolic Genes of *P. falciparum* from Laboratory Adapted and Atovaquone Resistant Strains

3.1 Introduction

The completion of the *P. falciparum* genome revealed a large number of genes which provide new insights into the biology of the parasite, the parasite-host interactions and pathogenesis, and which may eventually lead to identification of potential of new drug targets and vaccines. The *Plasmodium* covers ~23 megabase pairs genome comprised of 14 linear chromosomes, a circular plastid-like genome (apicoplast) and a linear mitochondria genome (25). Sequencing study by Gardner et al. (2002) estimated that malaria genome consists of more than 60% of the 5,409 predicted open reading frames (ORFs) and lack of similiarity with other known organism. Furthermore, the genomic nucleotide composition contains more than 80% A/T in coding regions and 90% in non-coding regions.

Over the last decade gene expression profiling has become an important tool in functional genomics and drug discovery. The study of gene expression in the genome has been recognised as transcriptomics. Gene expression is a measurement of the expression level of the genes as a result of transcription of DNA into messenger RNA (mRNA). Several molecular techniques have been developed for the high throughput analysis of gene expression such as DNA microarray, real-time PCR, massive parallel signature sequencing (MPSS), and serial analysis of gene expression (SAGE). These technologies provided tools

for researchers to address the roles of multiple genes in the complex cellular functions of *Plasmodium* (293).

The human malaria parasite *P. falciparum* expresses different types of proteins throughout of its life cycle. Mass spectrometry analyses reveal that at least 2391 genes are transcribed and translated into proteins in one or more stages of the parasite life cycle (74, 147). Florens, et al. (2002) reported that sporozoites distinctively express proteins which are unique to this stage. The proteomics studies also reveals that proteins involved in processing mRNAs and in protein synthesis (translation) are expressed at higher levels in gametocytes particularly female gametocytes than in other stages (285). The housekeeping genes are the most common genes and are expressed throughout the life cycle of *Plasmodium*. The housekeeping genes encode approximately 136 housekeeping proteins which include ribosomal proteins, transcription factors, histones and cytoskeletal proteins (97). Apart from the housekeeping proteins, the parasite expresses 472 crucial proteins which involved in the development of the parasite during the asexual replicative stages and 234 proteins are involved in parasites binding to the human host cell (invasive stages). There are 'host-specific genes" that encode 229 proteins present in mosquito and 417 proteins in mammalian host (77).

Many studies on the transcriptome rely on the microarray results and are quantitatively measured using real time PCR. Comparison studies of the transcription profile of mRNA and the translated protein in *P. falciparum* are still limited. The malaria parasite has an S-shaped wave of transcript pattern where 3,000 genes are expressed during the intraerythrocytic stage (25, 150, 156). The transcriptional regulation is rigidly programmed (hard-wired) and is not

greatly affected by environmental or drug perturbations (81, 112). This is unlike other organisms, such as *S. cerevisae*, *M. tuberculosis* and *Candida albicans* in which the mRNA transcription is more responsive to environmental or chemical perturbations (11, 24, 48, 81, 283).

Like other eukaryotic cells, *P. falciparum* is also equipped with transcriptional regulatory components i.e RNA polymerase II (82), TATA binding protein (TBP) and other putative orthologs to regulate the general transcription machinery i.e TFIIA, TFIIB, TFIIE, TFIIF, TFIID and TFIIH complexes (28, 112). The transcription of mRNA in the parasite is strongly regulated by parasite genotype and the factors responsible for transcription which are distributed throughout the genome. However, data from the *P. falciparum* genome indicates *P. falciparum* has a limited number of transcription factors (82).

In this chapter we performed an analysis of the expression profiles of mitochondrial genes from major metabolic pathways: glycolysis, the TCA cycle, the mitochondrial electron transport chain and sexual development protein in *P. falciparum* 3D7, 3D7-YDHODH.GFP and TM90-C2B using the Genome Lab™ GeXP Genetic Analysis System by Beckman & Coulter. The sexual development gene profiling is used as an indicator to determine any interference from sexual stages to the parasites genome. The aim of this study is to get a better understanding of the molecular changes that may be present in atovaquone resistant parasites (TM90-C2B) compared to 3D7. The 3D7-YDHODH.GFP strain is a transgenic 3D7 strain containing the yeast dihydroorotate dehydrogenase gene (yDHODH) which has previously been shown to confer an atovaquone resistant phenotype (Painter et al.,2007) and here is used as a control strain as it should have a similar gene expression profile to the parent 3D7. Of particular interest in this chapter is to determine whether the putative Y268S mutation (as it

has not been confirmed) in the bc_1 enzyme conferring atovaquone resistance in TM90-C2B parasites is accompanied by changes in gene expression of respiratory enzymes or related genes of energy metabolism.

3.2 Materials and Methods

3.2.1 Malaria Parasites

Three different *Plasmodium falciparum* malaria parasites were used in these studies; *P. falciparum* 3D7 (reference strain), TM90C2B the atovaquone resistant field isolate strain and 3D7-YDHODH.GFP. The atovaquone resistant TM90C2B was generously provided by Professor Dennis Kyle (College of Public Health, University of South Florida, USA) and was first isolated during a clinical phase 2 study to determine atovaquone efficacy in Thailand. 3D7-yDHODH·GFP, a transgenic derivative of *P. falciparum* 3D7 containing yeast dihydroorotate dihydrogenase gene was generated through electroporation of purified pHHyDHOD–GFP plasmid into ring stages of *P. falciparum* using a BioRad GenePulser (BioRad, UK) was prepared by David Johnson, Molecular and Biochemical Parasitology Group, Liverpool School of Tropical Medicine, UK. Purified pHHyDHOD–GFP plasmid was generously provided by Professor Akhil Vaidya (Drexel University College of Medicine, Philadelphia, USA). This plasmid contains a human dihydrofolate reductase gene as a WR99210-selectable marker (203). The parasites were grown in complete culture medium as described in section **2.1**.

3.2.2 Total RNA Extraction from *P. falciparum*

Total RNA extraction from ~10% synchronised trophozoite parasites of *P. falciparum* 3D7, 3D7-yDHODH·GFP (TX13) and TM90C2B falciparum malaria were carried out

following a modified protocol described by Lescuyer *et al* (1997). The parasites used for the RNA extraction were kept highly synchronous (>99% of tropozoite stage) using repeated cycles of the sorbitol-lysis technique (was described in section **2.9**), in order to avoid any potential cell-cycle dependent differences in gene expression. For RNA extraction, parasites were sedimented by centrifugation (3,000 x g for 5 minutes) followed by washing the parasite pellet in 5 volumes of cold PBS pH 7.4 and lysis in 0.05% saponin. Once the lysis of RBC was observed, the mixture was quickly spun at 5,000 x g for 5 minutes at 4 °C. The supernatant was discarded and the pellet was re-suspended in 1 ml of TRIzol reagent (Invitrogen, UK) for 10 minutes. The suspension was transferred into 1.5 ml RNase free microcentrifuge tubes and stored at -80 °C. The TRIzol parasite suspension was thawed on ice and mixed with 200 µl of chloroform ($1/5^{th}$ of total reaction volume). The mixture was vigorously shaken and then centrifuged at 10,000 x g for 15 minutes at 4 °C. The aqueous phase was removed and RNA was precipitated by adding an equal volume of ice cold isopropanol and incubated for 15 minutes at room temperature. After 15 minutes at room temperature the RNA was recovered by centrifugation at 10,000 x g for 10 minutes at 4 °C. The pellet was then washed with 75% (v/v) ethanol followed by centrifugation at 10,000 x g for 10 minutes. The RNA pellet was air dried at room temperature in a laminar flow hood for 10 minutes. The RNA pellet was re-suspended in 100 µl RNase-free water and followed by incubation at 60 °C for 10 minutes. The quality and concentration of extracted RNA was measured using NanoDrop spectrophotometer (NanoDrop Technologies, UK). The RNA is stored at – 80 °C until ready for cDNA synthesis. The RNA extraction from the *P. falciparum* strains was performed on at least 3 independent occasions. Aliquots of 75 ng from each pool of total RNA served as template for making target specific cDNA by reverse transcription in a single multiplex assay using the GenomeLab GeXP Start Kit (Beckman Coulter, UK) and the gene- specific primers.

3.2.2 qPCR Expression Study

3.2.2.1 Primer Design

Primers were designed using GenomeLab eXpress Profiler software (Beckman Coulter) following the GenomeLab TM User's Guidelines. The multiplex primers and genes are listed in appendix A1. The 48 genes were identified and selected for multiplex primer design. 23 genes encode enzymes of glycolysis, 14 genes component of the mitochondrial electron transport chain, 8 genes enzymes of the *Plasmodium* TCA cycle, 1 gene a protein involved in sexual development and 2 were normalisation genes (housekeeping genes). Nucleotide sequences of the genes were obtained from PlasmoDB data base (WWW.PlasmoDB.org). As an internal control a kanamycin resistance gene (KAN^r) was used in the PCR reactions. Each primer has a gene specific sequence and each primer is appended with a universal primer sequence by the software. The multiplex primer sets were custom made by Invitrogen, UK. GeXPS primer stocks (forward and reverse primers) were diluted in Diethylpyrocarbonate (DEPC) treated water (AMBION, UK) to final concentrations of 500 nM and 200 nM respectively.

3.2.3 RT and PCR

The RT reaction and PCR steps were carried out according to the manufacturer's recommended protocol (GenomeLab TM GeXP Start Kit, Beckman Coulter). A summary of the RT and PCR reactions is illustrated in Figure 3.1. The RT reaction was carried out in a 20-µl total volume reaction with a final concentration of 1 x RT buffer, 1 unit/µl reverse transcriptase and 500 nM reverse primer plex. 5 µl of KAN^r RNA was added per reaction which consisted of 25 ng/µl of *P. falciparum* total RNA. The RT reactions were as follows: 48 °C for 1 minute, 37 °C for 5 minutes, 42 °C for 60 minutes, 95 °C for 5 minutes and final hold at 4 °C. This was followed by PCR reaction of 20 µl volume with a final concentration

of 1 X PCR buffer, 5 mM $MgCl_2$, 200 nM forward primer, 0.7 µl of Thermo-Start DNA Polymerase (ABgene) and 9.3 µl of RT reaction sample. The PCR parameters were set at 95-°C for 10 minutes, 35 cycles of 94 °C for 30 seconds, 55 °C for 30 seconds, 68 °C for 1 minute and a final hold at 4 °C. Both RT and PCR reactions were carried out in BIORAD thermal cycler.

3.2.4 Gene Expression Analysis

The 40-µl reaction for GeXP analysis contained 1 µl undiluted PCR product, 0.5 µl DNA Size Standard-400 and 3.8 µl sample loading solution and run on a GenomeLab TM GeXP Genetic Analysis System (Beckman Coulter). The fluorescently labelled PCR fragments are separated by capillary electrophoresis based on size and detected and quantified by the GeXP Frag-3 system. To validate the experimental assay, a minimum of 3 replicates of every *Plasmodium* strain were used in this study. The result of GeXP was initially analysed using the Fragment Analysis module of the Genome Lab GeXP software. The GeXP software matches each fragment peak with the appropriate gene, and reports peak height for all peaks in the electrophortogram. As an extra precaution, manual analyses of the results were also carried out to validate data from the GeXp software programme. The pre-analysed data were subsequently exported to analyses using eXpress Profiler analysis software following manufacturer's protocols (Beckman Coulter 2004). Non-specific peaks were filtered out and expression was normalised using PF13_0305 elongation factor 1 alpha as the house keeping gene. The normalised gene expression data were then exported to Microsoft Excel 2007 for further analysis. Finally, Mann-Whitney test was performed to analyse the expression data using GraphPad Instat 3.

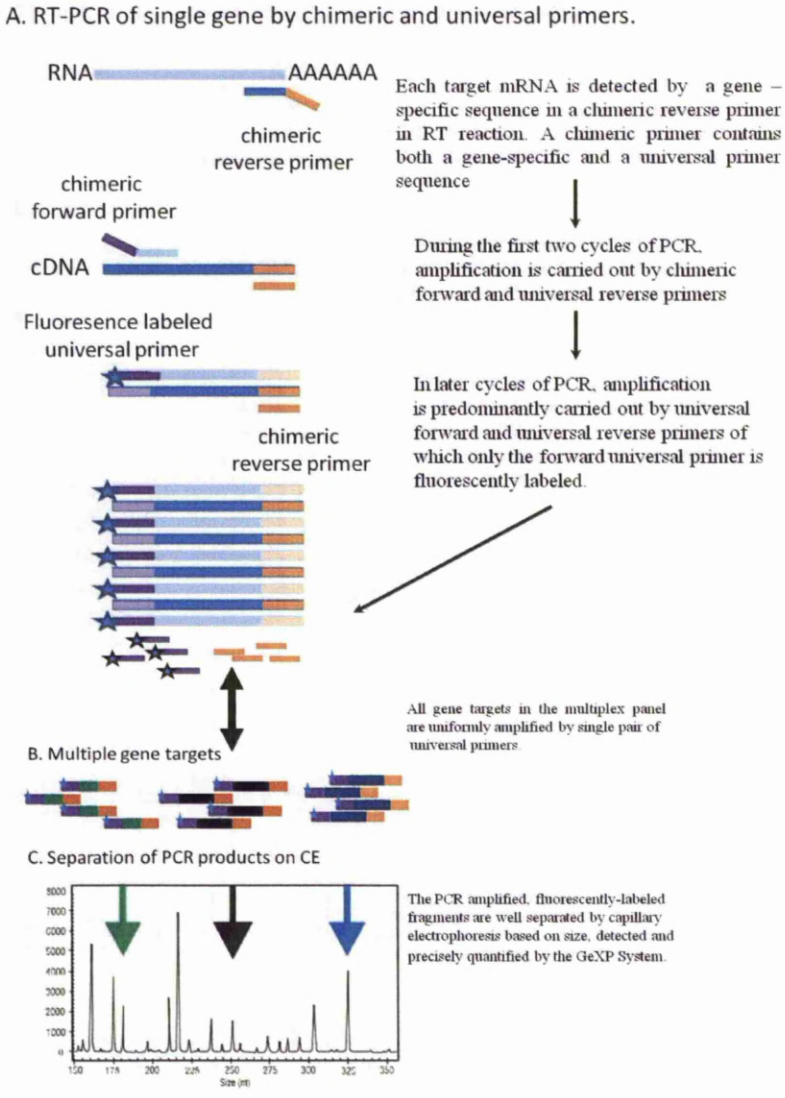

Figure 3.1: Schematic Illustration of Multiplex RT-PCR Assay

(A)Represents the reverse transcription and amplification using a universal tag at the 5' end of the chimeric primers. This step is followed by the conversion of a single pair of amplicons to synthesise a double stranded DNA template using the universal primers. (B) The PCR products from multiplex amplification were analysed using fluorescence capillary electrophoresis. The peak location represents the gene identity, and the peak area represents the gene expression level. (C) The multiplex PCR amplification products were analysed by fluorescence capillary electrophoresis and gene expression profiling are analysed using GeXp software programme. Adapted from BeckmanCoulter–Genome Lab^{TM} Genetic Analysis System.

3.2.5 Sequencing cytochrome b and the Rieske Iron-sulphur Protein of *P. falciparum* TM90C2B

The sequences of the primers used for *Pfx*-mediated PCR amplification of the genes encoding cytochrome *b* and the ISP from TM90C2B cDNA were as follows: Cyt *b* (forward) 5'-ATGAACTTTTACTCTATTAATTTAG; Cyt *b* (reverse) 5'-TATGTTTGCTTGGGAGCTGTAATC; ISP (forward) 5' ATGAATATTAAATATGTGGAAC; ISP (reverse) 5'-TCCAATTTTTATCGTATTTTCAT. The PCR reaction consisted of 96 °C for 10 minutes followed by 25 reaction cycles with melting (45 seconds), annealing (45 seconds) and extension (2 minutes) temperatures of 96-, 45- and 68 °C respectively, with a final 10 minute extension at 68 °C. The PCR reaction buffer contained 1 mM $MgSO_4$, 100 ng TM90C2B cDNA, 0.25 mM dA/C/G/TTP (1 mM total dNTP), 1x *Pfx* proprietary reaction buffer (Invitrogen), 2 µM forward/reverse primers and 1 unit of *Pfx* DNA polymerase (Invitrogen). Total reaction volume was 50 µl. The PCR reaction products were purified by 2% (w/v) agarose gel electrophoresis and sent for automated DNA sequencing (Lark Technologies, UK). Sequence chromatograms were inspected using the 4Peaks software package (mekentosj.com).

3.3 Results

3.3.1 Transcriptional Expression Profiles of Energy Metabolism Genes in Atovaquone Sensitive and Resistant Parasites

Quantitative RT-PCR was performed to determine the expression of energy metabolism genes from 3D7, 3D7-yDHODH·GFP and TM90C2B parasites. 48 candidate genes of energy metabolism from 3D7, 3D7-yDHODH·GFP and TM90C2B parasites were analysed using GeXP multiplex PCR. Data from each expression gene were normalised with

PF13-0305 elongation factor 1 alpha (housekeeping gene). Only 36 genes were able to generate amplifications that could be reliably analysed by eXpress Profiler analysis software. These 36 genes included those involved in glycolysis/fermentation, specific subunits of mitochondrial electron transport chain complexes, mitochondrial dehydrogenases and mitochondrial TCA cycle genes. Expression profiles from the various strains were measured from RNA taken from trophozoite-stage parasites on at least 3 independent occasions, expression was then normalised against the expression of a reference gene, elongation factor 1 alpha (see methods). Mean expression levels ($n \geq 3$) for all of the genes from the three strains are given in appendix 3. Figure 3.2 and 3.3 depict the relative fold change in gene expression for (a) 3D7-yDHODH·GFP/3D7 and (b) TM90C2B/3D7. The transgenic 3D7-yDHODH·GFP strain was generated from the 3D7 parent strain, therefore as expected, there was relatively little difference in the fold change in gene expression expressed as 3D7-yDHODH·GFP/3D7 (Figure 3.2). From this data also show that the gene expression values fell at or near 1 with the exception of the gene for NAD glutamate dehydrogenase.

Analysis of the fold change in gene expression of the atovaquone resistant strain TM90C2B compared to the atovaquone sensitive 3D7 strain revealed some significant differences between the two strains. Of note was the ~2 fold increase in expression of Complex III and Complex IV genes which included cytochromes *b*, *c* and c_1, the Rieske (ISP) subunit of bc_1, and subunits 1 and 2 of cytochrome *c* oxidase. Other genes also shown to be significantly up-regulated in expression by 2 fold included the hexose transporter, phosphoglycerate kinase and succinylCoA synthetase (Figure 3.3 and appendix 3). Both TM90C2B and 3D7 are able to generate gametocytes in the laboratory. Analysis of the sexual development gene pfs16 (PF11_0318) revealed no change in expression levels during replicates or between strains as shown in Figure 3.3 and appendix 3.

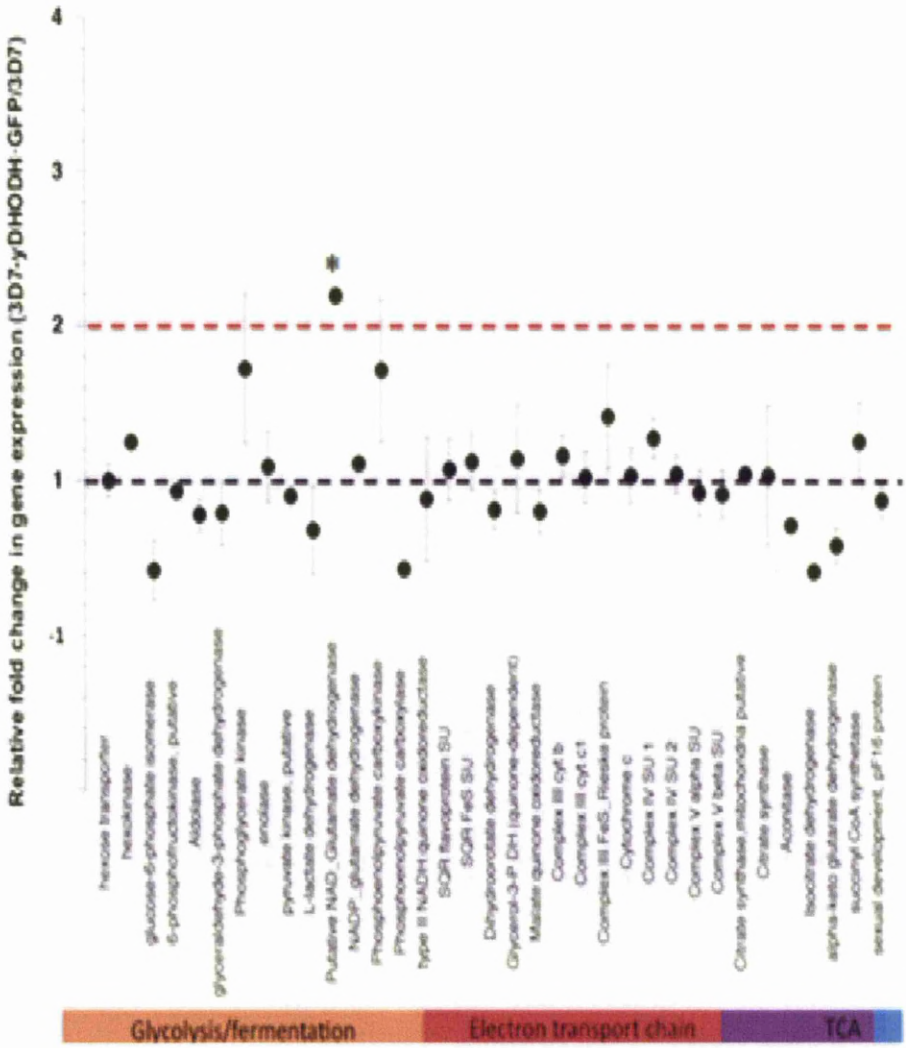

Figure 3.2: Relative Fold Changes in Gene Expression of Energy Metabolism Genes between Wild type (3D7) and Transgenic (3D7-yDHODH·GFP) *P.falciparum* Parasites

The relative fold change in gene expression for 3D7-yDHODH·GFP/3D7. Expression data is normalised against a reference gene (elongation factor 1 alpha) and is displayed as a mean fold change ± S.D from $n \geq 3$ independent experiments. Mean expression data ± S.D. ($n \geq 3$) is shown in Table S2. Asterix denotes significant difference $P \leq 0.05$.

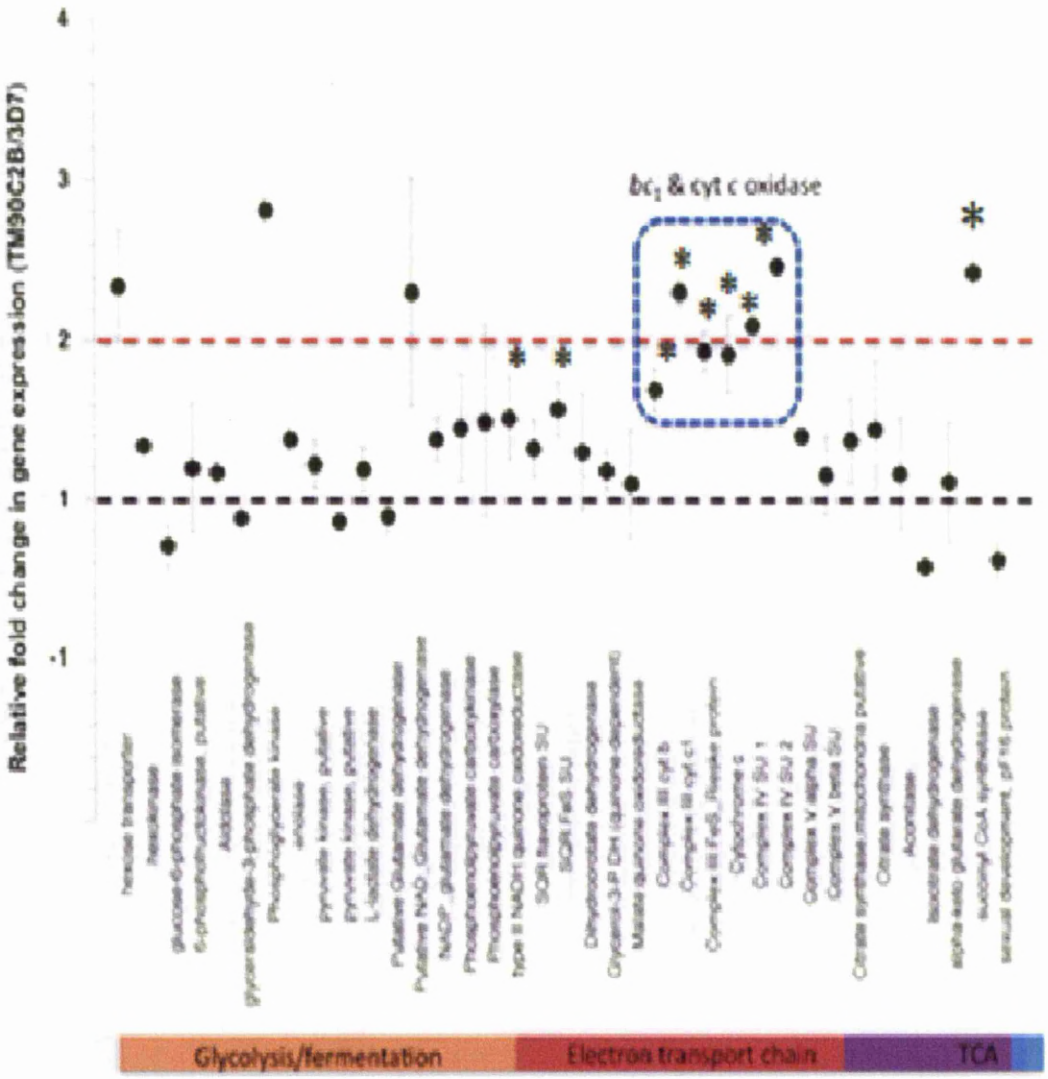

Figure 3.3: Relative Fold Changes in Gene Expression of Energy Metabolism Genes between Wild type (3D7) and Atovaquone Resistant (TM90C2B) *P. falciparum* Parasites

The relative fold change in gene expression for TM90C2B/3D7. Expression data is normalised against a reference gene (elongation factor 1 alpha) and is displayed as a mean fold change ± S.D from $n \geq 3$ independent experiments. Mean expression data ± S.D. ($n \geq 3$) is shown in Table S2. Dashed blue box indicates genes encoding for components of mitochondrial Complex III and IV. Asterix denotes significant difference $P \leq 0.05$.

3.3.2 Automated Sequencing of bc_1 Cytochrome *b* gene

Result from the automated sequencing of the mitochondrial cytochrome *b* gene PCR-amplified from *P. falciparum* TM90C2B cDNA confirmed the mutation of adenine to cytosine at nucleotide 803, resulting in the replacement of tyrosine by serine at amino acid position 268 (Figure 3.4). No additional mutations were observed in the nucleotide sequence of TM90C2B cytochrome *b* or the Rieske protein when compared to the control DNA (*P. falciparum* 3D7, data not shown).

3.4 Discussion

The GeXP analyser (Beckman Coulter) has been used for multiplex analysis of *Plasmodium* genes. The GeXP system uses capillary electrophoresis-based separation of modified endpoint PCR reactions to provide the relative intensity versus size for the targeted amplicons of RNA samples. The advantage of GeXP technology compared to the other technologies is that this system can analyse up to 35 genes using area under the curve (AUC). The AUC value represents the level of the transcription of individual gene. The expression of the individual genes will therefore be normalised with the house keeping gene which is also incorporated into the multiplexes (218). However, in this study only 36 out of 48 genes were able to be analysed confidently with $n \geq 3$. This is due to each multiplex primer requiring individual optimisation due to the dynamic range of the various genes. The quantitation of the expression level of the genes within the multiplexes is extremely variable. The level of gene expression is controlled by the abundance of the gene present in the genome. Some of the genes probably are low, moderate or highly abundant. Therefore removing or adding of multiplexes requires optimisation and this is an empirical process (218).

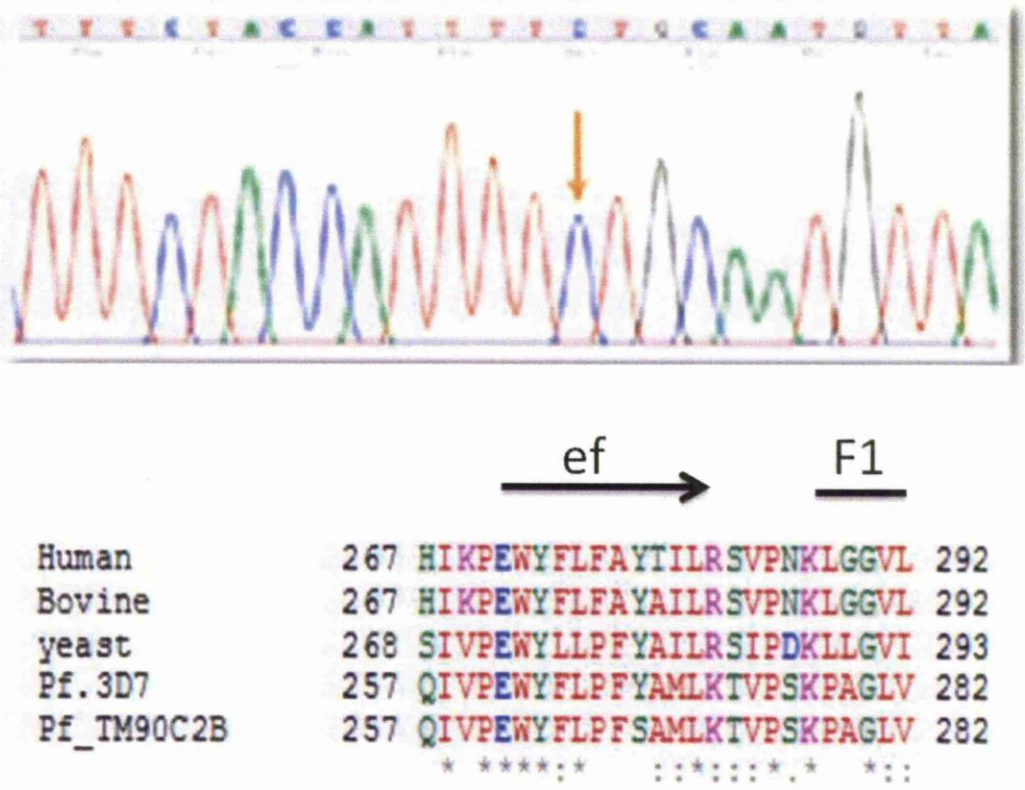

Figure 3.4: Automated DNA Sequencing of the Mitochondrial Cytochrome *b* Gene of TM90C2B

Automated DNA sequencing of the mitochondrial cytochrome *b* gene PCR-amplified from *P. falciparum* TM90C2B cDNA confirmed the mutation of adenine to cytosine at nucleotide 803, resulting in the replacement of tyrosine by serine at amino acid position 268. The consensus line shows (★)indicate identical residues; (:) indicate semi-conserved residues; (.) designated conserved residues.

In this chapter we have attempted to determine whether there is differential gene expression between the atovaquone resistant strains TM90C2B, 3D7-yDHODH·GFP (TX13) and the sensitive strain 3D7. Many studies have been conducted to investigate the underlying mechanisms of *Plasmodium* drug resistance. In many cases, the resistance mechanisms are mainly due to polymorphisms e.g mutation in the *pfcrt* gene for CQ resistance, point mutations in *pfdhfr* and *pfdhfs* conferring pyrimethamine and sulfadoxine resistance respectively, and *cyt b* point mutations conferring resistance to atovaquone.

The polymorphisms in the DNA sequence confer drug resistance through the changing of amino acid sequence of the protein product. Continuous exposure to the drugs may induce alternative mechanisms of gene regulation in the parasite genome to overcome the selective pressures of antimalarial drugs. The parasites regulate their gene function via the overexpression of transporter genes e.g *pfcrt* and *pfmdr*1, induction of alternative pathways to bypass the effect of the drug and repression of genes that control deleterious effects of the drugs (156).

In general mutations in DNA sequence result in major physiological changes even if the amino acid coding region is unchanged (50). However, in *Plasmodium* parasite, the determinant transcriptional regulation is still remain elusive (89). In this study it was possible to amplify most of the important genes involved in the mitochondrial electron transport chain. The TM90C2B strain is a clinical isolate which previously showed resistance to atovaquone. From genetic sequencing data it was shown that atovaquone resistance in this strain is probably conferred by a point mutation at position 268 cytochrome *b* of the parasite where tyrosine is replaced by serine (Y268S). Mutations at this site conferring atovaquone resistance

have been reported previously and have also included replacement of the tyrosine by asparagine or cysteine (29, 188, 241). This 268 codon of the *cytb* gene is a region encoding for the quinol oxidation site (Q_o) (131, 135). This phenomenon is also documented in another *Plasmodium* species (*P. yoelii*) (246).

Chapter 4 of this thesis describes the biochemical characterisation of the TM902CB bc_1 containing the Y268S point mutation. Therein it is hypothesised that the Y268S mutation affects the catalytic activity as well as the stability or folding of the bc_1 cytochrome *b*. It is therefore of interest to note that the expression data in this Chapter reveals a significant increase (~2 fold) in the level of expression of *cyt b*, *cyt* c_1 and iron-sulphur Rieske protein genes ($p \leq 0.05$, Mann-Whitney, Figure 3.3) in TM902CB compared to 3D7. In addition to this other mitochondrial complex enzymes are also shown to have a higher level of expression in the TM902CB strain compared to 3D7 including the genes encoding PfNDH2, SQR flavoprotein SU, cytochrome *c*, Complex IV SU1 and SU2 and Complex V alpha subunit. These data may be interpreted as to suggest that either (i) the parasite has upregulated specific genes to accommodate the Y268S cyt *b* mutation or (ii) selective pressure has selected for Y268S parasites that contain higher respiratory enzyme expression, but that this is a through natural variation and not a response by the parasite to drug pressure.

An analysis of transcriptome studies of other *P. falciparum* resistance genes such as *pfcrt*, *pfmdr1* and *pfdhfr-ts* suggests that point mutations do not affect the mRNA transcription level of the gene. The changes in the phenotype of the translated gene are mainly due to post-transcriptional regulation of the genes. Study of *P. falciparum* chloroquine (CQ) resistance shows a single polymorphism at amino acid 76 where lysine is replaced by thereonine

(K76T). The mutation of *pfcrt* gene has been identified as responsible for the CQ resistance in *P. falciparum*. Previous study of the transcriptome profiles of the parasite response to CQ showed the amplification of the *pfcrt* gene which led to the development of resistant parasites (94). However, the recent finding from the same authors indicates the mRNA level of the *pfcrt* is not affected by the drug perturbation (93), therefore indicates that there is no correlation between the *Pfcrt* mRNA expression level and CQ sensitivity (32, 56).

Johnson et al. (2008) demonstrated that the expression of PGH1 protein is increased in parasites pre-treated with phenobarbitone. PGH1 is the protein product of *pfmdr1*. This finding is supported by western blot analysis demonstrating a marked increase in the expression of the *P. falciparum* ABC transporter (118). However recent studies indicate increasing copy number does not necessarily confer drug resistance on its own (32). The drug resistance due to polymorphism of *pfmdr1* has no direct effect on parasite resistance to antimalarial drugs but it may involve other genes in the *Plasmodium* genome (32, 220).

Microarray and RT-PCR transcriptome studies on the *pfdhfr* conducted by Ganesan et al. (2008) demonstrated that DHFR-TS expression is slightly increased in Dd2 *P. falciparum* treated with WR99210. The Dd2 parasite clone was originated from clone W2 from Southeast Asia and is resistant to some antimalarial drugs but not WR99210. Results from their studies showed there are no significant differences between treated or non-treated cells with WR99210. They also demonstrated that the mRNA levels for the genes responsible for enzymes of pyrimidine or folate metabolism are not affected.

From this study most of the TM90C2B genes responsible for glycolysis and TCA cycle were not affected by the mutation in the bc_1 complex. This is in accordance with the finding from previous study by Llinas et al. (2006) which showed the genes belong to the functional categories such as glycolysis, cytoplasmic transcription, translation, the TCA cycle, the proteasome and plastid biosynthesis are tightly regulated in their gene expression profiles of 3 different *P. falciparum* strains (3D7, susceptible strain; Hb3, pyrimethamine resistant and Dd2, chloroquine resistant). From their findings gene regulation between species is similar. However, in a recent study genes responsible for specific metabolic pathways such as energy metabolism and nucleotide synthesis were shown to be down regulated at the ring stage of a *P. falciparum* artemisinin resistant strain and transcription of genes associated with protein metabolism significantly increased after the parasite matures (184). This is probably counteracting mechanisms of the parasite to fix the damage response caused by the the oxidative stress and/or protein alkylation of this drug (184).

Other genes which showed higher levels of expression in TM902CB compared to 3D7 (and 3D7-yDHODH·GFP) included the hexose transporter (PFB0210c), phosphoglycerate kinase and enolase. These are some of the genes whose products are responsible for the *Plasmodium* glycolytic pathway. The hexose transportor has been reported to be highly expressed during active stages in the *Plasmodium* life cycles (trophozoites and schizonts) (136). The hexose transporter is involved in the transport of fructose and glucose from the host plasma. From this finding we can hypothesise that atovaquone resistance may lead to a fitness cost (due to the reduced catalytic activity of the Y268 bc_1) which can be offset by an increase in glucose catabolism facilitated by an increase in glucose uptake. *Plasmodium* is dependent on glucose supply for growth and uses more glucose to generate ATP via fermentation during the trophozoite and schizont stages (78, 136, 199). Consistent with this

hypothesis our observation in the laboratory is that the growth rate of TM90C2B is slower than 3D7. This is in accordance with a study conducted by Fisher et al. (2004) who demonstrated that the growth rate of transgenic yeast with mutation at Y279C equivalent to the *Plasmodium* Y268 site(67, 127)had a two fold slower doubling time than the wild type yeast.

The gene expression of the 3D7-yDHODH·GFP strain was almost identical to the parent 3D7 strain, providing quality assurance of the methodology and robustness of the study. The only gene that was shown to be differentially expressed between 3D7 and 3D7-yDHODH·GFP was the putative (fungal-like) NAD-glutamate dehydrogenase (PF08_0132). Apart from this enzyme, *Plasmodium* also encodes another 2 genes for glutamate dehydrogenase (GDH); apicoplast NADP-dependent enzyme (PF14_0286) and cytosolic NADP-GDH (PF14_0164). Apicoplast NADP-dependent is targeted to the apicoplast in the generation of acetyl-coA for fatty acid metabolism and the cytosolic form is speculated to be involved in redox homeostasis in the *Plasmodium* mitochondria. To date there is very little information relating to the function of the fungal-like NAD-dependent GDH (199) and more studies will need to be conducted in order to explain the observed differential expression in the two strains. In this study some of the primers failed to amplify the targeted genes from the *P. falciparum* genome. Individual multiplexes would be required to optimise and probably some degree have to re-synthesis. Some of the primers used in this study were able to amplify the targeted gene in any of the *P. falciparum* strains, but there are some primer pairs fail to amplify. This is might be due to the small percentage of the targeted genes present in the genome, therefore leads to produce inaccurate expression value.

To date various high throughput technologies have been invented to either qualitatively or quantitatively measure groups of genes in a single analysis. Microarray technology is the most widely used in transcriptomic profiling of thousands genes from various group organisms. However, this technology has disadvantages such as a difficulty in analysing results of individual gene and cross hybridisation of signal between genes which can produce false positive or negative results, lack of optimisation of standard procedures and also not being cost effective for large samples. Therefore the GeXP profiling system provided an alternative technology in the study of gene quantitation. The results from the expression study must be analysed carefully. Direct evidence studies must be carried out in order to validate the data obtained from qPCR studies. Biochemical studies on the upregulated genes can be monitored by enzyme kinetics study. The translated protein also can be measured qualitatively using western blotting analysis because mRNA levels do not necessarily correlate with protein translational levels due to the presence of post-transcriptional gene silencing in *P. falciparum* (150, 237).

In conclusion, this chapter has described the transcriptional profile of energy metabolism genes from three strains with atovaquone resistant and sensitive phenotypes. The gene expression profile of the atovaquone resistant strain TM902CB showed higher levels of expression for genes encoding the bc_1 complex and related respiratory chain enzymes e.g. complex IV, PfNDH2 and Complex II, relative to the 3D7 atovaquone sensitive strain. As the Y268 mutation causes a fitness cost to the parasite, it is hypothesised that the observed differential expression may help the parasite to accommodate this mutation. It is likely that the differential expression patterns observed are more probably a result of selection of natural variation rather than due to a specific upregulation of genes in response to atovaquone. In the next Chapter, a biochemical characterisation of the respiratory enzymes of the 3D7 and

TM902CB strains is described and the results are discussed in context of the expression data presented here.

Chapter 4: Biochemical Characterisation of Atovaquone Resistant *P. falciparum* TM90C2B

4.1 Introduction

Atovaquone is a potent and effective antimalarial drug when used as a fixed-dose combination with proguanil (Malarone™), either for treating children and adults with uncomplicated *P. falciparum* malaria (201) or as chemoprophylaxis for preventing malaria in travellers (145).

Atovaquone, a hydroxynaphthoquinoe, is a competitive inhibitor of ubiquinone (CoQ), specifically inhibiting *Plasmodium* mitochondrial bc_1 activity (79). Loss of bc_1 activity results in a loss of mitochondrial function as evidenced by the collapse of the trans-membrane electrochemical potential (19, 246). It is believed that in asexual parasites, one of the essential functions of the mitochondrion is to provide orotate for pyrimidine biosynthesis through the activity of dihydroorotate dehydrogenase (DHODH). Consistent with this, inhibition of the bc_1 complex by atovaquone results in an increase in carbamoyl-aspartate and a reduction in UTP, CTP and dTTP (107, 292). A link between mitochondrial function and pyrimidine biosynthesis is further supported by the generation of an atovaquone resistant phenotype in transgenic *P. falciparum* parasites expressing CoQ-independent yeast DHODH (203). Atovaquone has also recently been shown to affect the conversion of fumarate to aspartate, further linking mitochondrial function with pyrimidine biosynthesis and also possibly purine metabolism (27).

At the structural level, details of atovaquone binding to cytochrome *b* are based on studies performed on model organisms and molecular modelling since a crystal structure of *Plasmodium* cytochrome *b* with bound atovaquone is not available. This notwithstanding, EPR spectroscopy of the Rieske [2Fe2S] cluster, site-directed mutagenesis of model organism cytochrome *b*, and gene sequencing of atovaquone-resistant *Plasmodium* strains demonstrate that atovaquone is most likely a competitive inhibitor of the parasite's cytochrome *b* Q_o (quinone oxidation) site reviewed in (130) and (14).

Atovaquone-resistant isolates of *P. falciparum* have been described following atovaquone or Malarone™ treatment failures. In these parasite lines, atovaquone resistance is often associated with a missense point mutation at position 268 in cytochrome *b*, exchanging tyrosine for serine (Y268S) or, less frequently, asparagine (Y268N) (16, 68, 72, 135, 188, 234) The resultant atovaquone resistant growth IC_{50} phenotype of these mutants is some 1000 fold higher than sensitive strains.

Position Y268 in cytochrome *b* is highly conserved across all phyla. It is located within the 'ef' helix component of the Q_o site, and it is likely that the side chain of this residue participates in a stabilising hydrophobic interaction with bound ubiquinol. Similarly, molecular modelling indicates a stabilising interaction of Y268 in the binding of atovaquone to yeast cytochrome *b* (130). In yeast, the introduction of the Y268S mutation (Y279S) results in an increase in IC50 for atovaquone inhibition of bc_1 enzymatic activity from 60 nM to >4000 nM (69). However, this is accompanied by a 70% reduction in bc_1 turnover, with EPR analysis showing an alteration of the iron sulphur protein (ISP) signal, indicative of a perturbation of the Q_o site (69, 276).

To date there are no available data on the effect of the atovaquone resistance mutation on the parasite bc_1 enzyme. *Plasmodium* cytochrome *b* shares a high degree of sequence and structural conservation with mammalian and yeast cytochrome *b*, however there are notable differences in key regions of the malaria parasite Q_o site. These include a four-residue deletion in the cd2 helix, which based on a homology model of the *P. falciparum* cytochrome *b* (constructed using bovine cytochrome b atomic coordinates as the structural template (18)) results in a 13-Å displacement of this structural element compared with the mammalian enzyme (18). Likewise, the α-carbon atom of the N-terminal proline of the ef helix (containing the catalytically essential 'PEWY' motif) is predicted to be displaced by 2 Å compared with the mammalian enzyme. The differences in *Plasmodium* cytochrome *b* compared to yeast or mammalian cytochrome *b* are manifested by the varying degrees of susceptibility to Q_o site inhibitors e.g. WR249685 is active at 3 nM against *P. falciparum* bc_1 compared to >13800 nM in bovine bc_1 and >5600 in yeast bc_1 (18).

In the previous chapter I reported the expression profile of energy metabolism genes from atovaquone sensitive and resistant parasites. In this chapter I have investigated the effect of mutation of tyrosine 268 on the enzymatic turnover and stability of *P. falciparum* bc_1.

4.2 Materials and Methods4.2.1 Preparation of Drug Stock Solutions

10 mM of drug/inhibitor stocks were prepared according to their solvent solubility Table 4.1 shows the list of drugs and inhibitors used in this study. Stock solutions were prepared and kept at -20 °C for 1 month. The endoperoxide drugs (artesunate and arthemeter), atovaquone and pyrimethamines were dissolved in dimethyl sulphoxide (DMSO) (Sigma Aldrich, UK) whereas chloroquine and sodium azide were dissolved in 50% ethanol and

distilled water respectively. These final drug dilutions and the rest of inhibitors (stigmatellin, myxothiazol, antimycin, thenyltrifluoracetylacetone (TTFA) and 5-fluro orotic acid) were diluted with culture medium (RPMI) and freshly prepared prior to studies being carried out.

4.2.2 Preparation of Parasite Inoculums

The preparation of the synchronised ring stage of malaria parasites used in drug inhibition assays was described in **Chapter 2 section 2.8** The final parasitaemia (2%) and haematocrit (1%) were prepared using the following formula:

$$\text{Vol. infected RBC required for parasitaemia} = \left(\frac{\text{Desired parasitaemia}}{\text{Actual parasitaemia}}\right) \times \text{total vol. required}$$

Parasite inoculums were prepared by adding 100 µl packed cell volume of a mixture of infected red blood cells (IRBCs) and uninfected red blood cells (URBCs) to 10 ml of culture medium.

4.2.3 Drug Inhibition Assay (IC_{50})

The following 2 to 4 fold serial dilutions were prepared to make 8 concentrations of drug. 50 µl of each diluted drug was dispensed in triplicate into 96 well microtitre plates (Microwell, Nunc, UK) followed with 50 µl of the parasite inoculum (2% parasitaemia, 1% haematocrit). Artemisinin was used at its highest concentration (1000 nM) as a positive control and complete culture medium served as the negative control. Plates were mixed by agitation and placed in a humidified chamber (Flow, UK), gassed for 3 minutes, and incubated at 37 °C for 48 hours. After 48 hours incubation, 100 µl of lysis buffer (20 mM Tris-HCl, pH 7.5, 5 mM EDTA, 0.008 % (w/v) saponin, 0.08 % (v/v) Triton X-100) supplemented with the fluorescent dye SYBR Green (0.2 µl of SYBR Green per 1 ml lysis buffer) was added to each well and gently mixed followed by incubation at room

Table 4.1: List of the Drugs/inhibitors used in Drug Inhibition Studies (IC_{50}) for Phenotypic Profiling of Atovaquone Sensitive and Resistant Strains of *Plasmodium falciparum*

Drug/Inhibitor	Molecular weight	Solvent	Source
Artesunate	384.42	DMSO	Novartis, Switzerland
Artemeter	298.38	DMSO	
Chloroquine	515.9	Ethanol:water (50:50%)	Novartis, Switzerland
Atovaquone	366.84	DMSO	Prof Paul O'Neill, (Department of Chemistry, Uni. of Liverpool)
Stigmatellin	514.65	RPMI	Sigma Aldrich, UK
Myxothiazol	487.68	RPMI	Sigma Aldrich, UK
Antimycin	548.63	RPMI	Sigma Aldrich, UK
Thenyltrifluoracetylacetone (TTFA)	114.03	Ethanol: water (90:10%)	Sigma Aldrich, UK
Sodium azide	65.01	Distilled water	Sigma Aldrich, UK
5-fluro orotic acid	192.1	RPMI	Sigma Aldrich, UK
Pyrimethamine	248.711	DMSO	

temperature for 1 hour. After incubation, plates were read at 485 nm (excitation) and 535 nm (emission) using a Varioskan fluorescence reader (Thermo Electron Corporation, Finland). The analysis is carried out by calculating fluorescence values and expressed in relative fluorescence units. IC_{50} values were calculated from the log of dose/response relationship as fitted with Grafit Software (Erithacus Software, Kent, United Kingdom). Results are given as the means of at least three separate experiments.

4.2.4 Preparation of free *P. falciparum* Cell Free Extracts

Free parasites were prepared from aliquots of infected erythrocytes (approximately 8 x 10^9 cells ml^{-1}) by adding 5 volumes of 0.15% (w/v) saponin in phosphate-buffered saline (137 mM NaCl, 2.7 mM KCl, 1.76 mM K_2HPO_4, 8.0 mM Na_2HPO_4, 5.5 mM D-glucose, pH 7.4) for 5 min, followed by three washes by centrifugation at 4,000 x g for 5 min. The pellet with parasites was resuspended in HEPES (25 mM) buffered RPMI containing a protease inhibitor cocktail (Complete Mini, Roche). Cell extract was prepared by repeated freeze-thawing in liquid N_2, followed by disruption with a sonicator probe (Vibra Cell; Bioblock Scientific) for 30s on ice with 15 pulses of 1 second (300 W each) at 1-s intervals.

4.2.5 Peparation of Decylubiquinol

The artificial quinol electron donor was prepared based on a previously described method (Fisher et al., 2004). The 2,3-dimethoxy-5-methyl-n-decyl-1,4-benzoquinone (decylubiquinone), an analogue of ubiquinone (Sigma), was dissolved (10 mg) in 400 µl of nitrogen-saturated hexane. An equal volume of aqueous 1.15 M sodium dithionite was added, and the mixture shaken vigorously until colourless. The upper, organic phase was collected, and the decylubiquinol recovered by evaporating off the hexane under N_2. The

decylubiquinol was dissolved in 100 µl of 96 % ethanol (acidified with 10 mM HCl) and stored in aliquots at -80 °C. Decylubiquinol concentration was determined spectrophotometrically from absolute spectra, using $\varepsilon_{288\text{-}320} = 4.14\ mM^{-1}\ cm^{-1}$.

4.2.6 Preparation of Reduced Cytochrome c

Reduced cytochrome *c* was prepared by mixing 100 µl of a 1 mM stock solution of equine cytochrome *c* (dissolved in 50 mM potassium phosphate, 2 mM EDTA, pH 7.5) with 20 µl of freshly prepared 100 mM sodium ascorbate (pH 7.5). The mixture was left on ice for 10 minutes to allow full reduction of the cytochrome. Ascorbate was removed by passing the reduced cytochrome through a PD-10 desalting column (Pharmacia) pre-equilibrated with 50 mM potassium phosphate, 2 mM EDTA (pH 7.5). The concentration of the reduced cytochrome *c* was assessed by redox difference spectrophotometry $\varepsilon_{550-542} = 18.1\ mM^{-1}\ cm^{-1}$).

4.2.7 Measurement of Decylubiquinol: Cytochrome c Oxidoreductase Activity

Cytochrome *c* reductase activity measurements were assayed in a Cary 4000 spectrophotometer at 500 versus 542 nm in a reaction buffer consisting of 50 mM potassium phosphate (pH 7.5), 2 mM EDTA, 10 mM KCN, and 30 µM equine cytochrome *c* (Sigma Aldrich, UK) at room temperature (67). The reaction volume was 700 µl. *P. falciparum* bc_1 was present as a crude membrane preparation ('cell-free extract') at a total protein concentration of 30-60 µg/ml. Cytochrome *c* reductase activity was initiated by the addition of decylubiquinol (5 - 50 µM), and kinetic data collected for four minutes. Initial rates (computer-fitted as zero-order kinetics) were measured as a function of decylubiquinol concentration, using $\varepsilon_{550-542} = 18.1\ mM^{-1}\ cm^{-1}$.

IC_{50} values of atovaquone against the bc_1 activity were obtained by adding of atovaquone in the reactions before the assays were carried out. The amount of DMSO in the assays must not exceed 0.3% (v/v) to avoid the side effect of DMSO on the enzymes. IC_{50} values were calculated using Kalidagraph and the equilibrium dissociation constant (K_i) of the binding of inhibitor was determined using Cheng-Prusoff equation (Cheng and Prusoff, 1973).

$$K_i = \frac{IC_{50}}{1 + \frac{[S]}{K_m}}$$

From this formular the binding affinity of atovaquone to bc_1 complex was calculated using the atovaquone IC_{50} values. S is substrate concentration to initiate the initial reaction velocity (V_0) and K_m is the half of concentration of the substrate that produces maximal velocity (V_{max}).

4.2.8 Preparation of *P. falciparum* Mitochondria using Percoll® Density Gradient Centrifugation

The frozen trophozoite stages of the RBC free parasites were fractionated in Percoll® gradient, enabling separation of an active mitochondrial fraction. Percoll® fractionation was prepared according to the protocol described by Kobayashi et al. (2007). The parasite free cell extract was sonicated 3 times using sonicator probe (Vibra Cell; Bioblock Scientific) for 30s on ice with 15 pulses of 1 second (300 W each) at 1-s intervals and subsequently centrifuged for 30 minutes at 10,000 x g for 30 minutes at 4 °C. The supernatant was discarded and the mitochondrial pellet was resuspended in 1.5 ml of MSE buffer (225 mM mannitol, 75 mM sucrose, 0.1 mM EDTA, 30 mM Tris.HCl; pH 7.4) and complete Roche protease inhibitor tablet (ratio MSE to parasite pellet 1:5). 23% of Percoll® (Sigma Aldrich, UK) in the final volume of mixture was added into the mixture and followed by 18 ml of cold MSE buffer. All

the procedures were carried out on ice. Percoll sample was centrifuged at 100,000 x g in Beckman 70Ti Beckman rotor for 1 hour at 4 °C. The mitochondrial gradient was fractionated from top to bottom using a plastic pipette (1 ml/fraction). The activity of decylubiquinol:cytochrome *c* oxidoreductase of every fraction was measured using $\varepsilon_{550-542}$ = 18.1 mM^{-1} cm^{-1} and the active fractions were pooled and kept at -80 °C for subsequent biochemical analysis.

4.2.9 The Specific Activities of *Plasmodium* Mitochondrial Respiratory Chain Complexes in Percoll® Fractionated Samples

The determination of direct specific activities of mitochondrial respiratory chain complexes were performed according to protocol described by Fisher et al. (2009). The direct PfNDH2 native assay was performed in a 1-mm cuvette contain 600 µl of 50 mM potassium phosphate, 2 mM EDTA (pH 7.5), 10 mM potassium cyanide and 15 mM NADH (prepared in assay buffer). 60 µl of the mitochondrial fraction was added to the cuvette, and the reaction was initiated by addition of 50 µM ubiquinone (Q1 Sigma Aldrich, UK) prepared in 100% ethanol. PfNDH2 activity was measured spectrophotometrically by monitoring the decrease in absorbance at 340 nm (NADH ε= 6.22 $mM^{-1}cm^{-1}$). Oxidation by the other dehydrogenases (malate, DHODH, glycerol and succinate) were measured in 600 µl total reactions contain assay buffer, 50 µM ubiquinone and 60 µl mitochondrial fraction. The reaction were initiated by addition of 50 µM Q1 and spectrophotometrically measured at 283 nm.

The decylubiquinol:cytochrome *c* oxidoreductase activity of the bc_1 complex cytochrome *b* and cytochrome *c* oxidation were performed according to the protocol

described by Fisher *et al.* (2004). The 600-µl reaction consisting of 50 mM potassium phosphate, 2 mM EDTA, 1 mM KCN (pH 7.5) was carried out at room temperature. 60 µl of the mitochondrial fraction and 30 µM of horse heart cytochrome *c* were added in preparation of the reaction mixture. The concentration of the stock solution of cytochrome *c* was determined spectrophotometrically at $\varepsilon_{550-542}$ =18.5 mM^{-1} cm^{-1} ,dithionite-reduced minus ferricyanide oxidised difference spectra in a Cary 4000 UV-visible spectrophotometer (Agilent Technologies, UK) (70). The reaction was started by the addition of 50 µM decylubiquinol (dQH2). Data were fitted as initial rate estimates (cytochrome c reduction) at $\varepsilon_{550-542}$ =18.5 mM^{-1} cm^{-1}.

The oxidation of cytochrome *c* was performed in a 600-µl reaction consisting of 50 mM potassium phosphate, 2 mM EDTA, 1 mM KCN (pH 7.5), 500 µM antimycin and 60 µl of mitochondrial fraction. The assay was started by the addition of 30 µM reduced cytochrome *c* and data were fitted as initial rate estimates (cytochrome *c* oxidation) at at $\varepsilon_{550-542}$ =18.5 mM^{-1} cm^{-1}.

4.2.10 Western Blot Analysis

Western blot analysis was carried out to validate the finding of the specific catalytic activities of PfNDH2 and cytochrome *c bc*1 complex from the mitochondrial fractions. Two peptides based antibodies were customed made from GenScript Corp., Piscataway, NJ, USA. The peptide 77-ESIRNFLRKKNGYC-110 of the *P. falciparum* putative NADH dehydrogenase (Swissprot ACC. Q81302) and 322-SHYDNSGRIRQGPA-335 of the *P. falciparum* ubiquinol-cytochrome *c* reductase iron-sulphur subunit (Swissprot Acc. Q8IL75) were selected, synthesized and used for immunization in the rabbit and generation of an

affinity-purified polyclonal antibody. The rabbit anti-PfNDH2 and anti-P*fbc*$_1$ polyclonal antibodies were lyophilized in phosphate buffered saline (pH 7.4) with 0.02% sodium azide as preservative. Lyophilized antibodies were reconstituted with Milli Q water and aliquots were stored at −20 °C until required.

Three type of protein samples from parasite cell free extract were used for western blotting analysis. The whole cell extract (P1), the soluble fraction (P2) and the insoluble membrane protein (P3) of *P. falciparum* 3D7 and TM90C2B were harvested from the trophozoite stage with a parasitaemia >8% by treatment with 0.15% (w/v) saponin in phosphate-buffered saline. After three washes in 25 mM HEPES-buffered RPMI 1640 medium by centrifugation at 4°C at 6,000 x g for 5 min, the cells were disrupted with a sonicating probe for 30s on ice (15 pulses of 1 second (300 W each) at 1-s intervals) in lysis buffer (50mM Tris-HCl, 150 mM NaCl, 2mM EDTA, pH 7.4) in presence of protease inhibitor cocktail (Complete Mini, Roche, Mannheim, Germany). The complete parasite lysate was separated into two parts. The first part of the lysate was labeled as P1 and kept at -80 °C until further analysis. The rest of the cell lysate was centrifuged at 17,000 x g for 30 min at 4 °C. The supernatant was discarded and the pellet containing insoluble proteins of the parasites was resuspended in lysis buffer consisting of 1% (w/v) n-dodecyl maltoside (SigmaAldrich, UK). The mixture was incubated on ice for 30 min. Solubilised membrane proteins (P2) were recovered from the supernatant after centrifugation at 4°C at 17,000 x g for 30 min. The pellet of the cell lysate (P3) which contained the insoluble part of the protein was resuspended in lysis buffer and finally both soluble and insoluble proteins were kept at -80 °C until further analysis. The protein concentrations were measured using Bradford assay using BSA as a standard following the method which was described in section **2.12.** 50 µg of each protein sample preparation (P1, P2 and P3) of 3D7 and TM90C2B were separated on a 10%

SDS-PAGE and transferred to Hybond ECL nitrocellulose (Amersham GE Healthcare UK) following the method which was described in section **2.14.** PfNDH2 recombinant protein from *E. coli* membrane preparation was used a positive control for PfNDH2 analysis and bovine mitochondrial membrane particles were used as a positive control. PfNDH2 and bovine mitochondrial membrane samples were prepared by Nick Fisher in our laboratory. Membranes were saturated overnight at 4 °C in blocking solution (5% dry milk, 0.05% Tween 20 in PBS solution) and immunodetection was carried out for 2 hours with the custom polyclonal antibody against the PfNDH2 and *P. falciparum* Rieske iron-sulphur protein respectively. HRP-conjugated goat anti-rabbit IgG secondary antibody (Abcam, UK) was used at 1:10000 dilution for 1 hour. The signal was visualized by chemiluminescence with ECL™Western Blotting Detection Reagent Kit (Amersham Biosciences, Piscataway, NJ), followed by exposure of the membranes to Kodak® BioMax™ MR film. For the membrane subjected to the detection of *P. falciparum* Rieske iron-sulphur protein, a second incubation of 1 h with a rabbit primary polyclonal antibody against *P. falciparum* aldolase was used as a control.

4.3 Results

4.3.1 Phenotypic Studies of *P. falciparum* Atovaquone Sensitive and Resistance Strains

Growth inhibition assays were performed to confirm the phenotypic profiles of the wild type (3D7) and atovaquone resistant strains (TM90C2B and 3D7-yDHODH·GFP) to therapeutic drugs and various specific electron transport inihibitors. The P. falciparum 3D7 is the reference strain that sensitive to all antimalarial drugs. The *P. falciparum* TM90C2B strain is a clinical isolate presented with a point mutation in the parasite *cyt b* gene resulting in a

Y268S substitution within the Q_o site (Smilkstein et al., 2008). Previous study shown this strain was resistant to inhibitors that targeted the Qo site include: atovaquone, myxothiazole and stigmatellin. However TM90C2B is fully sensitive to antimycin A. The 3D7-yDHODH·GFP is a transgenic derivative of *P. falciparum* 3D7 expressing ubiquinone-independent DHODH (yDHODH) from yeast. Previous studies have demonstrated that 3D7-yDHODH·GFP was highly resistant to atovaquone (Painter et al, 2007).

The IC_{50} analyses were carried out as described in section **4.2.5**. As expected, TM90C2B and 3D7-yDHODH·GFP were highly resistant to atovaquone with IC_{50} values $12.4 \times 10^3 \pm 1.6 \times 10^3$ nM and $5.8 \times 10^3 \pm 2.2 \times 10^3$ nM respectively. Both atovaquone resistant parasites were also resistant to the other bc_1-targeting inhibitor stigmatellin which acts on the Q_o site of the parasite's cytochrome *b*. TM90C2B was also confirmed to be resistant to other electron transport inhibitors (myoxothiazol and antimycin), 2-Thenoyltrifluoroacetone and also resistant to chloroquine and pyrimethamine (Table 4.2).

All three parasite strains are not resistant to the other inhibitors targeting the different mitochondrial respiratory complexes (sodium azide and 5-fluoro orotic acid) and were highly sensitive to artesunate which used as a positive control throughout of this study.

4.3.2 bc_1 Complex Steady-state Kinetic Parameters for Atovaquone Sensitive and Resistant strains

Figures 4.1 and 4.2 show the steady-state cytochrome *c* reductase activity measured spectrophotometrically at 550- *minus* 542 nm in *Plasmodium* cell-free extracts as a function

Table 4. 2: Growth Inhibition Profiles of *P. falciparum* 3D7, 3D7-yDHODH·GFP and TM90C2B Parasites

The data are expressed as mean ± S.E., acquired from multiple replicates performed on at least 3 independent occasions. The IC_{50} values were calculated by fitting of four-parameter logistic curves (Grafit software).

Drug	Target	3D7 IC_{50} (nM)	3D7-yDHODH·GFP IC_{50} (nM)	TM90C2B IC_{50} (nM)
Artesunate		1.6 ± 0.4	1.1 ± 0.13	0.5 ± 0.1
Chloroquine		11.4 ± 0.4	10.4 ± 0.4	70.6 ± 9.6
Atovaquone	bc_1 (Q_o)	0.8 ± 0.1	5.8 X 10^3 ± 2.2 X 10^3	12.4 X 10^3 ± 1.6 X 10^3
Stigmatellin	bc_1 (Q_o)	23.2 ± 4.2	4.1 X 10^3 ± 425	107 ± 13
Myxothiazol	bc_1 (Q_o)	33.3 ± 6.4	Not determined	564 ± 11
Antimycin	bc_1 (Q_i)	13.8 ± 2.2	Not determined	300 ± 34
2-Thenoyltrifluoroacetone	Succinate dehydrogenase	1.5 X 103 ± 245	1.4 X 10^3 ± 352	31.4 X 10^3 ± 965
Sodium Azide	Cyt aa_3	423 ± 45 X 10^3	586 X 10^3 ± 97 X 10^3	654 X 10^3 ± 102 X 10^3
5-fluoro orotic acid	Dihydroorotate dehydrogenase	6.1 ± 0.9	5.5 ± 0.4	6.3 ± 1.3
Pyrimethamine	Dihydrofolate reductase	31.5 ± 6.9	35.9 X 10^3 ± 9.9 X 10^3	>10,000

of decylubiquinol concentration. The apparent V_{max} and K_m for decylubiquinol and IC_{50} for atovaquone were calculated *via* linear regression (Kaleidagraph, Synergy Software) using kinetic data obtained from initial rate measurements. The presence of contaminating hemozoin precluded spectrophotometric determination of bc1 concentration in the Plasmodium cell-free extract, and so total protein concentration was measured using the Bradford method as describe in section **2.12.**

The bc_1 V_{max} for the TM90C2B strain was 60.2 ± 3.2 nmol cyt *c* reduced/min/mg protein and 62% of that observed in the control 3D7 strain (97.4 ± 5.1 nmol cyt *c* reduced/min/mg protein) using decylubiquinol and equine cytochrome *c* as substrates. The K_m for decylubiquinol increased to 18.5 ± 2.6 mM in the TM90C2B bc_1 *c.f.* 5.5 ± 1.1 mM in 3D7 bc_1 (Table 4:3). The IC_{50} value for atovaquone in the decylubiquinol:cyt *c* oxidoreductase assay increased approximately 100-fold in TM90C2B compared to 3D7 (6 ± 1.0 and 600 ± 90 nM) .The presence of contaminating hemozoin precluded spectrophotometric determination of bc_1 concentration in the *Plasmodium* cell-free extract, and so total protein concentration was measured using the Bradford method.

4.3.3 The Specific Activities of Percoll® Fraction of *Plasmodium* Mitochondrial Respiratory Chain Complexes

The subcellular location of the mitochondrial specific activities was determined by fractionation on a Percoll®gradient. Figure 4.3 shows that the mitochondrial fractions were detected in fractions 14–18, as determined by cytochrome *c* reductase activity spectrophotometrically measured at 550-542 nm. The fractions containing mitochondrial membrane (fractions 14-18) were pooled and kept followed by the bc_1 enzyme kinetic assay

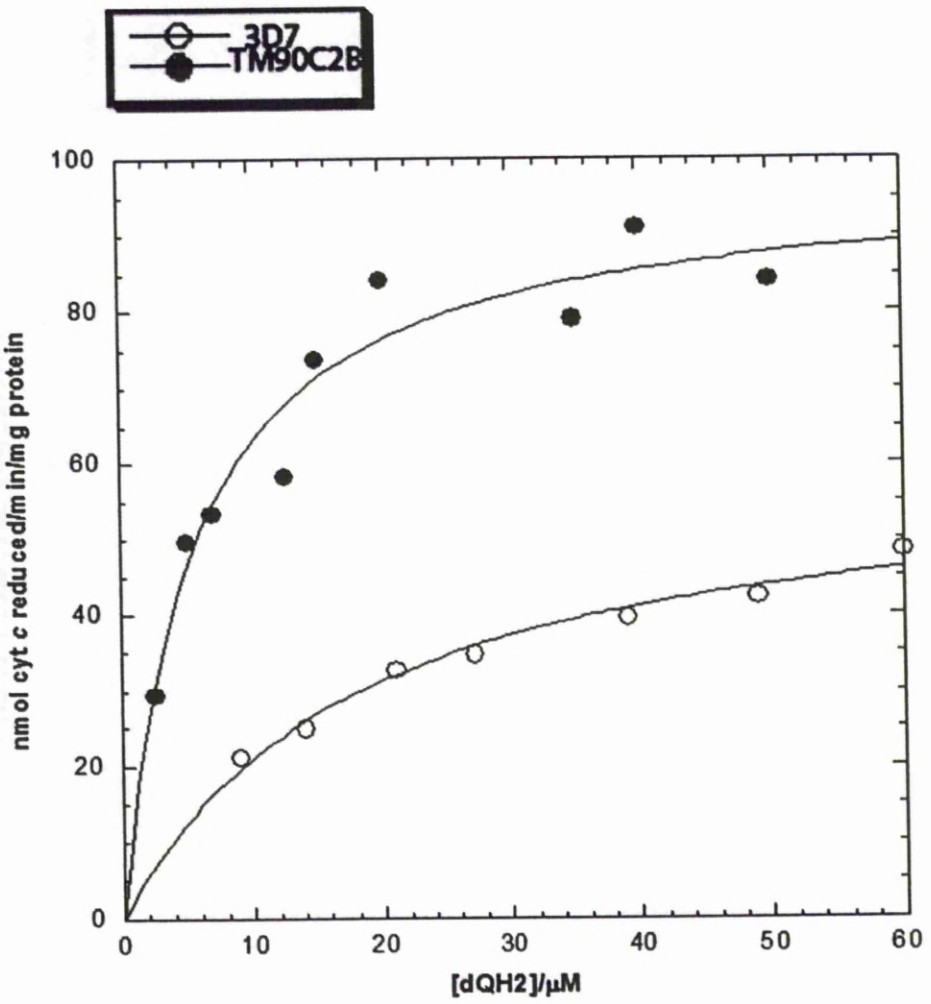

Figure 4.1: Steady-state decylubiquinol:cytochrome *c* oxidoreductase Activity of 3D7 and TM90C2B

Steady-state cytochrome *c* reductase activity of 3D7 and TM90C2B were measured spectrophotometrically at 550- *minus* 542 nm. The points are the mean initial velocity obtained at each QH_2 concentration indicated. The data were fitted to a Michaelis-Menten rectangular hyperbola using Kalidagraph (Synergy software). The reactions were started by the addition of decylubiquinol (5 - 50 μM). The K_m values were 5.5 ± 1.1and 18.5 ± 2.6 for 3D7 and TM90C2B respectively.

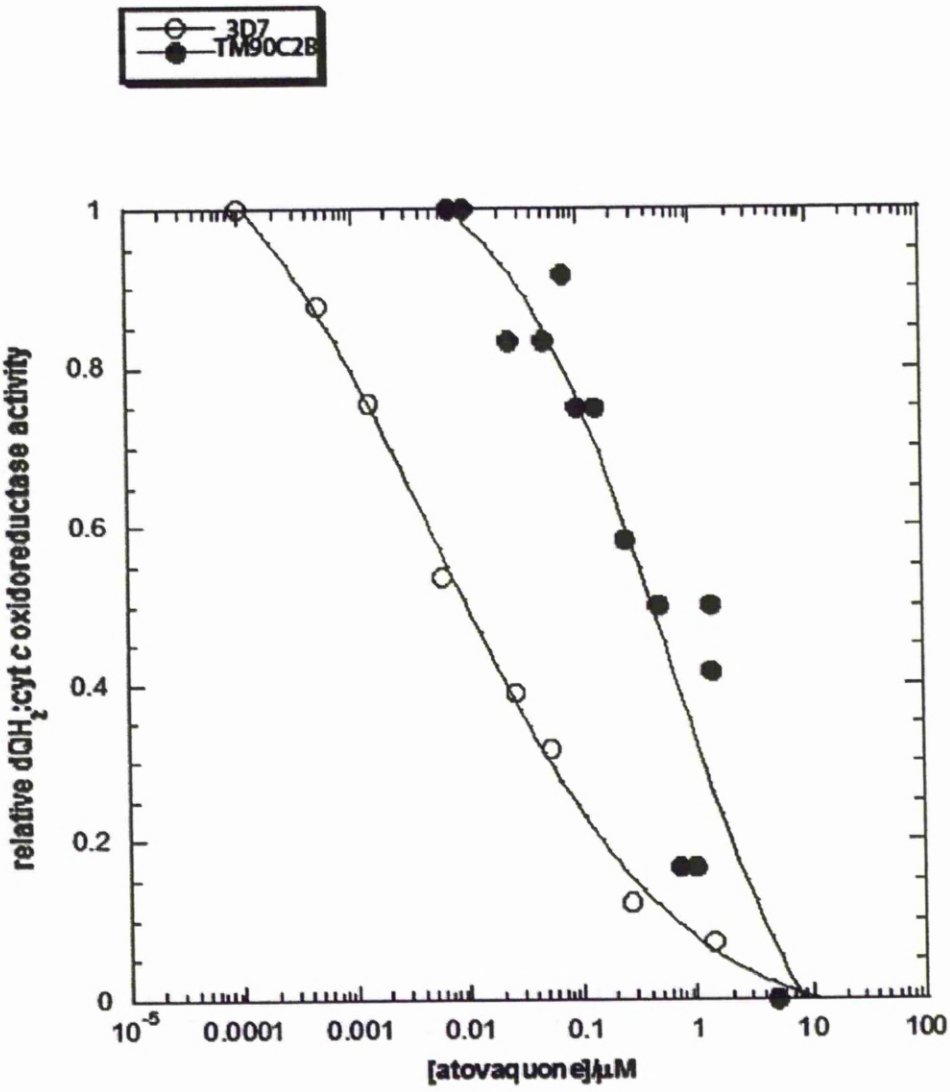

Figure 4.2: Determination of the IC_{50s} for Atovaquone against Cytochrome C reductase activity in a Cell-Free Extract of 3D7 and TM90C2B Malaria Parasites

The IC_{50} values for atovaquone in the decylubiquinol:cytochrome *c* oxidoreductase assay are 6 ± 1.0 nM (3D7) and 600 ± 90 nM (TM90C2B). The data were fitted using a four-parameter sigmoidal function in Kaleidagraph (Synergy Software).

Table 4.3: 'Cell-free extract' Steady-state Decylubiquinol:cytochrome *c* Oxidoreductase Activity and Atovaquone Sensitivity in *P. falciparum* strains 3D7 and TM90C2B

Enzyme activity was measured as described in Materials and Methods. The K_i values for atovaquone inhibition were calculated using the Cheng-Prusoff equation. The mean and S.E of each were obtained from three independent experiments.

P. falciparum strain	V_{max} (nmol cyt *c* reduced/min/mg protein)	K_m (dQH2, mM)	IC_{50} (atovaquone, nM)	K_i (atovaquone, nM)
3D7	97.4 ± 5.1	5.5 ± 1.1	6.4 ± 1.2	0.6
TM90C2B	60.2 ± 3.2	18.5 ± 2.6	600 ± 90	162

The specific activities of the mitochondrial Percoll®fractionation were carried out as described in section **4.2.9**. The specific activities of the mitochondrial respiratory enzyme complexes are expressed as nanomoles per gram per minute of mitochondrial protein as shown in Table 4.4. From the result quinone reductase activity was detected at 283 nm for all dehydrogenases except Complex II (succinate dehydrogenases). PfNDH2 displayed the highest turnover [(V_{max}/enzyme concentration)/time in seconds] amongst the dehydrogenases in both 3D7 and TM90C2B. The specific activities for both PfNDH2 and the bc_1 complex of TM90C2B were decreased by ~50% with respect to 3D7.

4.3.4 Western Blot Analysis

Western blot analyses were carried out to validate the data from the specific catalytic activities of PfNDH2 and bc_1 complex of 3D7 and TM90C2B malaria parasites. Figure 4.4 shows the comparison of the PfNDH2 expression in 3D7 and TM90C2B. Total protein (50 μg) for each sample of P1, P2, P3 (3D7 and TM90C2B) and recombinant PfNDH2 were separated 10% SDS-polyacrylamide gel and transferred to nitrocellulose membrane depicts the expression of PfNDH2 is more abundant than to TM90C2B. This is shown by a thick protein band of ~61 kDa in sample prepared from total cell lysate (P1) and also in insoluble (P3) parasite protein. From the membrane the protein of ~ 61 kDa was not detected in samples loaded from the soluble part of the parasite protein. This indicates the protein was prepared well since no contamination was detected in the lane containing soluble protein. Figure 4.5A and 4.5B show the western blot analysis of the protein expression of Riske iron sulphur protein from atovaquone sensitive (3D7) and resistant strain (TM90C2B). 50 μg of total protein for each sample of P1, P2, P3 (3D7 and TM90C2B) and aldolase were separated by 10% SDS-polyacrylamide gel and transferred to nitrocellulose membrane. Mutation of

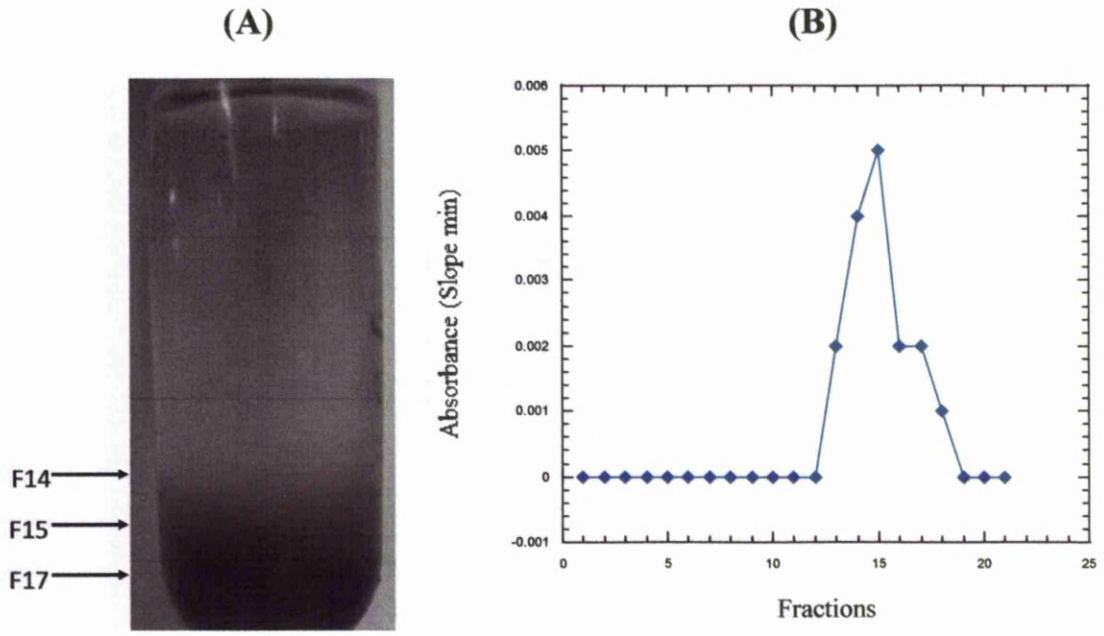

Figure 4.3: Percoll Density Gradient Centrifugation of Free-parasite Fractionations of TM90C2B *falciparum* Malaria Parasites

Picture A shows the formation of gradient separation of mitochondrial fractions in a 23% Percoll® gradient. Twenty one parasite fractions are generated and the numbers indicated are the fractions which produced the highest *bc*1 activities. (B) The activity of bc_1 started appearing in fraction 14 and the highest activity was detected in fraction 15. The activity started decreasing in fraction 17 and was completely undetected in fraction 19. The positive fractions (fraction 14-18 were pooled together and kept at -80 ^{0}C. Assay was performed in medium consisting of 50 mM potassium phosphate (pH 7.5), 2 mM EDTA and 10 mM KCN at room temperature. Quionol: cyt *c* oxidoreductase assay was done by adding 30 µM horseheart cyt *c* in the assay medium before adding 50 µM decylubiquinol to start the reaction (λ=550 nm - 542 nm).

Table 4. 4: The Specific Activities of 3D7 and TM90C2B *P. falciparum* Mitochondrial Respiratory Enzyme (Percoll fractionations)

Mitochondrial respiratory enzyme complexes	3D7 (nmole/mg/min)	TM90C2B (nmole/mg/min)
NADH-Q1	12.85 ± 0.83	6.41 ±1.53
QH2-cyt c	6.88 ± 1.31	2.84 ±1.54
Gly.-3-phosphate	3.99 ± 0.37	3.69 ± 1.07
Malate	5.99 ± 0.83	1.02 ± 0.54
DHODH	5.90 ± 2.10	3.07 ± 2.67
Cytochrome C oxidase	2.85 ± 0.12	0.83 ± 0.35

The specific activities of mitochondrial respiratory enzyme complexes were performed using Percoll® fractionations of *P. falciparum* 3D7 and TM90C2B. The quinone reduction rate was spectrophotometrically monitored at 283 nm (quinone reduction) for PfNDH2, glycerol-.3-.phosphate, malate and DHODH. The cytochrome *c* reductase activity and cytochrome *c* oxidation were measured spectrophotometrically at 550- *minus* 542 nm. Results are expressed as mean nanomoles per gram per minute of mitochondrial protein from at least 3 independent repeats.

cytochrome *b* can result in destabilisation of the bc_1 complex, with subsequent loss of the ISP (67).

The structural stability of the bc_1 complex in cell-free extracts prepared from the TM90C2B strain was assessed by monitoring ISP content *via* western blots as describe in section **4.2.10**. From the western blot analysis results show that the 3D7 bc_1 protein expression is higher compared to TM90C2B as indicated by a clear protein band at ~41 kDa. The western blot analysis was carried out to determine the amount of loaded protein was standardised using aldolase protein antibody. As shown in Figure 4.4B, aldolase protein bands have similar intensity in 3D7 and TM90C2B respectively.

4.4 Discussion

In this chapter the effect of the mutation in the bc_1 complex of *P. falciparum* TM90C2B was biochemically analysed and compared to the wild type 3D7 bc_1. An *in silico* model of atovaquone docked at the Q_o site of yeast cytochrome b has been described by Kessl et al. (2005). Cytochrome *b* mutations that modify the ubiquinol-binding pocket of the cytochrome complex and confer anti-malarial drug resistance in *S. cerevisiae* have also been described Kessl *et al* (2005). In these models, atovaquone is represented as a 'haem-distal' Q_o inhibitor, binding in a manner strongly reminiscent of stigmatellin, consistent with available EPR data (129). In the model, the hydroxyl moiety of the hydroxynaphthoquinone ring of atovaquone forms a hydrogen bond to the N atom of the imidazole group of His-181 in the Rieske iron-sulphur protein (lowering the redox potential of the [2Fe2S] cluster). A second H-bond is formed between atovaquone's hydroxynaphthoquinone carbonyl group and the carboxylate of the cytochrome *b* ef-loop residue Glu-272 *via* a bridging water molecule.

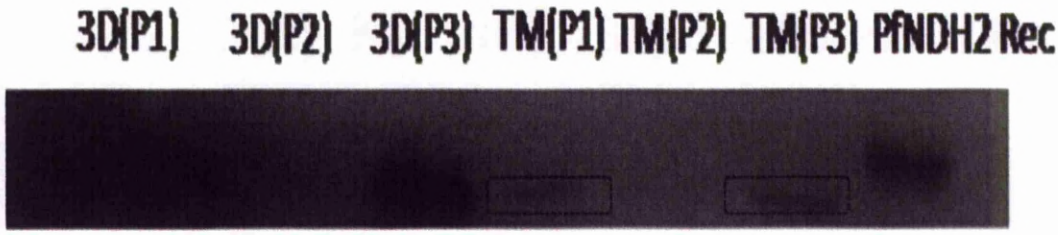

Figure 4.4: Western Blot Analysis of the *Plasmodium* Cell Free Extracts of 3D7 and TM90C2B Strains Using Polyclonal Antibodies against *P. falciparum* Putative NADH dehydrogenase

Western blot analysis of the *Plasmodium* cell free extract (P1), soluble protein (P2) and insoluble protein (P3) of PfNDH2 protein of 3D7 (3D) and TM90C2B (TM). The protein of ~ 61 kDa was visible in the P1 and P3 protein samples of 3D7 and TM90C23B respectively. The level of PfNDH2 protein in 3D7 was abundant compared to TM90C2B as shown on the membrane. No protein bands were detected from the soluble protein of 3D7 and TM90C2B indicating that PfNDH2 is in an insoluble form. PfNDH2 recombinant protein was used as a control to validate the specificity of the PfNDH2 polyclonal antibody against PfNDH2 *Plasmodium* protein samples.

(A)

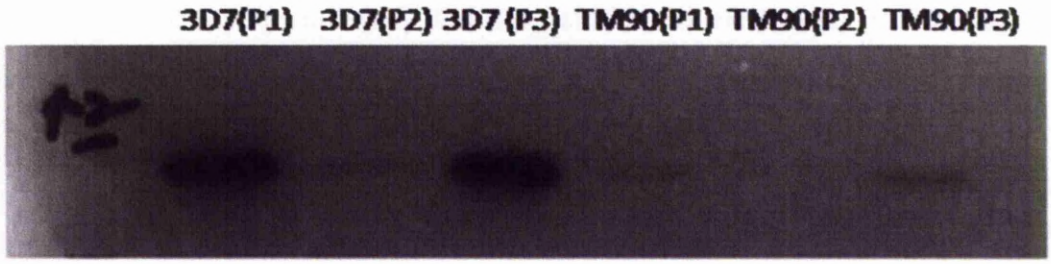

(B)

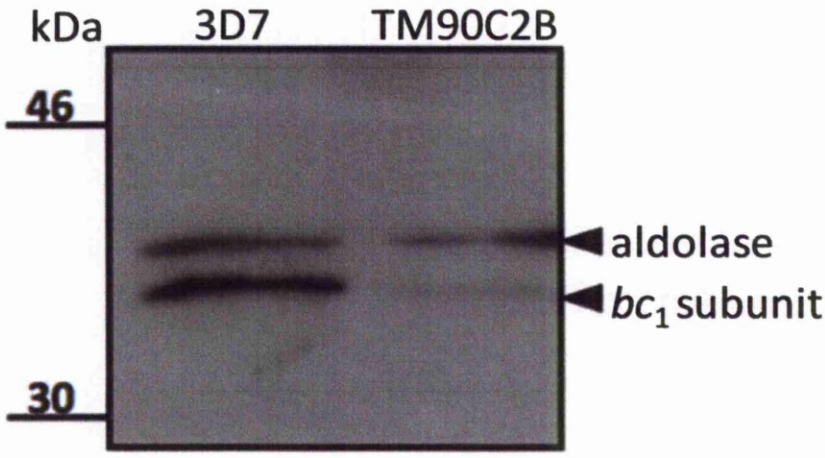

Figure 4.5: Western Blot Analysis of the *Plasmodium* Cell-Free Extract of 3D7 and TM90C2B Strains Using Polyclonal Antibodies against *P. falciparum* Ubiquinol-cytochrome *c* Reductase Iron-sulphur **subunit and Polyclonal Antibodies against *P. falciparum* aldolase**

Panel A shows the Western blot analysis of *Plasmodium* cell free extract (P1), soluble protein (P2) and insoluble protein (P3) of *P. falciparum* 3D7 and TM90C2B. The protein size ~41 kDa was detected in P1 and P3 protein samples from both 3D7 and TM90C2B and no protein bands were visible from the soluble preparation (P2). As shown on the membrane the expression of bc_1 protein of TM90C2B low compared to 3D7. This indicates the protein is affected by the presence of a point mutation at Y268S. (B) The same western blot analysis was carried out to determine the amount of loaded protein was standardised using aldolase protein antibody as a control. From the membrane shown the 3D7 bc_1 protein expression is higher compared to TM90C2B as indicated by a clear protein band at ~41 kDa. The positive control (aldolase) shows similar intensity bands in 3D7 and TM90C2B respectively.

The chlorophenyl ring of atovaquone in Kessl's yeast model sits in a hydrophobic pocket within cytochrome *b* formed from the side chains of Phe-121(transmembrane helix C), Phe-278 (ef loop) and Tyr-359 (transmembrane helix H). A similar pocket is likely to be formed by the corresponding residues in *P. falciparum* cytochrome *b* (Phe-115, Phe-267 and Phe-352). Y268 (*Plasmodium* notation), located within the ef helix, is highly conserved. In yeast, it has been suggested that the tyrosyl side chain of this residue participates in the positioning of Q_o-bound ubiquinol, and it has been postulated to contribute to stablising hydrophobic interactions with the naphthoquinone group of atovaquone (204) The structure of the yeast cytochrome bc_1 complex with a hydroxyquinone anion Q_o site inhibitor bound has been determined by (128, 204). Studies with mutant forms of bc_1 from the bacterium *Rhodobacter sphaeroides* indicated that an aromatic or large hydrophobic side-chain residue is required at this position within the ef helix for efficient catalytic activity (42). In addition, mutation of the equivalent residue in man (Tyr-279) has been linked with a variety of mitochondrial disorders that have been studied in yeast models (67, 280).

Data from phenotypic studies show that the TM90C2B strain is resistant to all mitochondrial electron transport inhibitors and also chloroquine. The chloroquine resistance mechanism is not addressed in this study. The resistance is probably due to a multi-drug resistance phenomenon which is rampant along the Thai/Cambodian border (177). This study also demonstrated the *P. falciparum* 3D7-yDHODH·GFP, the transgenic parasite bearing *S. cerevisae* DHODH was highly resistant to atovaquone. This finding is in accordance with the study conducted by Painter et al. (2007).

From the steady state study of free cell extracts of showed, V_{max} of crude preparations of TM90C2B bc_1 (60.2 ± 3.2 nmol cyt c reduced/min/mg protein) compared to the control

3D7 strain (97.4 ± 5.1 nmol cyt c reduced/min/mg protein) were similar to that observed for the yeast Y279C and S mutants (turnovers of 47 s^{-1} and 30 s^{-1} respectively, compared to the wild type value of 80 s^{-1}: (68). A confirmation study was conducted using a yeast model system which conferred Q_o-site mutations in cytochrome *b* (67, 69, 280). It should be noted that more deleterious effects on the yeast enzyme activity have been noted in Y279S preparations in other laboratories (127).

The three-fold increase in K_m observed for decylubiquinol in TM90C2B bc_1 coupled with the decrease in V_{max} suggests that the binding and/or positioning of the substrate ubiquinol within the Q_o site is impaired in TM90C2B compared to the wild type, consistent with mutation studies of this residue in other organisms. We note with interest the apparent instability of the ISP in TM90C2B as revealed by western blotting, which suggests a weakened interaction between this subunit and cytochrome *b*. This may be due to perturbation of the ef helix and surrounding protein structure at the Q_o site due to the introduced serinyl side chain, which may result in an increased electron transfer distance between bound ubiquinol and the ISP [2Fe2S] cluster and weakening or abolition of the hydrogen bond between 'haem-distal' Q_o ligands and His-181 of the ISP. The differences in bc_1 complex integrity observed in TM90C2B and the yeast Y279S mutant may arise from the potentially peculiar structure of the Q_o site and ISP docking surface in Apicomplexa (i.e. the four residue deletion in the N-terminal region of the cd2 helix (18).

We have shown that in *P. falciparum* the point mutation at codon Y268S affected the function of Complex 1. Results from the specific activities of the mitochondrial respiratory complexes showed that the PfNDH2 and bc_1 cytochrome *b* activities of TM90C2B were decreased (~ 50%) compared to 3D7. *Plasmodium* complex II is not detected using direct

measurement of succinate oxidation to fumarate. The measurement of succinate oxidation is performed spectrophotometrically at 283 nm measuring the reduction of dQ_1 as an electron acceptor. Potassium cyanide was used to block the normal path of electrons in the *Plasmodium* respiratory complex. The measurement of *Plasmodium* Complex II also can be performed using an artificial electron acceptor such as 2,6-dichlorophenolindophenol (DCPIP) measured at 600 nm or using PMS (phenazine methosulfate), or MTT (3-(4,5-dimethylthiazol-2-yl)-2,5-diphenyltetrazolium bromide) measured at 570 nm (180). The activity of succinate oxidation in 3D7 is measurable by linked assay with MTT and can be inhibited with atpenins (TTFA) and malonate (data not shown). However the catalytic efficiencies of the Complexes II were relatively low with K_{cat}/K_m= 600 and 5000 respectively when compared with other *Plasmodium* mitochondrial respiratory enzymes (134).

Western blot analysis was carried out to validate the kinetic studies of the dehydrogenases. Two peptide antibodies against *Plasmodium* NDH2 and Riske iron sulphur protein were designed and synthesized. The attempts to generate specific antibodies against cytochrome *b* were unsuccessful. The other mitochondrial dehydrogenases were not included in this analysis due to unavailability of the antibodies against the proteins. From the western blot analysis of complete lysates of cell free extract and membrane proteins, 3D7 PfNDH2 and Rieske iron sulphur protein were highly abundant compared to TM90C2B (Figure 4.4 and Figure 4.5). As described, the Y268S mutation in the parasite bc_1 may give rise to complex instability and difficulties in protein folding, resulting in the reduced western blot signal. At this stage however, it is not clear why the TM902CB strain has reduced expression of PfNDH2. One possibility may be that the two enzymes exist as a supercomplex, however no data is available at this stage to support this hypothesis. Supercomplexes have been identified in other species such as bovine and rat, fungi (*S. cereviasae* and *Podospora anserine*) and

Caenorhabditis elegans (reviewed by Lenaz and Genova, 2010). In these species, supercomplexes have been identified using techniques such as blue native PAGE (BN-PAGE) containing the enzymes Complex I, dimeric Complex III and Complex IV (Acin-Perez et al., 2008). In addition, supercomplexes have also been shown to contain Complex II and ATPase (2).

The interaction between Complex I and III (I.III) and Complex I, Complex III and Complex IV are the most described in the literature related to supercomplex studies. Bultema et al. (2009) proposed supercomplex forming megacomplexes of the inner mitochondrial structure in potato mitochondria. However the characterization of the supercomplexes by direct functional analysis via kinetic studies is still poor. Researchers speculated that the interaction between Complex I and Complex III is through electron flow by direct channeling of ubiquinone (152). The activity of the interaction between I and III is greater compared to the interaction between I, III and IV (229).

The effect of mutations in mitochondrial Complex III was reported recently by Suthammarak et al. (2010). For the first time they reported that presence of mutations in complex III of *C. elegans* affected the activity of the Complex I. Results from silver staining of native-PAGE gel and quantitative measurement of the amount of Complex IV indicated a significant loss of Complex IV from the I.II.IV supercomplexes compared to the wild type. The dissociation of Complex IV from the supercomplexes thus reduces the Complex I activity. From this finding mutations in one of the components of supercomplexes may lead to an imperfect confirmation and dysfunction of the proton pumping module.

The physical association between Complex I and Complex III is thought to involve the iron sulphur protein (ISP) (252). Western blot analysis of ISP content in cell-free extracts prepared from TM90C2B cultures revealed decreased levels of this subunit compared to the control 3D7 strain, with ISP content in the corresponding yeast mutant (Y279S) indistinguishable from wild type. Similarly, no loss of ISP content was observed in the yeast Y279A and Y279C mutants, although the Y279W mutation was found to be structurally destabilizing (67). A study by Kessl et al. (2005) demonstrated cytochrome *b* mutations modified the ubiquinol-binding pocket of the cytochrome bc_1 complex and conferred anti-malarial drug resistance in *S. cerevisiae*.

In conclusion, the mutation of codon Y268S in TM90C2B affects the binding of ubiquinone at Qo site in the *Plasmodium* bc_1 complex. Therefore extremely low turnover rates for the bc_1 activity of TM90C2B compared to 3D7 were observed. The mutation also affected the catalytic activities of other respiratory enzyme complexes. We speculate this might be due to supercomplex interactions between the enzymes in the respiratory chain of the *Plasmodium*. However the presence of supercomplexes in *Plasmodium* is not yet established. More research is needed to establish the relationship between mutations in one of the complexes affecting the allosteric mechanisms in the catalytic core of the putative supercomplex assembly.

Chapter 5: Molecular Characterisation of *P .falciparum* 3D7 Malate Quinone Oxidoreductase

5.1 Introduction

Malate or malic acid is a biochemically important organic compound with the chemical formula $C_4H_4O_5$ (Figure 5.1). Whilst chemical synthesis of this chiral compound yields both L- and D- enantiomers it should be noted that in nature only the L- enantiomer occurs.

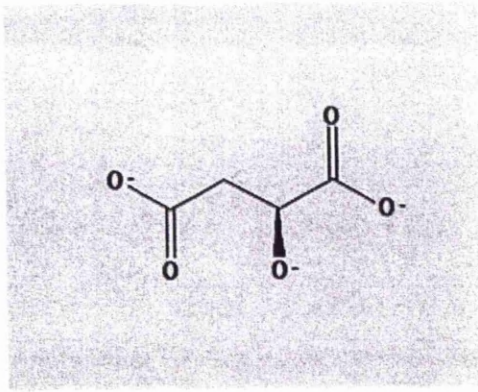

Figure 5.1: The Chemical Structure of L-malate

http://pubchem.ncbi.nlm.nih.gov .

In eukaryotes malate is involved in many biochemical reactions such as the TCA cycle, the malate-aspartate shuttle, and shuttling of acetate from the mitochondrial matrix to the cytosol. Malate is found in both the mitochondria and cytoplasm of many eukaryotic organisms. In the TCA cycle of eukaryotic organisms C_4 carbon is fixed and malate is oxidised to oxaloacetate (OAA) by malate dehydrogenase in the mitochondrial matrix resulting in CO_2 production (Figure 5.2). OAA cannot be transported directly into the mitochondrial matrix or transported back to the mitochondrial intermembrane space and is

effectively trapped. Therefore, OAA must be reduced to malate via the malate dehydrogenase enzyme. Reduced malate is transported through a malate α-ketoglutarate transporter, and subsequently oxidised to OAA. Malate also acts as a substrate for malic enzyme in the cytoplasm to form pyruvate. Pyruvate, the end product of the glycolysis pathway is transported to the mitochondrial matrix and subsequently oxisidised to form OAA (159).

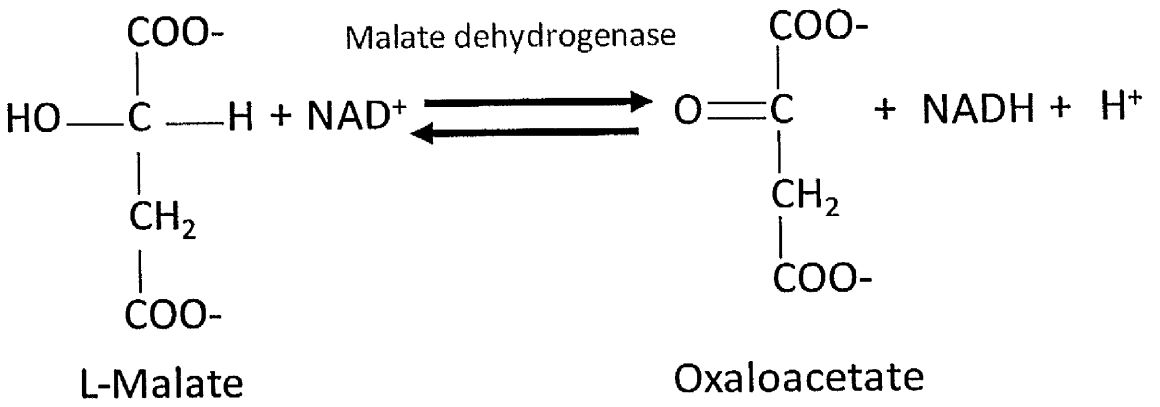

Figure 5.2: Oxidation Reaction of L-malate to OAA

Malate dehydrogenase catalyses the reversible conversion of L-malate to OAA. L- malate is oxidised to OAA and coupled with the reduction of NAD^+ to NADH + H^+.

Malate dehydrogenase (MDH; EC 1.1.1.37) is found in both eukaryotic and prokaryotic organisms. In eukaryotes malate is a substrate for distinct cytosolic and mitochondrial malate dehydrogenases whilst in prokaryotes, mitochondrial malate dehydrogenase (mtMDH) is replaced by the isozyme malate quinone oxidoreductase. In eukaryotic cells, MDH isozymes have been found in the cytosol as well as in other organelles such as mitochondria, chloroplasts, peroxisomes and glyoxysomes. MDH plays a major role in oxidative metabolism and other physiological functions depending on its biochemical characteristics and intracellular location (27, 176). This enzyme is involved in the aspartate aminotransferase reaction, which transfers the reducing equivalent (NADH or NADPH) from

the cytosol to mitochondria. mtMDH is a primary anaplerotic enzyme and reversibly interconverts malate and oxaloacetate (OAA) (159).

The other malate dehydrogenase isozyme from *Plasmodium* spp is malate:quinone oxidoreductase (MQO; E.C.1.1.99.16). MQO is a lipid-dependent, peripheral membrane-bound flavoprotein which catalyses the oxidation of L-malate to oxaloacetate. The *PfMQO* gene is encoded by chromosome 6 of *P. falciparum*. From the biochemical characterisation, MQOs can be divided into two major families. The 'actinobacterial' MQO including *Mycobacterium* spp., *Corynebacterium* spp., *Streptomyces* spp., *Nocardia* spp. and *Rhodococcus* spp. belong to one major bacterial MQO family (MQO1), while most ε-proteobacterial (*Helicobacter pylori*, *Campylobacter jejuni*) and apicomplexan (*P. falciparum*, *Toxoplasma gondii*, *Babesia bovis*) enzymes are members of the second group (MQO2) (182). MQO is identified to co-exist with an alternative complex I NADH dehydrogenase (NDH2) which is present in bacteria, fungi and plants (126). Gardner et al. (2002) predicted the presence of the NDH2 and MQO genes in the *P. falciparum* genome and both enzymes were predicted in the TCA cycle of *P. yoelli* and *P. falciparum*.

The role of MQO in the *Plasmodium* TCA cycle is as a substitute for other mitochondrial MDH isozymes (262, 269). In MQO, $FADH_2$ has been identified as the cofactor that donates electrons to the respiratory chain. This contradicts what occurs in cytoplasmic MDH, where NADH is oxidised to NAD^+ thus reduces OAA to malate. Electrons from $FADH_2$ are donated to ubiquinone which is subsequently oxisidised in the electron transport chain (185, 260, 262, 269).

In *Plasmodium* spp., studies conducted by Uyemura et al. (2004) showed the addition of malate as substrate generated a high membrane potential in *P. Yoelii*, whereas the addition of pyruvate, glutamate and other endogenous substrates produced low membrane potential. They showed the generation of membrane potential is through the stimulation of rotenone-insensitive respiration (NADH). They also reported the highest activity of membrane potential was completely inhibited after addition of antimycin A. *Plasmodium* malate quinone oxidoreductase is an FAD dependent enzyme which supplies electron to the electron transport chain, therefore no electrons are supplied from NAD (185). The presence of MQO in *P. yoelii* mitochondria is supported by the detection of a significant membrane potential when fumarate is used as a substrate. The recent studies conducted by Bulusu et al. (2011) indicate the presence of fumarate not a metabolic waste in *Plasmodium* spp. excretion products, but converted to aspartate by fumarase via malate and OAA intermediates. They also suggest the presence of another pathway whereby fumarate is converted directly to aspartate bypassing MDH pathway.

Recently the metabolomic evidence of the role of malate in *P. falciparum* was obtained by Olszewski et al. (2010). They have illustrated malate pathways in the *P. falciparum* TCA cycle (Figure 5.3). The metabolomic studies indicate malate is an end product for both oxidative and reductive branches of *Plasmodium* spp TCA cycle. The *Plasmodium* spp TCA cycle does not follow the canonical pathway where the TCA cycle is a cyclic pathway. Instead, a branched or bifurcated TCA cycle uses glutamate or glutamine as the major carbon source. These two amino acids donate their carbon skeleton to form 2-oxoglutarate. The 2-oxoglutarate either follows the cyclic pathway of TCA (oxidative branched) or the reducing branch of TCA cycle. In the oxidative branch fumarate is oxisidised

by fumarase to form malate, whilst in the reducing branch OAA is reduced by MQO to generate malate.

However, Tripathi et al. (2004) showed that PfMQO is functional only in combination with PfMDH, which is the sole supplier of malate to the *Plasmodium* TCA cycle. They demonstrated that PfMQO is significantly higher as compared to PfMDH (260). Study by Bulusu et al. (2011) demonstrated that the activity of MQO in the oxidation of malate to OAA is essentially irreversible. MQO cannot catalyse the reduction process of OAA to malate and we know OAA cannot be transported in or out of the intermembrane space to the mitochondrial matrix. OAA must be reduced by malate dehydrogenase in the mitochondrial intermembrane space, and subsequently transported into mitochondrial matrix through a malate-α-ketoglutarate transporter. In the mitochondrial matrix malate is re-oxidised by MQO to form OAA. OAA is then oxidised to form aspartate and finally transported out from the mitochondrial matrix through a glutamate-aspartate transporter.

The objective of this study was to characterise the malate quinone oxidoreductase enzyme from *P. falciparum* strain 3D7. The characterisation process involved several molecular biology techniques such as polymerase chain reaction, cloning and sequencing. This was followed by an expression study of the cloned gene in the *E. coli* host. The purification study of the overexpression of PfMQO recombinant protein in *E. coli* was performed and followed by subsequent biochemical assays such as steady-state enzyme kinetics. The information generated during this study will provide new insight into the molecular and biochemical properties of this protein. Due to the absence of this enzyme in

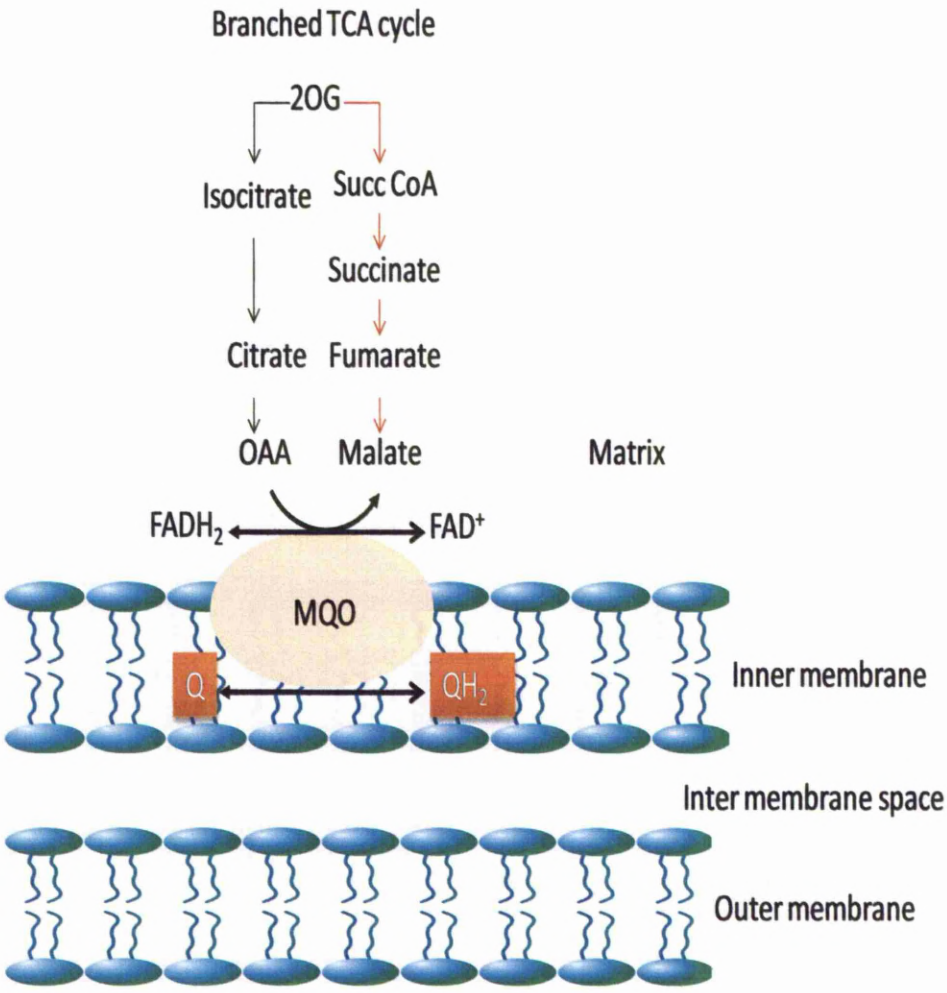

Figure 5.3: Topology of MQO in the *Plasmodium* Mitochondrial Inner Membrane

MQO is a single subunit enzyme and peripheral membrane protein where one part of the enzyme surface faces the mitochondrial matrix and the other part is embedded in the inner mitochondrial membrane. The TCA cycle of *P. falciparum* consists of oxidative pathway (red arrow) and reductive pathway (black arrow). Both pathways produce malate as the end product of the TCA cycle. MQO catalyses the reduction of OAA to malate and fumarate is oxidised by fumarase (fumarate hydratase) to malate in the oxidative pathway. $FADH_2$ is reduced to FAD^+, donating electrons to ubiquinone pool in the *P. falciparum* respiratory chain. Abbreviations: Q, ubiquinol; QH_2, ubiquinone; 2OG, 2-oxoglutarate; Succ CoA, succinyl-CoA. Figure is adapted from Olszewski et al. (2011).

mammalian mitochondria, we believed PfMQO may be a potential target for the development of new antimalarial drugs which selectively target the malarial mitochondria.

5.2 Materials and Methods

5.2.1 Bioinformatics

Bioinformatic studies were carried out using various applications freely available online. The database of the nucleotide and amino acid sequences of the putative PfMQO (Acc. No. PF3D7_ 061680) were extracted from PlasmoDB 8.0 website (www.plasmodb.org). The open reading frame (ORF) of the *PfMQO* gene was predicted using Biology WorkBench 3.2 programme hosted at http://workbench.sdsc.edu. The protein molecular weight and isoelectric point of PfMQO were predicted using the ProtParam programme hosted at http://www.expasy.org.

The prediction of subcellular location of PfMQO was performed using PFMpred (http://www.imtech.res.in/raghava/pfmpred) and PlasMit (http://gecco.org.chemie.uni-frankfurt.de) programmes. *P. falciparum* δ aminolevulinic acid synthetase (PfALAS, Acc. No. PF3D7_1440300) and *P. falciparum* malate dehydrogenase (PfMDH, Acc. No. PF3D7_0618500) were used as positive and negative controls.

The prediction of the internal transmembrane domains was performed using the TMHMM 2.0 prediction programme (http://www.cbs.dtu.dk) and the secondary structure of PfMQO was predicted using PSIPRED VIEW software (http://bioinf.cs.ucl.ac.uk) hosted by

University of Collage London, UK. *P. falciparum* dihydroorotate dehydrogenase (PfDHOODH) and type I phosphatidylserine decarboxylase (PfPSD) were used as positive and negative controls.

Multiple sequence alignment of MQO amino acid sequences from respective organisms was performed using ClustalW software (http://mobyle.pasteur.fr) using programme default parameters. The percentage of similarity of the PfMQO amino acid sequence (Uniprot Acc. no gi|46361119|emb|CAG25406.1) was determined by aligning the sequence with other MQOs encoded in other *Plasmodium* species and also from bacteria. The aligned sequences were putative MQO from *P. vivax* (Uniprot Acc. No. gi|148805058|gb|EDL46457.1), putative MQO from *P. berghei* (strain Anka) Uniprot Acc. No. tr|Q4Z5G1|Q4Z5G1_PLABA), putative MQO from *P. chabaudi* (Uniprot Acc. No. tr|Q4XW30|Q4XW30_PLACH), putative MQO from *P. knowlesi* (strain H) (Uniprot Acc. No. tr|B3L7N6|B3L7N6_PLAKH), probable MQO fragment from *P. yoelii yoelli* (Uniprot Acc. No.tr|Q7RE35|Q7RE35_PLAYO), MQO from *E. coli* (strain K12) (Uniprot Acc. No. sp|P33940) and MQO from *M. smegmatis* (strain ATCC 700084 / mc(2)155) (Uniprot Acc. No. sp|A0QVL2|MQO_MYCS2).

5.2.2 DNA Extraction

Genomic DNA was isolated from trophozoite stage synchronised *P. falciparum* (3D7) strain using a phenol chloroform extraction technique with modifications (153). Synchronised parasites were cultured in a 75-mm^2 flask containing complete RPMI medium until a parasitaemia of 7-8% was reached. Cells were centrifuged at 3000 x g for 5 minutes. The supernatant was discarded and the resultant pellet resuspended in 5 volumes of cold PBS pH 7.4. Subsequently, cells were centrifuged at 3000 x g for a further 5 minutes. The pellet was

resuspended in cold 5% (w/v) saponin (prepared in PBS). Following centrifugation at 3000 x g for 5 minutes, cells were digested with 50 µl proteinase K (0.1 mg/ml) in lysis buffer (40 mM Tris-HCl / 80 mM EDTA pH 8.0/ 2% (w/v) SDS). The mixture was incubated at room temperature for ~ 3 hours with intermittent shaking after which an equal volume of phenol/chloroform/isoamyl alcohol (25:24:1;v/v/v) was added, vigorously shaken and then centrifuged at 13,000 x g for 1 minute at room temperature. The aqueous phase was removed and DNA was precipitated by adding 1/10 volume 3M sodium acetate (pH 5.2) and 2.5 volumes of ice cold absolute ethanol with an overnight incubation at -20 °C. On the following day, the mixture was centrifuged at 13,000 x g for 30 minutes at 4 °C, followed by washing with 70% v/v ethanol. The mixture was centrifuged again at 13,000 x g for 5 minutes at 4°C. The supernatant was discarded and the DNA pellet was dried in a laminar flow hood. The DNA pellet was re-suspended in 100 µl DEPC-treated water (Ambion, UK) and stored at -80 °C until required.

5.2.3 Estimation of Nucleic Acid Concentration

The concentration of nucleic acids was estimated by measuring absorbance at 260 nm using a NanoDrop Nd-1000 UV/Vis Spectrophotometer (Labtech International, UK). DNA preparations which had a ratio of O.D. 260/280 in the range of 1.7-2.0 were regarded as pure and protein free (215).

5.2.4 Designing PCR Primers for *P. falciparum MQO* Gene

Each primer described herein was designed from the published genome sequence of the *P. falciparum MQO* putative gene (PF3D7_0616800) freely available from the PlasmoDB data base (http://plasmodb.org). Primers were custom synthesised by Invitrogen, UK. Five

primers were designed to cater for the different cloning processes to be used to incorporate the gene into the expression vectors. Two expression vectors were used in this study namely pET-15b (Novagen®, UK) and pUC19 (Invitrogen, UK). Two sets of primers were designed for each expression vector. One primer set was used to amplify the whole *PfMQO* gene and the second set was used to amplify the *PfMQO* gene region without the putative mitochondrial leader sequence. The leader sequence is a stretch of amino acid residues (~17-35 residues) located at the N-terminus of the mitochondrial protein. The signal of the leader peptides allows pre-proteins to be transported into the mitochondrial matrix. The transported protein eventually will be processed by matrix proteases (MPP) located in the mitochondrial matrix (97). The prediction of the putative PfMQO signal peptides was performed using SignalP 4.0 Server (www.cbs.dtu.dk). The primers used in this work are summarised in the following Table 5.1 Primer PF222MQO was a reverse primer for all primer sets.

5.2.5 Amplification of PfMQO Gene

The amplification of the *PfMQO* gene was carried out using a BIORAD PCR Thermocycler using genomic DNA (10 ng) obtained as per section **5.2.2**. High fidelity PCR reactions were prepared using Platinum® Pfx DNA Polymerase (Invitrogen, UK) according to protocol described by Invitrogen. This enzyme is a proprietary enzyme preparation containing recombinant DNA polymerase from *Pyrococcus* sp. Platinum® *Pfx* DNA Polymerase possesses a proofreading 3'-5' exonuclease activity which is highly possessive and thus increases the extension rate capability. The specificity and accuracy offered by this enzyme is higher than standard Taq DNA polymerase and therefore it is suited for PCR applications such as site-directed mutagenesis, expression and cloning. High fidelity of PCR reactions were performed in a final volume of 50 µl containing 1 x Pfx Amplification Buffer, 200 nmoles of primer (Invitrogen, UK), 10 mM dNTP mix (NewEngland Biolab,UK), 1 mM

$MgSO_4$, 10 ng DNA template and 1 unit Pfx DNA Polymerase. The PCR parameters were as follows; denaturation of templates at 95 °C for 3 minutes, annealing of primers at 46 °C for 30 seconds, and extension at 72 °C for 3 minutes and 15 seconds. After 30 cycles a final extension of 10 minutes was performed at 72 °C. The PCR products were visualised by electrophoresis using a 1.2% agarose gel stained with 0.5 µg/ml of ethidium bromide (120).

5.2.6 Purification of PCR Products

Prior to the cloning procedure, *PfMQO* PCR products were purified in order to remove agarose, excess nucleotides and primers. The PCR purification was carried out using Wizard® SV Gel and PCR Kit (Promega, UK). The membrane binding solution was added in an equal volume to PCR products and transferred into an SV minicolumn with a collection tube and incubated at for 1 minute at room temperature. The column assembly was centrifuged at 13,000 x g for 1 minute. The SV minicolumns were removed from the spin column assembly and the liquid in the collection tube discarded. 700 µl of membrane wash solution were added to the SV minicolumn. The SV minicolumn assemblies were centrifuged for 1 minute at 13,000 x g. The collection tubes were emptied as previously described and placed back on the SV minicolumns in the collection tubes. 5 µl of membrane wash solution were added followed by centrifugation for 5 minutes at 14,000 x g. The collection tubes were emptied and the column assemblies re-centrifuged for 1 minute with the microcentrifuge lid open to allow evaporation of any residual ethanol. The SV minicolumns were transferred to clean 1.5 ml microcentrifuge tubes and 50 µl of DEPC-treated water (Ambion, UK) was applied directly to the centre of the column. The reactions were incubated at room temperature for 1 minute. This was followed by centrifugation for 1 minute at 13,000 x g. The eluted PCR products were kept at 4 °C or –20 °C until required for cloning purposes.

Table 5.1: List of Primers Sequences used for PCR Analysis of *P. falciparum MQO* Gene

List of primers designed to amplify the targeted *PfMQO* gene from genomic DNA of *P. falciparum*. The highlighted sequences identify in bold the restriction sites incorporated during primer design.

Primer Name	Sequence	Incorporated Restriction Enzyme site	Expression Vector
P221LMQO (Forward)	5'-**CATATG**ATGATATGTGTTAAAA ATATTTTG-3'	*Nde*I	pET-15b
P222MQO (Reverse)	5'**GGATCC**TCATAAATAATTAACGGG ATATC-3'	*Bam*HI	pET-15b
PM225SMQO (Forward)	5'AC**CATATG**TTAAACGAACTACGTAAT AATAGG-3'	*Nde*I	pET-15b
PM227LMO (Forward)	5'AC**CTGCAGG**ATGATATGTGTTAAAAA TATTTTG-3'	*Pst*I	pUC19
PM226SMO (Forward)	5'**ACCTGCAGG**TTAAACGAACTACGTAAT AATAGG-3'	*Pst*I	pUC19

5.2.7 TA Cloning

PCR products amplified with primer pairs P221LMQO/P222MQO, PM225SMQO/P222MQO (incorporating restriction sites *Nde*I and *Bam*HI; Table 5.1) PM227LMO/P222MQO and PM226SMO/P222MQO (restriction sites *Pst*I and *Bam*HI; Table 5.1) were directly ligated into linearised pCR®II-TOPO (Invitrogen, UK). The ligation reaction consists of 1 µl plasmid pCR®II-TOPO (25 ng/µl) and 3 µl PCR product, 1 µl salt solution (1.2 M NaCl and 0.06 $MgCl_2$) and 5 µl DEPC-treated water (Ambion) in 10 µl of final volume.

5.2.8 Transformation of One Shot® TOP10 Chemically Competent *E. coli*

The ligation mixture of pCR®II-TOPO and the *MQO* gene amplicon were transformed into competent *E. coli* Top10 (Invitrogen, UK) by the heat shock method. 2 µl of the ligation mixture were added and mixed gently and incubated on ice for 30 minutes. Heat shock of the cells was carried out at 42 °C for 30 seconds followed by incubation on ice for a further 2 minutes. 250 µl of super optimal broth (SOC) medium were added into the reaction and tube was shaken horizontally at 37 °C for 60 minutes. SOC is commercially available from Invitrogen UK and consists of 2% Tryptone, 0.5% yeast extract, 10 mM NaCl, 2.5 mM KCl, 10 mM $MgCl_2$, 10 mM $MgSO_4$ and 20 mM glucose. 50 to 100 µl of the transformation reaction were spread on Luria Bertani (LB) agar plates consisting of 50 µg/ml ampicillin and IPTG/X-gal (40 µl 100 mM isopropyl-β-D thiogalactoside/40 µl 40 mg/ml 5-bromo-4-chloro-3-indoyl-β-D-galactosidase). Plates were incubated at 37 °C overnight. IPTG is known as an inducer of the lac operon and X-gal is a colourless chromogenic indicator containing a β-1,4 linkage to glucose. X-gal is metabolised by β-galactosidase to form 5-bromo-4-chloro-indoxyl which is spontaneously oxidized to the bright blue insoluble pigment 5,5'-dibromo-4,4'-

dichloro-indigo, and thus functions as an indicator. Efficiency of transformation was determined by examining the number of blue versus white colonies formed on LB-ampicillin-IPTG/X-gal agar plates. Only white colonies were chosen for analysis because blue colonies do not carry any insert. Screening was carried out on colonies selected from the LB-ampicillin agar plates. The selected colonies were subjected to a plasmid isolation step (miniprep or maxiprep) using a DNA purification system (Qiagen, UK).

5.2.9 Mini Preps of Plasmid DNA fom *E.coli* Cells

Mini preps of plasmid DNA from bacterial cells were carried out using QiaAmp kits (Qiagen, UK). A white colony from a fresh of LB agar plate was used to inoculate 10 ml LB medium containing appropriate antibiotics and incubated overnight at 37 °C in a shaking incubator. The bacterial culture was pelleted by centrifugation for 5 minutes at 10,000 x g. The supernatant was poured off and 250 µl of Cell Resuspension Solution (P1) was added and transferred to a microcentrifuge tube. This was followed by adding 250 µl of buffer P2 and mixing by inverting the tubes 4 times. Tubes were then left to stand for 5 minutes until the cell suspension turned blue indicating lysis of the cells. The mixture was neutralized by addition of 350 µl Buffer N3 neutralisation solution and immediately mixed thoroughly by inverting the tube. The bacterial lysate was subjected to centrifugation at 13,000 rpm for 10 minutes at room temperature. The cleared lysate was transferred into QIAprep spin column and was centrifuged at 13,000 rpm for 1 minute and the flow through discarded. The column was washed two times with 750 µl and 250 µl of buffer PE solution and centrifuged for 1 minute and 2 minutes, respectively, at 13,000 rpm at room temperature. Finally, the plasmid DNA was eluted in 100 µl DEPC-treated water by centrifugation at 13,000 rpm for 1 minute at room temperature. The DNA was quantitated using a NanoDrop spectrophotometer and was kept at -20 °C until required.

5.2.10 Screening of Positive Clones by Restriction Enzyme Analysis

Screening of the positives clones was carried out throughout this study to validate successful cloning and subcloning of the inserted gene into the vectors. This technique was also applied to assess the successful transformation of the ligated gene into the *E. coli* host. Generally, 1 µg of the plasmids were digested with 20 units of enzyme in 30 µl total volumes consisting of buffer and incubated at 37 °C for 1 hour. Bovine serum albumin (BSA) was added in some of the reactions. Each restriction enzyme composition in the digestion reaction will be described in detail in the following section. Enzymes and buffers were purchased from New England Biolabs. (UK). 10 µl of digested plasmid with 2 µl of 6 x loading dye were loaded onto a 1.2% agarose gel. Electrophoresis was conducted in 1 x TBE running buffer at 90 volts for 30 minutes and the gel was visualised under UV light.

5.2.11 Analysis by Automated Sequencing

200 ng of plasmid DNA that produced positive results by PCR and restriction enzyme analysis were sent for automated DNA sequencing (Cogenics, UK), where universal T7 primers were used for the sequencing reaction. The pCR®II/inserts then were designated as TOPO/pETPfLMQO, TOPO/pETPfSMQO, TOPO/pUCPfLMQO and TOPO/pUCPfSMQO. PfLMQO represents a complete nucleotide sequence of putative *PfMQO* gene and PfSMQO represents a putative *PfMQO* gene where the first 46 of the 1566 nucleotides have been removed from the putative *PfMQO* nucleotide sequence. These 46 nucleotides were predicted as a putative leader sequence signal of PfMQO using SignalP 4.0 Server software (www.cbs.dtu.dk).

5.2.12 Maxi Prep of Plasmid DNA fom *E.coli* Cells

Maxi preps of plasmid DNA from bacterial cells were carried out in order to get good yields of recombinant plasmid DNA for sub-cloning of TOPO/PfMQO into pET-15b and pUC19 expression vectors. A Qiagen Maxikit was used to purify recombinant plasmid from bacterial cells. A single colony of Top10 competent cells containing a *PfMQO* bearing plasmid from a streaked LB agar plate was inoculated into a starter culture of 5 ml LB/50 µg/ml ampicillin/25 µg /ml chloramphenicol and incubated overnight at 37 °C with vigorous shaking at 200 rpm. 200 µl of the starter culture were added into 100 ml LB/50 µg/ml ampicillin/25 µg /ml chloramphenicol broth and incubated at 37 °C overnight with vigorous shaking at 200 rpm. The culture was harvested by centrifugation at 6000 x g at 4 °C. The supernatant was discarded, and the bacterial pellet was re-suspended completely in 8 ml of Buffer P1 followed by 8 ml Buffer P2. The tube was mixed by inverting several times and then incubated at room temperature for 5 minutes. For the subsequent steps, all the mixing was carried out by inverting the samples 6 times. 8 ml of chilled Buffer S3 were added to the bacterial lysate and at this time the fluffy white precipitate containing genomic DNA, proteins, cell debris and SDS was produced. The lysate was poured into the barrel of a QIAfilter cartridge and incubated for 10 minutes at room temperature. The plunger was gently inserted into the QIAfilter Cartridge and the cell lysate was filtered into a 50 ml tube. 5 ml of Buffer BB 1 were added to the filtered lysate and the mixture was inverted 4-6 times. The lysate was transferred to a QIAGEN Plasmid *Plus* spin column attached to a vacuum pump. Approximately ~ 300 mbar pressure was applied until the liquid has been drawn through all the columns. 0.7 ml of Buffer ETR was added into the column and a vacuum was applied until the liquid had been drawn completely. This was followed by adding 0.7 ml Buffer PE and the same procedure was applied. The DNA column was centrifuged at 10,000 rpm for 1 minute to remove the residual wash buffer completely. The DNA was eluted in 400 µl of

Buffer EB and centrifuged at 10,000 rpm for 1 minute. The DNA purity was measured, followed by storage at -20 °C.

5.2.13 Double Restriction Enzyme Digestion

Double restriction enzyme digestion was carried out using specific enzymes that cut DNA at specific sites in the plasmids. The DNA fragments are cut at their unique recognition sequence at the recognition site by the specific enzyme. In this study the restriction enzyme digests were carried out to isolate the MQO fragments (TOPO/pETPfMQO and TOPO/pUCPfMQO) from the TOPO replication vector. The same procedure was also carried out on both expression vectors pET-15b and pUC19 to prepare for subsequent sucloning procedure. The TOPO plasmids encoding pET*MQO* genes (pETPfLMQO and pETPfSMQO) and pET-15b vector were digested with 20 units of *Nde*I and *Bam*HI, respectively. Reactions consisted of 3 µl NEB buffer III and 3 µl BSA in 30 µl total volume. The TOPO plasmids encoding pUC*MQO* and pUC19 vector were digested with 20 units *Pst*I and *Bam*HI in 30 µl total volume containing NEB buffer III. All reactions were incubated at 37 °C for 1 hour. 20 µl of digested plasmid mixed with an appropriate volume of 6 x loading dye were loaded to a 1.2% agarose gel. Electrophoresis was conducted in 1 x TAE running buffer at 90 volts for 30 minutes and the gel was visualised under UV light.

5.2.14 Agarose Gel Extraction

Agarose gel extraction was carried out using QIAquick®Gel Extraction Kit (Qiagen, UK). The ~1566 bp *MQO* DNA bands were excised from the agarose gel with a sterile scalpel. The gel slice was weighed in a 1.5-ml tube. 3 volumes of Buffer QG were added to 1 volume of the gel slice followed by incubation at 50 °C for 10 minutes. The mixture was

vortexed intermittently until the gel fragment was completely dissolved. After incubation, the sample was transferred into QIAquick spin column in a provided 2-ml collection tube and spun at high speed (13,000 rpm) for 1 minute. The flow through was discarded and the Qiaquick column was put back in the same collection tube. 0.5ml of Buffer QG was added to QIAquick column and centrifuged for 1 minute to remove all traces of agarose. The flow through was discarded and the QIAquick column was centrifuged for an additional 1 minute at 13,000 rpm. The QIAquick column was transferred into a clean 1.5-ml microcentrifuge tube and 50 µl DEPC-treated water (Ambion, UK) added before and centrifuging at maximum speed (13,000 rpm) for 1 minute. The DNA was checked for purity and concentration and subsequently kept in -20 °C.

5.2.15 Dephosphorylation of Linearlised Vector

Dephosphorylation of linearlised vector was carried out to prevent the religation of the double-digested expression vectors pET-15b and pUC19. 40 µl of double digested vector were incubated with 0.1 units Antarctic Phosphatase and 1 x Antarctic Phosphatase Buffer (NewEngland BioLabs, UK) in a total volume of 50 µl. The reaction was incubated at 37 °C for 30 minutes and then 65 °C for 5 minutes to terminate the enzymatic reaction.

5.2.16 Sub-cloning Reaction

The ligation process was carried out at vector: insert ratio of 1:3. The ligation mixture contained digested pET-15b, pUC19 and respective DNA fragments of pETPfLMQO, pETPfSMQO, pUCPfLMQO and pUCPfSMQO. The ligation reaction recipe was followed standard ligation reaction mixture that contained 1 unit of T4 DNA ligase and. 1 x T4 DNA ligase reaction buffer (50 mM Tris-HCl, 10 mM MgCl2, 10 mM Dithiothretol and 1 mM

ATP). Ligations were carried out at 14 °C for 2 hours. T4 DNA ligase was inactivated at 65 °C for 10 minutes prior to transformation into TOP10 chemically competent *E. coli* cells.

5.2.17 Transformation of Ligated Expression Vectors and *PfMQO* gene into One Shot® TOP10 Chemically Competent *E. coli*

The ligated expression vectors and *PfMQO* genes were transformed into *E. coli* TOP10 cells following the protocols as described in section **5.2.8** with the exception of an addition of X-gal for blue and white screening. The ligation mixture was transformed using heat-shock transformation into TOP10 chemically competent *E. coli* cells and plated on LB agar containing 50 μg/ml ampicillin.

5.2.18 Selection of Recombinants

7 colonies from each transformants were selected randomly for further analysis by restriction digestion. The colonies were subjected for small scale culture (5 ml LB containing 50 μg/ml ampicillin) and grown for overnight at 37 °C. This was followed by minipreparation using a QiaAmp (Qiagen, UK). This protocol was described in section **5.2.9**. The selected clones then were validated by digesting with *EcoR*V (pET-15b vector) and *Sph*I (pUC19 vector) respectively. The positive clones were designated as pET/PfLMQO, pET/PfSMQO, pUC/PfLMQO and pUC/PfSMQO.

5.2.19 Preparation of Competent *E. coli* BL21 (DE3) pLysS cells

The preparation of competent cells was carried out according to protocol described by (120). Non-competent BL21 (DE3) pLysS cells (Promega, UK) were plated on LB agar containing of 25 μg/ml chloramphenicol. The agar plate was incubated at 37 °C overnight. On the following day, a single bacterial colony was inoculated in 100 ml of LB/amp (25 μg/ml). The culture was incubated at 37 °C for 3-6 hours with vigorous shaking at 200 rpm. The bacterial growth was monitored spectrophotometrically at 600 nm. The growth of the cells was arrested by incubation on ice for 10 minutes after the OD_{600} reached 0.4. This was followed by centrifugation at 2700 x g for 10 minutes at 4 °C The supernatant was discarded and the bacterial pellet resuspended in 30 ml ice cold $MgCl_2$-$CaCl_2$ (80 mM $MgCl_2$/20 mM $CaCl_2$). The mixture was centrifuged at 2700 x g for 10 minutes at 4 °C. The supernatant was discarded and the pellet was resuspended in 2 ml ice cold buffer contain 0.1 M $CaCl_2$ and 500 μl of glycerol and mixed by gentle swirling. The resuspended cells were aliquoted into sterile 1.5 tubes and kept at -80 °C until ready to use.

5.2.20 Transformation of pET/PfMQO and pUC/PfMQO into *E. coli* BL21 (DE3) pLysS cells

The recombinant plasmids were transformed into the expression host *E. coli* BL21 (DE3) pLysS cells. 1-50 ng of recombinant PfMQO bearing plasmids (pET-15b and pUC19 clones) was added into 50 μl of competent BL21 cells. The mixtures were incubated on ice for 30 minutes, followed by heat shock at 42 °C for 45 seconds in a water bath. The mixture was incubated on ice for 5 minutes, 250 μl of SOC medium were added and the tube was shaken horizontally at 37 °C for 60 minutes. 50 to 100 μl of the cultures were spread on LB agar plates with 50 μg/ml ampicillin and 25 μg/ml chloramphenicol and incubated overnight at 37

°C (120). The positive clones form each transformant were screened by restriction enzymes analysis using *Eco*RV (pET expression system), *Sph*I, *Afl*III and *Bam*HI (pUC expression system).

5.2.21 Transformation of pET/PfMQO and pUC/PfMQO into *E. coli* Rosetta ™ (DE3)pLysS cells

The study of the protein expression of pET/PfMQOs and pUC/PfMQOs was also carried out in *E. coli* Rosetta™ (DE3)pLysS cells (Novagen, UK). Rosetta™ is a strain of BL21 designed to enhance the expression of eukaryotic proteins that contain codons rarely used in *E. coli*. The *E. coli* LysS contains tRNA genes argU, argW, ileX, glyT, leuW, proL, metT, thrT, tyrU, and thrU. The tRNA of the bacterial cells are supplied with seven rare codons (AUA, AGG, AGA, CUA, CCC, CGG and GGA) on a compatible chloramphenicol-resistant plasmid. The pLysS plasmid encodes T7 phage lysozyme, an inhibitor for T7 polymerase which reduces and almost eliminates expression from transformed T7 promoter containing plasmids when not induced (194). 1 µl of recombinant DNA from a transformed TOP10 cell minipreparation was directly applied to the cells and gently mixed. The tube was incubated on ice for 5 minutes and subsequently transferred to 42 °C water bath for heat shock for 30 seconds. 80 µl of SOC media was added and the tube was shaken horizontally at 37 °C for 60 minutes. 50 to 100 µl of the cultures were spread on LB agar plate with 50 µg/ml ampicillin and 25 µg/ml chloramphenicol and incubated overnight at 37 °C. The positive clones form each transformant were screened by restriction enzyme analysis using *Eco*RV and *Sph*I (pET-15b vector), *Afl*III (pUC19 vector) and double digestion with *Pst*I and *Bam*HI for the pUC expression system.

5.2.22 Determination of PfMQO Expression in *E. coli* Rosetta^{TM} (DE3)pLysS Cells

Small scale preparation of positive clones harbouring pET/PfLMQO and pET/PfSMQO, pUC/PfSMQO were carried out to determine the expression of the PfMQO recombinant protein in *E. coli* Rosetta cells. The glycerol stock of a PfMQOs positive clone were plated onto LB/50 μg/ml ampicillin/25 μg/ml chloramphenicol and incubated overnight at 37 °C. A single colony was used to inoculate 10 ml LB/50 μg/ml ampicillin/25 μg/ml broth. The cultures were incubated overnight at 37 °C in a shaking incubator at 200 rpm. 2.5 ml of the overnight cultures were inoculated into 50 ml LB/ 50 μg/ml ampicillin/ 25 μg/ml chloramphenicol and incubated at 37 °C with vigorous shaking at 200 rpm. The growth of the bacterial cells was monitored spectrophotometrically at 600 nm. Induction of protein expression by the addition of IPTG to a final concentration of 1 mM occurred once the OD_{600} reached 0.5-0.7. The cultures were continuously grown for an additional 4-5 hours. 1 ml of culture was pelleted and resuspended in 100 μl 1x SDS-PAGE sample buffer. Duplicate samples of bacterial lysates were prepared for Rapid Coomasive Blue Staining and western blot analysis. Samples of bacterial lysate were electrophorosed by 10% SDS-PAGE for 1 hour at 60 milliamp constant current. For western blot analysis, gel was electroblotted onto nitrocellulose membrane as previously describe in section **2.16**. The blotted membrane was incubated with monoclonal anti-polyhistidine antibody (Sigma Chemical Co. UK) at a dilution of 1:5000 for 2 hours in blocking buffer (5% skimmed milk powder in TBS-T). The blotted membrane was then washed 3 times in 1 x TBS-T, for 10 minutes each per wash. The membrane then was incubated for 1 hour with slow agitation with secondary antibody horseradish peroxidase (HRP) conjugated anti-mouse Ig antibody (Nordic Immunology) (1:10,000) in blocking buffer. Visualisation was performed using ECL reagent (Amersham, G.E Healthcare).

5.2.23 Determination of PfMQO Protein Solubility

This study was carried out to determine the solubility of the recombinant PfMQO protein using sample preparation as in previous section **5.2.22**. The bacterial pellets bearing for PfLMQO and PfSMQO were dissolved in 5 ml of lysis buffer (150 mM NaCl, 50 mM Tris.HCl, 1 mM EDTA pH 7.4). The bacterial suspension was centrifuged at 17,000 x g for 30 minutes at 4 °C. The supernatants were separated and the pellets were resuspended into the same lysis buffer (insoluble part). The insoluble part was divided into 2 (insoluble fraction and inclusion body). 20% of Triton X-100 was added into the inclusion body fraction to remove lipid and membrane associated protein but not solubilise the inclusion body. The mixture was incubated on rotary incubator for 30 minutes at 4 °C. This was followed by centrifugation at 17,000 x g for 30 minutes at 4 °C. The supernatant was carefully discarded from the pellet. The pellet was homogenised using glass tissue homogeniser to get a good yield. The homogenised pellet was resuspended in lysis buffer and kept at -80 °C. The soluble, insoluble and inclusion body fractions were diluted in 1% SDS loading buffer and electrophorised onto a 10% SDS polyacrylamide denaturing gel for 1 hour at 60 milliamp constant current and followed by rapid blue staining.

5.2.24 Time, Temperature and IPTG Induction Courses of PfMQO

The purpose of this study was to determine the optimal post-induction growth duration, temperature and IPTG concentration required for high level expression of soluble PfMQO. Only the positive clones of pET/PfLMQO and pET/PfSMQO were subjected to this study. The starter bacterial cultures were prepared as described in section **5.2.22**. The recombinant PfMQO was then designated as PfLMQO and PfSMQO. The parameters investigated were 22 °C, 30 °C and 37 °C, and 0.5 mM and 1 mM IPTG for the each

temperature. 5 ml bacterial culture was sampled at 3 hours and 5 hours, and overnight (post-IPTG induction). The samples were centrifuged at 3000 rpm for 20 minutes. The supernatants were discarded and pellets were resuspended in lysis buffer (150 mM NaCl, 50 mM Tris.HCl, 1 mM EDTA pH 7.4). Samples were kept on ice and sonicated using Vibra Cell probe sonicator at 80 ampitude 3 times for 10 seconds each until the sample was no longer viscous. The sonicated samples were centrifuged at 13,000 x g for 30 minutes. The supernatant containing soluble proteins was separated and the pellet (insoluble proteins) was resuspended in 1 ml of lysis buffer. Both soluble and insoluble fractions were diluted in 1% SDS loading buffer and electrophorised on a 10% SDS polyacrylamide denaturing gel for 1 hour at 60 milliamp constant current and followed by rapid blue staining.

5.2.25 Overexpression of PfMQO Recombinant Proteins

The overexpression of PfMQO protein was carried out based on the result obtained from the time and IPTG induction course study. 5 ml of starter culture of PfLMQO and PfSMQO bearing cells were inoculated into 100 ml LB/50 µg/ml ampicillin/25 µg/ml chloramphenicol growth media and grow at 37 °C in a shaking incubator at 200 rpm. The growth cultures were monitored spectrophotometrically at OD_{600} as described in section **5.2.21.** 1 mM of IPTG were added into the bacterial culture after OD_{600} of fermentation reached 0.6 to 0.8. The incubation temperature was reduced to 30 °C and the cultures were grown for an additional 3 hours. The cells were harvested by centrifugation at 3000 x g for 20 minutes at 4 °C. The cell pellets were frozen at -80 °C till further use.

5.2.26 Preparation of Clear *E. coli* Lysates under Native Conditions

Stored bacterial cells prepared as in section **5.2.25** were thawed on ice and resuspended in 5 ml of lysis buffer (150 mM NaCl, 50 mM Tris.HCl, 1 mM EDTA pH 7.4). 1 mg/ml lysozyme was added and the mixture kept on ice for 30 minutes. The cell mixture was sonicated on ice using a probe sonicator for 3 times at 80 amplitude with a 10-second cooling period between each burst. This was followed by centrifugation at 17,000 x g for 30 minutes at 4 °C. The supernatant was removed and divided into 2; C1 the soluble fraction which kept for SDS-PAGE analysis and S3 the soluble fraction which subjected to purify under native conditions. The pellet was resuspended in 500 µl of lysis buffer and divided into 2; insoluble fraction (C2) and insoluble fraction which was subjected to native purification (P3). Finally 50 µl of 100 % glycerol was added to the S3 and P3 samples. The mixtures were mixed thoroughly ready for purification under native condition.

5.2.27 Purification under Native Conditions

A 1:4 ratio 50 % Ni-NTA resin (Qiagen) was added to the soluble S3 and P3 fractions of PfLMQO. The mixtures were gently rotated for 60 minutes at 4 °C. Prior to loading the bacterial mixtures, the Ni-NTA columns were equilibrated three times with 600 µl sample wash buffer (50 mM NaH_2PO_4, 300 mM NaCl, 20 mM imidazole, pH 8.0) and centrifuged at 3000 rpm for 2 minutes at 4 °C . The mixture of of lysate and Ni-NTA was loaded into the column (Qiagen) and centrifuged at 16,000 g for 5 minutes at 4 °C. The flow through was collected and labelled as S4 and P4. The soluble and insoluble fractions were denoted as S and P throughout of this study. The columns were washed with wash buffer three times, followed by centrifugation and the flow through was collected. The flow throughs then were labelled as S5, S6, S7, P5, P6 and P7. Finally, the column was eluted twice with elution buffer

(50 mM Na_2PO_4, 300 mM NaCl, 20 mM imidazole pH 8.0) at 3000 rpm for 5 minutes at 4 °C . The samples were labelled as S8 and S9 (soluble) and P8 and P9 (insoluble). The eluted samples were diluted in 1 x SDS buffer and 1 x SDS loading buffer. Samples were subjected to electrophoresis on SDS-polyacrylamide gels containing 10% acrylamide for 1 hour at 60 milliamp constant current. The electroporated gels were stained using Expedion instant blue rapid staining (Expedion Protein Solutions, Cambridge, UK) and also using silver staining as described in section **2.15**.

5.2.28 Preparation of PfLMQO Inclusion Body for Purification under Denaturing Conditions

The cryostored bacterial cells bearing PfLMQO as in section **5.2.5** were thawed on ice and resuspended in 5 ml of lysis buffer (150 mM NaCl, 50 mM Tris HCl, 1 mM EDTA pH 7.4) and labelled as IB1. The resuspended cells were homogenised using Constant Systems Cell Disruptor (Constant Systems Ltd, UK) twice at 25 K. The cells were collected and 2 µl of DNAse I (Sigma Co., UK) and 0.5 mg/ml lysozyme (Sigma Co., UK) were added. The homogenised cells were labelled as IB2. The suspension was incubated for 20 minutes at room temperature on a rotating incubator for 20 minutes at room temperature. Triton X-100 was added to a final concentration of 2% v/v. The mixture was incubated on a rotating incubator for 30 minutes at 4 °C. After the incubation, the mixture was centrifuged at 17,000 x g for 30 minutes at 4 °C. The supernatant was separated and labelled as IB3. The pellet was resuspended in 1 ml of lysis buffer with complex protease inhibitor (Roche Co., UK) and followed by homogenised the cells using glass tissue homogenizer. The homogenised mixture was spun at 17000 x g for 30 minutes at 4 °C. The supernatant was discarded and the pellet was labelled as IB4 and kept at -80 °C. 1 ml of IB4 pellet was resuspended with buffer A (50

mM NaH_2PO_4, 300 mM NaCl, 5 mM Tris.Cl, 5 M GuHCl, pH 8.0) and followed by incubation overnight at 4 °C on the rotating incubator.

5.2.29 Purification under Denaturing Conditions

The purification began by equilibration of the Ni-NTA column by washing with 600 µl of Buffer A 3 times and centrifugation at 3000 rpm for 2 minutes at room temperature. The overnight inclusion bodies were centrifuged at 17,000 x g for 30 minutes at 4 °C and the supernatant was collected. The supernatant was separated and labelled as IB5. The pellet was resupended in 50 µl of lysis buffer contain Roche complex protease inhibitor. The mixture was labelled as IB6. 500 µl of IB6 was loaded to the spin column (Qiagen) and spun at 16,000 rpm for 5 minutes at room temperature. The flow through was collected and labelled as IBL1. This process was repeated and the second flow through was collected and labelled as IBL2. The column was washed 3 times with 600 µl of buffer A consisting 20 mM imidazole pH 8.0 and spun at 2,900 rpm for 2 minutes at room temperature. Every flow through was collected and labelled as IBW1, IBW2 and IBW3. Finally the column was eluted twice with 200 µl of Buffer B (50 mM NaPO4, 5 mM Tris.Cl, 500 mM imidazole, 30 mM NaCl and 5 mM GuHCl pH 7.5) and the elutes were labelled as IBE1 and IBE2. GuHCl should be separated from the samples by trichloroacetic acid (TCA) precipitation prior to SDS-PAGE analysis. A 100 µl of diluted samples were diluted to 10 µl of 10% TCA v/v with vortexing. The mixture was incubated for 20 minutes at 4 °C followed by centrifugation at 15,000 x g for 15 minutes at 4 °C. The supernatant was discarded and the pellet resuspended in 100 µl of cold ethanol. The sample was dried at 95 °C and subsequently resuspended in 1 x SDS sample buffer. 20 µg of proteins were separated under denaturing conditions on a 10% SDS polyacrylamide denaturing gel for 1 hour at 60 milliamp constant current and visualised by rapid blue staining and also stained by silver staining according to protocol described in section **2.15.**

5.2.30 Preparation of *E. coli* Rosetta Membranes

The PfLMQO expressed in *E. coli* Rosetta cells was prepared from LB broth containing 50 μg/ml ampicillin and 25 μg/ml chloramphenicol. As a control, *E. coli* Rosetta cells not transformed with the *PfMQO* gene was grown in LB broth containing only 25 μg/ml chloramphenicol. 10 ml of both bacterial cells were grown overnight at 37 °C at 200 rpm in a shaking incubator. The following day these cultures were propagated in 400 ml LB broth containing appropriate antibiotics and grown at 37 °C with 200 rpm until an OD 600 of 0.6 was reached (approximately 3 hours).The cells were induced with 1 mM IPTG and incubated for 4 h. The cells were harvested by centrifugation at 4000 x g for 20 min. Cells were resuspended in the 50 mM KPi /2mM EDTA pH 7.4) containing Roche protease inhibitor cocktail and kept on ice. This was followed by cell disruption using a cell disruptor at 25 K. The cell lysate was centrifuged at 10,000 rpm for 20 min at 4 °C to remove unbroken cells. Membranes were recovered from the supernatant by ultracentrifuging at 100,000 x g at 4 °C using Beckman Rotor JA 25.5 for 1 hour. The membranes were resuspended in 500 μl of 50 mM KPi/2 mM EDTA pH 7.4 contains protease inhibitor cocktail. The protein concentrations for both *E. coli* Rosetta control and *E. coli* Rosetta encoding PfMQO were carried out using Bradford assay as described in section **2.12** using BSA as a standard.

5.2.31 Measurement of MQO Enzyme Activities

Measurement of MQO activities either in native form in *E. coli* Rosetta cells or the recombinant PfMQO expressed in *E. coli* Rosetta were carried out using 2 types of electron donor. Both assays were perfomed spectrophotometrically using a Cary 300 Bio UV visible spectrophotometer. The first method is direct measurement using Q1 as electron acceptor and donor. The reaction was carried out in total volume of 700 ul of assay buffer (50 mM KPi/2 mM EDTA) pH 7.4, 50 μM Q-12,3-dimethoxy-5-methyl-6-(3-methyl-2-butenyl)-1,4-

benzoquinone (Sigma-Aldrich, UK) and 10 mM potassium cyanide (KCN) (Sigma-Aldrich, UK) at room temperature. The reaction was started by addition of L-malate (Sigma-Aldrich, UK) and the rate of Q1 reduction was determined by measuring the absorbance change at 273 nm.

The second assay was performed using 2,3-dichlorophenolindophenol (DCPIP) as an electron donor as described by (185). The MQO assays were carried out in a total reaction volume of 700 µl of assay buffer (50mM KPi/2 mM EDTA) pH 7.4 and 50 µM 2,3-dimethoxy-5-methyl-6-(3-methyl-2-butenyl)-1,4-benzoquinone (Sigma-Aldrich, UK) at room temperature. The first MQO assay was conducted by measuring the reduction of 50 µM 2,6-dichloroindophenol (DCPIP) (Sigma Aldrich, UK). The reaction was started by addition of 10 mM L-malate (Sigma, UK). The reduction of DCPIP was measured at 600 nm, and a differential absorption coefficient between oxidised and reduced DCPIP of 22 $cm^{-1}.mM^{-1}$ was assumed. The activity of DCPIP reduction was measured by subtracting the value of control activity (without the presence of substrate) in the reaction.

5.3 Results

5.3.1 Bioinformatic Analyses

The primary and secondary structure analyses of PfMQO were carried out using bioinformatic applications hosted by various domains online. The open reading frame and the molecular mass size of MQO were predicted using The Biology WorkBench 3.2 (http://workbench.sdsc.edu) and ProtParam programme hosted at http://www.expasy.org. The *PfMQO* gene shows an open reading frame (ORF) of 1566 bp with a predicted protein of 521

amino acids. The predicted molecular mass of PfMQO and isoelectric point (pI) are 59506.9 Da and 9.2 respectively.

The probability of PfMQO mitochondrial subcellular location was predicted using PFMpred (http://www.imtech.res.in/raghava/pfmpred) and PlasMit (http://gecco.org.chemie.uni-frankfurt.de/plasmit/) softwares that are freely available online. These softwares were used mainly to analyse *Plasmodium* subcellular protein. *P. falciparum* δ-aminolevulinic acid synthase and *P. falciparum* malate dehydrogenase (PfMDH) were used as positive and negative controls respectively. Table 5.2 shows the support vector machine (SVM) score of PFMpred result of 1.30 compared to 0.96 for δ-aminolevulinic acid synthetase and 0.0 for PfMDH. Similar analysis with PlasMit software using a neural network method shows that PfMQO and Pf δ-aminolevulinic acid synthase are mitochondrial proteins with a 91% reliability index (R.I) and that PfMDH is not a mitochondrial protein with a R.I of 99%.

Prediction of the transmembrane domains of *P. falciparum* proteins was carried out by TMHMM (http://www.cbs.dtu.dk/services/TMHMM/). PfDHODH and PfSD were selected as positive and negative membrane proteins control. The predictions of transmembrane domains plot of putative PfMQO, PfDHODH and PfSD are presented in Figure 5.5. Figure 5.5A shows the prediction result of PFMQO exhibiting only one transmembrane domain at amino acids position at 74-94 with a probability index of less than 0.75, suggesting that the PfMQO is unlikely the mitochondrial protein. In comparison, the PfDHODH in Figure 5.5B exhibits probability index 1, indicating that amino acids position 143-162 is likely the

```
      M  I  C  V  K  N  I  L  K  R  Y  K  N  S  P  L  N  E  L  R
1     atgatatgtgttaaaaatattttgaaaagatataaaaatagtccgttaaacgaactacgt  60
      N  N  R  K  Y  Y  E  G  S  F  V  K  S  I  K  F  S  T  S  N
61    aataataggaaatattatgaagggtcatttgtaaaaagtataaaatttagtacatcaaat  120
      Y  G  S  N  E  K  K  P  N  D  I  E  K  N  K  N  V  S  I  N
121   tatggaagtaatgaaaaaaaaccaaatgatattgaaaagaataagaatgtatctataaat  180
      L  N  E  G  N  I  L  Q  S  E  I  Y  D  T  V  V  I  G  G  G
181   cttaatgaaggtaatattttacaaagtgaaatatatgatacagttgtcataggaggaggg  240
      V  T  G  T  A  L  F  F  L  L  S  K  F  T  N  L  K  K  L  A
241   gtaacaggtactgctttgtttttttttattatctaaatttactaatttaaaaaagctagcc  300
      I  I  E  R  R  D  N  F  A  L  V  A  S  H  G  K  N  N  S  Q
301   ataattgaaagaagagataattttgctttagtagcatcacatggaaaaaataatagtcaa  360
      T  I  H  C  G  D  I  E  T  N  Y  S  F  E  K  A  K  F  I  K
361   acaattcattgtggtgatattgaaaccaattattcttttgaaaaagccaaatttataaaa  420
      R  Y  A  D  M  L  R  N  Y  L  T  N  I  P  K  E  K  R  E  N
421   agatatgctgatatgttaagaaattatttaacaaatatacctaaagaaaaaagagaaaac  480
      I  S  S  V  T  Q  K  M  V  L  G  V  G  E  K  E  C  Q  F  L
481   atatcaagtgttacacaaaaaatggttttaggtgtaggtgaaaaggaatgtcaattttta  540
      E  E  R  Y  P  V  F  R  Q  L  F  N  S  M  K  L  Y  N  K  D
541   gaagaaagatatcctgtatttagacaattatttaattccatgaaattatataataaagat  600
      D  I  H  E  V  E  P  R  V  A  L  K  D  S  H  T  L  R  E  E
601   gatatacatgaggtagaaccacgggttgctttaaaggattctcatacgttaagagaagaa  660
      Q  L  S  A  L  Y  M  P  P  E  L  T  T  C  D  Y  Q  K  L  S
661   caattatcagcattatatatgccaccagaattaaccacatgtgattatcaaaaattatcg  720
      E  S  F  I  E  S  A  R  T  V  P  N  K  T  I  S  I  N  L  L
721   gaaagttttattgaatctgcacgtactgtacccaataaaactatatctataaatttatta  780
      T  E  V  I  N  I  E  E  V  N  D  S  L  Y  K  I  H  T  N  K
781   acagaagtaattaatattgaagaagttaatgatagtttatataaaatacatacaaacaaa  840
      G  I  I  N  S  R  F  V  V  V  C  A  C  G  H  S  L  M  I  A
841   ggaatcattaattcgcgttttgttgtagtctgtgcatgcggacattcattaatgattgca  900
      Q  K  M  N  Y  G  L  E  Y  S  C  M  P  V  A  G  S  F  Y  F
901   caaaaaatgaattatggattagaatatagctgtatgcctgtagctggaagtttttatttt  960
      T  D  N  I  L  K  G  K  V  Y  T  I  Q  N  P  A  L  P  F  A
```

961 acggataatattttaaaagggaaagtatatactattcaaaatccagccttaccatttgca 1020

A V H G D P D I I E K G K T R F G P T A

1021 gccgtacatggagatccagatattattgagaaaggtaaaacgagatttggaccaacagct 1080

I P L P L L E R D N I K T L L D F L K V

1081 atacctttaccattgttagaaagagataatataaaaacattattggatttttaaaagta 1140

W N P D L S L F Q V Y Y N L F K D M T M

1141 tggaatccagatctaagtttatttcaagtatattataatttattcaaagatatgacaatg 1200

L K Y V A R N V L F E I P V L N K Y L F

1201 ttaaaatatgtagcacgtaacgttttatttgaaatcccagttttaaataaatatttattt 1260

L K D V K K I I P S L T I K D L T Y C V

1261 ttaaaagatgttaaaaaaattattccatcattaaccataaaagacttaacatattgtgtt 1320

G Y G G V R P Q L I N K K S K K L I L G

1321 ggttatggaggtgttcgaccacaactcataaataaaaaaagtaaaaaattaattcttgga 1380

E G K I D P G K N I I F N I T P S P G A

1381 gagggaaaaatcgatccaggaaaaaatattatctttaacattacaccttcacctggagca 1440

T T C L G N G E F D M N T I C E R L N A

1441 accacatgtttaggtaatggagaatttgatatgaacacaatatgtgaaagacttaacgca 1500

K I N K N D V K K Y L Y E G E Y P V N Y

1501 aaaattaacaaaaatgatgtgaaaaaatatttatatgaaggcgaatatcccgttaattat 1560

L *

1561 ttatga 156

Figure 5.4: Analysis of the Predicted Putative *PfMQO* Open Reading Frame (ORF), Start and Stop Codons

Analysis of the predicted *PfMQO* Open Reading Frame (ORF), Start and Stop Codons. *PfMQO* open reading frame of 1566 bp encoding a polypeptide 521 amino acid residues in length. Start and stop codons are underlined. The *PfMQO* gene was predicted using The Biology WorkBench 3.2 (http://workbench.sdsc.edu).

Table 5.2: Subcellular Location Predictions of *P.falciparum* Mitochondrial Proteins

	PFMpred		PlasMit	
Protein	SVM score	Final Prediction	R.I (%)	Final Prediction
Malate quinine oxidoreductase ,putative *P.falciparum* 3D7	1.30	MP	91	Possibly MP
Malate dehydrogenase, *P falciparum* 3D7	0.0	NMP	99	NMP
δ-aminolevulinic acid synthetase, *P. falciparum* 3D7 (PfALAS)	0.96	MP	91	Possibly MP

Subcellular location predictions of *P.falciparum* mitochondrial proteins using PFMpred and PlasMit bioinformatic methods. The prediction was done at default parameters of the web server. This table show the SVM score MitPred and R.I PlasMit analyses indicate the putative PfMQO is likely a mitochondrial protein. Pf δ-aminolevulinic acid synthetase and PfMDH proteins used as positive and negative controls. Abbreviations: SVM, Support Vector Machine; R.I, Reliability Index; MP; mitochondrial protein; NMP, non-mitochondrial protein.

transmembrane protein. Meanwhile, Figure 5.5C exhibits the transmembrane protein negative control plot. The PfSD probability index value is less than 0.75 indicates the amino acids sequence is unlikely the transmembrane protein.

The secondary structure of PfMQO was predicted using PSIPRED software (http://bioinf.cs.ucl.ac.uk/psipred) hosted by University of Collage London, UK. A grapic output of the predicted secondary structure of the putative PfMQO is shown in Figure 5.6. The stuctural composition is predicted to be 26% alpha Helix content, 22% strand and 52% coil.

The multiple alignment of MQO amino acid sequence from representative organisms was performed using ClustalW Multiple sequence alignment (http://mobyle.pasteur.fr/cgi-bin/portal.py) web server. The MQO amino acid sequences of *Plasmodium* spp., *E. coli* and *M. smegmatis* were extracted from sequence database of UniProt Knowledgebase UniProtKB (www.uniprot.org) website.The putatitve PfMQO amino acid sequence was compared with MQO amino acid sequences from other *Plasmodium* species, *E. coli* and *M. smegmatis*. Figure 5.7 shows that the putative PfMQO has 80% similiarity to putative PvMQO and putative PcMQO , 74% to PbMQO, 75% to putative PkMQO, 77% to probable PyMQO, 7% to EcMQO and 10% to MsMQO.

5.3.2 Amplification of *PfMQO* Gene

Using specific primers, as mentioned in materials and methods section **5.2.5.**, genomic DNA of *P. falciparum* strain 3D7 was subjected to amplification by PCR. The primers

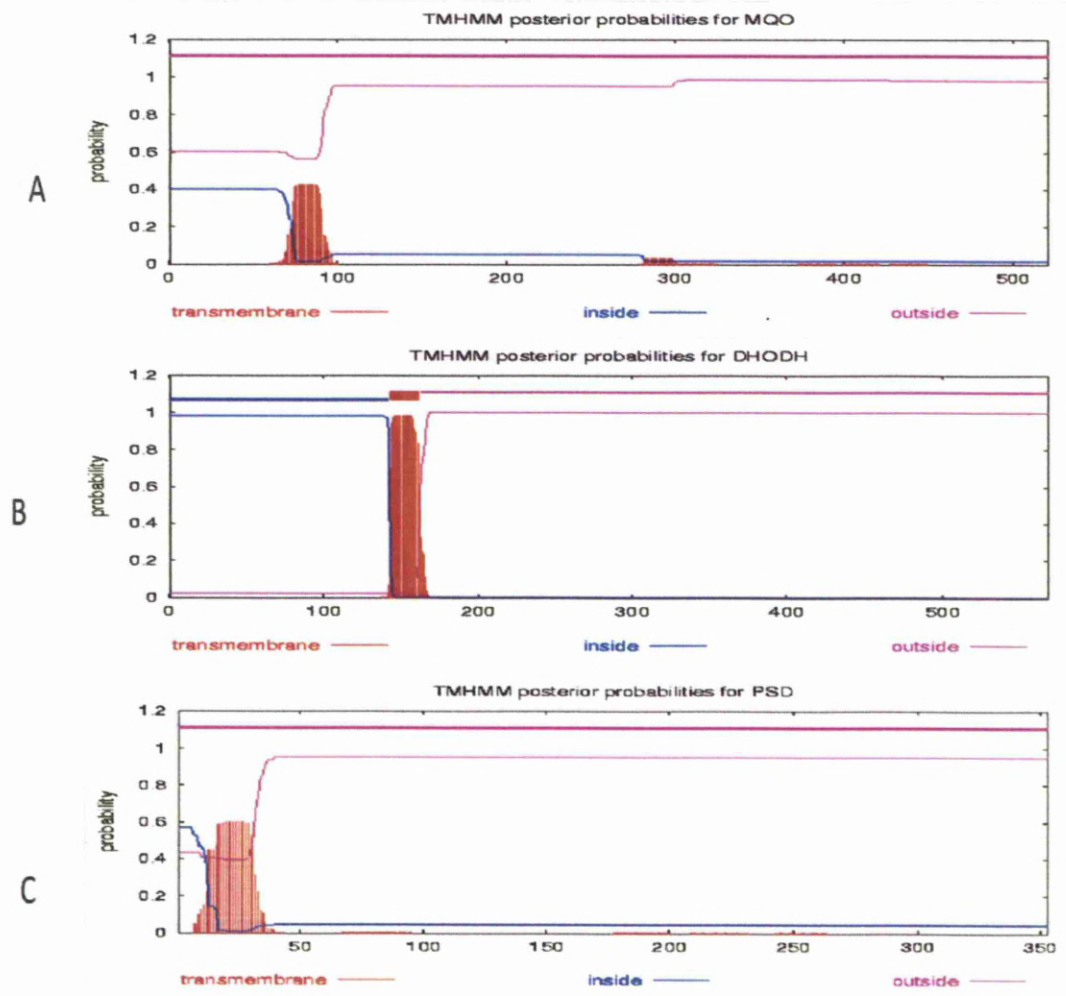

Figure 5.5: Graphical Representation of the Predicted Topologies of Putative PfMQO, PfDHOODH and PfPSD

Graphical representation of the transmembrane helices prediction in *P.falciparum* PfMQO, PfDHODH and PfPSD proteins. The plot was generated with TMHMM Server v. 2.0 (www.cbs.dtu.dk?services/TMHMM) shows the posterior probabilities of inside/outside/TM helices. The red lines indicate the number of predicted transmembrane helices, the blue lines indicate the inside region of the protein and the pink lines indicate the outside region of the the protein. X-axis indicates the amino acid number, Y-axis indicates the probability that the amino acid is located within the membrane, outside the cell or in the cytoplasm. The prediction gives the most probable location and orientation of transmembrane helices in the sequence at the top of the plot (between 1 and 1.2).The probability >0.75 indicate significant results and the maximum probability is 1 to indicate that amino acids are the transmembrane protein. The transmembrane regions of the PfMQO and PfPSD proteins have a probility lower than 0.75 and PfDHODH is close to 1. Therefore, suggesting that PfDHODH is most likely the transmembrane protein whereas PfMQOand PfPSD are no

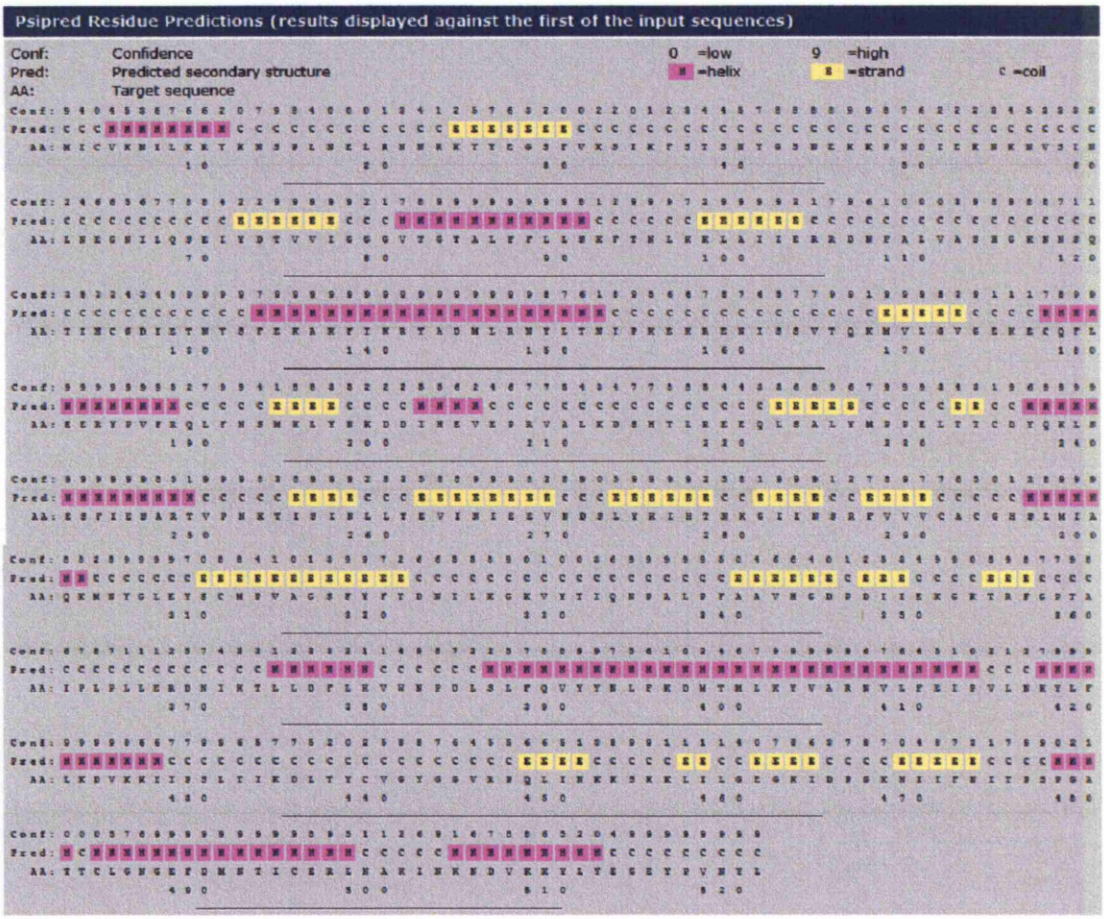
Psipred Residue Predictions (results displayed against the first of the input sequences)
Conf: Confidence
Pred: Predicted secondary structure
AA: Target sequence
0 =low
9 =high
H =helix
E =strand
C =coil

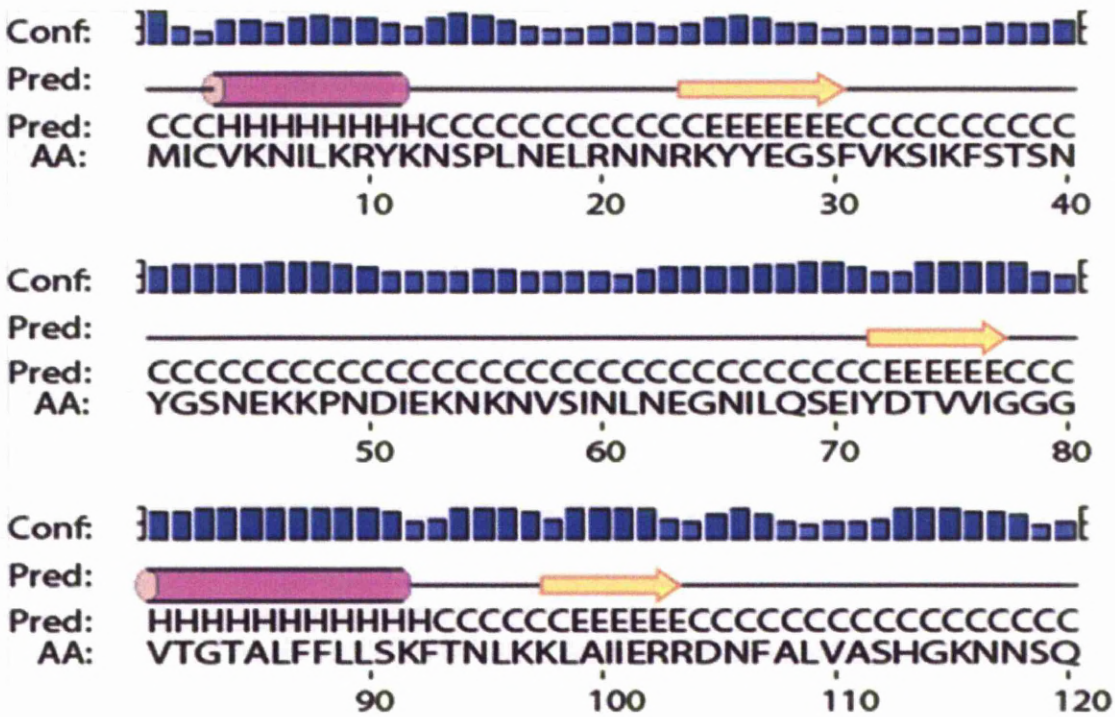
Conf:
Pred:
Pred: CCCHHHHHHHHHCCCCCCCCCCCCEEEEEEECCCCCCCCCC
AA: MICVKNILKRYKNSPLNELRNNRKYYEGSFVKSIKFSTSN
10
20
30
40
Conf:
Pred:
Pred: CCCCCCCCCCCCCCCCCCCCCCCCCCCCCCCCCCCEEEEECCC
AA: YGSNEKKPNDIEKNKNVSINLNEGNILQSEIYDTVVIGGG
50
60
70
80
Conf:
Pred:
Pred: HHHHHHHHHHHHCCCCCCEEEEEECCCCCCCCCCCCCCCCCC
AA: VTGTALFFLLSKFTNLKKLAIIERRDNFALVASHGKNNSQ
90
100
110
120

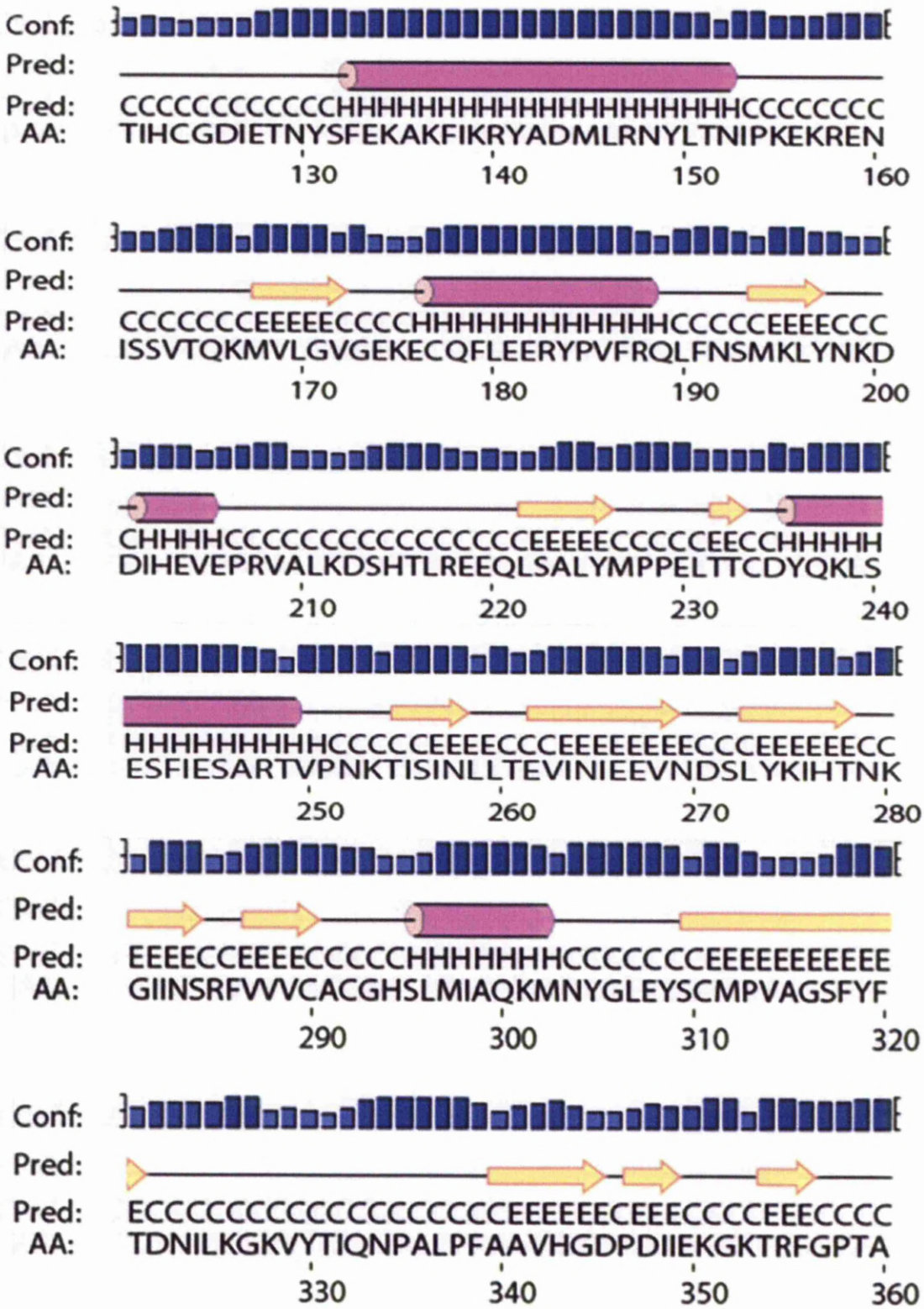
Conf:
Pred:
Pred: CCCCCCCCCCCCHHHHHHHHHHHHHHHHHHHHHCCCCCCCC
AA: TIHCGDIETNYSFEKAKFIKRYADMLRNYLTNIPKEKREN
130 140 150 160
Conf:
Pred:
Pred: CCCCCCCEEEEECCCCHHHHHHHHHHHHHCCCCCEEEECCC
AA: ISSVTQKMVLGVGEKECQFLEERYPVFRQLFNSMKLYNKD
170 180 190 200
Conf:
Pred:
Pred: CHHHHCCCCCCCCCCCCCCCEEEEECCCCCEECCHHHHH
AA: DIHEVEPRVALKDSHTLREEQLSALYMPPELTTCDYQKLS
210 220 230 240
Conf:
Pred:
Pred: HHHHHHHHHCCCCCEEEECCCEEEEEEECCCEEEEEECC
AA: ESFIESARTVPNKTISINLLTEVINIEEVNDSLYKIHTNK
250 260 270 280
Conf:
Pred:
Pred: EEEECCEEEECCCCCHHHHHHHCCCCCCCEEEEEEEEEEE
AA: GIINSRFVVVCACGHSLMIAQKMNYGLEYSCMPVAGSFYF
290 300 310 320
Conf:
Pred:
Pred: ECCCCCCCCCCCCCCCCCCCEEEEEECEEECCCCEEECCCC
AA: TDNILKGKVYTIQNPALPFAAVHGDPDIIEKGKTRFGPTA
330 340 350 360

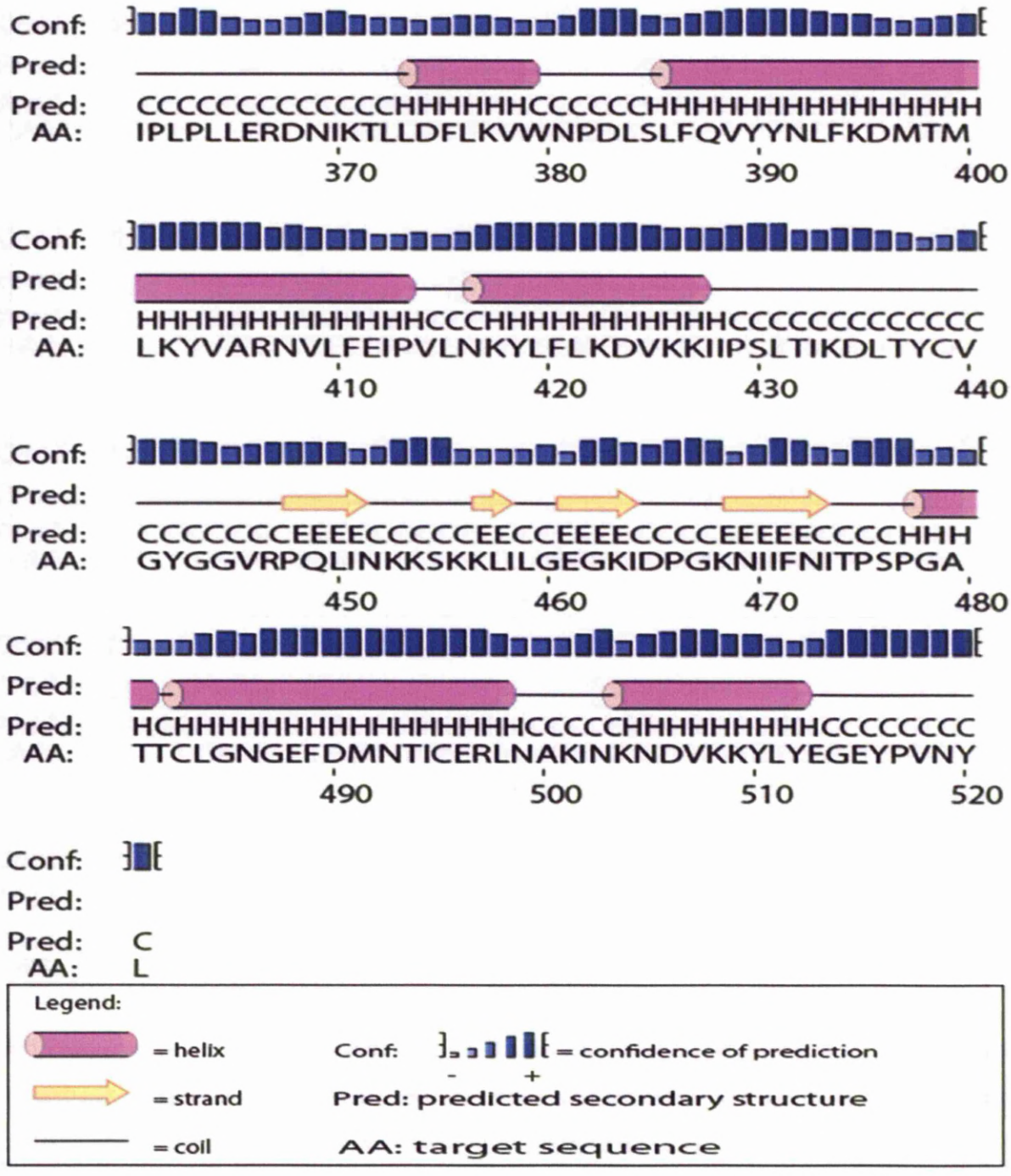

Figure 5.6: The Amino Acid Sequence of the Putative PfMQO with Predicted Secondary Structure by PSIPRED

(A) Schematic of putative PfMQO residue prediction. The H stands for helix, C for coil and E for strand. The structural composition of the protein is predicted to be 26% helix content, 22% strand and 52% coil content. (B) Grapical output of putative PSIPRED for PfMQO. The blue bars for each amino acid represents the confidence of each prediction. The taller the bar indicates the higher level of confidence. 'Pink cylinder' corresponds to a helix, 'yellow arrow' to a strand and 'black line'to a coil and finally 'AA' stands for the target sequence.

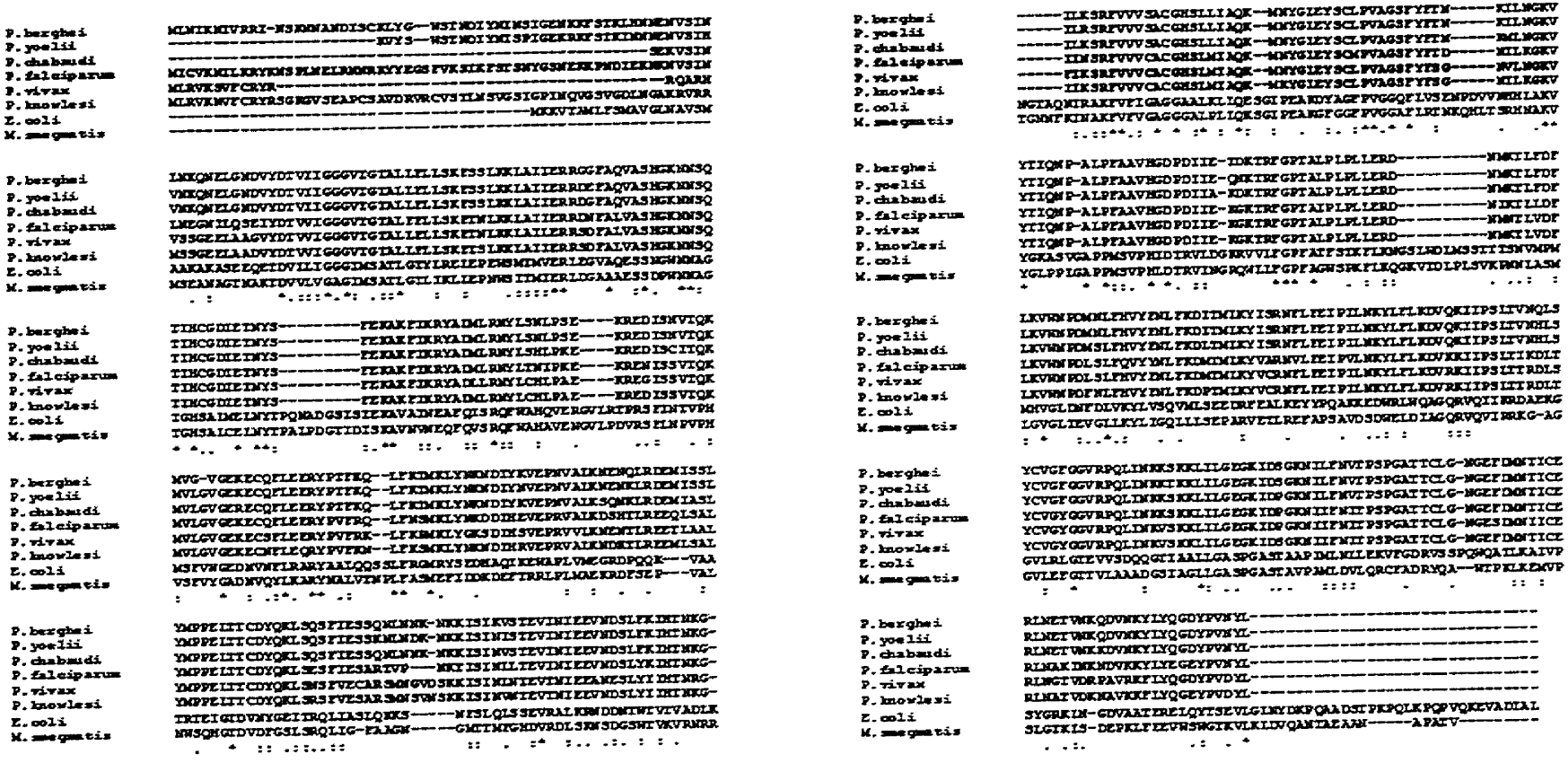

Figure 5.7: Sequence Alignment Results for MQOs from Representative Organism

Multiple sequence alignment for MQO of different *Plamodium* species, *E. coli* and *M. smegmatis* were generated using ClustalW programme (http://mobyle.pasteur.fr/cgi-bin/portal.py). This alignment shows that the putative PfMQO has an 80% similiarity to putative PvMQO and putative PcMQO, 74% to PbMQO, 75% to putative PkMQO, 77% to probable PyMQO, 7% to EcMQO and 10% to MsMQO. The consensus lines (*) indicate identical residues; (:) indicate semi-conserved residues; (.) designated conserved residues.

(Table 5.1) were designed to facilitate cloning into the expression vectors pET-15b and pUC19. The two sets of primers incorporated restriction enzyme sites as follows: *Nde*I and *Bam*HI for pET-15b and *Pst*I and *Bam*HI for pUC19. The putative *PfLMQO* gene and *PfSMQO* without leader sequence (signal peptide sequence) were amplified by PCR and yielded single amplicon of ~1566 bp (LMQO) and ~1529 bp (SMQO) respectively. Figure 5.8 indicates that the PCR conditions have been optimised and primers are specific for the targeted gene. The size of the PfSMQO fragment is smaller than PfLMQO due to a deletion of the putative leader sequence from the putative *PfMQO* gene. The predicted putative leader sequence comprising "catatatgatatgtgttaaaaatattttgaaaagatataaaaatagtccg" nucleotides were predicted using SignalP 4.0 Server programme (www.cbs.dtu.dk).

5.3.3 Screening of Positive Clones of *PfMQO* in TOP 10 *E. coli* host

The amplicons of the *PfMQO* gene were initially cloned to the Invitrogen pCR®II-TOPO® vector using the TOPO TA cloning kit (Invitrogen). TOPO TA cloning providing fast and efficient cloning strategies for direct cloning of the PCR products into a plasmid vector. *Taq* polymerase which was used in PCR reaction has added a single deoxyadenosine (A) at the 3' ends of the PCR products thus facilitating the direct cloning into the T overhanging 3′ deoxythymidine sites located in the multiple cloning site (MCS) of the linearised TOPO vector as shown in Figure 5.9. The cloning of PCR products into the TOPO vector created 5,571 bp TOPO/PfL*MQO* and 5,529 bp TOPO/PfS*MQO* respectively.

The success of the PfLMQO and PfS*MQO* cloning were validated using restriction enzyme analysis as described in section **5.2.13**. White colonies from each transformantion

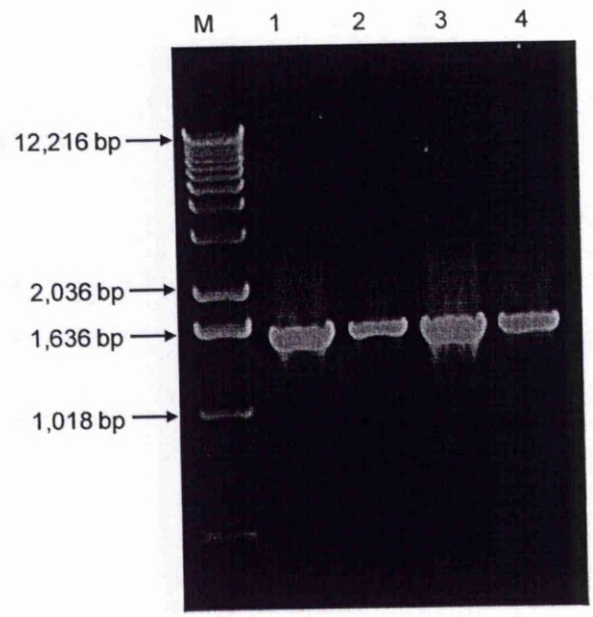

Figure 5. 8: Amplification of *P. falciparum* 3D7 *MQO* .

Agarose gel electrophoresis showing PCR amplification of putative *PfMQO* gene from *P. falciparum* 3D7. Lane M contains 1 kb DNA molecular weight marker (Invitrogen), lanes 1, 2, 3, and 4 show the PCR products of PfpETLMQO, PfpETSMQO, PfpUCLMQO and PfpUCSMQO. Lanes 1-4 show a single band of size ~ 1.6 kb. The PCR products were visualised on a 1.2% agarose gel.

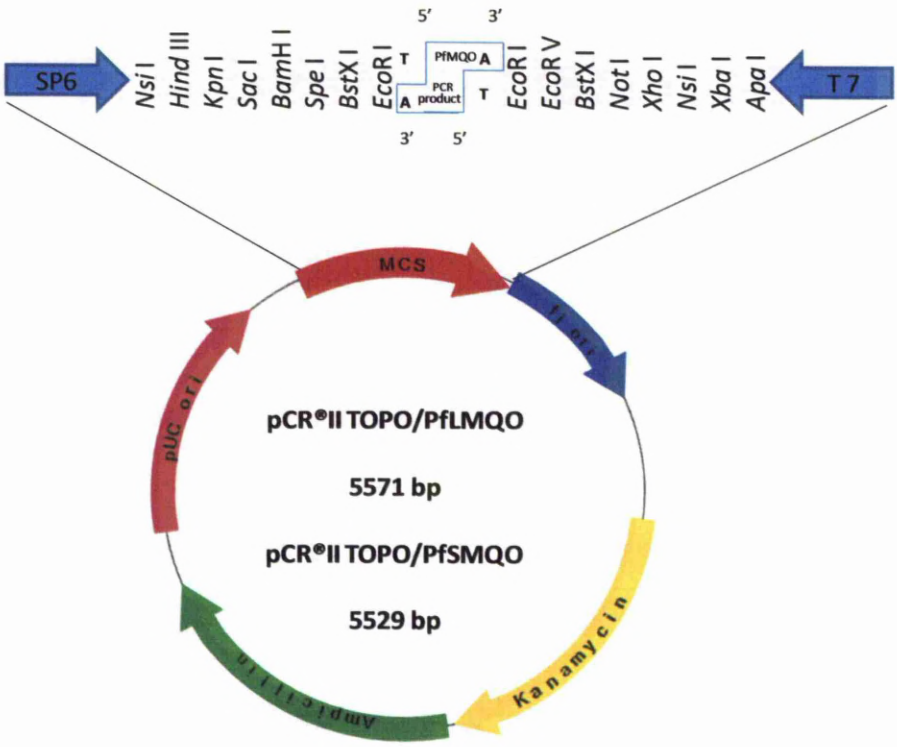

Figure 5.9: Plasmid Map of pCR®II-TOPO® Bearing the *P. falciparum MQO* gene within the Multiple Cloning Site (MCS)

pCR®II-TOPO® (Invitrogen) has been used to construct the recombinant *PfMQO* directly from a PCR reaction. The pCR®II-TOPO® Invitrogen vector is a 4.0-kb linearised vector with a overhanging deoxythymidine (T) residue at the 3' ends to make it easy for the PCR products that possess single deoxyadenosine (A) at 3' ends to ligate efficiently with the vector. The pCR®II-TOPO® vector contains a *lac* promoter to allow the expression of the *lacZ* gene gene which encodes the first 146 amino acid of β-galactosidase. Interruption of *lacZ* by the insertion of PCR product may give rise to white colonies. The presence of both the kanamycin and ampicillin resistance genes in the vector allows for selection and maintainance in *E. coli*. The vector contains a f1 origin of replication for propagation in *E. coli*. The vector also carries the T7 promoter and M13 forward and reverse priming sites for *in vivo* and *in vitro* transcription of sense RNA and sequencing of the insert. The plasmid map was generated using NetPlasmid software hosted by http://www.justbio.com

were picked and cultured overnight in LB medium containing 50 μg/ml ampicillin. The white colonies represent the recombinant *lacZ* gene with foreign DNA, whereas the blue colonies The recombinant plasmids were sent to Cogenics Ltd, UK for automated sequencing using their M13 primers. The positive *PfMQO* clones showed 100% identity when aligned with the published putative *PfMQO* gene sequence using the BLAST programme (http://blast.ncbi.nlm.nih.gov). The recombinant plasmids were designated as TOPO/pETPfLMQO, TOPO/pETPfS*MQO*, TOPO/pUCPfLMQO and TOPO/pUCPfS*MQO*.

5.3.4 Subcloning of TOPO/pET and TOPO/pUC (PfLMQO and PfSMQO) into pET-15b and pUC19 Expression Vectors

The plasmids TOPO/pETPfMQOs and TOPO/pUCPfMQOs were subcloned into pET-15b and pUC19 expression vectors. This was carried out by double digestion of the plasmid to excise the *MQO* fragment from the TOPO vector and subsequent ligation to the appropriate vector (pET-15b or pUC19). The TOPO/pETPfMQOs were double digested using *Nde*I and *Bam*HI, whilst the TOPO/pUCPfMQOs were digested with *Pst*I and *Bam*HI. Figure 5.10A shows the results of the digests with DNA fragment size of ~4.0 kb and ~1.6 kb corresponding to the pCR®-TOPO vector and *PfMQO* fragments respectively. Figure 5.10B shows the 3 DNA fragments ~ 4.0 kb, ~ 1.6 kb and 1118 bp that corresponding to bands corresponding to pCR®-TOPO vector, *PfMQO* and the second *Pst*I restriction site within the pCR®-TOPO vector. All clones were produced expected band size in agreement with the predicted DNA fragment size generated using NEBcutter V2.0 programme (tools.neb.com/NEBcutter2). The DNA fragments were excised, as described in section **5.2.14** from 1.2% agarose gels and pooled together in order to achieve a higher concentration of the *PfMQO* gene. The *PfMQO* fragments from pETPfLMQO and pETPfSMQO were ligated to linearised pET-15b and PfLMQO and pUCPfSMQO to pUC19 expression vectors.

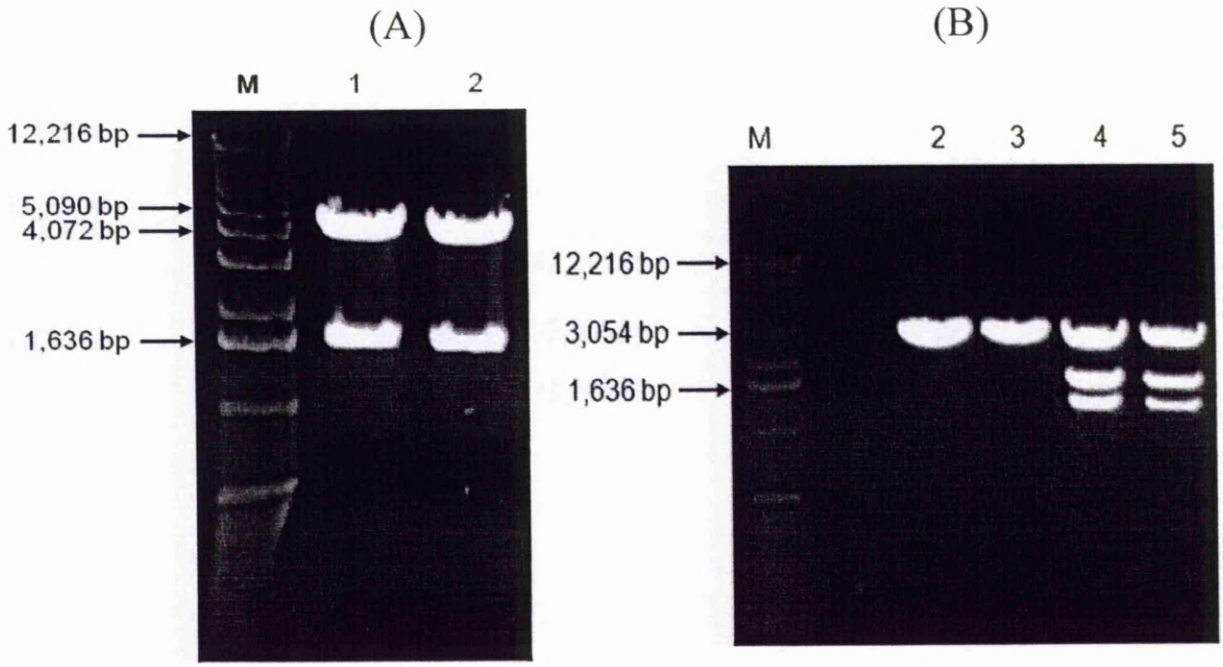

Figure 5. 10: Restriction Enzyme Digestion Analysis of Transformed Colonies of pCR®II-TOPO/PfMQO

Panel A: Lanes 1 TOPO/pETPfLMQO and lane 2 TOPO/pETPfSMQO produced 2 bands of approximately ~4 kb and ~1.6 kb corresponding to pCR®-TOPO vector and *PfMQO* fragment respectively when digested with *Nde*I and *Bam*HI. Panel B: Lane 2 and 3 are undigested TOPO/pUCPfLMQO and TOPO/pUCPfSMQO. Lanes 4 and 5 contain digested TOPO/PfLMQO and TOPO/PfSMQO, respectively. The digest used *Pst*I and *Bam*HI and produced 3 bands sizes of ~4 kb, ~1.6 kb and ~1118 bp corresponding to pCR®-TOPO vector, *PfMQO* and the second *Pst*I restriction site within the pCR®-TOPO vector. Lanes designated M contain 1 kb DNA ladder (Invitrogen)

The ligation of the expression vector and plasmid was described in section **5.2.16**. The ligated plasmid and insert created the 7274 bp and 7229 bp plasmids (pET-15/pETPfLMQO and pet-15b/pETPfSMQO) respectively and 4257 bp and 4218 bp plasmids (pUC19/pUCPfLMQO and pUC19/pUCPfSMQO) respectively. The DNA fragment of *PfMQO* was cloned between the restriction sites of *Nde*I and *Bam*HI for pET-15b and *Pst*I and *Bam*HI for pUC19. The cloning of the insert into the vector is diagrammatically illustrated in Figure 5.11(pET-1b) and Figure 5.12 (pUC19).

The ligation reactions were transformed into *E. coli* TOP10 cells as described in section **5.2.16**, and plated on LB agar plates containing 50 μg/ml ampicillin which were incubated overnight at 37 °C. Colonies were picked and subjected to overnight culture followed by miniprep DNA isolation. Figure 5.13A shows results of the positive colonies of pET/PfLMQO and pET/PfSMQO that produced 3 bands sizes ~4229 bp, ~1897 bp and ~1153 bp, and ~4229 bp, ~1855 bp and ~1153 bp respectively when digested with *EcoR*V. Figure 5.13B the positive clones of pUC/PfLMQO and pUC/PfSMQO produced 2 bands of approximately 3253 bp, 1004 bp.and 3243, 965 bp respectively when digested with *Sph*I. Positive clones were processed for glycerol stock cryopreservation. The positive recombinant plasmids were designated as pET/PfLMQO, pET/PfSMQO, pUC/PfLMQO and pUC/PfSMQO.

5.3.5 Transformation of pET/PfMQOs and pUC/PfMQOs into BL21 (DE3)pLysS E. coli

The positive recombinant plasmids were subjected to transformation into the expression *E. coli* BL21(DE3)pLysS cells. *E. coli* BL21(DE3)pLysS cells are under the control of T7 promoter expression system which allows higher protein expression. This strain

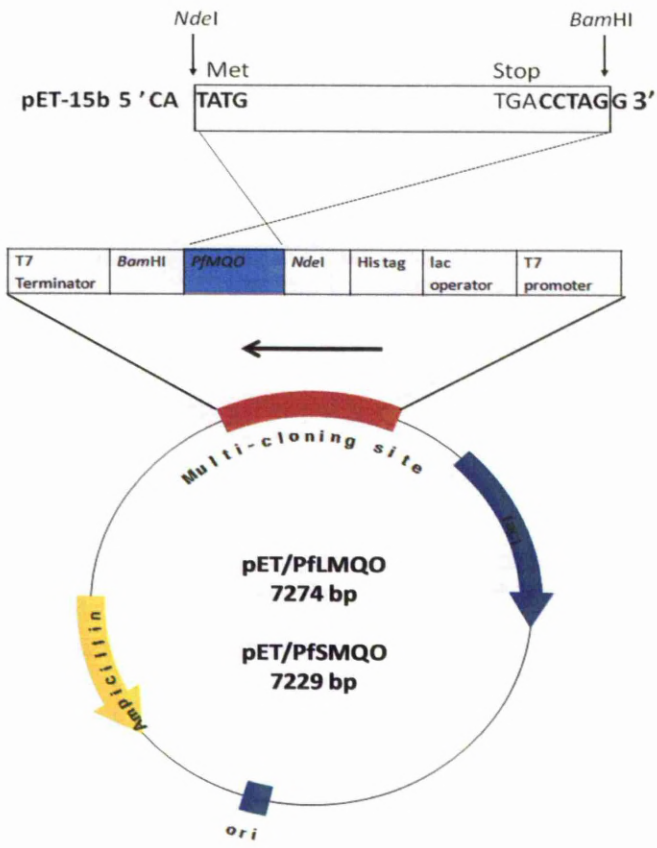

Figure 5.11: Schematic Representation of the pET-15b Expression Vector Bearing *P. falciparum MQO* gene

The pET-15b plasmid contains a T7 promoter region, a lacI gene, a sequence coding for six histidine residues and an ampicillin resistance gene that enables selection. The plasmid construction was carried out by excising the PFMQO from pCR®II-TOPO® vector and ligated into *Nde*I and *Bam*HI restriction sites under the control of T7 promoter. The sucessfull of the PfMQO cloning into the expression vector, yielding the N-terminal His-tagged recombinant protein.The plasmid map was generated using NetPlasmid software hosted by http://www.justbio.com.

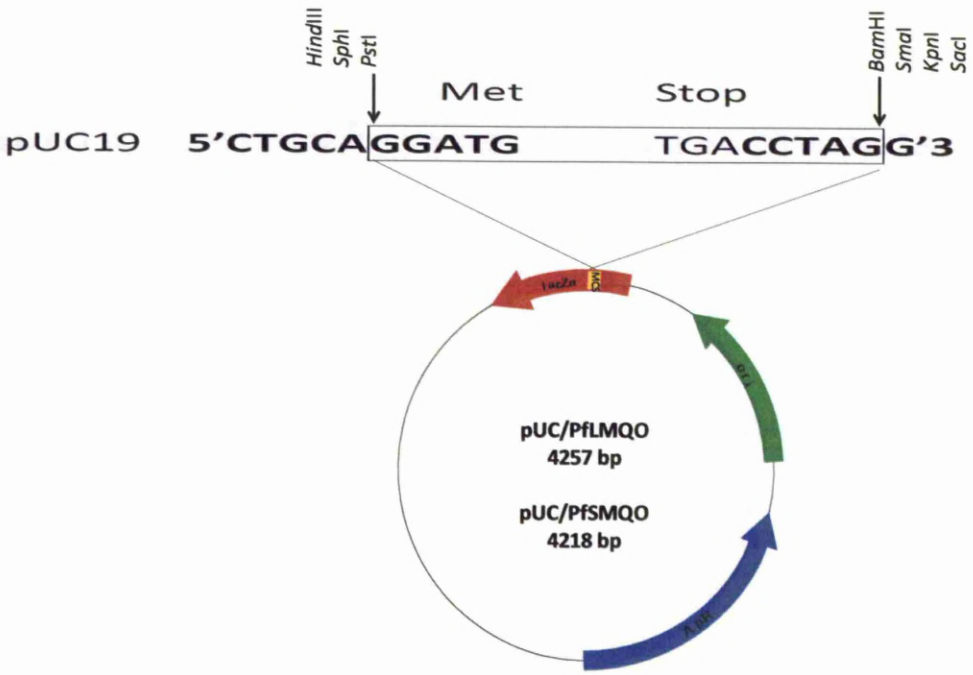

Figure 5.12: Schematic Representation of the pUC19 Expression Vector Bearing *P. falciparum MQO* gene

The pUC19 plasmid contains a *lacZ* gene which has similar features to pCR®II-TOPO® vector. The presence of the lacZ gene allows recombinants to be selected by blue/white screening. pUC19 also possesses the ampicillin resistance gene (Apr) that enables selection. The plasmid construction was carried out by excising the *PfMQO* from pCR®II-TOPO® vector and ligating into the pUC19 multiple cloning sites (between *Pst*I and *Bam*HI restriction sites). The plasmid map was generated using NetPlasmid software hosted by http://www.justbio.com.

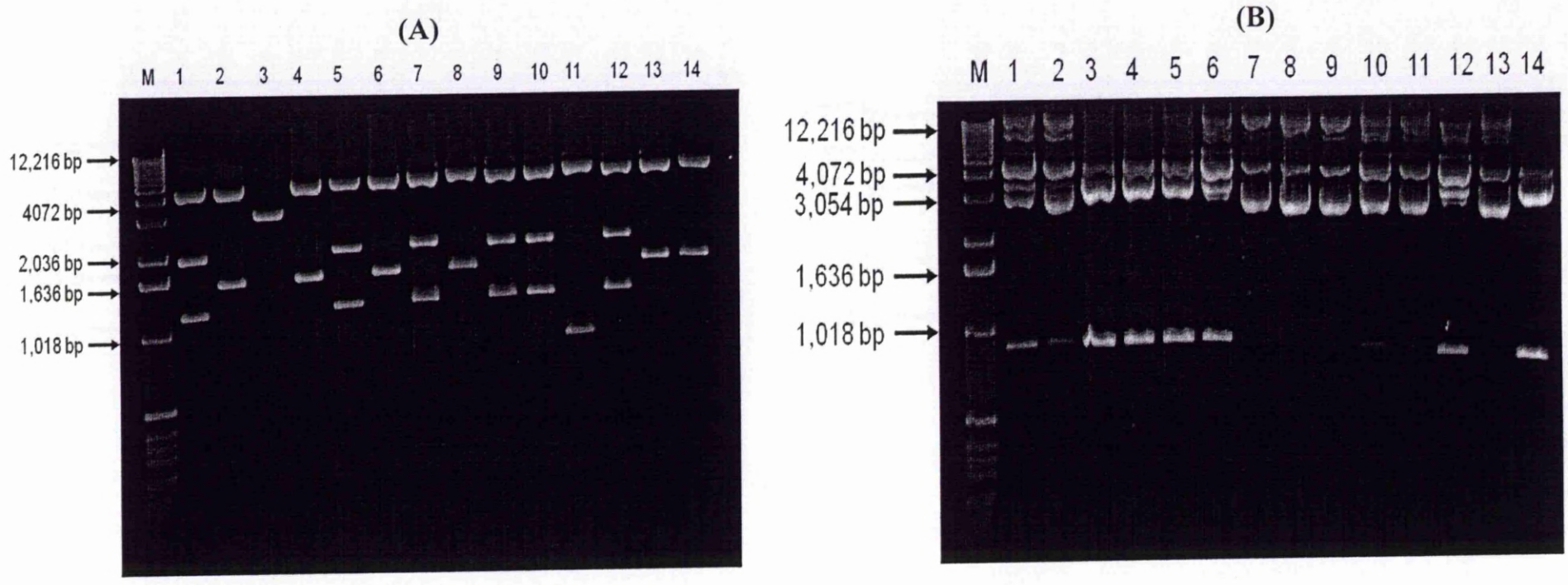

Figure 5.13: Screening of Positive Clones of pET-15b and pUC19 Transformed into *E. coli* TOP 10

Panel A, lanes 1-7 consist of putative pET/PfLMQO digests and lanes 8-14 consist of putative pET/PfSMQO digests. The positive clones for pET/PfLMQO and pET/PfSMQO produced 3 bands of approximately 4229 bp, 1897 bp and 1153 bp, and 4229 bp, 1855 bp and 1153 bp respectively when digested with *EcoR*V. Panel B; Lanes 1-7 consist of putative pUC/PfLMQO digests, and lanes 8-14 consist of putative pUC/PfSMQO digests. the positive clones of pUC/PfLMQO and pUC/PfSMQO produced 2 bands of approximately 3253 bp, 1004 bp.and 3243, 965 bp respectively when digested with *Sph*I.Lanes designated M contain 1 kb DNA ladder (Invitrogen).Panel A, lanes 2, 3, 4, 6, 7, 8, 9, 11, 13 and 14; and lanes 7, 8, 9, 10, 11, and 13 in panel B appeared with wrong sizes of DNA fragments therefore was excluded from further analysis.

carries both the DE3 lysozyme and the plasmid pLysS. DE3 consists of T7 bacteriophage gene I encoding T7 RNA polymerase under the control of the *lac* UV5 promoter. pLysS carries the gene encoding for T7 lysozyme which lowers the expression level of recombinant genes by inhibiting basal level of T7 RNA polymerase but does not affected the expression level of recombinant protein following induction by IPTG. The transformants were plated onto the LB agar plate consisting 25 μg/ml chloramphenicol and 50 μg/ml ampicillin. The same procedure was repeated where single colonies were picked and used to inoculate LB broth consisting 50 μg/ml ampicillin and 25 μg/ml chloramphenicol and subjected to minipreps preparation. Results from Figure 5.14A show that the positive pET/PfLMQO and pET/PfSMQO clones produced 3 bands of approximately 4229 bp, 1897 bp and 1153 bp, and 4229 bp, 1855 bp and 1153 bp respectively when digested with *Eco*RV. Whilts in Figure 5.14B positive clones for pUC/PfLMQ and pUC/SMQO produced 3 bands of approximately 2079 bp, 1224 bp and 954 bp and 2079 bp, 1185 and 954 bp when digested with *Afl*III.

5.3.6 Transformation of Pet/PfMQOs and PUC/PfMQOs into *E. coli* Rosetta (DE3) pLysS

The positive recombinant DNAs were retransformed into *E. coli* Rosetta (DE3) after expression in BL21(DE3) pLysS cells was not detectable. The 'maxi prep' preparations were carried out to get the highest purity and concentration of plasmids. The same screening procedures were carried out as described in section **5.2.13**. Figure 5.15A and 5.15B produced similar results as described in section 5.3.5. Restriction enzyme analysis using *Sph*I was carried out and from the finding showed that the positive clones of pUC/PfLMQO and pUC/PfSMQO produced 2 bands with approximately 3253 bp, 1004 bp.and 3243, 965 bp respectively.

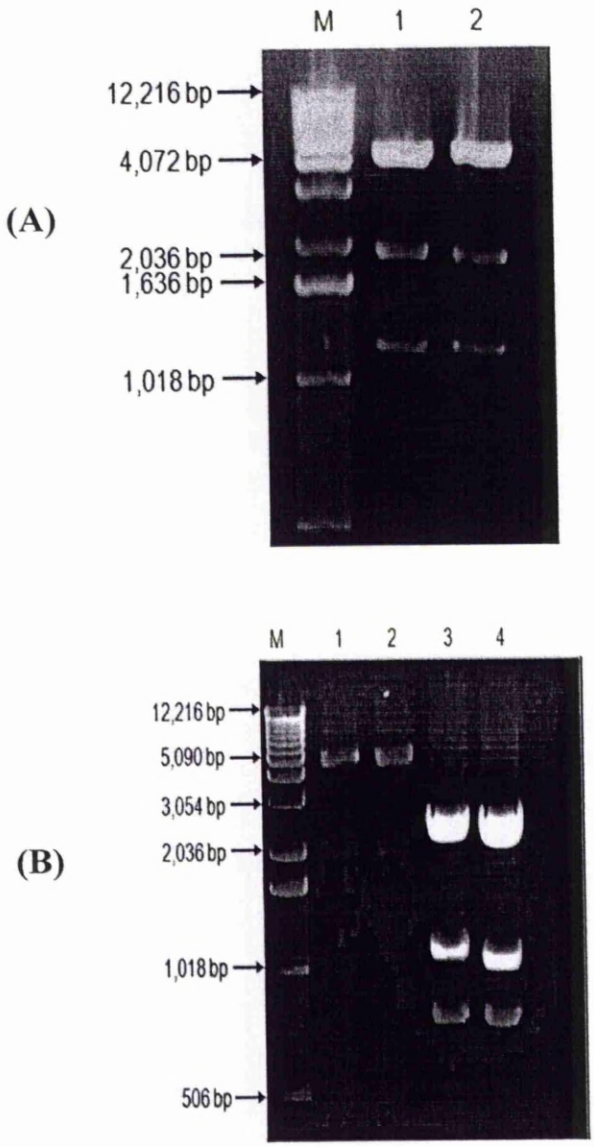

Figure 5.14: Screening of Positive Clones of pET-15b and pUC19 Transformed into BL21 (DE3) pLysS *E. coli*

Panel A; Lanes 1 and 2 consist of pET/PfLMQO and pET/PfSMQO. The positive clones for pET/PfLMQO and pET/PfSMQO produced 3 bands of approximately 4229 bp, 1897 bp and 1153 bp, and 4229 bp, 1855 bp and 1153 bp respectively when digested with *EcoR*V. Figure B; lanes 1 and 2 consist of undigested pUC/PfLMQO and pUC/PfSMQO. The positive clones for pUC/PfLMQO and pUC/PfSMQO (lanes 3 and 4) produced 3 bands of approximately 2079, 1224 bp, 1224 bp and 2079 bp, 1185 bp, 954 bp respectively when digested with *Afl*III. Lanes designated M contain 1 kb DNA ladder (Invitrogen).

5.3.7 Expression Studies of PfMQOs in *E. coli* Rosetta (DE3) pLysS

Small scale cultures of positive clones selected from restriction enzyme analysis were subjected to 1-mM IPTG induction at 30 °C to express the predicted ~60 kDa PfMQO protein. Immunodetection using monoclonal anti-polyhistidine antibody as primary antibody followed by secondary antibody horseradish peroxidase (HRP) anti-mouse Ig antibody (Nordic Immunology) was carried out to determine the expression of recombinant PfMQO in both pET-15b and pUC19 expression vectors. Figure 5.16 (lanes 1 and 2) show both PfLMQO and PfSMQO cloned into pET-15b expression vector were producing a band ~ 60 kDa as analysed on a 10% SDS-PAGE. From Figure 5.18 it is also evident that PfSMQO was less expressed compared to PfLMQO.

5.3.8 Solubility Studies of PfLMQO and PfSMQO Recombinant Proteins

The solubility assay of the proteins was carried out to determine the presence of overexpressed protein in a soluble fraction, insoluble fraction or in the form of an inclusion body. The fractions of soluble material, insoluble material and inclusion bodies of homogenised *E. coli* Rosetta cells producing PfLMQO and PfSMQO were analysed on a 10% SDS-PAGE and stained with InstantBlue ™ (Expedon) stain. Results from Figure 5.17 shows the expressed proteins are found exclusively associated with the insoluble fractions (i.e. in the pellet fraction and in inclusion bodies). Inclusion bodies are insoluble and biologically inactive aggregates of partially folded protein. This is frequently seen when a recombinant protein is overexpressed either in the cytoplasm or periplasm of the *E. coli* bacterial host. This is usually associated with high initial expression of the protein thus forming a homogeneous aggregate of the overexpressed protein.

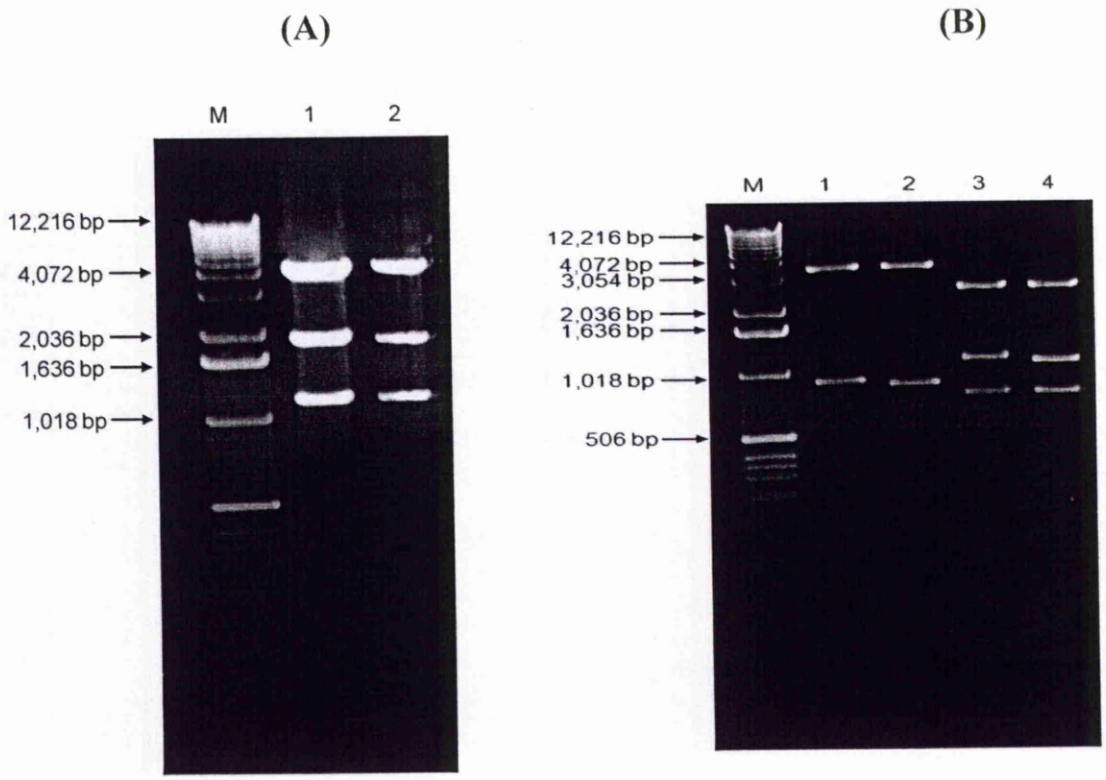

Figure 5.15: Screening of Positive Clones of pET-15b and pUC19 Transformed into Rosetta (DE3) *E. coli*

Panel A; Lanes 1 and 2 consist of pET/PfLMQO and pET/PfSMQO. The positive clones for pET/PfLMQO and pET/PfSMQO produced 3 bands sizes 4229 bp, 1897 bp and 1153 bp, and 4229 bp, 1855 bp and 1153 bp respectively when digested with *EcoR*V. Figure B; lanes 1 and 2 consist of pUC/PfLMQO and pUC/PfSMQO. Lanes 3 and 4 represent the positive clones of pUC/PfLMQO and pUC/PfSMQO produced 2 bands of approximately 3253 bp, 1004 bp.and 3243, 965 bp respectively when digested with *Sph*I. The positive clones for pUC/PfLMQO and pUC/PfSMQO produced 3 bands approximately 2079, 1224 bp, 1224 bp and 2079 bp, 1185 bp, 954 bp respectively when digested with *Afl*III. Lanes designated M contain 1 kb DNA ladder (Invitrogen).

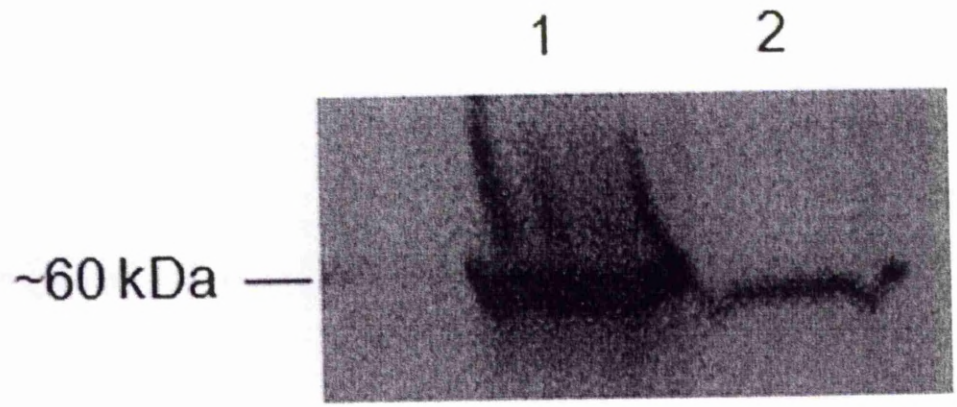

Figure 5.16: The Expression Study of PfMQO

Lanes 1 and 2 consist of pET/PfLMQO and pET/PfSMQO expressed in *E. coli* Rosetta . The ~ 60 kDa proteins were visible in the pET-15b expression system after immunodetection with monoclonal anti-oligohistidine antibody.

5.3.9 Time, Temperature and IPTG Induction Studies of Recombinant PfLMQO and PfSMQO in *E. coli* Rosetta (DE3) Cells

Time, temperature and IPTG induction studies of recombinant PfLMQO and PfSMQO expressed in the pET-15b system were carried out to determine the optimal post-induction duration, temperature and IPTG concentration as described in section **5.2.24**. The bacterial cells were grown in LB broth containing of 50 μg/ml ampicillin and 25 μg/ml chloramphenicol. The cells were grown at three different temperatures (22, 30 and 37 °C), and two IPTG concentrations (0.5 and 1 mM). SDS-PAGE gels stained with InstantBlue ™ (Expedon) stain exhibit the recombinant PfLMQO protein in the insoluble fraction. A band of ~60 kDa became visible after 3 hours post-induction at all temperatures and IPTG concentrations (Figure 5.18A). However, the level of protein expressed is less at the 0.5 mM IPTG concentration at all temperatures. An IPTG concentration of 1 mM and a post-induction time of 3 hours were found to be optimal for the maximal expression of PfLMQO. This is shown by the appearance of bands of ~ 60 kDa with higher intensities compared with other protein bands after eletrophoresis onto a 10% acrylamide SDS-PAGE (Figure 5.18A). The level of expression started to decline after 5 hours incubation (Figure 5.19A) and the protein was completely degraded after overnight incubation (Figure 5.20A) in all test conditions. At the same time, results on the expression level of PfSMQO shown the recombinant PfSMQO protein is less compared to PfLMQO. This is shown in Figure 5.18B and Figure 5.19B which the protein band ~60 kDa is barely visible compared to PfLMQO. This is observed in different temperatures and IPTG concentions.

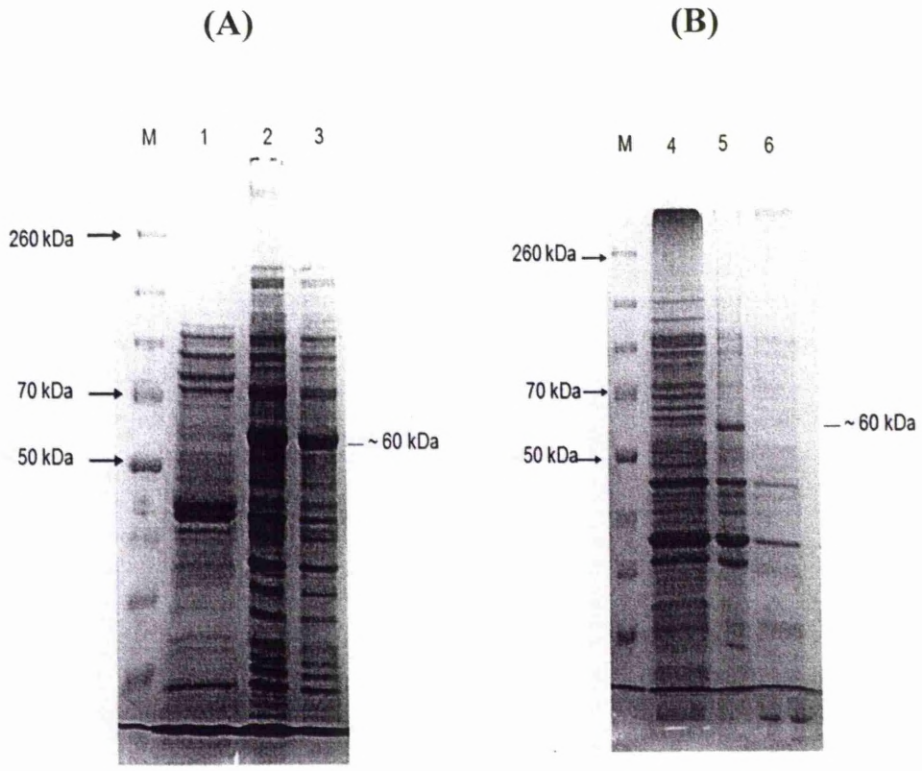

Figure 5.17: Solubilty Study of PfLMQO and PfSMQO

Solubility study of PfLMQO and PfSMQO grown at 30 °C with 1 mM IPTG. Panel A (PfLMQO) : Lane 1, soluble fraction, lane 2, insoluble fraction and lane 3, inclusion body. Panel B (PfSMQO) : Lane 4 insoluble fraction, lane 5 inclusion bodies and lane 6 soluble fraction. Lane M, protein molecular weight Spectra Broad Range Protein marker (Fermentas). The recombinant protein's ~ 60 kDa are clearly visible in the lanes containing insoluble fractions and in the inclusion body preparation of PfLMQO. The recombinant protein ~ 60 kDa is clearly visible in the inclusion body preparation and only a small band of the expected protein size is present in the insoluble preparation of PfSMQO. It clearly shows that the ~ 60 kDa recombinant protein was not detected in soluble fractions of either PfLMQO or PfSMQO.

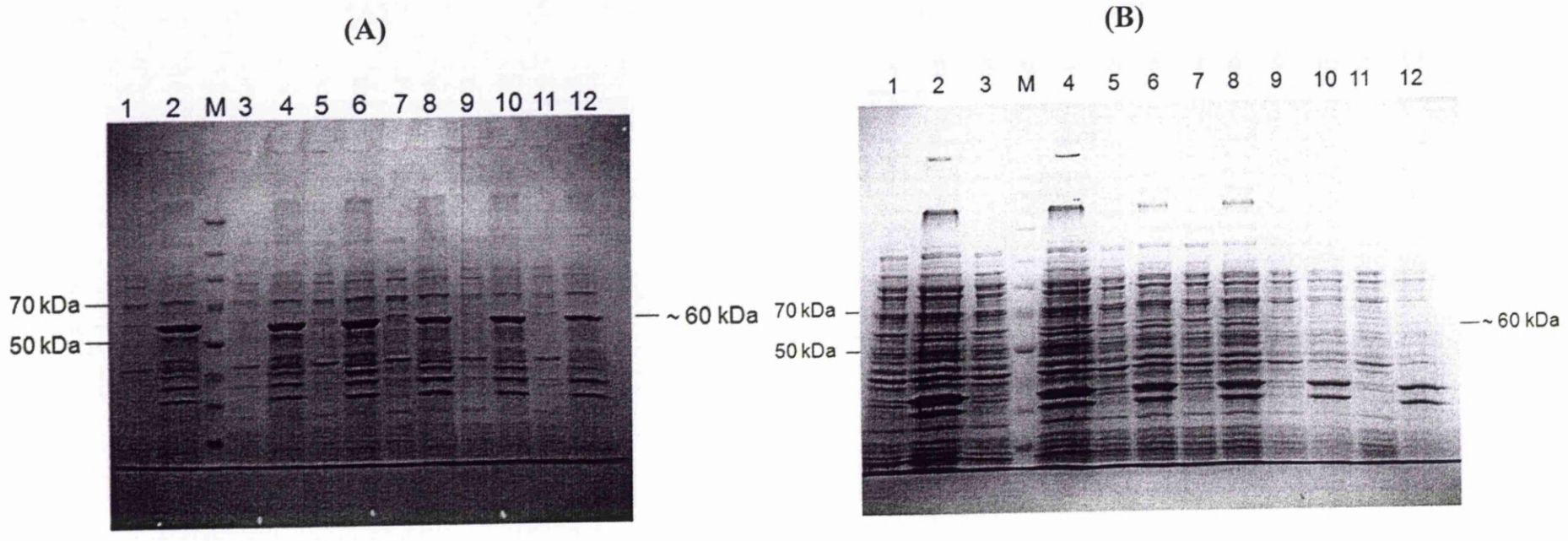

Figure 5.18: Three Hours Post IPTG Induction Course Studies of PfLMQO and PfSMQO

SDS-PAGE analysis of time and IPTG induction course studies of PfLMQO (A) and PfSMQO (B) produced in *E. coli* Rosetta after 3 hours induction. The odd and even number represent soluble and insoluble fractions respectively. Lanes 1-2 (37 °C , 1.0 mM IPTG), lanes 3-4 (37 °C , 0.5 mM IPTG), lanes 5-6 (30 °C , 1.0 mM IPTG), lanes 7-8 (30 °C , 0.5 mM IPTG), lanes 9-10 (22 °C , 1.0 mM IPTG) and lanes 11-12 (22 °C , 0.5 mM IPTG). Lane M Spectra Broad Range Protein marker (Fermentas). Panel A (PfLMQO) shows the visible recombinant proteins bands ~ 60 kDa detected in the insoluble fraction lanes and no obvious band detected in soluble fraction lanes. Panel B (PfSMQO) shows the protein bands ~60 kDa in the insoluble fraction lanes were not clearly visible but the bands can still be distinguished from the soluble fraction lane.

5.3.10 Purification of PfLMQO Recombinant Protein

The PfLMQO recombinant protein was expressed in Rosetta *E .coli* cells grown in LB medium consisting 50 μg/ml ampicillin and 25 μg/ml chloramphenicol. The expression of protein is under the control of T7 promoter in the pET-15b plasmid. The pET-15b vector carries a oligo-histidine (His-tag) sequence which is located at the N-terminus of purified protein. Most His-tag purification systems work efficiently with 6xHis-tagged proteins under denaturing and native conditions in low or high salt buffers. The protein binding to Ni-NTA matrices can be eluted by imidazole. Low concentration of imidazole are suggested to reduce non-specific binding of host proteins with histidines. From the SDS-PAGE gels (Figure 5.21 A and B) the PfLMQO was not purifiable using a Ni-NTA column (Qiagen). No single band size ~60 kDa is visible from eluted samples from either soluble or insoluble fractions loaded as seen on lane S8 and lane S9 (soluble fraction) and P8 and P9 (insoluble). The clear recombinant protein bands were detected from the pellet preparation which is presented at the at the positions C2 adn P3.

Based on this finding, purification under denaturing conditions was carried out. The purification under denaturing conditions was started by inclusion bodies preparation from the insoluble fractions of the bacterial cells. The inclusion bodies preparation was described in section **5.2.28.** The SDS polyacrylamide gel (Figure 5:22) shows the PLMQO purified from inclusion bodies under denaturing condition. As shown, ~ 60 kDa protein bands were evident in eluted samples E1 and E2 of the inclusion body preparation. Using a strong denaturant such as 6M GuHCl the N terminal 6xHis tag of the recombinant protein is exposed thus improve binding of the protein to the Ni-NTA matrix. Therefore, improving the efficiency of the purification and potential nonspecific binding is minimised.

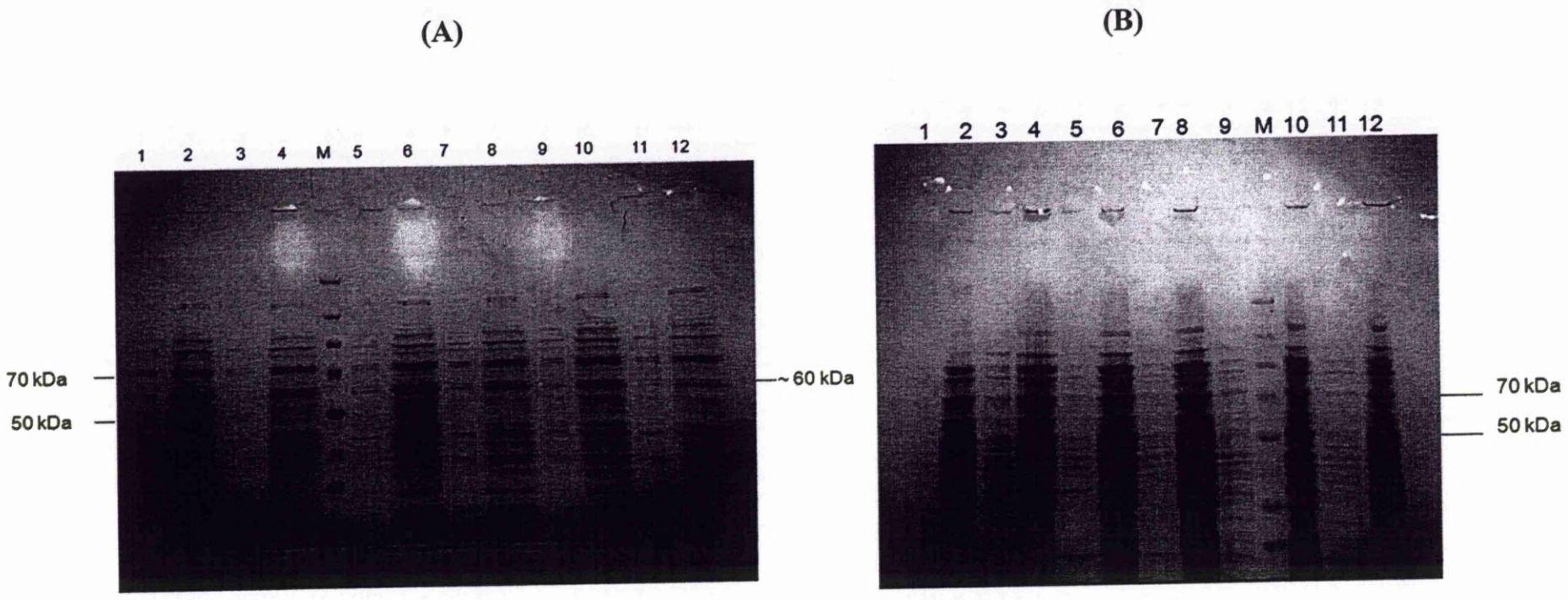

Figure 5.19: Five Hours Post IPTG Induction Course Studies of PfLMQO and PfSMQO

SDS-PAGE analysis of time and IPTG induction course studies of PfLMQO (A) and PfSMQO (B) produced in *E. coli* Rosetta after 3 hours induction. The odd and even number represent soluble and insoluble fractions respectively. Lanes 1-2 (37 °C , 1.0 mM IPTG), lanes 3-4 (37 °C , 0.5 mM IPTG), lanes 5-6 (30 °C , 1.0 mM IPTG), lanes 7-8 (30 °C , 0.5 mM IPTG), lanes 9-10 (22 °C , 1.0 mM IPTG) and lanes 11-12 (22 °C , 0.5 mM IPTG). Lane M Spectra Broad Range Protein marker (Fermentas). Panel A (PfLMQO) shows the visible recombinant proteins bands ~ 60 kDa detected in the insoluble fraction lanes and no obvious band detected in soluble fraction lanes. Panel B (PfSMQO) shows the protein bands ~60 kDa in the insoluble fraction lanes were not clearly visible but the bands can still be distinguished from the soluble fraction lane.

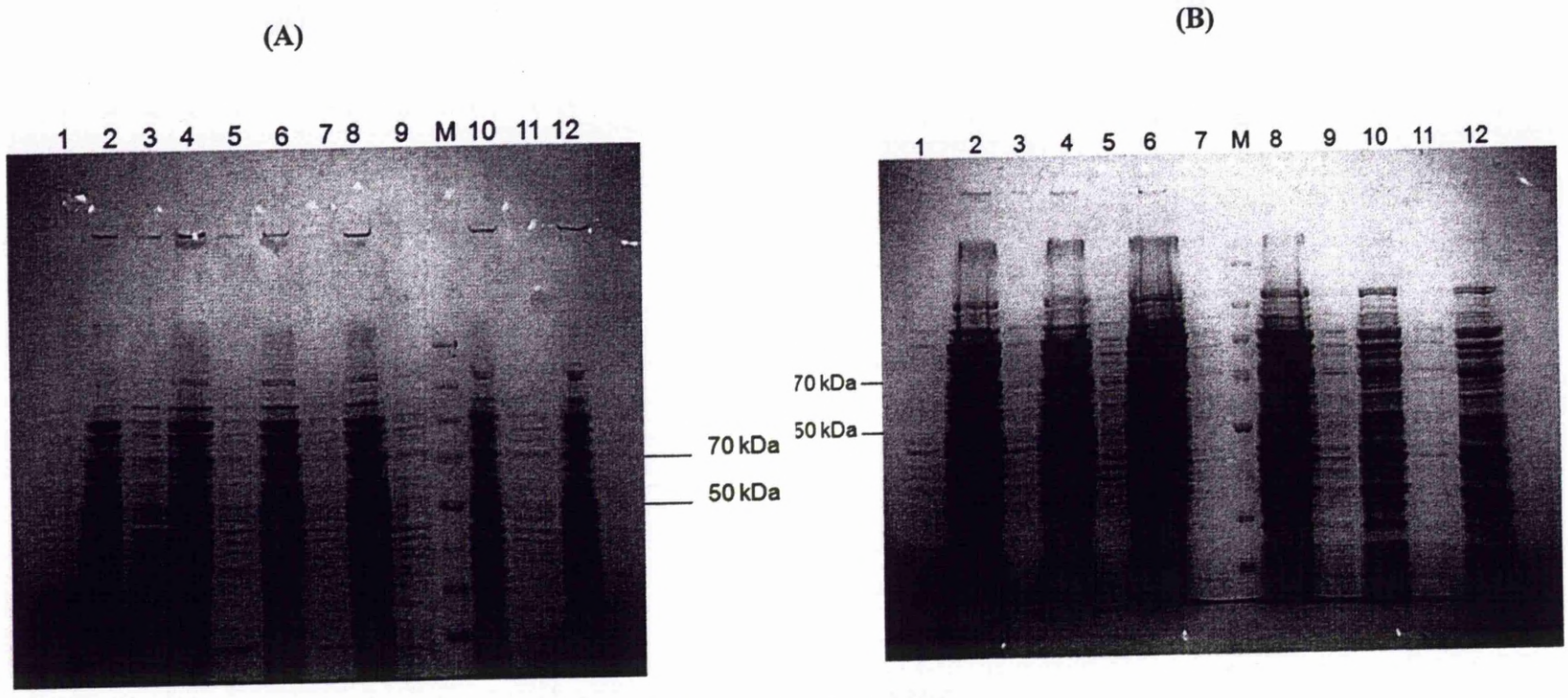

Figure 5.20: Overnight Post IPTG Induction Course Studies of PfLMQO and PfSMQO

SDS-PAGE analysis of time and IPTG induction course studies of PfLMQO (A) and PfSMQO (B) produced in *E. coli* Rosetta after 3 hours induction. The odd and even number represent soluble and insoluble fractions respectively. Lanes 1-2 (37 °C , 1.0 mM IPTG), lanes 3-4 (37 °C , 0.5 mM IPTG), lanes 5-6 (30 °C , 1.0 mM IPTG), lanes 7-8 (30 °C , 0.5 mM IPTG), lanes 9-10 (22 °C , 1.0 mM IPTG) and lanes 11-12 (22 °C , 0.5 mM IPTG). Lane M Spectra Broad Range Protein marker (Fermentas). The recombinant protein for both PfLMQO (A) and PfSMQO (B) were not detected in all bacterial cells grown at different concentrations of IPTG.

5.2.11 Measurement of MQO Activity

The enzyme activity study of recombinant PfMQO and the native form of MQO were measured spectrophotometrically using direct and indirect enzyme assays as described in section **5.2.31.** The direct assay was performed to monitor the level of Q1 reduction measured at 23 nm. The Q1 reduction is not measurable for either PfLMQO or MQO protein expressed in *E. coli* cells. Following this, the indirect linked assay was performed to measure the Q1 reduction by indirectly measuring the reduction rate of DCPIP. The results produced by this assay were very inconsistent when the same parameter was repeated.

5.4 Discussion

Malate quinone oxidoreductase (MQO) is a dehydrogenase enzyme presumably located in the inner mitochondrial membrane of *P. falciparum*. MQO is involved in the respiratory chain of the *Plasmodium* mitochondria and donates electrons to co-enzyme Q using $FADH_2$ as a co-factor. Recently a study conducted by Olszewski et al. (2010) showed the role of MQO in the branched architecture of the *Plasmodium* TCA cycle. MQO has been demonstrated as an enzyme which reduces OOA to malate.

PfMQO has been partially characterised using bioinformatic and genomic approaches. The characterisation of PfMQO was performed using computational analysis due to the absence of direct evidence of PfMQO protein. The characterisation of PfMQO started with prediction of the open reading frame (ORF) of the putative PfMQO sequence which is available from PlasmoDB. This was followed by prediction of the molecular weight and the

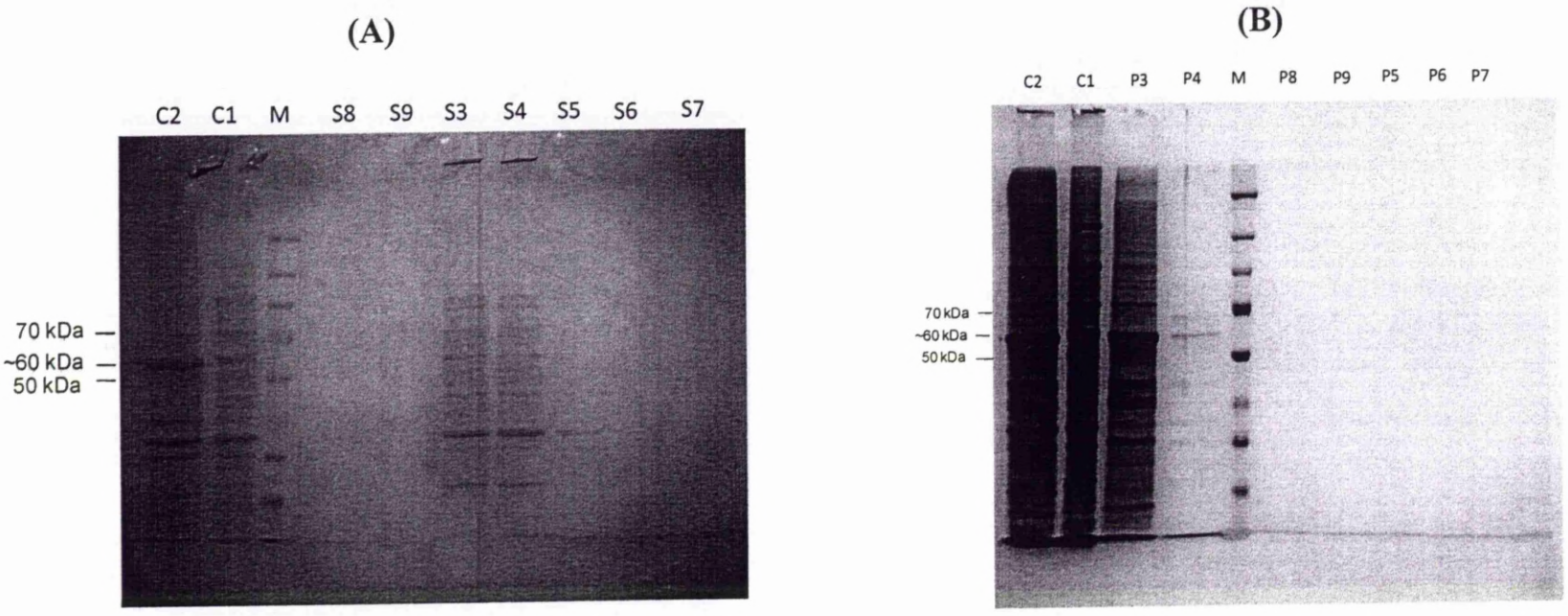

Figure 5.21: SDS-PAGE Analysis of PfLMQO Purified under Native Conditions

A recombinant PfLMQO protein was expressed in *E. coli* Rosetta cells grown in LB medium for 3 hours with 1 mM IPTG at 30 °C. Panel A and B show native purification of 6xHis-tagged protein of soluble and insoluble fractions respectively. Panel A: C2 insoluble fraction, C1 soluble fraction, S8 first elution, S9 second elution, S3 bacterial lysate, S4 flow through, S6 wash 1 and S7 wash 2. Panel B: C2 insoluble fraction, C1 soluble fraction, P3 insoluble lysate, P4 flow through, P5 wash 1, P6 wash 2, P7 wash 3, P6 elute 1 and P7 elute 2. . No single band was detected from eluted samples loaded in lane S8, S9, P8 and P9. M indicates Spectra broad range protein marker. The ~60 kDa bands were visible in lanes containing insoluble fraction (C2) and cell lysate sample (P3) indicating that the PfLMQO protein is not purifiable under native conditions.

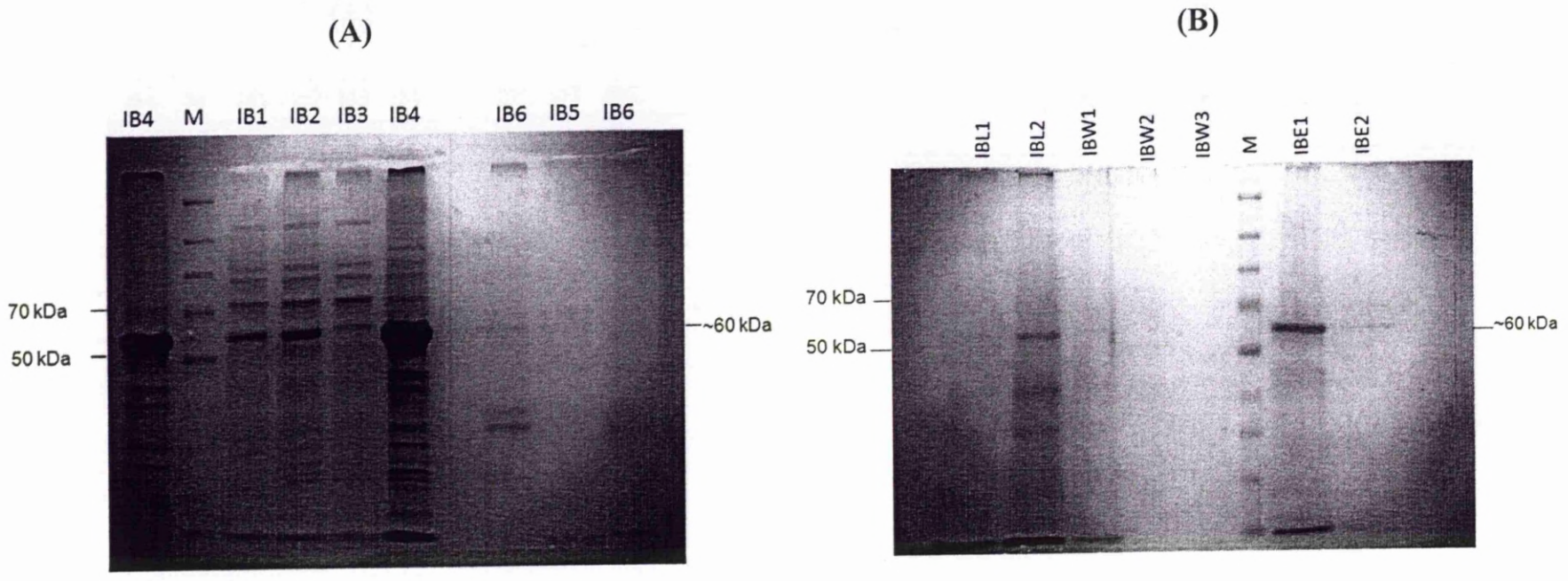

Figure 5.22: SDS-PAGE Analysis of Purified PfLMQO under Denaturing Conditions

Recombinant PfLMQO protein was expressed in *E. coli* Rosetta cells grown in LB medium for 3 hours with 1 mM IPTG at 30 °C. Panel A and B show denaturing purification of 6xHis-tagged proteins of inclusion bodies. Panel A: IB1 insoluble fraction, IB2 homogenised pellet, IB3 supernatant of homogenised pellet, IB4 homogenised pellet after treatment with buffer A, IB5 supernatant of IB4, IB6 resuspended pellet of IB4 before loading into Ni-NTA column. Panel B: IBL1 flow through, IBL2 second flow through, IBW1 wash 1, IBW2 wash 2, IBE 1 elute 1 and IBE 2 elute 2. M indicates Spectra broad range protein marker. The bands~60 kDa are visible in all samples loaded from pellet of inclusion bodies and eluted samples. The protein band is not visible from samples loaded from supernatant and wash samples. This indicates the inclusion body derived PfLMQO is successfully purified under denaturing conditions.

isoelectric point of the protein using the amino acid sequence of the PfMQO. The final destination of the targeted protein was predicted using PFMpred and PlasMit softwares that was mainly invented to predict the sublocation of plasmodial protein. PFMpred is using Support Vector Machine (SVM) model to predict *Plasmodium* membrane proteins type based on split amino acid composition (SAAC) and position-specific scoring matrix (PSSM) profile therefore offering better prediction results (272). Another prediction system (PlasMit prediction system) is used a neural network system that predicts the subcellular *P. falciparum* protein (Bender 2003) location based on the relative frequencies of amino acids in different regions. The probability of PfMQO targeting the mitochondria was compared to two other known *Plasmodium* proteins; PfALAS and PfMDH. Selection of controls is based on known subcellular location of *Plasmodium* proteins from selected publications which predicted that the PfALAS located in *Plasmodium* mitochondrial membrane (270) and PfMDH is a cytoplasmic protein (213). Both results (PFMpred and PlastMit) predicted that PfMQO is located in *Plasmodium* mitochondrial membrane with the probability SVM score and R.I of 1.30 and 91% respectively. Therefore, these analyses indicate that PfMQO is likely a mitochondrial protein. This result is in agreement with 2 control proteins where PfALAS (positive control) SVM score was 0.96 and 91% R.I showing that the PfALAS protein is probably located in the mitochondrial subcellular membrane. Whereas, the negative control showed a 0.0 SVM score and a 99% R.I showing that PfMDH is 99% not a mitochondrial protein.

Determination of membrane protein topology is a fundamental aspect in the process of characterisation of unknown protein. However, the prediction of membrane domains only provides the structural predictions e.g number of transmembrane segments and their orientation across the membrane. The topology of PfMQO was carried out using TMHMM,

Split 4.0 server software. This programme is based on a hidden Markov model algorithm that predicts the location of the transmembrane topology of targeted protein with 97-98% accuracy (137). Figure 5.5, shows the graphical presentation of predicted transmembrane helices results of PfMQO in comparison with PfDHOODH and PfPSD proteins. This result showed that the probability score of PfMQO was less than 0.7 compared to PfDHOODH and PSD probability scores. The probability score for PfDHOODH (positive control) was close to 1 and 0.6 for PfPSD (negative control). Therefore, it is clearly demonstrated that the PfDHOODH is most likely the integral protein while PfMQO and PfPSD are most likely non-membrane proteins. This prediction result has been supported by secondary structure prediction using PSIPRED software indicating the presence of alpha helices, beta sheet and coil although no trasmembrane helices were predicted. These bioinformatic data indicate that PfMQO is not an integral mitochondrial membrane protein but most likely a peripheral membrane protein. The peripheral membrane protein is often found in close association with integral membrane protein (100). As a peripheral membrane protein, PfMQO is associated with the membrane but does not penetrate the hydrophobic core of the membrane. Part of PfMQO is exposed to mitochondria matrix and part of it is bound to the mitochondrial membrane. Hence, this protein can be removed without the disruption of the membrane structure. This is in accordance with study conducted by Molenaar et al. (1998) which demonstrated that the MQO is a peripheral mitochondrial membrane protein in *C. glutamicum*.

From the multiple alignment of the putative PfMQO amino acid sequence it is indicated that the PfMQO is highly conserved within the *Plasmodium* genome with 85% similarity to putatitive PvMQO and putative PyMQO, 74% to putative PcMQO and 75% to putative PkMQO.

It has also been demonstrated that the PfMQO has low similarity to prokaryotes MQO (less than 10% similarity to EcMQO and MsMQO). This low similarity provides major advantages for future characterisation of the protein expressed in the prokaryotic host system.

In this study, the putative *PfMQO* genes (PfLMQO and PfSMQO) were successfully amplified using designated primers. PfLMQO and PfSMQO fragments produced band sizes approximately 1566 bp and 1529 bp respectively. Result on the agarose gel showed that the DNA fragment size of PfSMQO was sligltly lower than PfLMQO. This is due to the absence of the leader sequence from the putative *PfSMQO* gene sequence. The expecting leader sequence was carried out using SignalIP 4.0 programme. The prediction result showed that the signal peptide cleavage site was located at N-terminus (1-37 amino acid sequence) of the putative PfMQO. The forward primer for PfSMQO was designed to start at the start codon (ATG) located at the end terminus of the expecting leader sequence. In general, the role of the leader sequence coding region is involved in the stability of the mRNA and for its efficient translation. The *Plasmodium* mitochondrial and apicoplast genome are generally encoded by nuclear genes and the products are targeted into the organelles (82, 169, 269). Nucleated synthesised proteins must be imported into the mitochondria via various pathways. The most common pathway is through an N-terminal leader peptide or presequence (96, 269). The leader protein signal eventually will be removed by the action of a mitochondrial processing protease (MPP) once the protein reached the mitochondrial matrix. From this study, it is shown that the absence of leader sequence in the putative *PfSMQO* gene does affect the level of the expression recombinant protein as shown in Figure 5.17. The removal of leader sequence from the putative *PfMQO* gene does affect the expression of the recombinant protein. Figure 5.19 shows that the band size of ~60 kDa appear clearly on SDS-PAGE for PfLMQO and less for PfSMQO. The molecular mass size of the protein calculated

using Protparam indicated that the size of PfSMQO is 57 kDa less 2 kDa than PfLMQO (59 kDa). However this was not obviously seen on the SDS-PAGE gels in solubility studies.

To produce recombinant PfLMQO and PfSMQO in *E. coli*, the PfMQO genes were cloned into pET-15b and pUC19 expression vectors. The constructs for PFLMQOs and PfSMQOs for the pET-1b vector were fused to an oligo-histidine tag at the N-terminus which facilitates purification. The rationale of using 2 different expression systems is to optimise the translation of the protein under different promoters. The pET-15b possesses a T7 promoter whilst pUC19 has a *lac* promoter. The pET system is the most powerful system developed for the cloning and expression of recombinant proteins in *E. coli*. This system has been provided with a strong bacteriophage T7 promoter which controls the translational and transcriptional process of the inserted gene. The expression of the targeted protein is controlled by host T7 RNA polymerase which under the control of *lacUV* gene which inducible by addition of IPTG. This system has a capability to produce up to 50% of the total protein after a few hours post induction. Unlike in pET-15b, the expression of recombinant PfMQO in pUC19 was controlled by the *lac* promoter. PfLMQO and PfSMQO DNA segments were inserted in-frame with *lacZ* gene and expressed as a fusion protein consisting a portion of the beta-galactosidase. Similarly to *lacUV* gene in pET-15b, *lacZ* gene is also inducible with IPTG. However the expression studies of the PfLMQO and PfSMQO using pUC19 expression vector did not show satisfactory results.

Two *E. coli* hosts, BL21 and Rosetta, have been used in this study. The PfMQO recombinant proteins were not expressable in BL21 cells. Therefore, the constructed PfMQO clones were retransformed into *E. coli* Rosetta. Substantial expression of PFLMQO was obtained in the *E. coli* Rosetta (DE3) strain, which is specifically engineered to enhance expression of eukaryotic proteins containing codons rarely used in *E. coli*. The western blot

result shows that the recombinant his tagged PfLMQO and PfSMQO cloned in pET-15b plasmid were reacted with IgG anti-His antibodies This show the recombinant PfMQO proteins were successfully expressed in pET-15b under controlled of T7 promoter.

The solubility tests were carried out to determine the optimum conditions of the expressed protein by checking at various times after induction. Intracelluar protein content is often a balance between the amount of soluble protein in the cells, the formation of inclusion bodies and protein degradation. The recombinant proteins were detectable after 3 hours incubation and slowly degraded after 5 hours post IPTG induction in all conditions. This suggests the optimum temperature for PfLMQO expression is 30 °C - 37 °C with 1 mM IPTG. Meanwhile the bacterial growth at 22 °C showed no overproduction when induced with 0.5 mM or 1 mM IPTG. The temperature is a crucial element in the expression and the solubility of the recombinant protein. Growth at lower temperature will reduce expression levels but will lead to solubility of the protein. The overnight cultures did produce recombinant protein. This is in accordance with finding from study conducted by (267) which showed that the MQO protein is active only during exponential growth, and when the cells reach stationary phase, it appears to be broken down.

Molenaar et al. (1998) demonstrated that *C. glutamicum* MQO is identified as a mitochondrial membrane bound protein that can be released from the membrane by addition chelator. .Part of the enzyme is embedded in inner mitochondrial membrane and the other part is in the matrix of mitochondria. As intracellular membrane proteins, the proteins are frequently sequestered into insoluble inclusion bodies. As shown in Figure 5:17 both PfLMQO and PfSMQO were found associated with inclusion bodies. This is possibly due to overloading of the folding pathway during over-expression of the protein or the hydrophobic

interactions between protein chains which increase the probability of mis-folding. The proteins solubility was predicted using a programme developed by Wilkinson and Harrison in the year 1991 (http:www.biotech.ou.edu) (282), showed that the PfLMQO and PfSMQO recombinant proteins had 89.3% and 86.6% chance of formation of inclusion bodies respectively when over expressed in *E. coli*. Protein solubility increases with increasing net charge (positive and negative). Consequently turns in the protein structure are most difficult to form. The high concentration of residues forming turns may be indicative of slow folding protein. A traditional approach to improve the solubility of recombinant protein involves reducing the synthesis rate of target gene product by decreasing the IPTG inducer and cell growth at lower temperature (227). However, the use of low temperature affects the transcription and translation rates therby reducing the strength of hydrophobic interactions that contribute to protein mis-folding (13).

From the results in this study, the PfMQO recombinant proteins were obviously associated with inclusion bodies. Figure 5.17 shows the protein is purifiable under denaturating conditions and the bands sizes ~ 60 kDa appeared on a 10% SDS-PAGE gels. By introducing strong denaturants such as 6 M GuHCl, 8 M urea and variety of detergents such as Triton™ X-100, NP-40, dodecyl β D-maltoside and octyl β D-glucoside in combination with reducing agents such as 20 mM DTT or β-mercaptoethanol it may greatly improve the solubility of the proteins. Mostly proteins purified under denaturing conditions are in the inactive form. Therefore, dialyzing process needs to be carried out in order to remove their denaturants and refold the proteins back into their active states.

The optimal conditions for solubilisation have to be determined by varying the pH and ionic strength of the denaturants and reducing agents in the washing buffer. The growth temperature is also important to minimise the formation of inclusion bodies. As mentioned

earlier growth at lower temperature will improve the solubility but reduce the degree of protein expression. The optimisation will take some time due to the distinctive character of each protein. Due to the limitations of time, this work had to be stopped at the purification under denaturing conditions. Further purification trials are currently being carried out in our laboratory to overcome the problem of formation of inclusion bodies by using different growth temperatures and IPTG concentrations.

The attempt to measure the activities of the PfLMQO was performed using membrane preparations of *E. coli* Rosetta cells. The reduction of Q1 was indirectly measured by measuring the reduction rate of DCPIP. However, we are unable to generate the consistent findings due to the data irregularity using the same parameters (data not shown). The explanation behind this is possibly due to the protein existing in inclusion bodies. A previous MQO kinectics study conducted by Molenaar et al. (1998) demonstrated that the reduction of DCPIP was recorded using partially purified recombinant *C. glutamicum*. The *C. glutamicum MQO* gene of is cloned and expressed in the MQO negative *C. glutamicum* strain. The specific activity of the recombinant MQO enzyme activity was four-fold higher (5-10 μmol DCPIP reduced/ $nmol.min^{-1}.mg^{-1}$protein) compared to membrane preparation from wild type *C. glutamicum*. The presence of inclusion bodies is not documented. From their study it was also suggested that the usage of EDTA or ethylene glycol tetraacetic acid (EGTA) in the assay buffer strip off the enzyme thus affected the MQO activity. Mark et al. (2004) also demonstrated that the combination of EDTA and Mg^{2+} inhibited enzyme activity of *E.coli* NADH dehydrogenase. EDTA disrupts the outer membrane of *E. coli* cells by removing positive charges, causing the negatively charged heads of the phospholipids to repel each other (117, 163). Then, the lysozyme is able to access the peptidoglycan to cleave the C1 N-

acetyl muramic acid (NAM) to C4-N-acetyl glutamic (NAG) glycosidic linkage thus causing cell lysis.

In conclusion, the characterisation of the putative PfMQO is partially complete using the bioinformatic approaches and also from the direct evidence through molecular and biochemical data. The primary and the secondary structure of PfMQO are solely dependent on the bioinformatics data. However, this data must be interpreted carefully. Bear in mind that it is only prediction and as we understand with all predictions, accuracy can be highly variable. Functional characterisation such as crystallography study, NMR, mutagenesis and the susceptibility of the protein to proteolytic enzymes have to be carried out in order to directly characterise this protein. The successful expression of the PfMQO in *E. coli* is a good start, but the existence of the PfMQO in inclusion bodies is a major obstacle which has to be solved before the other studies can be performed.

Finally, PfMQO is a good target to study for new antimalarial drugs which target malarial mitochondria. The absence of this enzyme in the mammalian host is a good criterion as a drug target. Furthermore the gene is highly conserved among the other *Plasmodium* species as shown in Figure 5.7 and has very low similarity to the bacterial MQOs. Therefore, the absence of MQO in any eukaryotic organisms means that this enzyme has great potential for the development of a new drug target for malarial chemotherapy if shown to be essential during the parasite's life cycle in the human host.

Chapter 6: General Discussion and Conclusion

There were two main focuses in this study. The first was to characterise the atovaquone resistant parasite TM90C2B using molecular and biochemical analysis. This was followed by the molecular characterisation of the putative *Plasmodium* mitochondrial malate quinone oxidoreductase (PfMQO).

6.1 Molecular and Biochemical Characterisation of the Atovaquone Resistant Phenotype in the Malaria Parasite *P. falciparum*

TM90C2B is an atovaquone resistant *P. falciparum* parasite clinically isolated from patients on the Thai and Cambodia border (242). The resistant parasite emerged shortly after atovaquone was administered as a single treatment to malaria patients. The antifolate drug proguanil was subsequently given in combination with atovaquone (A:P; Malarone®) to overcome the problem of resistance typically associated with the individual drugs (247). Currently, A:P is widely used for malaria chemoprophylaxis among travellers visiting malaria endemic areas. Atovaquone is a hydroxynaphthoquinoe and acts as a competitive inhibitor of ubiquinol through its binding to the ubiquinol oxidation site (Q_o) in the *Plasmodium* bc_1 complex. The benzopyranone ring of atovaquone binds to the bc_1 complex via the hydroxyl group Glu-272 of cytochrome b and the carbonyl group His-181 of the Rieske iron sulphur protein (114, 129).

Plasmodium complex III is composed of two monomeric units (10 and 11) consisting of ten different polypeptides. The catalytic cores of cytochrome bc_1 are composed of three subunits: cytochrome *b*, cytochrome c_1 and Rieske iron-sulphur protein ([2Fe2S] ISP). These subunits are directly involved in electron transfer within the *Plasmodium* respiratory chain and thus coupled with vectorial translocation of protons across the inner mitochondrial membrane. The generation of an electrochemical gradient and thus ATP (by F_0F_1 ATP synthase (complex V) is unique to certain other eukaryotic cells and does not occur within the *Plasmodium* parasite.

The *Plasmodium* cyt*b* gene is encoded by mitochondrial DNA (mtDNA) and this means any polymorphisms, such as substitutions or insertions, are parentally inherited (3, 41). The accumulation of these base substitutions or insertions through the generations introduces mutations to the gene sequence. The mtDNA mutation rate has been reported as approximately 10-fold higher than the mutation rate of nuclear DNA (36). In addition, mitochondrial complexes I and III have been identified as major contributors to the production of cellular reactive oxygen species (ROS) (186). The superoxide anion produces ROS in the cells and continuous exposure produces damage in various cells and causes the aging process in human. ROS are responsible for oxidative damage to mtDNA and the mitochondrial respiratory chain system (217). Mutations in mtDNA thus affect the mRNA and tRNA and consequently the translated protein (222).

As shown in **Chapter 3,** the TM90C2B strain was shown to harbour a point mutation in the *Pfcytb* gene resulting in the substitution of a tyrosine to a serine at residue 268. This mutation was shown in Chapter 4 to affect catalytic turnover and substrate affinity, as well as atovaquone binding. Western blot analysis also indicated reduced levels of bc_1 protein in the

TM90C2B strain compared to the wild type 3D7 strain bc_1. However, the results of the expression profiles (**Chapter 3**) showed the complex III genes *cytb*, $cytc_1$ and Fes_Rieske expression levels were higher (~ 2 fold) in TM90C2B compared to 3D7. Two hypotheses can be put forward to explain these apparently inconsistent data. The first is that the described Y268S mutation causes bc_1 instability and/or possibly protein folding problems which result in a reduction in bc_1 protein levels. It is then possible that in order to accommodate for this, the TM90C2B parasite was selected through natural selection to contain an increase level of expression of Complex III genes, which aid to off-set the poor folding/stability issues of the mutated protein.

A second hypothesis is that the gene mutation giving rise to the Y268S mutation causes an increase in the degradation rate of the mRNA and its translated protein. The impairment of protein translation is apparently due to the level of translated mutant proteins exceeding the threshold value of the wild type proteins. This threshold is dependent on the instability of the mutated protein and the amount of wild type tRNA (103). The mutant protein phenotype only appears when the amount of mutated mRNA and tRNA reach a level twice that of the wild type (222). Similarly in this scenario, the TM90C2B strain's higher expression levels of Complex III genes help to off-set the issues of mRNA instability.

Interestingly, **Chapter 4** also showed that protein levels of PfNDH2 were lower in the TM90C2B strain than the 3D7 strain. It is tempting to speculate therefore that the regulation/control of protein expression/translation of both PfNDH2 and bc_1 are somehow shared or that the Y268S mutation has a deleterious effect upon PfNDH2 translation/stability. As mentioned in Chapter 4, mitochondria from animals and plants have been shown to possess respiratory supercomplexes, but it is not clear at this stage if *Plasmodium* also

possesses a supercomplex containing PfNDH2 and Complex III, and if so how this phenomenon would impact on the stability/translation of both of these proteins.

6.2 Critical Assessment of the Methodology (Chapters 3 & 4)

In this study the expression level of selected metabolite genes were measured using the GeXP PCR technique. The GeXP qPCR technique is a novel, universal technique to study up 35 genes in one reaction compared to 5 genes for real time PCR (RT-PCR). The amplicons of the PCR are highly quantitative and detected using fluorescence based capillary electrophoresis system. The advantage of this technique is the number of genes that can be analysed in one reaction therefore reducing cost per sample. The GeXP technique is recommend to validate data from a microarray study. Nevertheless, additional techniques could have been used to support the GeXP technique (e.g. single RT-PCRs on key genes), or, additional primers could have been used for each gene to confirm the data.

(i) The GeXP data was colected from trophozoite-stage parasites and time permitting it would have been interesting to perform the same experiment of ring-stage and schizont-stage parasites. These data would have confirmed that the differential expression observed between 3D7 and TM90C2B was present throughout the asexual life cycle.

(ii) To our knowledge TM90C2B is the only atovaquone resistant parasite that has been successfully lab adapted. In future experiments it would be interesting to determine the gene expression from different atovaquone resistant isolates and determine whether similar expression/translation phenomena are observed.

(i) Enzymatic activities for the dehydrogenases were measured using direct measurement of the quionone reductase activity at 283 nm. The measurement was carried out by reducing the path length to 1 mm to overcome the interference of hemozoin in the reaction. This is an improvement from many studies that use linked assays with artificial electron acceptors DCPIP, MTT or horse heart cytochrome c. The mitochondrial Percoll® fractionation was carried out to improve sensitivity when measuring the quinone reductase activity in *Plasmodium* strains, but perhaps the assays would have benefitted further from an initial purification of the mitochndria. Although very labour intensive this would have improved the relative activity of the membrane fractions and therefore improved the signal to noise ratio of the measurements.

6.3 Molecular Characterisation of *P. falciparum* 3D7 malate quinone oxidoreductase (PfMQO)

The *Plasmodium* parasite consumes more energy than the host cell and is solely dependent on glucose fermentation for energy generation (238). Whilst the *Plasmodium* genome has been encoded for all the necessary TCA enzymes their function is still debatable (82). Despite not generating ATP, the *Plasmodium* TCA cycle is believed to be involved in mitochondrial redox homeostasis and *de novo* pyrimidine biosynthesis (262).

In the canonical TCA cycle, malate is oxidised to OAA by mitochondrial malate dehydrogenase (mtMDH). However in the *Plasmodium* parasite, mitochondrial MDH is replaced by MDH isoenzyme malate quinone oxidoreductase (MQO). Instead of using NAD(P) as a co-factor, MQO uses $FADH_2$ and directly transfers electrons to ubiquinone (185, 262). This is partly a defence mechanism in the *Plasmodium* biology to minimise the effect of oxidative damage due to the generation of free radicals. The degradation of haemoglobin increases the production of ROS but by directly transfering the electrons to ubiquinone they minimise the oxidative damage (262).

The transcriptome data (PlasmoDB) showes that the intraerythrocytic parasites express the highest MQO level during the trophozoite and late schizont stages. Interestingly most of the enzymes in the *Plasmodium* TCA cycle also showed high expression at this stage (25). A recent study by Olszewski et al. (2010) demonstrate the presence of a branched a TCA cycle in *Plasmodium.* The *Plasmodium* TCA cycle comprises of an oxidative branch (canonical TCA) and a reductive branch. However only the reductive branch is functionally active and

the oxidative branch is not involved in the cycle. The LC-MS data analysis showed malate is the end product from both the oxidative and reductive branch of the TCA cycle. According to Olzewski et al. (2010), malate is reduced to OAA in the reductive arm and also by the oxidation of fumarate to malate by the fumarate hydratase (fumarase) enzyme (200, 262). However, a study by Bulusu et al., (2011) indicates the reduction of OAA to malate is only catalysed by MDH. Unlike MDH, MQO is irreversible and only catalyses the oxidation of malate to OAA. Olszewski et al. (2010) also found the functional TCA cycle in *Plasmodium* parasite is entirely depending on the reductive arm where OAA is reduced to malate. Therefore the role of PfMQO in TCA cycle in *Plasmodium* is unclear. Previous studies hypothesised that MQO is replacing mitochondrial MDH in catalysing oxidation of malate to OAA (262, 269). But this latest finding indicates MQO is likely to be responsible only in the *Plasmodium* respiratory chain by donating electrons directly to ubiquinone pool.

The bioinformatic data analysis in **Chapter 5** indicates that PfMQO is a peripheral mitochondrial membrane protein. Biologically as a peripheral membrane protein, the interaction with the membrane is not very strong. By using mild denaturing conditions with chelators or detergents the protein can be dissociated from the membrane. In this study putative *PfMQO* gene was successfully cloned and expressed in *E. coli* Rosetta cells. However the expression of PfMQO was in the form of an insoluble protein. We successfully cloned the putative *PfMQO* gene into the expression vector pET-15b which was equipped with the T7 promoter. A similar study conducted by Tripathi et al. (2004) failed to express *PfMQO* gene using the pQE30 expression system with T5 promoter.

PfMQO was expressed at high levels in *E. coli* Rosetta under the T7 promoter. The overexpression of eukaryotic proteins in *E. coli* usually triggers the induction of heat shock

proteins and other stress responses this causes recombinant proteins to form as inclusion bodies (34). However, the expressed recombinant proteins are often present in a misfolded form and need to refold back into their native form. As previously mentioned in **Chapter 5,** the formation of inclusion bodies can be reduced by lowering the growth temperature, by coexpression of the gene with molecular chaperones or by using disulfide isomerase (34). The solubility of the recombinant proteins can also be improved by introducing a fusion partner (tag) for example N-utilisation substance A (NusA), maltose binding protein (MBP), thioredoxin (TRX) or glutathione S-transferase (GST) (47).

6.4 Critical Assessment of the Methodology (Chapter 5)

(i) The methodology used for cloning and expression of recombinant PfMQO followed a traditional route using commercial vectors and expression strains. Within the constraints of these techniques a number of additional studies/approaches could have been made. The first is in the codon usage of the gene. An *E. coli*-friendly codon usage could have been used for the *MQO* gene (e.g. by synthesis of the gene) to aid expression. In addition, the gene could have been truncated at both the C- and N-terminal to improve solubility/folding. As mentioned in Chapter 5, time constraints ment that a number of different growth conditions and IPTG treatment regimens were not tested in order to minimise inclusion body formation. In addition as mentioned a number of further manoeuvre could have been attempted to improve the solubility of the recombinant proteins such as the introduction of a fusion partner (tag) for example N-utilisation substance A (NusA), maltose binding protein (MBP), thioredoxin (TRX)

or glutathione S-transferase (GST) as well as the replacement with a less aggressive promoter than the one used in the commercially vector.

(ii) Steady state kinetics with the recombinant protein gave inconsistent data. It would have been useful to have attempted to follow the MQO activity by the monitoring of substrate and product using LC-MS/MS, using appropriate controls.

6.5 Future Work

Based on the outputs from this thesis, a number of future studies could be designed towards meeting the original objectives. These include:

(i) Demonstrate the presence of supercomplexes in *Plasmodium*. This could be performed by threshold-effect studies (222) or by analyses of BLUE Native gel followed by a 2 dimensional SDS PAGE followed by proteomic LC-MS/MS analysis (88, 286).

(ii) To date there is no crystal structure for the *Plasmodium* bc_1 complex and most studies of atovaquone resistance rely on the *S. cerevisae* yeast model. An in silico model has been described by Kessl et al., (2003) to demonstrate the binding of atovaquone to the Q_o binding site of the cytochrome b. It would therefore be very beneficial to crystalise the parasite bc_1 and determine its three dimensional structure. A major obstacle to this is obviously the insufficient amount of starting materials (i.e. the parasite cell free extracts). Typically 5-15 mg/ml of concentrated pure mitochondrial

protein is required to start crystallisation of the protein (Chayen and Saridakis 2008). As a comparison 10 mg of pure recombinant protein can be harvested from 1 litre of *E. coli* culture (Tripathi et al., 2004). This is particularly challenging as the *Plasmodium* parasite has only one mitochondrion therefore lots of parasites are required. In addition, the mutation within the mtDNA of the TM90C2B strain slows the growth rate when compared to the 3D7 strain. However, with time, it should be possible to collect enough mitochondrial membrane for such a preparation.

(iii) Expression of PfMQO using non-bacterial expression systems, such as insect cell lines and the cell-free system used for many membrane transporters (20). This could be attempted in addition to other bacterial expression systems that use less aggressive promoters, e.g. using slow growing organisms such as *Mycobacterium smegmatis*.

6.6 Conclusion

Atovaquone TM90C2B was partially characterised at the genomic and biochemical level. The mutation at Q_o site in bc_1 complex was demonstrated by automated sequencing. The effect of the mutation at the mRNA level was determined by GeXP PCR and showed the high expression of the genes in the complex. The effect of the mutation at the functional level was carried out by direct biochemical assays which showed the low catalytic activities of bc_1 in TM90C2B compared to 3D7. The mutation in the bc_1 complex also affected the activity of PfNDH2. The level of translated protein was quantified using western blotting and showed TM90C2B to have less Rieske Fe-S protein than 3D7.

The PfMQO was partially characterised successfully using bioinformatic and molecular techniques. In order to complete the characterisation of the protein, biochemical studies must be carried out. This could be followed by studies to crystalise the protein and then trials with the different inhibitors. The function of PfMQO in the malaria parasite is still not clear. Further studies are needed to understand the properties of the protein and thus provide new insight into the physiology of the MQO protein assemblage within the *Plasmodium* mitochondria. Eventually data from this study would provide a system for identification of inhibitors for anti-MQO activity as target drug sites in the *Plasmodium* mitochondria.

References

1. **Abdalla, S., D. J. Weatherall, S. N. Wickramasinghe, and M. Hughes.** 1980. The anaemia of P. falciparum malaria. British Journal of Haematology **46:**171-183.
2. **Acin-Perez, R., P. Fernandez-Silva, M. L. Peleato, A. Perez-Martos, and J. A. Enriquez.** 2008. Respiratory active mitochondrial supercomplexes. Molecular cell **32:**529-39.
3. **Afonso, A., Z. Neto, H. Castro, D. Lopes, A. C. Alves, A. M. Tomas, and V. D. Rosario.** 2010. Plasmodium chabaudi chabaudi malaria parasites can develop stable resistance to atovaquone with a mutation in the cytochrome b gene. Malaria Journal**:**135.
4. **Agnanndji, S. T., Lell,B et al.** 2011. First results of phase 3 trial of RTS,S/AS01 malaria vaccine in African children. New England Journal of Medicine **365:**1863-75.
5. **Aikawa, M.** 1988. Morphological changes in erythrocytes induced by malarial parasites. Biology of the Cell **64:**173-181.
6. **Alkadi, H. O.** 2007. Antimalarial drug toxicity: A review. Chemotherapy **53:**385-391.
7. **Angulo, I., and M. Fresno.** 2002. Cytokines in the pathogenesis of and protection against malaria. Clinical and Diagnostic Laboratory Immunology **9:**1145-1152.
8. **Arnot, D. E., and K. Gull.** 1998. Ninth Malaria Meeting of the British Society for Parasitology, University of Liverpool, 15-17 September 1997: The Plasmodium cell-cycle: Facts and questions. Annals of Tropical Medicine and Parasitology **92:**361-365.
9. **Bai, T., M. Becker, A. Gupta, P. Strike, V. J. Murphy, R. F. Anders, and A. H. Batchelor.** 2005. Structure of AMA1 from Plasmodium falciparum reveals a clustering of polymorphisms that surround a conserved hydrophobic pocket. Proceedings of the National Academy of Sciences of the United States of America **102:**12736-12741.
10. **Ballou, W. R., J. Rothbard, and R. A. Wirtz.** 1985. Immunogenicity of synthetic peptides from circumsporozoite protein of Plasmodium falciparum. Science **228:**996-999.
11. **Bammert, G. F., and J. M. Fostel.** 2000. Genome-wide expression patterns in Saccharomyces cerevisiae: Comparison of drug treatments and genetic alterations affecting biosynthesis of ergosterol. Antimicrobial Agents and Chemotherapy **44:**1255-1265.
12. **Banerjee, R., J. Liu, W. Beatty, L. Pelosof, M. Klemba, and D. E. Goldberg.** 2002. Four plasmepsins are active in the Plasmodium falciparum food vacuole, including a protease with an active-site histidine. Proceedings of the National Academy of Sciences of the United States of America **99:**990-995.
13. **Baneyx, F., and M. Mujacic.** 2004. Recombinant protein folding and misfolding in Escherichia coli. Nature Biotechnology **22:**1399-1407.
14. **Barton, V., N. Fisher, G. A. Biagini, S. A. Ward, and P. M. O'Neill.** 2010. Inhibiting Plasmodium cytochrome bc1: a complex issue. Current Opinion in Chemical Biology **14:**440-446.
15. **Bassat, Q., C. Guinovart, B. Sigauque, I. Mandomando, P. Aide, J. Sacarlal, T. Nhampossa, A. Bardaji, L. Morais, S. MacHevo, E. Letang, E. MacEte, J. J. Aponte, A. Roca, C. MenÃ©ndez, and P. L. Alonso.** 2009. Severe malaria and concomitant bacteraemia in children admitted to a rural Mozambican hospital. Tropical Medicine and International Health **14:**1011-1019.
16. **Berry, A., A. Senescau, J. Lelievre, F. Benoit-Vical, R. Fabre, B. Marchou, and J. F. Magnaval.** 2006. Prevalence of Plasmodium falciparum cytochrome b gene mutations in isolates imported from Africa, and implications for atovaquone resistance. Transactions of the Royal Society of Tropical Medicine and Hygiene **100:**986-988.
17. **Biagini, G. A., P. G. Bray, S. A. Ward, and D. L. Mayers.** 2009. Mechanisms of Antimalarial Drug Resistance Antimicrobial Drug Resistance, p. 561-574, Antimicrobial Drug Resistance. Humana Press, Totowa, NJ, U.S.A.
18. **Biagini, G. A., N. Fisher, N. Berry, P. A. Stocks, B. Meunier, D. P. Williams, R. Bonar-Law, P. G. Bray, A. Owen, P. M. O'Neill, and S. A. Ward.** 2008. Acridinediones: Selective and potent inhibitors of the malaria parasite mitochondrial bc1 complex. Molecular Pharmacology **73:**1347-1355.

inhibitors of the malaria parasite mitochondrial bc1 complex. Molecular Pharmacology **73:**1347-1355.

19. **Biagini, G. A., P. Viriyavejakul, P. M. O'Neill, P. G. Bray, and S. A. Ward.** 2006. Functional characterization and target validation of alternative complex I of Plasmodium falciparum mitochondria. Antimicrobial Agents and Chemotherapy **50:**1841-1851.
20. **Birkholtz, L. M., G. Blatch, T. L. Coetzer, H. C. Hoppe, E. Human, E. J. Morris, Z. Ngcete, L. Oldfield, R. Roth, A. Shonhai, L. Stephens, and A. I. Louw.** 2008. Heterologous expression of plasmodial proteins for structural studies and functional annotation. Malaria Journal **7.**
21. **Blackman, M. J., H. G. Heidrich, S. Donachie, J. S. McBride, and A. A. Holder.** 1990. A single fragment of a malaria merozoite surface protein remains on the parasite during red cell invasion and is the target of invasion-inhibiting antibodies. Journal of Experimental Medicine **172:**379-382.
22. **Bloland, P. B.** 2001. Drug resistance in malaria. WHO report **WHO/CDS/CSR/DRS/2001.4.**
23. **Booker, M. L., C. M. Bastos, M. L. Kramer, R. H. Barker, Jr., R. Skerlj, A. B. Sidhu, X. Deng, C. Celatka, J. F. Cortese, J. E. G. Bravo, K. N. C. Llado, A. E. Serrano, I. Angulo-Barturen, M. Belen Jimenez-Diaz, S. Viera, H. Garuti, S. Wittlin, P. Papastogiannidis, J.-w. Lin, C. J. Janse, S. M. Khan, M. Duraisingh, B. Coleman, E. J. Goldsmith, M. A. Phillips, B. Munoz, D. F. Wirth, J. D. Klinger, R. Wiegand, and E. Sybertz.** 2010. Novel Inhibitors of Plasmodium falciparum Dihydroorotate Dehydrogenase with Anti-malarial Activity in the Mouse Model. Journal of Biological Chemistry **285:**33054-33064.
24. **Boshoff, H. I. M., T. G. Myers, B. R. Copp, M. R. McNeil, M. A. Wilson, and C. E. Barry Iii.** 2004. The transcriptional responses of Mycobacterium tuberculosis to inhibitors of metabolism. Novel insights into drug mechanisms of action. Journal of Biological Chemistry **279:**40174-40184.
25. **Bozdech, Z., M. Llinas, B. L. Pulliam, E. D. Wong, J. Zhu, and J. L. DeRisi.** 2003. The transcriptome of the intraerythrocytic developmental cycle of Plasmodium falciparum. PLoS Biology **1:**5.
26. **Brettler, D. B., B. R. Bloom, S. T. Goldstein, C. N. Shapiro, W. R. Ballou, J. A. Stoute, and J. Cohen.** 1997. A recombinant circumsporozoite protein vaccine against malaria [3] (multiple letters). New England Journal of Medicine **336:**1759-1761.
27. **Bulusu, V., V. Jayaraman, and H. Balaram.** 2011. Metabolic Fate of Fumarate, a Side Product of the Purine Salvage Pathway in the Intraerythrocytic Stages of Plasmodium falciparum. The Journal of Biological Chemistry **286:**9236-45.
28. **Callebaut, I., K. Prat, E. Meurice, J. P. Mornon, and S. Tomavo.** 2005. Prediction of the general transcription factors associated with RNA polymerase II in Plasmodium falciparum: Conserved features and differences relative to other eukaryotes. BMC Genomics **6.**
29. **Canfield, C. J., M. Pudney, and W. E. Gutteridge.** 1995. Interactions of atovaquone with other antimalarial drugs against Plasmodium falciparum in vitro. Experimental Parasitology **80:**373-381.
30. **Carlton, J. M., S. V. Angiuoli, B. B. Suh, T. W. Kooij, M. Pertea, J. C. Silva, M. D. Ermolaeva, J. E. Allen, J. D. Selengut, H. L. Koo, J. D. Peterson, M. Pop, D. S. Kosack, M. F. Shumway, S. L. Bidwell, S. J. Shallom, S. E. Van Aken, S. B. Riedmuller, T. V. Feldblyum, J. K. Cho, J. Quackenbush, M. Sedegah, A. Shoaibi, L. M. Cummings, L. Florens, J. R. Yates, J. D. Raine, R. E. Sinden, M. A. Harris, D. A. Cunningham, P. R. Preiser, L. W. Bergman, A. B. Vaidya, L. H. Van Lin, C. J. Janse, A. P. Waters, H. O. Smith, O. R. White, S. L. Salzberg, J. C. Venter, C. M. Fraser, S. L. Hoffman, M. J. Gardner, and D. J. Carucci.** 2002. Genome sequence and comparative analysis of the model rodent malaria parasite Plasmodium yoelii yoelii. Nature **419:**512-519.
31. **Cecchini, G.** 2003. Function and structure of complex II of the respiratory chain, p. 77-109, Annual Review of Biochemistry, vol. 72.
32. **Chaijaroenkul, W., S. A. Ward, M. Mungthin, D. Johnson, A. Owen, P. G. Bray, and K. Na-Bangchang.** 2011. Sequence and gene expression of chloroquine resistance transporter

(pfcrt) in the association of in vitro drugs resistance of Plasmodium falciparum. Malaria Journal **10:**42.

33. **Chen, Q., F. Pettersson, A. M. Vogt, B. Schmidt, S. Ahuja, P. Liljestrom, and M. Wahlgren.** 2004. Immunization with PfEMP1-DBL1 alpha generates antibodies that disrupt rosettes and protect against the sequestration of Plasmodium falciparum-infected erythrocytes. Vaccine **22:**2701-2712.
34. **Cheng, C.-H., and W.-C. Lee.** 2010. Protein solubility and differential proteomic profiling of recombinant Escherichia coli overexpressing double-tagged fusion proteins. Microbial Cell Factories **9:**63.
35. **Chiodini, P. L., C. P. Conlon, D. B. A. Hutchinson, J. A. Farquhar, A. P. Hall, T. E. A. Peto, H. Birley, and D. A. Warrell.** 1995. Evaluation of atovaquone in the treatment of patients with uncomplicated Plasmodium falciparum malaria. Journal of Antimicrobial Chemotherapy **36:**1073-1078.
36. **Contamine, V., and M. Picard.** 2000. Maintenance and integrity of the mitochondrial genome: A plethora of nuclear genes in the budding yeast. Microbiology and Molecular Biology Reviews **64:**281-315.
37. **Coteron, J. M., M. Marco, J. Esquivias, X. Deng, K. L. White, J. White, M. Koltun, F. El Mazouni, S. Kokkonda, K. Katneni, R. Bhamidipati, D. M. Shackleford, I. Angulo-Barturen, S. B. Ferrer, M. Belen Jimenez-Diaz, F.-J. Gamo, E. J. Goldsmith, W. N. Charman, I. Bathurst, D. Floyd, D. Matthews, J. N. Burrows, P. K. Rathod, S. A. Charman, and M. A. Phillips.** 2011. Structure-Guided Lead Optimization of Triazolopyrimidine-Ring Substituents Identifies Potent Plasmodium falciparum Dihydroorotate Dehydrogenase Inhibitors with Clinical Candidate Potential. Journal of Medicinal Chemistry **54:**5540-5561.
38. **Cowman, A. F., and B. S. Crabb.** 2006. Invasion of red blood cells by malaria parasites. Cell **124:**755-766.
39. **Cox-Singh, J., and B. Singh.** 2008. Knowlesi malaria: newly emergent and of public health importance? Trends in Parasitology **24:**406-10.
40. **Crawford JM, F. M. a. R. D.** 2003. Molecular Medical Parasitology. Academic Press.
41. **Creasey, A., K. Mendis, J. Carlton, D. Williamson, I. Wilson, and R. Carter.** 1994. Maternal inheritance of extrachromosomal DNA in malaria parasites. Molecular and Biochemical Parasitology **65:**95-8.
42. **Crofts, A. R., M. Guergova-Kuras, R. Kuras, N. Ugulava, J. Li, and S. Hong.** 2000. Proton-coupled electron transfer at the Q(o) site: what type of mechanism can account for the high activation barrier? Biochimica et biophysica acta **1459:**456-66.
43. **Cummings, J. F., M. D. Spring, R. J. Schwenk, C. F. Ockenhouse, K. E. Kester, M. E. Polhemus, D. S. Walsh, I. K. Yoon, C. Prosperi, L. Y. Juompan, D. E. Lanar, U. Krzych, B. T. Hall, L. A. Ware, V. A. Stewart, J. Williams, M. Dowler, R. K. Nielsen, C. J. Hillier, B. K. Giersing, F. Dubovsky, E. Malkin, K. Tucker, M. C. Dubois, J. D. Cohen, W. R. Ballou, and G. Heppner.** 2010. Recombinant Liver Stage Antigen-1 (LSA-1) formulated with AS01 or AS02 is safe, elicits high titer antibody and induces IFN-gamma/IL-2 CD4+ T cells but does not protect against experimental Plasmodium falciparum infection. Vaccine **28:**5135-5144.
44. **Dahl, E. L., and P. J. Rosenthal.** 2008. Apicoplast translation, transcription and genome replication: targets for antimalarial antibiotics. Trends in Parasitology **24:**279-284.
45. **Dahlström, S., M. I. Veiga, P. Ferreira, A. Mårtensson, A. Kaneko, B. Andersson, A. Björkman, and J. P. Gil.** 2008. Diversity of the sarco/endoplasmic reticulum Ca2+-ATPase orthologue of Plasmodium falciparum (PfATP6). Infection, Genetics and Evolution **8:**340-345.
46. **Dame, J. B., J. L. Williams, T. F. McCutchan, J. L. Weber, R. A. Wirtz, W. T. Hockmeyer, W. Lee Maloy, J. David Haynes, I. Schneider, D. Roberts, G. S. Sanders, E. Premkumar Reddy, C. L. Diggs, and L. H. Miller.** 1984. Structure of the gene encoding the immunodominant surface antigen on the sporozoite of the human malaria parasite plasmodium falciparum. Science **225:**587-593.

47. **Davis, G. D., C. Elisee, D. M. Newham, and R. G. Harrison.** 1999. New fusion protein systems designed to give soluble expression in Escherichia coli. Biotechnology and bioengineering **65:**382-8.
48. **De Backer, M. D., T. Ilyina, X. J. Ma, S. Vandoninck, W. H. M. L. Luyten, and H. V. Bossche.** 2001. Genomic profiling of the response of Candida albicans to itraconazole treatment using a DNA microarray. Antimicrobial Agents and Chemotherapy **45:**1660-1670.
49. **Deng, X., R. Gujjar, F. El Mazouni, W. Kaminsky, N. A. Malmquist, E. J. Goldsmith, P. K. Rathod, and M. A. Phillips.** 2009. Structural plasticity of malaria dihydroorotate dehydrogenase allows selective binding of diverse chemical scaffolds. Journal of Biological Chemistry **284:**26999-27009.
50. **Denver, D. R., K. Morris, J. T. Streelman, S. K. Kim, M. Lynch, and W. K. Thomas.** 2005. The transcriptional consequences of mutation and natural selection in Caenorhabditis elegans. Nature Genetics **37:**544-548.
51. **Dinglasan, R. R., J. M. Porter-Kelley, U. Alam, and A. F. Azad.** 2005. Peptide mimics as surrogate immunogens of mosquito midgut carbohydrate malaria transmission blocking targets. Vaccine **23:**2717-2724.
52. **Dondorp, A. M., F. Nosten, P. Yi, D. Das, A. P. Phyo, J. Tarning, K. M. Lwin, F. Ariey, W. Hanpithakpong, S. J. Lee, P. Ringwald, K. Silamut, M. Imwong, K. Chotivanich, P. Lim, T. Herdman, S. S. An, S. Yeung, P. Singhasivanon, N. P. J. Day, N. Lindegardh, D. Socheat, and N. J. White.** 2009. Artemisinin resistance in Plasmodium falciparum malaria. New England Journal of Medicine **361:**455-467.
53. **Douglas, A. D., A. R. Williams, J. J. Illingworth, G. Kamuyu, S. Biswas, A. L. Goodman, D. H. Wyllie, C. Crosnier, K. Miura, G. J. Wright, C. A. Long, F. H. Osier, K. Marsh, A. V. Turner, A. V. S. Hill, and S. J. Draper.** 2011. The blood-stage malaria antigen PfRH5 is susceptible to vaccine-inducible cross-strain neutralizing antibody. Nature Communications **2.**
54. **Dudkina, N. V., J. Heinemeyer, S. Sunderhaus, E. J. Boekema, and H. P. Braun.** 2006. Respiratory chain supercomplexes in the plant mitochondrial membrane. Trends in Plant Science **11:**232-240.
55. **Duraisingh, M. T., T. Triglia, S. A. Ralph, J. C. Rayner, J. W. Barnwell, G. I. McFadden, and A. F. Cowman.** 2003. Phenotypic variation of Plasmodium falciparum merozoite proteins directs receptor targeting for invasion of human erythrocytes. EMBO Journal **22:**1047-1057.
56. **Durrand, V., A. Berry, R. Sem, P. Glaziou, J. Beaudou, and T. Fandeur.** 2004. Variations in the sequence and expression of the Plasmodium falciparum chloroquine resistance transporter (Pfcrt) and their relationship to chloroquine resistance in vitro. Molecular and Biochemical Parasitology **136:**273-285.
57. **Eastman, R. T., and D. A. Fidock.** 2009. Artemisinin-based combination therapies: A vital tool in efforts to eliminate malaria. Nature Reviews Microbiology **7:**864-874.
58. **Eckstein-Ludwig, U., R. J. Webb, I. D. A. Van Goethem, J. M. East, A. G. Lee, M. Kimura, P. M. O'Neill, P. G. Bray, S. A. Ward, and S. Krishna.** 2003. Artemisinins target the SERCA of Plasmodium falciparum. Nature **424:**957-961.
59. **Egan, T. J.** 2008. Haemozoin formation. Molecular and Biochemical Parasitology **157:**127-136.
60. **Ekvall, H.** 2003. Malaria and anemia. Current Opinion in Hematology **10:**108-114.
61. **Epstein, J. E., K. Tewari, K. E. Lyke, B. K. L. Sim, P. F. Billingsley, M. B. Laurens, A. Gunasekera, S. Chakravarty, E. R. James, M. Sedegah, A. Richman, S. Velmurugan, S. Reyes, M. Li, K. Tucker, A. Ahumada, A. J. Ruben, T. Li, R. Stafford, A. G. Eappen, C. Tamminga, J. W. Bennett, C. F. Ockenhouse, J. R. Murphy, J. Komisar, N. Thomas, M. Loyevsky, A. Birkett, C. V. Plowe, C. Loucq, R. Edelman, T. L. Richie, R. A. Seder, and S. L. Hoffman.** 2011. Live attenuated malaria vaccine designed to protect through hepatic CD8 + T cell immunity. Science **334:**475-480.
62. **Feagin, J. E.** 1992. The 6-kb element of Plasmodium falciparum encodes mitochondrial cytochrome genes. Molecular and Biochemical Parasitology **52:**145-148.

63. **Feagin, J. E.** 2000. Mitochondrial genome diversity in parasites. International Journal for Parasitology **30:**371-390.
64. **Ferguson-Miller, S., and G. T. Babcock.** 1996. Heme/copper terminal oxidases. Chemical Reviews **96:**2889-2907.
65. **Fidock, D. A., R. T. Eastman, S. A. Ward, and S. R. Meshnick.** 2008. Recent highlights in antimalarial drug resistance and chemotherapy research. Trends in Parasitology **24:**537-544.
66. **Fisher, N., P. G. Bray, S. A. Ward, and G. A. Biagini.** 2007. The malaria parasite type II NADH:quinone oxidoreductase: an alternative enzyme for an alternative lifestyle. Trends in Parasitology **23:**305-310.
67. **Fisher, N., C. K. Castleden, I. Bourges, G. Brasseur, G. Dujardin, and B. Meunier.** 2004. Human Disease-related Mutations in Cytochrome b Studied in Yeast. Journal of Biological Chemistry **279:**12951-12958.
68. **Fisher, N., and B. Meunier.** 2008. Molecular basis of resistance to cytochrome bc1 inhibitors. FEMS Yeast Research **8:**183-192.
69. **Fisher, N., and B. Meunier.** 2005. Re-examination of inhibitor resistance conferred by Qo-site mutations in cytochrome b using yeast as a model system. Pest management science **61:**973-8.
70. **Fisher, N., A. J. Warman, S. A. Ward, and G. A. Biagini.** 2009. Chapter 17 Type II NADH: Quinone Oxidoreductases of Plasmodium falciparum and Mycobacterium tuberculosis. Kinetic and High-Throughput Assays, p. 303-320, Methods in Enzymology, vol. 456.
71. **Fitch, C. D.** 2004. Ferriprotoporphyrin IX, phospholipids, and the antimalarial actions of quinoline drugs. Life Sciences **74:**1957-1972.
72. **Fivelman, Q. L., G. A. Butcher, I. S. Adagu, D. C. Warhurst, and G. Pasvol.** 2002. Malarone treatment failure and in vitro confirmation of resistance of Plasmodium falciparum isolate from Lagos, Nigeria. Malaria Journal **1:**1.
73. **Flint, D. H., M. H. Emptage, and J. R. Guest.** 1992. Fumarase A from Escherichia coli: Purification and characterization as an iron-sulfur cluster containing enzyme. Biochemistry **31:**10331-10337.
74. **Florens, L., M. Washburn, N. Muster, D. Wolters, M. Gardner, R. Anthony, D. Haynes, K. Moch, J. Sacci, A. Witney, N. Grainger, A. Holder, Y. Wu, J. Yates Iii, and D. Carucci.** 2002. Presented at the Proceedings 50th ASMS Conference on Mass Spectrometry and Allied Topics.
75. **Foth, B. J., L. M. Stimmler, E. Handman, B. S. Crabb, A. N. Hodder, and G. I. McFadden.** 2005. The malaria parasite Plasmodium falciparum has only one pyruvate dehydrogenase complex, which is located in the apicoplast. Molecular Microbiology **55:**39-53.
76. **Francis, S. E., D. J. Sullivan Jr, and D. E. Goldberg.** 1997. Hemoglobin metabolism in the malaria parasite Plasmodium falciparium. Annual Review of Microbiology **51:**97-123.
77. **Fraunholz, M. J.** 2005. Systems biology in malaria research. Trends in Parasitology **21:**393-395.
78. **Fry, M., and J. E. Beesley.** 1991. Mitochondria of mammalian Plasmodium spp. Parasitology **102:**17-26.
79. **Fry, M., and M. Pudney.** 1992. Site of action of the antimalarial hydroxynaphthoquinone, 2-[trans-4-(4'-chlorophenyl) cyclohexyl]-3- hydroxy-1,4-naphthoquinone (566C80). Biochemical Pharmacology **43:**1545-1553.
80. **Funes, S., E. Davidson, A. Reyes-Prieto, S. Magallon, P. Herion, M. P. King, and D. Gonzalez-Halphen.** 2002. A green algal apicoplast ancestor. Science **298:**2155.
81. **Ganesan, K., N. Ponmee, L. Jiang, J. W. Fowble, J. White, S. Kamchonwongpaisan, Y. Yuthavong, P. Wilairat, and P. K. Rathod.** 2008. A genetically hard-wired metabolic transcriptome in Plasmodium falciparum fails to mount protective responses to lethal antifolates. Plos Pathogens **4.**
82. **Gardner, M. J., N. Hall, E. Fung, O. White, M. Berriman, R. W. Hyman, J. M. Carlton, A. Pain, K. E. Nelson, S. Bowman, I. T. Paulsen, K. James, J. A. Eisen, K. Rutherford, S. L. Salzberg, A. Craig, S. Kyes, M. S. Chan, V. Nene, S. J. Shallom, B. Suh, J. Peterson, S. Angiuoli, M. Pertea,**

J. Allen, J. Selengut, D. Haft, M. W. Mather, A. B. Vaidya, D. M. A. Martin, A. H. Fairlamb, M. J. Fraunholz, D. S. Roos, S. A. Ralph, G. I. McFadden, L. M. Cummings, G. M. Subramanian, C. Mungall, J. C. Venter, D. J. Carucci, S. L. Hoffman, C. Newbold, R. W. Davis, C. M. Fraser, and B. Barrell. 2002. Genome sequence of the human malaria parasite Plasmodium falciparum. Nature **419**:498-511.

83. **Garnham, P. C.** 1966. Comments on biology of human malaria. Military Medicine **131**:Suppl:961-962.
84. **Gassis, S., and P. K. Rathod.** 1996. Frequency of drug resistance in Plasmodium falciparum: A nonsynergistic combination of 5-fluoroorotate and atovaquone suppresses in vitro resistance. Antimicrobial Agents and Chemotherapy **40**:914-919.
85. **Gaur, D., D. C. G. Mayer, and L. H. Miller.** 2004. Parasite ligand-host receptor interactions during invasion of erythrocytes by Plasmodium merozoites. International Journal for Parasitology **34**:1413-1429.
86. **Genton B, A.-Y. F., Betuela I, Anders RF, Saul A, Baea K, Mellombo M, Taraika J, Brown GV, Pye D, Irving DO, Felger I, Beck HP, Smith TA, Alpers MP. .** 2003. Safety and immunogenicity of a three-component blood-stage malaria vaccine (MSP1, MSP2, RESA) against Plasmodium falciparum in Papua New Guinean children. Vaccine **8**:30-41.
87. **Ghumra, A., P. Khunrae, R. Ataide, A. Raza, S. J. Rogerson, M. K. Higgins, and J. Alexandra Rowe.** 2011. Immunisation with recombinant PfEMP1 domains elicits functional rosette-inhibiting and phagocytosis-inducing antibodies to Plasmodium falciparum. PLoS ONE **6**.
88. **Gómez, L. A., J. S. Monette, J. D. Chavez, C. S. Maier, and T. M. Hagen.** 2009. Supercomplexes of the mitochondrial electron transport chain decline in the aging rat heart. Archives of Biochemistry and Biophysics **490**:30-35.
89. **Gonzales, J. M., J. J. Patel, N. Ponmee, L. Jiang, A. Tan, S. P. Maher, S. Wuchty, P. K. Rathod, and M. T. Ferdig.** 2008. Regulatory hotspots in the malaria parasite genome dictate transcriptional variation. PLoS Biology **6**.
90. **Goodman, C. D., V. Su, and G. I. McFadden.** 2007. The effects of anti-bacterials on the malaria parasite Plasmodium falciparum. Molecular and Biochemical Parasitology **152**:181-191.
91. **Gordon, D. M., T. W. McGovern, U. Krzych, J. C. Cohen, I. Schneider, R. LaChance, D. G. Heppner, G. Yuan, M. Hollingdale, M. Slaoui, P. Hauser, P. Voet, J. C. Sadoff, and W. R. Ballou.** 1995. Safety, immunogenicity, and efficacy of a recombinantly produced Plasmodium falciparum circumsporozoite protein-hepatitis B surface antigen subunit vaccine. Journal of Infectious Diseases **171**:1576-1585.
92. **Grau, G. E., C. D. Mackenzie, R. A. Carr, M. Redard, G. Pizzolato, C. Allasia, C. Cataldo, T. E. Taylor, and M. E. Molyneux.** 2003. Platelet accumulation in brain microvessels in fatal pediatric cerebral malaria. Journal of Infectious Diseases **187**:461-466.
93. **Gunasekera, A. M., A. Myrick, K. L. Roch, E. Winzeler, and D. F. Wirth.** 2007. Plasmodium falciparum: Genome wide perturbations in transcript profiles among mixed stage cultures after chloroquine treatment. Experimental Parasitology **117**:87-92.
94. **Gunasekera, A. M., S. Patankar, J. Schug, G. Eisen, and D. F. Wirth.** 2003. Drug-induced alterations in gene expression of the asexual blood forms of Plasmodium falciparum. Molecular Microbiology **50**:1229-1239.
95. **Haldar, K., and N. Mohandas.** 2009. Malaria, erythrocytic infection, and anemia. Hematology / the Education Program of the American Society of Hematology. American Society of Hematology. Education Program:87-93.
96. **Hammen, P. K., and H. Weiner.** 1998. Mitochondrial leader sequences: structural similarities and sequence differences. The Journal of experimental zoology **282**:280-3.
97. **Hammen, P. K., and H. Weiner.** 1998. Mitochondrial leader sequences: Structural similarities and sequence differences. Journal of Experimental Zoology **282**:280-283.
98. **Hartgers, F. C., B. B. Obeng, Y. C. M. Kruize, A. Dijkhuis, M. McCall, R. W. Sauerwein, A. J. F. Luty, D. A. Boakye, and M. Yazdanbakhsh.** 2009. Responses to malarial antigens are altered in helminth-infected children. Journal of Infectious Diseases **199**:1528-1535.

99. **Hartwig, C. L., A. S. Rosenthal, J. D'Angelo, C. E. Griffin, G. H. Posner, and R. A. Cooper.** 2009. Accumulation of artemisinin trioxane derivatives within neutral lipids of Plasmodium falciparum malaria parasites is endoperoxide-dependent. Biochemical Pharmacology **77:**322-336.

100. **Harvey Lodish, A. B., S Lawrence Zipursky, Paul Matsudaira, David Baltimore, James Darnell.** 2000. Molecular Cell Biology, 4th edition ed. New York: Freeman, New York.

101. **Hayton, K., and X. Z. Su.** 2008. Drug resistance and genetic mapping in Plasmodium falciparum. Current Genetics **54:**223-239.

102. **Hayward, R. E.** 2000. Plasmodium falciparum phosphoenolpyruvate carboxykinase is developmentally regulated in gametocytes. Molecular and Biochemical Parasitology **107:**227-240.

103. **Helm, M.** 2006. Post-transcriptional nucleotide modification and alternative folding of RNA. Nucleic Acids Research **34:**721-33.

104. **Higgins, M. K.** 2008. The structure of a chondroitin sulfate-binding domain important in placental malaria. Journal of Biological Chemistry **283:**21842-21846.

105. **Hirschey, M. D., T. Shimazu, E. Goetzman, E. Jing, B. Schwer, D. B. Lombard, C. A. Grueter, C. Harris, S. Biddinger, O. R. Ilkayeva, R. D. Stevens, Y. Li, A. K. Saha, N. B. Ruderman, J. R. Bain, C. B. Newgard, R. V. Farese Jr, F. W. Alt, C. R. Kahn, and E. Verdin.** 2010. SIRT3 regulates mitochondrial fatty-acid oxidation by reversible enzyme deacetylation. Nature **464:**121-125.

106. **Hodder, A. N., P. E. Crewther, and R. F. Anders.** 2001. Specificity of the protective antibody response to apical membrane antigen 1. Infection and Immunity **69:**3286-3294.

107. **Hoffman, D. L., and P. S. Brookes.** 2009. Oxygen sensitivity of mitochondrial reactive oxygen species generation depends on metabolic conditions. Journal of Biological Chemistry **284:**16236-16245.

108. **Hoffman, S. L., P. F. Billingsley, E. James, A. Richman, M. Loyevsky, T. Li, S. Chakravarty, A. Gunasekera, R. Chattopadhyay, M. Li, R. Stafford, A. Ahumada, J. E. Epstein, M. Sedegah, S. Reyes, T. L. Richie, K. E. Lyke, R. Edelman, M. B. Laurens, C. V. Plowe, and B. K. L. Sim.** 2010. Development of a metabolically active, non-replicating sporozoite vaccine to prevent Plasmodium falciparum malaria. Human Vaccines **6:**97-106.

109. **Horsefield, R., V. Yankovskaya, G. Sexton, W. Whittingham, K. Shiomi, S. Omura, B. Byrne, G. Cecchini, and S. Iwata.** 2006. Structural and computational analysis of the quinone-binding site of complex II (succinate-ubiquinone oxidoreductase): A mechanism of electron transfer and proton conduction during ubiquinone reduction. Journal of Biological Chemistry **281:**7309-7316.

110. **Hosler, J. P.** 2004. The influence of subunit III of cytochrome c oxidase on the D pathway, the proton exit pathway and mechanism-based inactivation in subunit I. Biochimica et Biophysica Acta - Bioenergetics **1655:**332-339.

111. **Huang, Y., M. J. Lemieux, J. Song, M. Auer, and D. N. Wang.** 2003. Structure and mechanism of the glycerol-3-phosphate transporter from Escherichia coli. Science **301:**616-620.

112. **Hughes, K. R., N. Philip, G. Lucas Starnes, S. Taylor, and A. P. Waters.** 2010. From cradle to grave: RNA biology in malaria parasites. Wiley Interdisciplinary Reviews - RNA **1:**287-303.

113. **Hunt, N. H., and G. E. Grau.** 2003. Cytokines: Accelerators and brakes in the pathogenesis of cerebral malaria. Trends in Immunology **24:**491-499.

114. **Hunte, C., J. Koepke, C. Lange, T. Rossmanith, and H. Michel.** 2000. Structure at 2.3 angstrom resolution of the cytochrome bc(1) complex from the yeast Saccharomyces cerevisiae co-crystallized with an antibody Fv fragment. Structure with Folding & Design **8:**669-684.

115. **Hyde, J. E.** 2007. Drug-resistant malaria - An insight. FEBS Journal **274:**4688-4698.

116. **Janka, J. J., O. A. Koita, B. TraorÃ©, J. M. TraorÃ©, F. Mzayek, V. Sachdev, X. Wang, K. Sanogo, L. SangarÃ©, L. Masur, H. Masur, G. J. Kato, M. T. Gladwin, and D. J. Krogstad.** Increased pulmonary pressures and myocardial wall stress in children with severe malaria. Journal of Infectious Diseases **202:**791-800.

117. **Ji Hae Chung, P. K., Patrick Yang, Nelson Yang, Frances Levitt.** 2005. The Enzyme Kinetics of NADH Dehydrogenase After the Addition of the Inhibitory Molecules, EDTA and Mg2+. Journal of Experimental Microbiology and Immunology **7:**7-13.
118. **Johnson, D. J., A. Owen, N. Plant, P. G. Bray, and S. A. Ward.** 2008. Drug-regulated expression of Plasmodium falciparum P-glycoprotein homologue 1: A putative role for nuclear receptors. Antimicrobial Agents and Chemotherapy **52:**1438-1445.
119. **Jones, M. K., and M. F. Good.** 2006. Malaria parasites up close. Nature Medicine **12:**170-171.
120. **Joseph Sambrook, P. M.** 2001. Molecular Cloning: A Laboratory Manual. CSH Press.
121. **Joy, D. A., X. Feng, J. Mu, T. Furuya, K. Chotivanich, A. U. Krettli, M. Ho, A. Wang, N. J. White, E. Suh, P. Beerli, and X. Z. Su.** 2003. Early origin and recent expansion of Plasmodium falciparum. Science **300:**318-321.
122. **Kanehisa, M., S. Goto, S. Kawashima, and A. Nakaya.** 2002. Thed KEGG databases at GenomeNet. Nucleic Acids Research **30:**42-46.
123. **Karunaweera, N., D. Wanasekara, V. Chandrasekharan, K. Mendis, and R. Carter.** 2007. Plasmodium vivax: Paroxysm-associated lipids mediate leukocyte aggregation. Malaria Journal **6.**
124. **Kaslow, D. C.** 2002. Transmission-blocking vaccines. Chemical Immunology **80:**287-307.
125. **Keller, C. C., G. C. Davenport, K. R. Dickman, J. B. Hittner, S. S. Kaplan, J. B. Weinberg, P. G. Kremsner, and D. J. Perkins.** 2006. Suppression of prostaglandin E 2 by malaria parasite products and antipyretics promotes overproduction of tumor necrosis factor-Î±: Association with the pathogenesis of childhood malarial anemia. Journal of Infectious Diseases **193:**1384-1393.
126. **Kerscher, S. J.** 2000. Diversity and origin of alternative NADH:ubiquinone oxidoreductases. Biochimica et biophysica acta **1459:**274-83.
127. **Kessl, J. J., K. H. Ha, A. K. Merritt, B. B. Lange, P. Hill, B. Meunier, S. R. Meshnick, and B. L. Trumpower.** 2005. Cytochrome b mutations that modify the ubiquinol-binding pocket of the cytochrome bc1 complex and confer anti-malarial drug resistance in Saccharomyces cerevisiae. Journal of Biological Chemistry **280:**17142-17148.
128. **Kessl, J. J., K. H. Ha, A. K. Merritt, B. B. Lange, P. Hill, B. Meunier, S. R. Meshnick, and B. L. Trumpower.** 2005. Cytochrome b mutations that modify the ubiquinol-binding pocket of the cytochrome bc₁ complex and confer anti-malarial drug resistance in Saccharomyces cerevisiae. Journal of Biological Chemistry **280:**17142-17148.
129. **Kessl, J. J., B. B. Lange, T. Merbitz-Zahradnik, K. Zwicker, P. Hill, B. Meunier, H. PÃ¡lsdÃ³ttir, C. Hunte, S. Meshnick, and B. L. Trumpower.** 2003. Molecular basis for atovaquone binding to the cytochrome bc₁ complex. Journal of Biological Chemistry **278:**31312-31318.
130. **Kessl, J. J., S. R. Meshnick, and B. L. Trumpower.** 2007. Modeling the molecular basis of atovaquone resistance in parasites and pathogenic fungi. Trends in Parasitology **23:**494-501.
131. **Khositnithikul, R., P. Tan-Ariya, and M. Mungthin.** 2008. In vitro atovaquone/proguanil susceptibility and characterization of the cytochrome b gene of Plasmodium falciparum from different endemic regions of Thailand. Malaria Journal **7.**
132. **Kilejian, A., and J. Olson.** 1979. Proteins and glycoproteins from human erythrocytes infected with Plasmodium falciparum. Bulletin of the World Health Organization **57:**101-107.
133. **Kirk, K., H. A. Horner, and J. Kirk.** 1996. Glucose uptake in Plasmodium falciparum-infected erythrocytes is an equilibrative not an active process. Molecular and Biochemical Parasitology **82:**195-205.
134. **Kita, K., H. Hirawake, H. Miyadera, H. Amino, and S. Takeo.** 2002. Role of complex II in anaerobic respiration of the parasite mitochondria from Ascaris suum and Plasmodium falciparum. Biochimica et Biophysica Acta (BBA) - Bioenergetics **1553:**123-139.
135. **Korsinczky, M., N. Chen, B. Kotecka, A. Saul, K. Rieckmann, and Q. Cheng.** 2000. Mutations in Plasmodium falciparum cytochrome b that are associated with atovaquone resistance are located at a putative drug-binding site. Antimicrobial Agents and Chemotherapy **44:**2100-2108.

136. **Krishna, S., C. J. Woodrow, R. J. S. Burchmore, K. J. Saliba, and K. Kirk.** 2000. Hexose transport in asexual stages of Plasmodium falciparum and Kinetoplastidae. Parasitology Today **16:**516-521.
137. **Krogh, A., B. Larsson, G. Von Heijne, and E. L. L. Sonnhammer.** 2001. Predicting transmembrane protein topology with a hidden Markov model: Application to complete genomes. Journal of Molecular Biology **305:**567-580.
138. **Krotoski, W. A.** 1985. Discovery of the hypnozoite and a new theory of malarial relapse. Transactions of the Royal Society of Tropical Medicine and Hygiene **79:**12-20.
139. **Krungkrai, J.** 2004. The multiple roles of the mitochondrion of the malarial parasite. Parasitology **129:**511-524.
140. **Krungkrai, J.** 1995. Purification, characterization and localization of mitochondrial dihydroorotate dehydrogenase in Plasmodium falciparum, human malaria parasite. Biochimica et Biophysica Acta - General Subjects **1243:**351-360.
141. **Kublin, J. G., F. K. Dzinjalamala, D. D. Kamwendo, E. M. Malkin, J. F. Cortese, L. M. Martino, R. A. G. Mukadam, S. J. Rogerson, A. G. Lescano, M. E. Molyneux, P. A. Winstanley, P. Chimpeni, T. E. Taylor, and C. V. Plowe.** 2002. Molecular markers for failure of sulfadoxine-pyrimethamine and chlorproguanil-dapsone treatment of Plasmodium falciparum malaria. Journal of Infectious Diseases **185:**380-388.
142. **Kumar, N.** 2002. Malaria: Progress, problems and plans in the genomic era. International Journal for Parasitology **32:**1537-1538.
143. **Kyes, S., P. Horrocks, and C. Newbold.** 2001. Antigenic variation at the infected red cell surface in malaria, p. 673-707, Annual Review of Microbiology, vol. 55.
144. **La Raja, M.** 2002. Erythrophagocytosis by peripheral monocytes in Plasmodium falciparum malaria. Haematologica **87**.
145. **Lalloo, D. G., D. Shingadia, G. Pasvol, P. L. Chiodini, C. J. Whitty, N. J. Beeching, D. R. Hill, D. A. Warrell, and B. A. Bannister.** 2007. UK malaria treatment guidelines. Journal of Infection **54:**111-121.
146. **Lambros, C., and J. P. Vanderberg.** 1979. Synchronization of Plasmodium falciparum erythrocytic stages in culture. The Journal of parasitology **65:**418-20.
147. **Lasonder, E., Y. Ishihama, J. S. Andersen, A. M. W. Vermunt, A. Pain, R. W. Sauerwein, W. M. C. Eling, N. Hall, A. P. Waters, H. G. Stunnenbergt, and M. Mann.** 2002. Analysis of the Plasmodium falciparum proteome by high-accuracy mass spedrometry. Nature **419:**537-542.
148. **Lavazec, C., S. Sanyal, and T. J. Templeton.** 2007. Expression switching in the stevor and Pfmc-2TM superfamilies in Plasmodium falciparum. Molecular Microbiology **64:**1621-1634.
149. **Lavazec, C., S. Sanyal, and T. J. Templeton.** 2006. Hypervariability within the Rifin, Stevor and Pfmc-2TM superfamilies in plasmodium falciparum. Nucleic Acids Research **34:**6696-6707.
150. **Le Roch, K. G., J. R. Johnson, L. Florens, Y. Zhou, A. Santrosyan, M. Grainger, S. F. Yan, K. C. Williamson, A. A. Holder, D. J. Carucci, J. R. Yates Iii, and E. A. Winzeler.** 2004. Global analysis of transcript and protein levels across the Plasmodium falciparum life cycle. Genome Research **14:**2308-2318.
151. **Lenaz, G., and M. L. Genova.** 2009. Structural and functional organization of the mitochondrial respiratory chain: A dynamic super-assembly. International Journal of Biochemistry & Cell Biology **41:**1750-1772.
152. **Lenaz, G., and M. L. Genova.** 2010. Structure and Organization of Mitochondrial Respiratory Complexes: A New Understanding of an Old Subject. Antioxidants & Redox Signaling **12:**961-1008.
153. **Lescuyer, P., S. Picot, V. Bracchi, J. Burnod, J. Austin, A. Perard, and P. Ambroise-Thomas.** 1997. Detection of RAPD markers correlated with chloroquine resistance in Plasmodium falciparum. Genome Research **7:**747-753.
154. **Li, G. Q., X. B. Guo, L. C. Fu, H. X. Jian, and X. H. Wang.** 1994. Clinical trials of artemisinin and its derivatives in the treatment of malaria in China. Transactions of the Royal Society of Tropical Medicine and Hygiene **88:**S5-S6.

155. **Lim, L., and G. I. McFadden.** 2010. The evolution, metabolism and functions of the apicoplast. Philosophical Transactions of the Royal Society B: Biological Sciences **365:**749-763.
156. **Llinas, M., Z. Bozdech, E. D. Wong, A. T. Adai, and J. L. DeRisi.** 2006. Comparative whole genome transcriptome analysis of three Plasmodium falciparum strains. Nucleic Acids Research **34:**1166-1173.
157. **Looareesuwan, S., C. Viravan, H. K. Webster, D. E. Kyle, D. B. Hutchinson, and C. J. Canfield.** 1996. Clinical studies of atovaquone, alone or in combination with other antimalarial drugs, for treatment of acute uncomplicated malaria in Thailand. American Journal of Tropical Medicine and Hygiene **54:**62-66.
158. **Looareesuwan, S., P. Wilairatana, K. Chalermarut, Y. Rattanapong, C. J. Canfield, and D. B. A. Hutchinson.** 1999. Efficacy and safety of atovaquone/proguanil compared with mefloquine for treatment of acute Plasmodium falciparum malaria in Thailand. American Journal of Tropical Medicine and Hygiene **60:**526-532.
159. **M.Cox, D. L. N. a. M.** 2008. Lehniger Principles of Biochemistry, Fifth Edition ed. W.H. Freeman and Company.
160. **Maeda T, S. T., Harb OS, Roos DS, Takeo S, Suzuki H, Tsuboi T, Takeuchi T, Asai T.** 2009. Pyruvate kinase type-II isozyme in Plasmodium falciparum localizes to the apicoplas. Parasitol.Int **58:**101-105.
161. **Malaguarnera, L., R. M. Imbesi, S. Pignatelli, J. SimporÃ¨, M. Malaguarnera, and S. Musumeci.** 2002. Increased levels of interleukin-12 in Plasmodium falciparum malaria: Correlation with the severity of disease. Parasite Immunology **24:**387-389.
162. **Malkin, E. M., A. P. Durbin, D. J. Diemert, J. Sattabongkot, Y. Wu, K. Miura, C. A. Long, L. Lambert, A. P. Miles, J. Wang, A. Stowers, L. H. Miller, and A. Saul.** 2005. Phase 1 vaccine trial of Pvs25H: A transmission blocking vaccine for Plasmodium vivax malaria. Vaccine **23:**3131-3138.
163. **Mark Madden, C. S., Kathy Tse, Ambrose Wong.** 2004. The Inhibitory Effect of EDTA and Mg2+ on the Activity of NADH Dehydrogenase in Lysozyme Lysis. Journal of Experimental Microbiology and Immunology **5:**8-15.
164. **Marks, F., V. Von Kalckreuth, R. Kobbe, S. Adjei, O. Adjei, R. D. Horstmann, C. G. Meyer, and J. May.** 2005. Parasitological rebound effect and emergence of pyrimethamine resistance in Plasmodium falciparum after single-dose sulfadoxine-pyrimethamine. Journal of Infectious Diseases **192:**1962-1965.
165. **Martin, W., and R. G. Herrmann.** 1998. Gene transfer from organelles to the nucleus: How much, what happens, and why? Plant Physiology **118:**9-17.
166. **Matuschewski, K.** 2006. Getting infectious: Formation and maturation of plasmodium sporozoites in the Anopheles vector. Cellular Microbiology **8:**1547-1556.
167. **McCarthy, J. S., and M. F. Good.** Whole parasite blood stage malaria vaccines: A convergence of evidence. Human Vaccines **6.**
168. **McCollum, A. M., A. C. Poe, M. Hamel, C. Huber, Z. Zhou, Y. P. Shi, P. Ouma, J. Vulule, P. Bloland, L. Slutsker, J. W. Barnwell, V. Udhayakumar, and A. A. Escalante.** 2006. Antifolate resistance in Plasmodium falciparum: Multiple origins and identification of novel dhfr alleles. Journal of Infectious Diseases **194:**189-197.
169. **McFadden, G. I.** 2000. Mergers and acquisitions: malaria and the great chloroplast heist. Genome biology **1.**
170. **McFadden, G. I., and D. S. Roos.** 1999. Apicomplexan plastids as drug targets. Trends in Microbiology **7:**328-333.
171. **McMillan, P. J., L. M. Stimmler, B. J. Foth, G. I. McFadden, and S. Muller.** 2005. The human malaria parasite Plasmodium falciparum possesses two distinct dihydrolipoamide dehydrogenases. Molecular Microbiology **55:**27-38.
172. **Meshnick, S. R., T. E. Taylor, and S. Kamchonwongpaisan.** 1996. Artemisinin and the antimalarial endoperoxides: From herbal remedy to targeted chemotherapy. Microbiological Reviews **60:**301-315.

173. **Metenou, S., B. DembÃ©le, S. Konate, H. Dolo, S. Y. Coulibaly, Y. I. Coulibaly, A. A. Diallo, L. Soumaoro, M. E. Coulibaly, D. Sanogo, S. S. Doumbia, M. Wagner, S. F. TraorÃ©, A. Klion, S. Mahanty, and T. B. Nutman.** 2009. Patent filarial infection modulates malaria-specific type 1 cytokine responses in an IL-10-dependent manner in a filaria/malaria-coinfected population. Journal of Immunology **183:**916-924.

174. **Mideo, N., T. Day, and A. F. Read.** 2008. Modelling malaria pathogenesis. Cellular Microbiology **10:**1947-1955.

175. **Miller, L. H., D. I. Baruch, K. Marsh, and O. K. Doumbo.** 2002. The pathogenic basis of malaria. Nature **415:**673-679.

176. **Minarik, P., N. Tomaaskova, M. Kollarova, and M. Antalak.** 2002. Malate Dehydrogenases - Structure and function. General Physiology and Biophysics **21:**257-265.

177. **Mita, T., K. Tanabe, and K. Kita.** 2009. Spread and evolution of Plasmodium falciparum drug resistance. Parasitology International **58:**201-209.

178. **Mitchell, G. H., A. W. Thomas, G. Margos, A. R. Dluzewski, and L. H. Bannister.** 2004. Apical Membrane Antigen 1, a Major Malaria Vaccine Candidate, Mediates the Close Attachment of Invasive Merozoites to Host Red Blood Cells. Infection and Immunity **72:**154-158.

179. **Miura, K., D. B. Keister, O. V. Muratova, J. Sattabongkot, C. A. Long, and A. Saul.** 2007. Transmission-blocking activity induced by malaria vaccine candidates Pfs25/Pvs25 is a direct and predictable function of antibody titer. Malaria Journal **6**.

180. **Miyadera, H., K. Shiomi, H. Ui, Y. Yamaguchi, R. Masuma, H. Tomoda, H. Miyoshi, A. Osanai, K. Kita, and S. Omura.** 2003. Atpenins, potent and specific inhibitors of mitochondrial complex II (succinate-ubiquinone oxidoreductase). Proceedings of the National Academy of Sciences of the United States of America **100:**473-477.

181. **Mkulama, M. A. P., S. Chishimba, J. Sikalima, P. Rouse, P. E. Thuma, and S. Mharakurwa.** 2008. Escalating Plasmodium falciparum antifolate drug resistance mutations in Macha, rural Zambia. Malaria Journal **7**.

182. **Mogi, T., Y. Murase, M. Mori, K. Shiomi, S. Mura, M. P. Paranagama, and K. Kita.** 2009. Polymyxin B identified as an inhibitor of alternative NADH dehydrogenase and malate: Quinone oxidoreductase from the gram-positive bacterium mycobacterium smegmatis. Journal of Biochemistry **146:**491-499.

183. **Mohammed, A. O., G. Elghazali, H. B. Mohammed, M. I. Elbashir, S. Xu, K. Berzins, and P. Venge.** 2003. Human neutrophil lipocalin: A specific marker for neutrophil activation in severe Plasmodium falciparum malaria. Acta Tropica **87:**279-285.

184. **Mok, S., M. Imwong, M. J. Mackinnon, J. Sim, R. Ramadoss, P. Yi, M. Mayxay, K. Chotivanich, K. Y. Liong, B. Russell, D. Socheat, P. N. Newton, N. P. J. Day, N. J. White, P. R. Preiser, F. Nosten, A. M. Dondorp, and Z. Bozdech.** 2011. Artemisinin resistance in Plasmodium falciparum is associated with an altered temporal pattern of transcription. BMC Genomics **12**.

185. **Molenaar, D., M. E. van der Rest, and S. Petrovic.** 1998. Biochemical and genetic characterization of the membrane-associated malate dehydrogenase (acceptor) from Corynebacterium glutamicum. European journal of biochemistry / FEBS **254:**395-403.

186. **Muller, F. L., Y. Liu, and H. Van Remmen.** 2004. Complex III releases superoxide to both sides of the inner mitochondrial membrane. Journal of Biological Chemistry **279:**49064-49073.

187. **Muller, I. B., and J. E. Hyde.** 2010. Antimalarial drugs: Modes of action and mechanisms of parasite resistance. Future Microbiology **5:**1857-1873.

188. **Musset, L., B. Pradines, D. Parzy, R. Durand, P. Bigot, and J. Le Bras.** 2006. Apparent absence of atovaquone/proguanil resistance in 477 Plasmodium falciparum isolates from untreated French travellers. Journal of Antimicrobial Chemotherapy **57:**110-115.

189. **Na-Bangchang, K., and J. Karbwang.** 2009. Current status of malaria chemotherapy and the role of pharmacology in antimalarial drug research and development. Fundamental and Clinical Pharmacology **23:**387-409.

190. **Nahrevanian, H., and M. J. Dascombe.** 2003. The role of nitric oxide and its up/downstream molecules in malaria: cytotoxic or preventive? The Southeast Asian journal of tropical medicine and public health **34 Suppl 2**:44-50.
191. **Nair, S. C., C. F. Brooks, C. D. Goodman, A. Strurm, G. I. McFadden, S. Sundriyal, J. L. Anglin, Y. Song, S. N. Moreno, and B. Striepen.** 2011. Apicoplast isoprenoid precursor synthesis and the molecular basis of fosmidomycin resistance in Toxoplasma gondii. Journal of Experimental Medicine **208**:1547-1559.
192. **Nair, S. C., and B. Striepen.** 2011. What do human parasites do with a chloroplast anyway? PLoS Biology **9**.
193. **Nosten, F., and N. J. White.** 2007. Artemisinin-based combination treatment of falciparum malaria. The American journal of tropical medicine and hygiene **77**:181-192.
194. **Novagen** 2004, posting date. Novagen User Protocol Competent Cells. [Online.]
195. **O'Neill, P. M., V. E. Barton, and S. A. Ward.** 2010. The molecular mechanism of action of artemisinin - The debate continues. Molecules **15**:1705-1721.
196. **Ockenhouse, C. F., P. F. Sun, D. E. Lanar, B. T. Wellde, B. Ted Hall, K. Kester, J. A. Stoute, A. Magill, U. Krzych, L. Farley, R. A. Wirtz, J. C. Sadoff, D. C. Kaslow, S. Kumar, L. W. Preston Church, J. M. Crutcher, B. Wizel, S. Hoffman, A. Lalvani, A. V. S. Hill, J. A. Tine, K. P. Guito, C. De Taisne, R. Anders, T. Horii, E. Paoletti, and W. R. Ballou.** 1998. Phase I/IIa safety, immunogenicity, and efficacy trial of NYVAC-Pf7, a poxvectored, multiantigen, multistage vaccine candidate for Plasmodium falciparum malaria. Journal of Infectious Diseases **177**:1664-1673.
197. **Ogutu, B. R., O. J. Apollo, D. McKinney, W. Okoth, J. Siangla, F. Dubovsky, K. Tucker, J. N. Waitumbi, C. Diggs, J. Wittes, E. Malkin, A. Leach, L. A. Soisson, J. B. Milman, L. Otieno, C. A. Holland, M. Polhemus, S. A. Remich, C. F. Ockenhouse, J. Cohen, W. R. Ballou, S. K. Martin, E. Angov, V. A. Stewart, J. A. Lyon, D. G. Heppner Jr, and M. R. Withers.** 2009. Blood stage malaria vaccine eliciting high antigen-specific antibody concentrations confers no protection to young children in Western Kenya. PLoS ONE **4**.
198. **Ogutu, B. R., and C. R. J. C. Newton.** 2004. Management of seizures in children with falciparum malaria. Tropical Doctor **34**:71-75.
199. **Olszewski, K. L., and M. Llinas.** 2011. Central carbon metabolism of Plasmodium parasites. Molecular and Biochemical Parasitology **175**:95-103.
200. **Olszewski, K. L., M. W. Mather, J. M. Morrisey, B. A. Garcia, A. B. Vaidya, J. D. Rabinowitz, and M. Llinas.** 2010. Branched tricarboxylic acid metabolism in Plasmodium falciparum. Nature **466**:774-778.
201. **Osei-Akoto A, O. L., Owusu- Ofori S.** 2009. Atovaquone-proguanil for treating uncomplicated malaria (Review), The Cochrane Collaboration. John Wiley & Sons, Ltd.
202. **Pagola, S., P. W. Stephens, D. S. Bohle, A. D. Kosar, and S. K. Madsen.** 2000. The structure of malaria pigment [beta]-haematin. Nature **404**:307-310.
203. **Painter, H. J., J. M. Morrisey, M. W. Mather, and A. B. Vaidya.** 2007. Specific role of mitochondrial electron transport in blood-stage Plasmodium falciparum. Nature **446**:88-91.
204. **Palsdottir, H., C. G. Lojero, B. L. Trumpower, and C. Hunte.** 2003. Structure of the yeast cytochrome bc1 complex with a hydroxyquinone anion Qo site inhibitor bound. Journal of Biological Chemistry **278**:31303-31311.
205. **Parroche, P., F. N. Lauw, N. Goutagny, E. Latz, B. G. Monks, A. Visintin, K. A. Halmen, M. Lamphier, M. Olivier, D. C. Bartholomeu, R. T. Gazzinelli, and D. T. Golenbock.** 2007. Malaria hemozoin is immunologically inert but radically enhances innate responses by presenting malaria DNA to Toll-like receptor 9. Proceedings of the National Academy of Sciences of the United States of America **104**:1919-1924.
206. **Patarroyo, G., L. Franco, R. Amador, L. A. Murillo, C. L. Rocha, M. Rojas, and M. E. Patarroyo.** 1992. Study of the safety and immunogenicity of the synthetic malaria SPf66 vaccine in children aged 1-14 years. Vaccine **10**:175-178.
207. **Perlmann, P., and M. Troye-Blomberg.** 2002. Malaria and the immune system in humans. Chemical Immunology **80**:229-242.

208. **Peters, J. M., N. Chen, M. Gatton, M. Korsinczky, E. V. Fowler, S. Manzetti, A. Saul, and Q. Cheng.** 2002. Mutations in cytochrome b resulting in atovaquone resistance are associated with loss of fitness in Plasmodium falciparum. Antimicrobial Agents and Chemotherapy **46:**2435-2441.

209. **Petersen, I., R. Eastman, and M. Lanzer.** 2011. Drug-resistant malaria: Molecular mechanisms and implications for public health. FEBS Letters **585:**1551-1562.

210. **Peterson, M. G., V. M. Marshall, J. A. Smythe, P. E. Crewther, A. Lew, A. Silva, R. F. Anders, and D. J. Kemp.** 1989. Integral membrane protein located in the apical complex of Plasmodium falciparum. Molecular and Cellular Biology **9:**3151-3154.

211. **Phillips, R. E., S. Looareesuwan, and D. A. Warrell.** 1986. The importance of anaemia in cerebral and uncomplicated falciparum malaria: Role of complications, dyserythropoiesis and iron sequestration. Quarterly Journal of Medicine **58:**305-323.

212. **Potter, S., T. Chan-Ling, H. J. Ball, H. Mansour, A. Mitchell, L. Maluish, and N. H. Hunt.** 2006. Perforin mediated apoptosis of cerebral microvascular endothelial cells during experimental cerebral malaria. International Journal for Parasitology **36:**485-496.

213. **Pradhan, A., A. K. Tripathi, P. V. Desai, P. K. Mukherjee, M. A. Avery, L. A. Walker, and B. L. Tekwani.** 2009. Structure and function of Plasmodium falciparum malate dehydrogenase: Role of critical amino acids in co-substrate binding pocket. Biochimie **91:**1509-1517.

214. **Price, R. N., J. A. Simpson, F. Nosten, C. Luxemburger, L. Hkirjaroen, F. T. Kuile, T. Chongsuphajaisiddhi, and N. J. White.** 2001. Factors contributing to anemia after uncomplicated falciparum malaria. American Journal of Tropical Medicine and Hygiene **65:**614-622.

215. **Promega** 2008, posting date. Promega Technical Bulletin Genomic DNA Purification Instructor's Manual. Promega. [Online.]

216. **Quashie, N. B., B. D. Akanmori, D. Ofori-Adjei, B. Q. Goka, and J. A. L. Kurtzhals.** 2006. Factors contributing to the development of anaemia in Plasmodium falciparum malaria: What about drug-resistant parasites? Journal of Tropical Pediatrics **52:**254-259.

217. **Raha, S., and B. H. Robinson.** 2000. Mitochondria, oxygen free radicals, disease and ageing. Trends in Biochemical Sciences **25:**502-508.

218. **Rai, A. J., R. M. Kamath, W. Gerald, and M. Fleisher.** 2009. Analytical validation of the GeXP analyzer and design of a workflow for cancer-biomarker discovery using multiplexed gene-expression profiling. Analytical and Bioanalytical Chemistry **393:**1505-1511.

219. **Ralph, S. A., G. G. van Dooren, R. F. Waller, M. J. Crawford, M. J. Fraunholz, B. J. Foth, C. J. Tonkin, D. S. Roos, and G. I. McFadden.** 2004. Metabolic maps and functions of the Plasmodium falciparum apicoplast. Nature Reviews Microbiology **2:**203-216.

220. **Reed, M. B., K. J. Sallba, S. R. Caruana, K. Kirk, and A. F. Cowman.** 2000. Pgh1 modulates sensitivity and resistance to multiple antimalarials in Plasmodium falciparum. Nature **403:**906-909.

221. **Rich, P. R.** 2003. The molecular machinery of Keilin's respiratory chain. Biochemical Society Transactions **31:**1095-1105.

222. **Rossignol, R., B. Faustin, C. Rocher, M. Malgat, J. P. Mazat, and T. Letellier.** 2003. Mitochondrial threshold effects. Biochemical Journal **370:**751-762.

223. **Roth Jr, E.** 1990. Plasmodium falciparum carbohydrate metabolism: A connection between host cell and parasite. Blood Cells **16:**453-460.

224. **Rowe, J. A., A. Claessens, R. A. Corrigan, and M. Arman.** 2009. Adhesion of Plasmodium falciparum-infected erythrocytes to human cells: Molecular mechanisms and therapeutic implications. Expert Reviews in Molecular Medicine **11.**

225. **Rutgers, T., D. Gordon, A. M. Gathoye, M. Hollingdale, W. Hockmeyer, M. Rosenberg, and M. De Wilde.** 1988. Hepatitis B surface antigen as carrier matrix for the repetitive epitope of the circumsporozoite protein of Plasmodium falciparum. Bio/Technology **6:**1065-1070.

226. **Sagara, I., A. Dicko, R. D. Ellis, M. P. Fay, S. I. Diawara, M. H. Assadou, M. S. Sissoko, M. Kone, A. I. Diallo, R. Saye, M. A. Guindo, O. Kante, M. B. Niambele, K. Miura, G. E. D. Mullen, M. Pierce, L. B. Martin, A. Dolo, D. A. Diallo, O. K. Doumbo, L. H. Miller, and A.**

Saul. 2009. A randomized controlled phase 2 trial of the blood stage AMA1-C1/Alhydrogel malaria vaccine in children in Mali. Vaccine **27:**3090-3098.

227. **Sarensen, H. P., and K. K. Mortensen.** 2005. Soluble expression of recombinant proteins in the cytoplasm of Escherichia coli. Microbial Cell Factories **4.**

228. **Sato, S., B. Clough, L. Coates, and R. J. M. Wilson.** 2004. Enzymes for heme biosynthesis are found in both the mitochondrion and plastid of the malaria parasite Plasmodium falciparum. Protist **155:**117-125.

229. **Schafer, E., H. Seelert, N. H. Reifschneider, F. Krause, N. A. Dencher, and J. Vonck.** 2006. Architecture of active mammalian respiratory chain supercomplexes. The Journal of Biological Chemistry **281:**15370-5.

230. **Scheibel, L. W., A. Adler, and W. Trager.** 1979. Tetraethylthiuram disulfide (Antabuse) inhibits the human malaria parasite Plasmodium falciparum. Proceedings of the National Academy of Sciences of the United States of America **76:**5303-7.

231. **Schofield, L., and G. E. Grau.** 2005. Immunological processes in malaria pathogenesis. Nature Reviews Immunology **5:**722-735.

232. **Schofield, L., L. Vivas, F. Hackett, P. Gerold, R. T. Schwartz, and S. Tachado.** 1993. Neutralizing monoclonal antibodies to glycosylphosphatidylinositol, the dominant TNF-Î±-inducing toxin of Plasmodium falciparum: Prospects for the immunotherapy of severe malaria. Annals of Tropical Medicine and Parasitology **87:**617-626.

233. **Schumann, R. R.** 2007. Malarial fever: Hemozoin is involved but toll-free. Proceedings of the National Academy of Sciences of the United States of America **104:**1743-1744.

234. **Schwartz, E., M. Parise, P. Kozarsky, and M. Cetron.** 2003. Delayed onset of malaria - Implications for chemoprophylaxis in travelers. New England Journal of Medicine **349:**1510-1516.

235. **Schwolbel, B., M. Alifrangis, A. Salanti, and T. Jelinek.** 2003. Different mutation patterns of atovaquone resistance to Plasmodium falciparum in vitro and in vivo: Rapid detection of codon 268 polymorphisms in the cytochrome b as potential in vivo resistance marker. Malaria Journal **2:**1-7.

236. **Seeber, F., and D. Soldati-Favre.** 2010. Metabolic pathways in the apicoplast of apicomplexa, p. 161-228, International Review of Cell and Molecular Biology, vol. 281.

237. **Sherman, I. W.** 1979. Biochemistry of Plasmodium (malarial parasites). Microbiological Reviews **43:**453-495.

238. **Sherman, I. W.** 1998. Malaria: parasite biology, pathogenesis, and protection. ASM Press, Washington, D.C.

239. **Skerlj, R. T., C. M. Bastos, M. L. Booker, M. L. Kramer, R. H. Barker, Jr., C. A. Celatka, T. J. O'Shea, B. Munoz, A. B. Sidhu, J. F. Cortese, S. Wittlin, P. Papastogiannidis, I. Angulo-Barturen, M. Belen Jimenez-Diaz, and E. Sybertz.** 2011. Optimization of Potent Inhibitors of P. falciparum Dihydroorotate Dehydrogenase for the Treatment of Malaria. Acs Medicinal Chemistry Letters **2:**708-713.

240. **Slavic, K., U. Straschil, L. Reininger, C. Doerig, C. Morin, R. Tewari, and S. Krishna.** 2010. Life cycle studies of the hexose transporter of Plasmodium species and genetic validation of their essentiality. Molecular Microbiology **75:**1402-1413.

241. **Smilkstein, M. J., I. Forquer, A. Kanazawa, J. X. Kelly, R. W. Winter, D. J. Hinrichs, D. M. Kramer, and M. K. Riscoe.** 2008. A drug-selected Plasmodium falciparum lacking the need for conventional electron transport. Molecular and Biochemical Parasitology **159:**64-68.

242. **Smilkstein, M. J., I. Forquer, A. Kanazawa, J. X. Kelly, R. W. Winter, D. J. Hinrichs, D. M. Kramer, and M. K. Riscoe.** 2008. A drug-selected Plasmodium falciparum lacking the need for conventional electron transport. Molecular and Biochemical Parasitology **159:**64-8.

243. **Smith, J. D., C. E. Chitnis, A. G. Craig, D. J. Roberts, D. E. Hudson-Taylor, D. S. Peterson, R. Pinches, C. I. Newbold, and L. H. Miller.** 1995. Switches in expression of plasmodium falciparum var genes correlate with changes in antigenic and cytoadherent phenotypes of infected erythrocytes. Cell **82:**101-110.

244. **Snow, R. W., C. A. Guerra, A. M. Noor, H. Y. Myint, and S. I. Hay.** 2005. The global distribution of clinical episodes of Plasmodium falciparum malaria. Nature **434:**214-217.
245. **Srivastava, I. K., J. M. Morrlsey, E. Darrouzet, F. Daldal, and A. B. Vaidya.** 1999. Resistance mutations reveal the atovaquone-binding domain of cytochrome b in malaria parasites. Molecular Microbiology **33:**704-711.
246. **Srivastava, I. K., H. Rottenberg, and A. B. Vaidya.** 1997. Atovaquone, a broad spectrum antiparasitic drug, collapses mitochondrial membrane potential in a malarial parasite. Journal of Biological Chemistry **272:**3961-3966.
247. **Srivastava, I. K., and A. B. Vaidya.** 1999. A mechanism for the synergistic antimalarial action of atovaquone and proguanil. Antimicrobial Agents and Chemotherapy **43:**1334-1339.
248. **Stanway, R. R., T. Witt, B. Zobiak, M. Aepfelbacher, and V. T. Heussler.** 2009. GFP-targeting allows visualization of the apicoplast throughout the life cycle of live malaria parasites. Biology of the Cell **101:**415-430.
249. **Stoute, J. A., A. O. Odindo, B. O. Owuor, E. K. Mibei, M. O. Opollo, and J. N. Waitumbi.** 2003. Loss of red blood cell-complement regulatory proteins and increased levels of circulating immune complexes are associated with severe malarial anemia. Journal of Infectious Diseases **187:**522-525.
250. **Surolia, N., and G. Padmanaban.** 1991. Chloroquine inhibits heme-dependent protein synthesis in Plasmodium falciparum. Proceedings of the National Academy of Sciences of the United States of America **88:**4786-4790.
251. **Surolia, N., and A. Surolia.** 2001. Erratum: Triclosan offers protection against blood stages of malaria by inhibiting enoyl-ACP reductase of Plasmodium falciparum (Nature Medicine (2000) 7 (167-173)). Nature Medicine **7:**636.
252. **Suthammarak, W., P. G. Morgan, and M. M. Sedensky.** 2010. Mutations in mitochondrial complex III uniquely affect complex I in Caenorhabditis elegans. The Journal of biological chemistry **285:**40724-31.
253. **Takala, S. L., D. Coulibaly, M. A. Thera, A. H. Batchelor, M. P. Cummings, A. A. Escalante, A. Ouattara, K. Traore, A. Niangaly, A. A. Djimde, O. K. Doumbo, and C. V. Plowe.** 2009. Extreme polymorphism in a vaccine antigen and risk of clinical malaria: implications for vaccine development. Science translational medicine **1.**
254. **Tanner, M., T. Teuscher, and P. L. Alonso.** 1994. SPf66 malaria vaccine trial: An update. Parasitology Today **10:**79.
255. **Taylor, H. M., M. Grainger, and A. A. Holder.** 2002. Variation in the expression of a Plasmodium falciparum protein family implicated in erythrocyte invasion. Infection and Immunity **70:**5779-5789.
256. **Thera, M. A., O. K. Doumbo, D. Coulibaly, M. B. Laurens, A. K. Kone, A. B. Guindo, K. Traore, M. Sissoko, D. A. Diallo, I. Diarra, B. Kouriba, M. Daou, A. Dolo, M. Baby, M. S. Sissoko, I. Sagara, A. Niangaly, I. Traore, A. Olotu, O. Godeaux, A. Leach, M. C. Dubois, W. R. Ballou, J. Cohen, D. Thompson, T. Dube, L. Soisson, C. L. Diggs, S. L. Takala, K. E. Lyke, B. House, D. E. Lanar, S. Dutta, D. G. Heppner, and C. V. Plowe.** 2008. Safety and immunogenicity of an AMA1 malaria vaccine in Malian children: Results of a phase 1 randomized controlled trial. PLoS ONE **5.**
257. **Thera, M. A., and C. V. Plowe.** 2012. Vaccines for malaria: How close are we?, p. 345-357, Annual Review of Medicine, vol. 63.
258. **Tonkin, C. J., G. G. Van Dooren, T. P. Spurck, N. S. Struck, R. T. Good, E. Handman, A. F. Cowman, and G. I. McFadden.** 2004. Localization of organellar proteins in Plasmodium falciparum using a novel set of transfection vectors and a new immunofluorescence fixation method. Molecular and Biochemical Parasitology **137:**13-21.
259. **Triglia, T., J. G. T. Menting, C. Wilson, and A. F. Cowman.** 1997. Mutations in dihydropteroate synthase are responsible for sulfone and sulfonamide resistance in Plasmodium falciparum. Proceedings of the National Academy of Sciences of the United States of America **94:**13944-13949.

260. **Tripathi, A. K., P. V. Desai, A. Pradhan, S. I. Khan, M. A. Avery, L. A. Walker, and B. L. Tekwani.** 2004. An alpha-proteobacterial type malate dehydrogenase may complement LDH function in Plasmodium falciparum: Cloning and biochemical characterization of the enzyme. European Journal of Biochemistry **271**:3488-3502.
261. **Tuteja, R.** 2007. Malaria - An overview. FEBS Journal **274**:4670-4679.
262. **Uyemura, S. A., S. Luo, M. Vieira, S. N. J. Moreno, and R. Docampo.** 2004. Oxidative Phosphorylation and Rotenone-insensitive Malate- and NADH-Quinone Oxidoreductases in Plasmodium yoelii yoelii Mitochondria in Situ. Journal of Biological Chemistry **279**:385-393.
263. **Vaidya, A. B., R. Akella, and K. Suplick.** 1989. Sequences similar to genes for two mitochondrial proteins and portions of ribosomal RNA in tandemly arrayed 6-kilobase-pair DNA of a malarial parasite. Molecular and Biochemical Parasitology **35**:97-108.
264. **Vaidya, A. B., and M. W. Mather.** 2000. Atovaquone resistance in malaria parasites. Drug Resistance Updates **3**:283-287.
265. **Vaidya, A. B., and M. W. Mather.** 2009. Mitochondrial evolution and functions in malaria parasites, p. 249-267, Annual Review of Microbiology, vol. 63.
266. **Vaidya, A. B., and M. W. Mather.** 2005. A post-genomic view of the mitochondrion in malaria parasites, p. 233-250, Current Topics in Microbiology and Immunology, vol. 295.
267. **Van der Rest, M. E., C. Frank, and D. Molenaar.** 2000. Functions of the membrane-associated and cytoplasmic malate dehydrogenases in the citric acid cycle of Escherichia coli. Journal of Bacteriology **182**:6892-6899.
268. **Van Dooren, G. G., M. Marti, C. J. Tonkin, L. M. Stimmler, A. F. Cowman, and G. I. McFadden.** 2005. Development of the endoplasmic reticulum, mitochondrion and apicoplast during the asexual life cycle of Plasmodium falciparum. Molecular Microbiology **57**:405-419.
269. **Van Dooren, G. G., L. M. Stimmler, and G. I. McFadden.** 2006. Metabolic maps and functions of the Plasmodium mitochondrion. FEMS Microbiology Reviews **30**:596-630.
270. **Varadharajan, S., S. Dhanasekaran, Z. Q. Bonday, P. N. Rangarajan, and G. Padmanaban.** 2002. Involvement of Î´-aminolaevulinate synthase encoded by the parasite gene in de novo haem synthesis by Plasmodium falciparum. Biochemical Journal **367**:321-327.
271. **Vaughan, A. M., M. T. O'Neill, A. S. Tarun, N. Camargo, T. M. Phuong, A. S. I. Aly, A. F. Cowman, and S. H. I. Kappe.** 2009. Type II fatty acid synthesis is essential only for malaria parasite late liver stage development. Cellular Microbiology **11**:506-520.
272. **Verma, R., G. C. Varshney, and G. P. S. Raghava.** 2010. Prediction of mitochondrial proteins of malaria parasite using split amino acid composition and PSSM profile. Amino Acids **39**:101-110.
273. **Vogetseder, A., C. Ospelt, M. Reindl, M. Schober, and E. Schmutzhard.** 2004. Time course of coagulation parameters, cytokines and adhesion molecules in Plasmodium falciparum malaria. Tropical Medicine and International Health **9**:767-773.
274. **Waller, R. F., and G. I. McFadden.** 2005. The apicoplast: A review of the derived plastid of apicomplexan parasites. Current Issues in Molecular Biology **7**:57-80.
275. **Warrell, D. A.** 1997. Cerebral malaria: Clinical features, pathophysiology and treatment. Annals of Tropical Medicine and Parasitology **91**:875-884.
276. **Wenz, T., P. Hellwig, F. MacMillan, B. Meunier, and C. Hunte.** 2006. Probing the role of E272 in quinol oxidation of mitochondrial complex III. Biochemistry **45**:9042-9052.
277. **White, N. J.** 2008. Qinghaosu (artemisinin): The price of success. Science **320**:330-334.
278. **WHO.** 2010. World Malaria Report.
279. **WHO.** 2008. World Malaria Report. World Health Organization.
280. **Wibrand, F., K. Ravn, M. Schwartz, T. Rosenberg, N. Horn, and J. Vissing.** 2001. Multisystem disorder associated with a missense mutation in the mitochondrial cytochrome b gene. Annals of neurology **50**:540-3.
281. **Wiesner, J., A. Reichenberg, S. Heinrich, M. Schlitzer, and H. Jomaa.** 2008. The plastid-like organelle of apicomplexan parasites as drug target. Current Pharmaceutical Design **14**:855-871.

282. **Wilkinson, D. L., and R. G. Harrison.** 1991. Predicting the solubility of recombinant proteins in Escherichia coli. Nature Biotechnology **9**:443-448.
283. **Wilson, M., J. DeRisi, H. H. Kristensen, P. Imboden, S. Rane, P. O. Brown, and G. K. Schoolnik.** 1999. Exploring drug-induced alterations in gene expression in Mycobacterium tuberculosis by microarray hybridization. Proceedings of the National Academy of Sciences of the United States of America **96**:12833-12838.
284. **Winter, R. W., J. X. Kelly, M. J. Smilkstein, R. Dodean, D. Hinrichs, and M. K. Riscoe.** 2008. Antimalarial quinolones: Synthesis, potency, and mechanistic studies. Experimental Parasitology **118**:487-497.
285. **Wirth, D. F.** 2002. Biological revelations. Nature **419**:495-496.
286. **Wittig, I., H. P. Braun, and H. Schägger.** 2006. Blue native PAGE. Nature Protocols **1**:418-428.
287. **Woods, S. A., S. D. Schwartzbach, and J. R. Guest.** 1988. Two biochemically distinct classes of fumarase in Escherichia coli. Biochimica et Biophysica Acta - Protein Structure and Molecular Enzymology **954**:14-26.
288. **Wrenger, C., and S. Muìller.** 2003. Isocitrate dehydrogenase of Plasmodium falciparum: Energy metabolism or redox control? European Journal of Biochemistry **270**:1775-1783.
289. **Xiang, H., J. McSurdy-Freed, G. S. Moorthy, E. Hugger, R. Bambal, C. Han, S. Ferrer, D. Gargallo, and C. B. Davis.** 2006. Preclinical drug metabolism and pharmacokinetic evaluation of GW844520, a novel anti-malarial mitochondrial electron transport inhibitor. Journal of Pharmaceutical Sciences **95**:2657-2672.
290. **Yankovskaya, V., R. Horsefield, S. Tornroth, C. Luna-Chavez, H. Miyoshi, C. Leger, B. Byrne, G. Cecchini, and S. Iwata.** 2003. Architecture of succinate dehydrogenase and reactive oxygen species generation. Science **299**:700-704.
291. **Yeates, C. L., J. F. Batchelor, E. C. Capon, N. J. Cheesman, M. Fry, A. T. Hudson, M. Pudney, H. Trimming, J. Woolven, J. M. Bueno, J. Chicharro, E. Fernnandez, J. M. Fiandor, D. Gargallo-Viola, F. G. De Las Heras, E. Herreros, and M. L. Leon.** 2008. Synthesis and structure-activity relationships of 4-pyridones as potential antimalarials. Journal of Medicinal Chemistry **51**:2845-2852.
292. **Yeo, A. E. T., K. K. Seymour, K. H. Rieckmann, and R. I. Christopherson.** 1997. Effects of dual combinations of antifolates with atovaquone or dapsone on nucleotide levels in Plasmodium falciparum. Biochemical Pharmacology **53**:943-950.
293. **Young, J. A., and E. A. Winzeler.** 2005. Using expression information to discover new drug and vaccine targets in the malaria parasite Plasmodium falciparum. Pharmacogenomics **6**:17-26.
294. **Zameitat, E., A. J. Pierik, K. Zocher, and M. Loffler.** 2007. Dihydroorotate dehydrogenase from Saccharomyces cerevisiae: Spectroscopic investigations with the recombinant enzyme throw light on catalytic properties and metabolism of fumarate analogues. FEMS Yeast Research **7**:897-904.
295. **Zhang, L., and A. Hach.** 1999. Molecular mechanism of heme signaling in yeast: The transcriptional activator Hap1 serves as the key mediator. Cellular and Molecular Life Sciences **56**:415-426.
296. **Zhu, G., X. Shi, and X. Cai.** 2010. The reductase domain in a Type i fatty acid synthase from the apicomplexan Cryptosporidium parvum: Restricted substrate preference towards very long chain fatty acyl thioesters. BMC Biochemistry **11**.

Appendices

Appendix 1: Molecular Basic of Antimalarial Drug Resistance

Antimalarial Drug	Resistance gene	Mode of action	Amino acid residue	Polymorphism	Location
CQ	*Pfcrt*	Drugs and metabolite transporter	K76T	Lysine to threonine	Chromosome 7
Pyrimethamine, cycloguanil, chlorcycloguanil	*Pfdhfr*	Dihydrfolate reductase enzyme for folate biosynthesis, pyrimidine metabolism	N51I, C59R, S108N, I164L	Asparagine to isoleucine, cystine to arginine, serine to asparagines, isoleucine to leucine	Chromosome 4
Sulphonamides and sulfones	*Pfdhps*	Dihydropteroate synthetase for folate biosynthesis	A436S/F, A437G, K540E, A518G, A613S/T	Alanine to serine/phenylalanine, alanine to glycine, lysine to glutamate, alanine to glycine, alanine to serine/threonine	Chromosome 8
Atovaquone	Cytochrome *b*	Mitochondrial electron transport chain	Y268S	Tyrosine to serine	Not assigned
CQ, MQ,QN	*Pfmdr-1/Pfpgh-1*	ABC transporter	N86Y	Asparagine to tyrosine	Chromosome 5
CQ,QN,SP	*Pfmrp-1*	ABC transporter	H191Y,S437A	Histidine to tyrosine, serine to alanine	Chromosome 1
CQ,MQ,QN,SP	*Pfnhe-1*	ABC transporter	Ms4760		Locus at chromosome 9 and 13

Pfcrt, *Plasmodium* chloroquine resistance transporter gene; *Pfmdr/Pfpgh*-1 gene, multidrug resistance p-glycoprotein pump, *Pfdhfr*, dihydrofolate reductase gene; *Pfdhps, Plasmodium* dihydropteroate synthase gene. Numbers refer to the positions of point mutations associated with resistance.

Appendix 2: Primers used for GeXP to Quantitate Major Metabolism Gene Expression Profiles of *P. falciparum* (3D7, TM90C2B and 3D7-YDHODH.GFP)

No	Name of Gene	Forward Primer Sequence	Reverse Primer Sequence	Product Size
1	PFB0210c hexose transporter	AGGTGACACTATAGAATACTGCAAGCTTGGCATCATTA	GTACGACTCACTATAGGGAGCTTTTGTCGCTCCTCCATA	250
2	PFF1155w hexokinase	AGGTGACACTATAGAATAGCATGCAACAGCATCACAAT	GTACGACTCACTATAGGGATTTCGCTGGAATAGCAGCTC	305
3	PF14_0341 glucose-6-phosphate isomerase	AGGTGACACTATAGAATAACCCTTATCAATTGCTTTTGGA	GTACGACTCACTATAGGGATGCTGACCATTTGTACCAGG	358
4	*PF14_0341 glucose-6-phosphate isomerase	AGGTGACACTATAGAATATGGGTAGGAGGTCGATTTTC	GTACGACTCACTATAGGGATTCATCCATATCATGACAACCA	151
5	PFI0755c 6-phosphofructokinase, putative	AGGTGACACTATAGAATAGGCCATTTAGGTAATGCACG	GTACGACTCACTATAGGGACCATCCCTTGCTTTATCGTC	207
6	PF11_0294 ATP-dependent phosphofructokinase, putative	AGGTGACACTATAGAATACCTGGCAGGAATAGCTGTAGA	GTACGACTCACTATAGGGACGCTGTATGCCCAGGTATTT	273
7	*PF11_0294 ATP-dependent phosphofructokinase, putative	AGGTGACACTATAGAATACTCTCATGGACTCCTGGCA	GTACGACTCACTATAGGGAGAACAGGTGCTACAGAGGGG	219

8	PF14_0425 Aldolase	AGGTGACACTATAGAATACACCAGCCTTACCAG GTGTT	GTACGACTCACTATAGGGATTTCCTTGCCATGTGT TCAA	200
9	PF14_0598 glyceraldehyde-3- phosphate dehydrogenase	AGGTGACACTATAGAATATTGGGGAAAATGCCA AGTAG	GTACGACTCACTATAGGGAGGGGCGGACATAATA ACCTT	151
10	PFI1105w Phosphoglycerate kinase	AGGTGACACTATAGAATATCTTGATGCTGGTCC AAAAA	GTACGACTCACTATAGGGAGTGAGGCTCCTCCAC CTGTA	297
11	PFD0660w phosphoglycerate mutase, putative	AGGTGACACTATAGAATACCCTCTTCCAAGACA TTCAAA	GTACGACTCACTATAGGGATTCAAAGGGGAGGTG AGAAA	332
12	PF10_0155 enolase	AGGTGACACTATAGAATAAAATGAATGGGGATG GTCAA	GTACGACTCACTATAGGGAGGGATCCTCCATTGA TAACG	228
13	*PF10_0155 enolase	AGGTGACACTATAGAATACTGGTGCCTCCACTG GTATT	GTACGACTCACTATAGGGATCCAATCAATTTTGG AGCAA	165
14	PF10_0363 pyruvate kinase 2 putative	AGGTGACACTATAGAATAACATTCTCGCACATA GCGAA	GTACGACTCACTATAGGGATGTTCAAAATTTTCCG ACGC	179
15	PFF1300w pyruvate kinase, putative	AGGTGACACTATAGAATAATCCATGACCAAGAA CCCAA	GTACGACTCACTATAGGGACACCTGCAGTTTCTCC TGAA	144
16	*PF13_0141	AGGTGACACTATAGAATAGCACCAAAAGCAAA	GTACGACTCACTATAGGGACCAGCCAAATCGTCA	249

	L-lactate dehydrogenase	AATCGT	TAAGTG	
17	PF13_0141 L-lactate dehydrogenase	AGGTGACACTATAGAATAATGGCACCAAAAGCA AAAAT	GTACGACTCACTATAGGGAAGCTTTTCCATGTGGC ATGT	243
18	PF13_0269 Glycerol kinase	AGGTGACACTATAGAATATGATGGAGGCATGAC AAAAA	GTACGACTCACTATAGGGATCGACAGCTTTATTCC ATTCG	289
19	*PF13_0269 Glycerol kinase	AGGTGACACTATAGAATATGATGGAGGCATGAC AAAAA	GTACGACTCACTATAGGGAAGAACTGCAGCACCA AGAGAA	151
20	PF14_0286 Putative Glutamate dehydrogenase	AGGTGACACTATAGAATATGCTTTTCCATGTGCA ACAC	GTACGACTCACTATAGGGACCTCCAGCATTAGCA GCTTT	214
21	*PF14_0286 Putative Glutamate dehydrogenase	AGGTGACACTATAGAATATGCAAACATGCCAAC ACATA	GTACGACTCACTATAGGGATACAGCTACCCCTCC AGCAT	137
22	PF08_0132 Putative NAD_Glutamate dehydrogenase	AGGTGACACTATAGAATAGAAGGTCGGCATTAA GTTGC	GTACGACTCACTATAGGGATAATCAACTCGGGGC TTGTC	265
23	PF14_0164 NADP_glutamate dehydrogenase	AGGTGACACTATAGAATAAGGAGGTAAAGGTG GTTCGG	GTACGACTCACTATAGGGACCAATTTCTCGACCA CCAAC	193
24	PF13_0234 Phosphoenolpyruvate carboxykinase	AGGTGACACTATAGAATACATCACAATTCAACT CCAGCA	GTACGACTCACTATAGGGAGACAACGTTCATCCC AACCT	335

25	PF14_0246 Phosphoenolpyruvate carboxylase	AGGTGACACTATAGAATATGGGCTCATAGAGGA AGACG	GTACGACTCACTATAGGGAGTTCGAATAGCTTGT GTTGGG	243
26	PF13_0144 lactate/malate DH putative	AGGTGACACTATAGAATAATGGCGGGTGTTCTT CATAG	GTACGACTCACTATAGGGATATCTTGGAAGGGGG ACCAT	165
27	PFC0831w triosephophate isomerase, putative	AGGTGACACTATAGAATATTCGGACCATTTACA GGAGAA	GTACGACTCACTATAGGGATCGTAAGAGCTCCAT CATTTTG	280
28	PFC0831w triosephophate isomerase, putative	AGGTGACACTATAGAATATTCCAAAAATCAACC AACTGTC	GTACGACTCACTATAGGGATCACTCGAATTATTCC GTTCG	204
29	PF11_0157 Glycerol-3-phosphate dehydrogenase	AGGTGACACTATAGAATATGGGGAACAGTCGTT TCAA	GTACGACTCACTATAGGGAATGGCTCTTGCGTTTT TCTT	351
30	*PF11_0157 Glycerol-3-phosphate dehydrogenase	AGGTGACACTATAGAATATGTTATAGCCTTAGG GGTTGGA	GTACGACTCACTATAGGGACTTCCTCCCAAACAT GTGGT	226
31	PFI0735c type II NADH:quinone oxidoreductase	AGGTGACACTATAGAATATAGCTGTAGGGGCAA AAACG	GTACGACTCACTATAGGGAATCAGCAAATTCTGC GGTAA	264
32	PF10_0334 Succinate quinone oxidoreductase (SQR) flavoprotein subunit (SU)	AGGTGACACTATAGAATAAAAATTTTTGCGGGA GTTGA	GTACGACTCACTATAGGGAATGCTGATGCAGCTT CTCCT	236
33	PFL0630w SQR iron-sulphur (FeS) SU	AGGTGACACTATAGAATACCAGCCACCTTAATG CAAG	GTACGACTCACTATAGGGAGGCTGGATCTAAACC TTTTGG	193

34	PFF0160c Dihydroorotate dehydrogenase	AGGTGACACTATAGAATAGCAGGTGCTTCAGTT TGTCA	GTACGACTCACTATAGGGACTTTTGCTATGCTTTC GGC	186
35	PFC0275w Glycerol-3-P DH (quinone-dependent)	AGGTGACACTATAGAATAGCCTTAGATGCAGCC ACAAG	GTACGACTCACTATAGGGAGCGCTCTTTCTGCTAA TGCT	221
36	PFF0815w Malate:quinone oxidoreductase	AGGTGACACTATAGAATATTACACCTTCACCTG GAGCA	GTACGACTCACTATAGGGATAACGGGATATTCGC CTTCA	172
37	Mal_MITO_3 Complex III cyt b	AGGTGACACTATAGAATAATACATGCACGCAAC AGGTG	GTACGACTCACTATAGGGATTGCACCCCAATAAC TCATTT	228
38	PF14_0597 Complex III cyt c1	AGGTGACACTATAGAATAGTGGTGCATCTCCAC CTGAT	GTACGACTCACTATAGGGAGGAGTGGTGGAGGCA TAGAA	214
39	PF14_0373 Complex III Fes Rieske protein	AGGTGACACTATAGAATATGAACCGTCAAATCA TCCAC	GTACGACTCACTATAGGGACGCTAGCCAATTCAC CTTTC	165
40	PF14_0038 Cytochrome c	AGGTGACACTATAGAATAAAAAAGGGCGCTAA GCTTTT	GTACGACTCACTATAGGGATTTCTTCCATAAAATC CGTGC	144
41	MAL_MITO_2 Complex IV SU 1	AGGTGACACTATAGAATAGCCAGGATTATTCGG AGGAT	GTACGACTCACTATAGGGAAAGTCCATCCAGTTC CACCA	207
42	PF13_0327 Complex IV SU 2	AGGTGACACTATAGAATACCATTTTGGGCAAGA ACAAG	GTACGACTCACTATAGGGACCGGAGGTGATTCAA CTTCAT	257
43	PFB0795w Complex V alpha SU	AGGTGACACTATAGAATATCGAGACAATGGAAA ACG	GTACGACTCACTATAGGGATCCCGGGGGTCTTCTT AAT	137
44	PFL1725w Complex V beta SU	AGGTGACACTATAGAATATTTTTGCTGGTGTAG GGGAA	GTACGACTCACTATAGGGATGACCATATACAAGC GCAGC	179
45	PF10_0218	AGGTGACACTATAGAATATCAAATTCAAGTTAT	GTACGACTCACTATAGGGAACTTGCATTTCCACCC	242

	Citrate synthase, mitochondrial putative	TGGTGCG	TCAT	
46	*PF10_0218 Citrate synthase, mitochondrial putative	AGGTGACACTATAGAATACACACTTTCCAGATG ACCCA	GTACGACTCACTATAGGGACCAATGGATCTAGAA AGGGC	233
47	PFF0455w Citrate synthase	AGGTGACACTATAGAATAGAAAAGTTCCTTTCT TTCATTTTG	GTACGACTCACTATAGGGATGTCTCCAGAAAAAG GCTGG	186
48	*PFF0455w Citrate synthase	AGGTGACACTATAGAATATCACGATTACTTAGT TTTACGGCA	GTACGACTCACTATAGGGATGTACATATTGCCTTG CTGGG	144
49	PF10_0218 Citrate synthase mitochondrial putative	AGGTGACACTATAGAATACACACTTTCCAGATG ACCCA	GTACGACTCACTATAGGGACCAATGGATCTAGAA AGGGC	233
50	PF13_0229 Aconitase	AGGTGACACTATAGAATATGGAGCAAGAAGAG GAAATGA	GTACGACTCACTATAGGGACCCAATCTCTTGAACT CCCA	258
51	PF13_0242 Isocitrate dehydrogenase	AGGTGACACTATAGAATACCAATCTGATGCTGT TGCTC	GTACGACTCACTATAGGGAATGGGCAGCTTCTGA AACAC	137
52	PF08_0045 Alpha-keto glutarate dehydrogenase	AGGTGACACTATAGAATAAATCGCTGGACAAGG AATTG	GTACGACTCACTATAGGGACCTGACCTTGCATCTA TTGGA	172
53	PF11_0097 Succinyl CoA synthetase	AGGTGACACTATAGAATACACGAATTGTTATGC ATCCG	GTACGACTCACTATAGGGAATGATTCCAGGACAA TTGGG	235
54	PFF0895w Malate dehydrogenase	AGGTGACACTATAGAATAGCTAAAGCATCTGCA GCATTT	GTACGACTCACTATAGGGAGGAATTCAACTGGAT GTGCC	221

55	PF07_0073 seryl-tRNA synthetase, putative	AGGTGACACTATAGAATACAAGTAGCAGGTCATCGTGG	GTACGACTCACTATAGGGACAAGTTCGGCACATTCTTCC	200
56	**PF13_0305 elongation factor 1 alpha	AGGTGACACTATAGAATATGTCATTGATGCACCAGGTC	GTACGACTCACTATAGGGATGAAAAGGCACCTTCGAAAC	158
57	***Kan(r)	AGGTGACACTATAGAATAATCATCAGCATTGCATTCGATTCCTGTTTG	GTACGACTCACTATAGGGAATTCCGACTCGTCCAACATC	325
58	PF11_0318 sexual development, pF16 protein	AGGTGACACTATAGAATACATTCAACCGAACATGCAAA	GTACGACTCACTATAGGGAATGGAATATTTTGCAAGGGG	240

Primers 1-30 represent genes involved in glycolysis, 31-44 mitochondrial electron transport chain, 45-54 the TCA cycle, 55-56 housekeeping genes, 57 Kan (r); kanamycin RNA internal positive control gene and 58 a gene encoding a sexual developmental protein.* re-synthesised.**Gene used for normalisation. *** Internal control.

Appendix 3: Fold Change in Expression for Key Energy Metabolism Genes of the Atovaquone Resistant Strain TM90C2B and the 3D7-yDHODH-GFP Transgenic Compared to The Atovaquone Sensitive 3D7 Strain

Gene		3D7			TM90-C2B			3D7-YDHODH.GFP (TX13)			Fold Changes		Man Whitney P<0.05	
		Mean	S.E	N	Mean	S.E	N	Mean	S.E	N	TM90/ 3D7	TX13/ 3D7	3D7/ TM90	TX13/3D7
PFB0210c	Hexose Transporter	0.138	0.007	6/6	0.324	0.049	3/3	0.138	0.015	5/5	2.34	1.00	0.024*	0.247
PFF1155w	Hexokinase	0.071	0.004	2/3	0.095	-	1/3	0.088	0.001	2/3	1.34	1.25	-	0.90
PF14_0341	Glucose-6-phosphate isomerase	0.920	0.012	2/3	0.648	0.119	3/3	0.386	0.179	3/3	0.71	0.42	0.20	0.20
PFI0755c	6-phospho fructokinase, putative	0.220	0.018	3/3	0.264	0.089	2/3	0.205	0.009	3/3	1.20	0.93	0.90	0.40
PF14_0425	Aldolase	0.404	0.078	3/3	0.472	0.033	2/3	0.313	0.042	3/3	1.17	0.78	0.80	0.40
PF14_0598	Glyceraldehyde-3-phosphate dehydrogenase	0.834	0.109	3/3	0.735	0.006	2/3	0.656	0.174	3/3	0.88	0.79	0.80	0.70
PFI1105w	Phosphoglycerate kinase	0.121	0.053	3/3	0.339	0.009	2/3	0.207	0.058	3/3	2.81	1.72	0.20	0.40
PF10_0155	Enolase	0.642	0.030	3/3	0.886	0.039	5/5	0.701	0.146	2/3	1.38	1.09	0.09	0.54
PF10_0363	Pyruvate kinase 2, putative	0.094	0.020	2/3	0.115	0.014	2/3	ND	-	5/5	1.22	-	0.67	-
PFF1300w	Pyruvate kinase, putative	0.903	0.075	3/3	0.774	0.020	2/3	0.817	0.024	2/3	0.86	0.90	0.40	0.70
PF13_0141	L-lactate dehydrogenase	0.597	0.049	5/5	0.712	0.083	2/3	0.408	0.172	2/3	1.19	0.68	0.38	0.39

PF14_0286	Putative Glutamate dehydrogenase	0.354	0.078	3/3	0.316	0.036	3/3	N.D	N.D	N.D	0.89	-	0.90	-
PF08_0132	Putative NAD-glutamate dehydrogenase	0.098	0.022	3/3	0.225	0.070	2/3	0.214	0.005	2/3	2.30	2.19	0.20	0.20
PF14_0164	NADP-glutamate dehydrogenase	0.102	0.009	6/6	0.142	0.014	2/3	0.114	-	1/3	1.38	1.11	0.20	-
PF13_0234	Phosphoenol pyruvate carboxykinase	0.084	0.014	6/6	0.122	0.029	3/3	0.143	0.039	5/5	1.45	1.71	0.381	0.052
PF14_0246	Phosphoenol-pyruvate carboxylase	0.169	0.003	6/6	0.253	0.101	3/3	0.073	-	1/3	1.49	0.43	0.548	-
PFI0735c	Type II NADH: quinone oxidoreductase	0.088	0.003	6/6	0.133	0.022	3/3	0.078	0.035	3/3	1.51	0.88	0.024*	0.548
PF10_0334	SQR flavoprotein SU	0.041	0.004	5/5	0.054	0.007	3/3	0.044	0.008	5/5	1.32	1.07	0.095	0.429
PFL0630w	SQR FeS SU	0.098	0.005	6/6	0.153	0.016	3/3	0.110	0.018	5/5	1.57	1.12	0.024*	0.662
PFF0160c	DHODH	0.087	0.002	6/6	0.114	0.032	3/3	0.071	0.011	4/4	1.30	0.81	0.381	0.247
PFC0275w	Glycerol 3-P DH (quinone dependent)	0.153	0.007	6/6	0.181	0.018	3/3	0.175	0.054	5/5	1.18	1.14	0.381	0.537
PFF0815w	MQO	0.176	0.003	6/6	0.195	0.060	3/3	0.141	0.025	5/5	1.10	0.80	0.517	0.055
CYTb	Complex III cyt b	0.671	0.101	5/6	1.134	0.087	3/3	0.779	0.0921	5/5	1.69	1.16	0.024*	1.000
PF14_0597	Complex III cyt c1	0.118	0.009	5/6	0.272	0.0097	3/3	0.121	0.020	5/5	2.30	1.02	0.016*	0.632
PF14_0373	Complex III Fes_Rieske protein	0.239	0.017	6/6	0.463	0.030	3/3	0.338	0.080	5/5	1.93	1.41	0.028*	0.199
PF14_0038	Cytochrome c	0.413	0.066	5/6	0.787	0.100	3/3	0.424	0.073	5/5	1.91	1.03	0.243	0.234
MAL_MITO_2	Complex IV SU1	0.438	0.031	5/5	0.916	0.009	3/3	0.556	0.057	5/5	2.09	1.27	0.027*	0.054
PF13_0327	Complex IV SU2	0.121	0.010	6/6	0.298	0.006	3/3	0.126	0.015	5/5	2.46	1.04	0.026*	0.247
PFB0795w	Complex V alpha SU	0.325	0.003	6/6	0.457	0.014	3/3	0.299	0.050	5/5	1.40	0.92	0.026*	1.000
PFL1725w	Complex V beta SU	0.135	0.010	6/6	0.156	0.007	3/3	0.124	0.015	5/5	1.15	0.92	0.714	0.126
PF10_0218	Citrate synthase, mitochondria putative	0.149	-	1/3	0.204	0.040	2/3	0.155	0.005	2/3	1.37	1.04	-	-

PFF0455w	Citrate synthase like protein putative	0.294	0.135	2/3	0.423	0.125	5/6	0.301	0.135	2/3	1.44	1.03	0.587	0.667
PF13_0229	Aconitase	0.143	0.026	2/3	0.166	0.050	2/3	0.102	0.0001	2/3	1.17	0.71	1.00	0.333
PF13_0242	Isocitrate dehydrogenase	0.324	0.058	2/3	0.187	0.018	2/3	0.131	0.012	2/3	0.58	0.41	0.245	0.149
PF08_0045	Alpha-keto glutarate dehydrogenase	0.230	0.051	3/3	0.255	0.086	2/3	0.133	0.026	2/3	1.11	0.58	1.000	0.100
PF11_0097	Succinyl CoA synthetase	0.148	0.011	3/3	0.359	0.013	2/3	0.185	0.037	2/3	2.42	1.25	0.200	0.700
PFF0895w	Malate dehydrogenase	0.062	-	1/5	0.217	-	1/3	N.D	-	-	-	-	-	-
PF11_0318	Sexual Development, PF16 protein	0.012	0.002	3/3	0.008	0.001	3/3	0.011	0.001	4/6	0.62	0.87	0.200	0.723

Gene expression is normalised to internal reference gene (elongation factor 1 alpha). The * symbol indicates significant differences in expression between 3D7 and TM90-C2B, 3D7 or 3D7-YDHODH.GFP. (N): figures in the numerator represent number of experiments showing results and denominators represent number of total of experimens run. N.D: smples did not produce results. Purple boxes represent genes involved in glycolysis, blue; genes involved in mitochondrial electron transport chain and red; are genes in *Plasmodium* TCA cycle.